

1-1-2015

Development Of Inlet And Vacuum Ionization Methods For Characterization Of Biological Materials By Mass Spectrometry

Beixi Wang
Wayne State University,

Follow this and additional works at: http://digitalcommons.wayne.edu/oa_dissertations

 Part of the [Analytical Chemistry Commons](#)

Recommended Citation

Wang, Beixi, "Development Of Inlet And Vacuum Ionization Methods For Characterization Of Biological Materials By Mass Spectrometry" (2015). *Wayne State University Dissertations*. Paper 1175.

This Open Access Dissertation is brought to you for free and open access by DigitalCommons@WayneState. It has been accepted for inclusion in Wayne State University Dissertations by an authorized administrator of DigitalCommons@WayneState.

**DEVELOPMENT OF *INLET* AND *VACUUM* IONIZATION
METHODS FOR CHARACTERIZATION OF BIOLOGICAL
MATERIALS BY MASS SPECTROMETRY**

by

BEIXI WANG

DISSERTATION

Submitted to Graduate School

of Wayne State University,

Detroit, Michigan

in partial fulfillment of the requirements

for the degree of

DOCTOR OF PHILOSOPHY

2015

MAJOR: CHEMISTRY (Analytical)

Approved by:

Advisor

Date

DEDICATION

*This dissertation is dedicated to
my parents: **Heling Jia**
and **Jihai Wang***

ACKNOWLEDGEMENTS

Wayne State University is not only the starting of my career, but also a new chapter in my life. During my graduate study here, I have learned more than just analytical chemistry. The environment of the university, the city, and the country has provided me a great opportunity to reach advanced research equipment, brilliant scientists, and the foundation to be a successful person. First and foremost, I sincerely acknowledge my advisor, Prof. Sarah Trimpin, for accepting me as a member in her lab five years ago, believing that I would be good at research despite my imperfect English at that time. I am thankful for her guidance, continuous encouragement, and support throughout my PhD period. I am also grateful to my committee members, Prof. Charles McEwen, Prof. Tamara Hendrickson, Prof. Tiffany Mathews, and previous member Prof. Jin Cha, for providing feedback on my research and their support in reading this thesis, especially Prof. McEwen for his inspiration as an outstanding scientist and his help when I was looking for jobs. Our collaborator, Prof. Charles Wilkins, is also acknowledged for access to his instrument and his support in my job search. Thank you to Prof. Ken Mackie and Dr. James Wager-Miller for providing us with tissue sections, and Prof. Arthur Suits and Dr. Lu Yan for their assistance with lasers.

I would like to thank the previous Trimpin group members, Dr. Ellen Inutan, Corinne Lutomski, and Tarick El-Baba for their continuous help and assistance. They have accompanied me through my happy and difficult times in the lab, especially Ellen for welcoming me into this lab and teaching me everything patiently from the beginning. The current Trimpin group members, Dr. Chih-Wei Liu, Dr. Shubha Chakrabarty, Kevin Joss,

Bryan Harless, and Casey Foley for their help and proof reading my manuscripts especially when I was writing my thesis. I have learned a lot by teaching you when you first joined the lab.

I would also like to acknowledge my family for their love, support, and encouragement for my whole life. Specifically, my brilliant mother has always been my number one mentor and my best friend, supporting me in what I do and providing me her life experience. I appreciate that I have inherited at least a little bit of her mind and nature to learn new things and giving presentations. Thank you to my aunt, Huiqing Wang, for giving me the greatest support while I am here in a foreign country and her insightful advice on career selection.

Last but not least, I would like to thank my friends, Xun Bao, Dong Fang, Chenchen He, Lorelie Imperial, Jing Li, Yuanyuan Yang, Zhijin Lin, Yue Ren, Zhifang Zhou, especially Xun and Chenchen for sharing my happiness and accompanying me through down times, and Lorelie for being my elder “younger sister”. I could not accomplish what I have done without the help from my beloved friends.

PREFACE

This dissertation is based closely on the following refereed publications:

Chapter 4: B. Wang, C. B. Lietz, E. D. Inutan, S. M. Leach, S. Trimpin, Producing Highly Charged Ions without Solvent Using Laserspray Ionization: A Total Solvent-Free Analysis Approach at Atmospheric Pressure. *Anal. Chem.*, **2011**, *83*, 4076-4084.

Chapter 5: B. Wang, E. D. Inutan, S. Trimpin, A New Approach to High Sensitivity Liquid Chromatography-Mass Spectrometry of Peptides using Nanoflow Solvent Assisted Inlet Ionization. *J. Am. Soc. Mass Spectrom.* **2012**, *23*, 442-445.

Chapter 6: B. Wang, S. Trimpin, High Throughput Solvent Assisted Ionization *Inlet* (SAII) for Use in Mass Spectrometry. *Anal. Chem.* **2014**, *86*, 1000-1006.

Chapter 7: B. Wang, E. Tisdale, C. L. Wilkins, S. Trimpin, Matrix Assisted Ionization Vacuum for High Resolution Fourier Transform Ion Cyclotron Resonance Mass Spectrometers. *Anal. Chem.* **2014**, *86*, 6792-6796.

Chapter 8: B. Wang, C. L. Dearing, J. Wager-Miller, K. Mackie, and S. Trimpin, Drug Detection and Quantification Directly from Tissue using Novel Ionization Methods for Mass Spectrometry, *Anal. Chem.*, submitted.

TABLE OF CONTENTS

Dedication	ii
Acknowledgement	iii
Preface	v
List of Schemes and Tables	vii
List of Figures	ix
List of Abbreviations	xiii
Chapter 1 Introduction	1
Chapter 2 Materials and Instrumentation.	23
Chapter 3 Fundamental Understanding	28
Chapter 4 Producing Highly Charged Ions without Solvent Using Laserspray Ionization: A Total Solvent-Free Analysis Approach at Atmospheric Pressure	36
Chapter 5 A New Approach to High Sensitivity Liquid Chromatography-Mass Spectrometry of Peptides using Nanoflow Solvent Assisted Inlet Ionization	62
Chapter 6 High Throughput Solvent Assisted Ionization <i>Inlet</i> (SAII) for Use in Mass Spectrometry	71
Chapter 7 Matrix Assisted Ionization Vacuum for High Resolution Fourier Transform Ion Cyclotron Resonance Mass Spectrometers	89
Chapter 8 Drug Detection and Quantification Directly from Tissue using Novel Ionization Methods for Mass Spectrometry	102
Chapter 9 Conclusion and Further Prospectus	124
Appendixes	127
Bibliography	172
Abstract	208
Autobiographical Statement	210

LIST OF SCHEMES AND TABLES

Scheme 1.1. Technology development needed to expand the use of mass spectrometry for clinical applications.....	3
Scheme 1.2. Representation of the basic components of a mass spectrometer.....	3
Scheme 1.3. Schematic representation of MALDI process in vacuum (A) and at atmospheric pressure (B).....	5
Scheme 1.4. Examples of common MALDI matrices.	7
Scheme 1.5. Schematic representation of ESI.....	11
Scheme 1.6. Schematic representation of TOF analyzer in both linear and reflectron detection modes.	14
Scheme 1.7. Schematic representation of a quadrupole analyzer.....	15
Scheme 1.8. Schematic representation of a linear quadrupole ion trap mass analyzer.....	16
Scheme 1.9. Schematic representation of the principle of FT-ICR MS.	17
Scheme 3.1. Schematic representation of the fundamental understanding of <i>inlet</i> ionization. SAI is displayed in the scheme by pipetting analyte solution right in front of the heated inlet tube linking AP and vacuum of the mass spectrometer.....	31
Scheme 3.2. Schematic representation of: (A) <i>Inlet</i> ionization methods that produce ions with the assistance of heat and vacuum drop, ionization occurs in the inlet tube of the mass spectrometer (B) <i>Vacuum</i> ionization methods the utilize proper matrix occurring by exposing to vacuum. (1) Laserspray ionization; (2) matrix assisted ionization; (3) solvent assisted ionization	35
Scheme 6.1. Pictures of the SAI source setup using (A) a single pipet, (B) an 8-channel pipet, (C) a 96-pipet array.....	78
Scheme 8.1. Schematic representation of the workflow of SAI and typical LC-tandem MS methods. (I) Half of the brain tissue section from drug-treated mouse was scraped off from the glass slide, the other half was preserved for surface analysis. (II) From the preserved tissue section, surface SAI was performed in (A) discontinuous mode and (B) continuous mode. (C) Typical sample work-up and analysis by either LC-ESI-MS/MS or SAI direct injection.	111

Table 3.1. Microscopic images of 3-NBN, coumarin and bronopol showing the sublimation of these matrices at room temperature and atmospheric pressure.34

Table 8.1. Amounts of clozapine quantified by typical LC-ESI-MS/MS and surface SAI in discontinuous mode.121

LIST OF FIGURES

- Figure 3.1.** LSII-MS spectrum of ubiquitin (MW 8570) using 2,5-DHAP matrix. The matrix/analyte mixture was ablated by (A) ultraviolet (B) visible and (C) infrared laser29
- Figure 3.2.** MS and MS/MS spectrum of myelin basic protein fragment (MW 1832) using by (A) LSII and (B) MAII using 2,5-DHAP as matrix, and (C) SAII using water with 0.1% formic acid as solvent.....31
- Figure 3.3.** Analysis of ubiquitin aqueous solution by cold ionization. (A) Picture of a 10 μ L ubiquitin aqueous solution spotted on dry ice and introduced into the cold extended inlet assisted by dry ice sublimation. (B) Mass spectrum of ubiquitin.....32
- Figure 4.1.** LSI-IMS-MS of angiotensin I (Ang. I) with 2,5-DHAP matrix using solvent-free sample preparation, a TSA approach: left panel (A) mass spectrum and right panel (B) 2-D plot of drift time versus m/z 44
- Figure 4.2.** LSI-IMS-MS of (A) non- β -amyloid component of Alzheimer’s disease (NAC) and (B) bovine insulin (BI) with 2,5-DHAP matrix using solvent-free sample preparation, a TSA approach: left panel (1) mass spectrum and right panel (2) 2-D plot of drift time versus m/z 47
- Figure 4.3.** Solvent-free mass spectra of angiotensin I obtained from (A) SYNAPT G2, a TSA approach, using a home-built desolvation device and 150 °C source temperature after using different grinding times and frequencies during homogenization of 2,5-DHAP matrix/angiotensin I...49
- Figure 4.4.** Microscopy images of liquid droplets produced by laser (N_2) ablation of (A) 2,5-DHAP and (B) 2,5-DHB matrixes after the material was ground for 30 s in the TissueLyser II.....51
- Figure 4.5.** LSI-IMS-MS of a mixture of angiotensin I and sphingomyelin with 2,5-DHAP matrix using the solvent-free sample preparation method, a TSA approach: left panel (A) mass spectrum and right panel (B) 2-D plot of drift time versus m/z53
- Figure 4.6.** LSI-IMS-MS of crude petroleum oil with 2,5-DHAP matrix using solvent-free sample preparation, a TSA approach: left panel (A) mass spectrum and right panel (B) 2-D plot of drift time versus m/z 55
- Figure 5.1.** Pictures showing the setup for LC-nSAII. Side view of MS inlet in which the tip of the fused silica capillary tube of the LC column is placed about 0.1 mm out of the orifice inlet entrance of the mass spectrometer (A) directly or (B) by use of a “PicoTip” attached to the end of the fused silica capillary tube.....68

Figure 5.2. LC-nSAII-MS/MS mass spectrum of 100 fmol μL^{-1} BSA tryptic digest with 1 μL injection at a flow rate of 800 nL min^{-1} using the setup shown in Figure 5.1(A).	69
Figure 5.3. nSAII-LC/MS base peak chromatograms of 10 fmol μL^{-1} BSA tryptic digest with 1 μL injection at a flow rate of 400 nL min^{-1} using the “PicoTip” extension shown in Figure 5.1(B).	70
Figure 6.1. A mixture of phosphorylated peptides was pipetted into the inlet. 1 μL of 2.5 pmol μL^{-1} solution was used for each acquisition. Mass spectra of the mixture were obtained in (A) positive acquisition mode at 150 °C and (B) negative acquisition mode at 400 °C.	78
Figure 6.2. Multiplexing SAII-MS using the 8-channel pipet at an inlet temperature of 150 °C. The analysis of 5 tips filled (3 μL) with 3 different samples with solvent (S) between each two samples. (A) Total ion chromatogram (TIC): (1) Mass spectra and (2) mapping of the location of individual analytes: (B) 2.5 pmol μL^{-1} leucine enkephalin (LE, m/z 556), (C) 1 pmol μL^{-1} galanin (Gal, m/z 1053), and (D) 1 pmol μL^{-1} ubiquitin (Ubi, m/z 1224).	82
Figure 6.3. Mapping using the 8-channel pipet. (I): (A) Schematic representation of content in each pipette tip. (B) The mapping of m/z 270 peak. (II): (A) TIC and (B) Mass spectra extracted from (1) 0.02 min, (2) 0.17 min, and (3) 0.34 min of the TIC.	83
Figure 6.4. SAII mass spectra of ubiquitin at inlet temperature of 250 °C. Solutions of 3 μL of 1 pmol μL^{-1} were introduced by (A) manually pipetting and (B) vacuum drawing.	84
Figure 6.5. SAII-MS using 84 tips mounted on a 96-well pipet tip holder with the inlet temperature at 250 °C acquired in ~5 min. (I) Total ion current. (II) Mass spectra of (A) 1 pmol μL^{-1} clozapine, (B) 2.5 pmol μL^{-1} leucine enkephalin, (C) 1 pmol μL^{-1} sphingomyelin, (D) 1 pmol μL^{-1} galanin, (E) 5 pmol μL^{-1} bovine insulin (in methanol:water with acetic acid), (F) 1 pmol μL^{-1} ubiquitin, and (G) 10 pmol μL^{-1} lysozyme.	86
Figure 6.6. Mapping of clarithromycin from tablet in a 384-microtiter plate using the 8-channel pipet. (I) Picture of loading tablet solution and pure solvent from microtiter plate to pipette. (II)(A) Schematic representation of content in each pipette tip. (B) The mapping of a major fragment at m/z 590.3.	88

Figure 7.1. Mass spectra of ubiquitin using 3-NBN as matrix obtained on the high vacuum MALDI source of the Apex FT-ICR mass spectrometer (A) without (MAIV) and (B) with the use of a laser (LSIV) for matrix:analyte ablation.....	96
Figure 7.2. Picture of MAIV operating on the ESI source of the Apex FT-ICR mass spectrometer.....	100
Figure 7.3. MAIV mass spectra of (A) +9 charge state of ubiquitin and (B) +10 charge state of lysozyme using 3-NBN as matrix obtained on the ESI source of the Apex FT-ICR mass spectrometer.....	102
Figure 8.1. Fast surface assessment using a SAI method employing surface extraction by 1 μL of MeOH in discontinuous mode. (A) TIC of the entire duration of sample analysis including exposure of solvent to surface to ionization in inlet. (B) Mass spectrum extracted from the TIC with the inset showing the isotopic distribution of protonated clozapine ions.....	115
Figure 8.2. Fast surface assessment using the SAI method employing surface extraction by 1 μL of MeOH in continuous mode. (A) TIC of the whole analysis for ~ 1.4 min. (B) SAI-CID-MS of the protonated clozapine ions (1) directly extracted from tissue surface and (2) from synthesized clozapine chemical solution.....	117
Figure 8.3. Calibration curves of clozapine (A) using SAI by pipetting standard clozapine:clozapine-d8 solutions at different concentration ratio with clozapine-d8 at 2 pmol μL^{-1} , signal intensity ratio is plotted against concentration ratio; and (B) using LC-ESI-MS/MS with standard clozapine solutions at different concentration, peak area of the fragment ion at m/z 270 is plotted against concentration.....	118
Figure 8.4. The right half of a 20 μm brain tissue section from drug-treated mouse was quantified by SAI method in discontinuous mode. Solution of 1 μL of each of the four standard clozapine:clozapine-d8 mixtures at different concentration ratios was used for surface extraction and then pipetted into the heated inlet of the mass spectrometer. Calibration curves were obtained by plotting the signal intensity ratio against the concentration ratio.....	120
Figure 8.5. 20 μm brain tissue sections from drug-treated and control mice were analyzed by MAIV operating at intermediate pressure. Solution of 0.5 μL 3-NBN/clozapine:clozapine-d8 mixture was spotted on the tissue section and the sample was loaded into the commercially available vacuum chamber. The intensity ratio was plotted against concentration ratio. Insets show the microscopy images of the matrix/clozapine:clozapine-d8 spotted on tissue section before and after MAIV analysis.....	122

Figure 8.6. Calibration curve obtained by spotting 4 μ L 3-NBN/clozapine:clozapine-d8 mixture on control mouse brain tissue sections. The glass slide holding the half-covered tissue was then sealed to the vacuum on a modified skimmer cone. Ion intensity ratio was plotted against concentration ratio. The inset shows a picture of the modified skimmer cone and a half-covered tissue section.....124

LIST OF ABBREVIATIONS

Ang I	angiotensin I
AP	atmospheric pressure
APCI	atmospheric pressure chemical ionization
API	atmospheric pressure ionization
APPI	atmospheric pressure photon ionization
ASAP	atmospheric solids analysis probe
BI	bovine insulin
BSA	bovine serum albumin
CHCA	α -cyano-4-hydroxycinnamic acid
CI	chemical ionization
CID	collision induced dissociation
CLA	clarithromycin
2-D	2-dimensional
DART	direct analysis in real time
DESI	desorption electrospray ionization
2,5-DHAP	2,5-dihydroxyacetophenone
2,5-DHB	2,5-dihydroxybenzoic acid
EI	electron ionization
ESI	electrospray ionization
ECD	electron capture dissociation
ETD	electron transfer dissociation
FAB	fast atom bombardment
FT-ICR	Fourier transform ion cyclotron resonance
Gal	galanin

IMS	ion mobility spectrometry
IP	intermediate pressure
LC	liquid chromatography
LE	leucine enkephalin
LIT	linear ion trap
LSII	laserspray ionization <i>inlet</i>
LSIV	laserspray ionization <i>vacuum</i>
Lys	lysozyme
MAII	matrix assisted ionization <i>inlet</i>
MAIV	matrix assisted ionization <i>vacuum</i>
MALDI	matrix-assisted laser desorption/ionization
MS	mass spectrometry
MW	molecular weight
<i>m/z</i>	mass-to-charge ratio
NAC	non- β -amyloid component of Alzheimer's disease
3-NBN	3-nitrobenzotrile
Nd:YAG	neodymium-doped yttrium aluminum garnet
nESI	nano-electrospray ionization
NMR	nuclear magnetic resonance
2-NPG	2-nitrophenol
nSAII	nano-solvent assisted ionization <i>inlet</i>
QqTOF	quadrupole time-of-flight
SAII	solvent assisted ionization <i>inlet</i>
SIMS	secondary ion mass spectrometry
SM	sphingomyelin

TIC	total ion chromatogram
TOF	time-of-flight
TSA	total solvent-free analysis
Ubi	ubiquitin
UPLC	ultrahigh performance liquid chromatography
UV	ultraviolet

CHAPTER 1

INTRODUCTION

1.1 Long-Term Goals

Analytical technologies for biological compounds have developed rapidly and become essential and indispensable in life science, pharmaceutical chemistry, clinical, and health care fields. For example, diseases are driven by molecular modifications in the cell, such as some cancers that result from the phosphorylational modification on amino acid residues of proteins.^{1,2} Analyses on the cellular levels is therefore important for disease diagnoses and treatment. In the real world, analysis of complex materials is difficult, mainly due to issues of sensitivity, dynamic range, solubility, and complexity.³ Brain tissue is an example of a complex material. It is composed of lipids, peptides, proteins, and carbohydrates, as well as other substances^{4,5} that build up the brain structure and maintain brain functions. There are also numerous exogenous species accumulating in brain tissue, such as drugs from disease treatment or drug addiction.⁶ In addition to the fact that the amount of lipids in cells is overwhelmingly higher than proteins,^{4,5} the structure diversity of lipids is much more significant than other compounds.^{7,8} Therefore the analysis of a compound of interest from a complex environment becomes more difficult.

A number of analytical technologies have been developed to analyze complex biological compounds in order to understand property/function relationships. To name a few, separation methods such as gas chromatography, liquid chromatography (LC), and thin layer chromatography were developed to separate components from complex mixtures, with the separation usually taking minutes to hours.^{9,10} Spectroscopy methods

such as ultraviolet-visible absorption spectroscopy is used to detect, identify and quantify atoms and molecules, but often lacks sensitivity and specificity.⁹ Nuclear magnetic resonance (**NMR**) spectroscopy elucidates structural information of organic compounds, but usually requires milligrams or milliliters of samples.¹¹ Immunoassays are commonly used in clinical analyses for targeted proteins and have high specificity, but the development of antibodies for this purpose is costly and time consuming.¹²

Mass spectrometry (**MS**) has a number of advantages for providing molecular information relative to other spectroscopic methods, has matched sensitivity and less cost for consumables than immunoassays while overcoming problems like cross-reactivity with metabolites, and achieving higher speed than traditional separation methods applicable for high-throughput analyses.⁹⁻¹⁵ The disadvantages of MS include the relatively costly instrumentation, lack of robustness, and requirement for trained operators and expertise.^{12,16,17} **Scheme 1.1** lists the challenges that need to be addressed to promote MS to have further practical utility, taking clinical analyses as an example.¹⁸ Higher sensitivity and dynamic range are required to observe all components from complex substrates.¹⁹ For example, signals from lipids often dominate the mass spectrum, while peptides, proteins, and small molecules may not be observable.^{20,21} Separation technologies prior to MS, e.g. LC-MS, can help to reduce the complexity and improve the dynamic range and specificity. Tandem MS with, for example, collision induced dissociation (**CID**) can improve specificity by requiring specific fragmentation transitions. This method can also provide structural information for e.g. peptides and drugs.^{22,23} Reproducibility and spatial resolution are desired for quantification and exact location, to differentiate e.g. the diseased tissue from the healthy area.²⁴ Data acquisition of MS for

rapid response in, for example, emergency rooms or surgical facilities need to be fast. The instrumentation and consumables should be financially affordable and simple to use.^{12,17} Therefore, MS has particular value in biological material characterization.

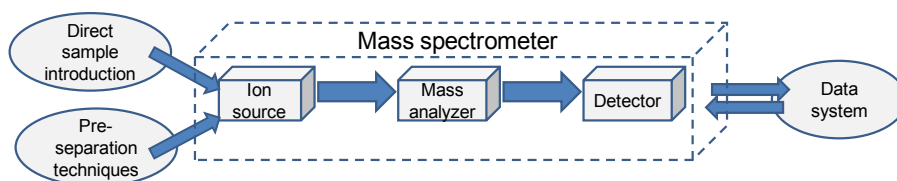
Scheme 1.1 Technology development needed to expand the use of MS for clinical applications [Adopted from Reference 18]. Points highlighted in red will be covered in this thesis.

- A. Sensitivity and dynamic range:** to observe *all* components (e.g., lipids and proteins, **hydrophilic and hydrophobic**, low and high abundance) directly from native and complex environment (e.g., **tissue**, plasma, serum, urine), improvements needed include:
- 1. Separation:** to deal with complexity and isoforms (**LC, mass resolution**, IMS)
 - 2. Specificity:** **fragmentation** (MS/MS: CID, ETD) for confirmation and ID (bottom up, top down)
 - 3. Reproducibility:** for **quantitation**
 - 4. Spatial resolution:** for **location** (with and without a laser)
- B. Speed:** of **data acquisition** and **interpretation**
- C. Robust, simple and cheap:** **automation, disposables**

1.2 General Introduction on Mass Spectrometry and Tandem Mass Spectrometry

The essential components of a mass spectrometer are the ionization source, the mass analyzer, and the detector (**Scheme 1.2**). Samples can be introduced into the ion source by direct sample introduction. Alternatively, complex materials can be passed through other separation methods prior to MS and then introduced via the interface, e.g. LC-MS to be discussed in **Section 1.3.2**. Analyte molecules are converted to gas-phase ions in the ion source; the ions are subsequently separated in the mass analyzer according to their mass-to-charge ratio (m/z) and are detected by the detector. The result is displayed as a mass spectrum of m/z versus relative ion intensity.

Scheme 1.2. Representation of the basic components of a mass spectrometer.



Tandem MS is used for the ions of interest to undergo a second or more mass spectrometric analysis. The ions at a certain m/z are selected (MS^1) and fragmented intentionally; the fragment ions are separated by the mass analyzer (MS^2). This process can be repeated several times for MS^n analysis. The intentional fragmentation is typically achieved by CID, electron-capture dissociation (**ECD**), or electron-transfer dissociation (**ETD**).²⁵ CID employs a collision gas (e.g. N_2 , He) to collide with the gas-phase analyte ions and results in fragmentation. For example, when a peptide ion encounters the collision gas, the peptide N-C bonds are cleaved so that smaller peptide fragments are analyzed to provide structural information. This is a harsh process that fragile sites, e.g. a phosphate group on a peptide, is easily cleaved off; on the contrary, ETD is a softer dissociation process that normally retains the phosphate group on the structure.²⁶ The radical anion of a small molecule, e.g. flouranthene, is generated and reacts with the analyte ions. The electron transfers from flouranthene to the analyte ion, and the excess energy obtained by the analyte ion leads to fragmentation. CID and ETD are frequently used in structural analysis such as peptide sequencing and proteomics.²⁶

This dissertation is focusing on ionization methods, and specifically coupling a novel ionization process with different mass analyzers. Therefore, a more detailed description of ionization methods and mass analyzers will be provided in the next sections.

1.3 Ionization for Mass Spectrometry

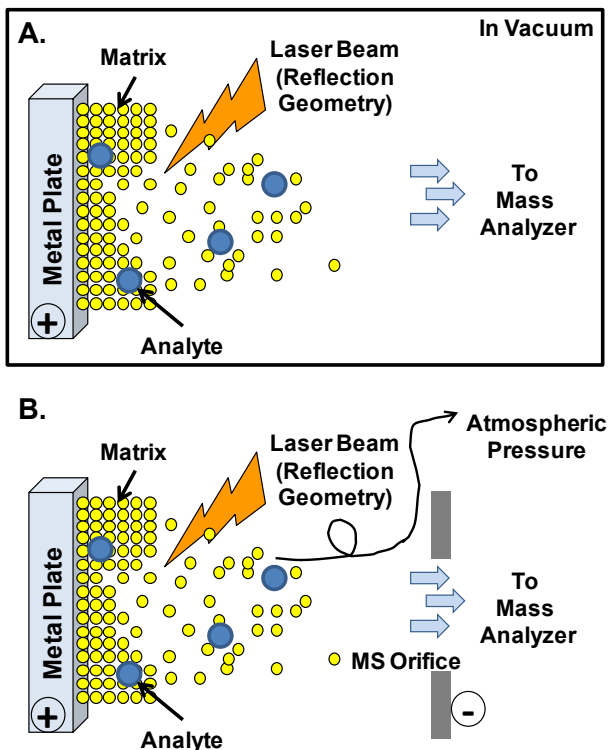
Any form of MS analysis can only occur when molecules are efficiently converted to gas-phase ions. Various ionization methods have been developed over decades. Early invented ionization methods include electron ionization (**EI**),²⁷ chemical ionization (**CI**),²⁸ fast atom bombardment (**FAB**),²⁹ secondary ion mass spectrometry (**SIMS**),³⁰ etc.

Matrix-assisted laser desorption/ionization (MALDI)^{31,32} and electrospray ionization (ESI),³³ developed during the 1980's, are currently the two most widely used “soft” ionization methods in MS and are capable of ionizing non-volatile compounds from biological materials. The inventors shared the Nobel Prize in Chemistry in 2002. This section focuses on the principles of operation, sample preparation, fundamental, and application aspects of MALDI, ESI, and a few ambient ionization methods.

1.3.1 Matrix-Assisted Laser Desorption/Ionization (MALDI)

MALDI was developed as a vacuum ionization method (**Scheme 1.3.A**) and has been extended to atmospheric pressure (**AP**) (**Scheme 1.3.B**).

Scheme 1.3. Schematic representation of the MALDI process in vacuum (**A**) and at atmospheric pressure (**B**).

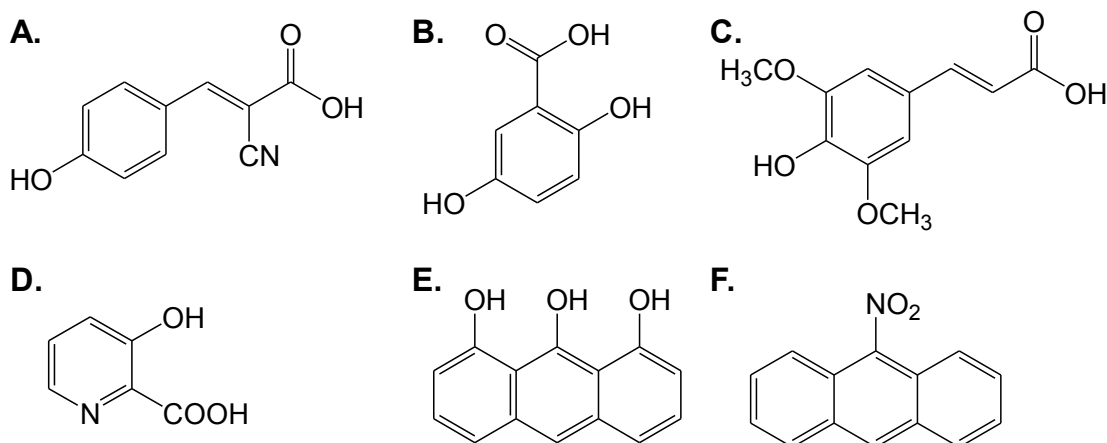


1) Vacuum MALDI

Traditional MALDI utilizes a ultraviolet (UV) laser in vacuum to ablate the surface of matrix:analyte crystals on a target plate in reflection geometry. The ions produced are accelerated by the voltage (~20 kV) applied on the target sample plate, and guided by focusing lens to the mass analyzer (**Scheme 1.3.A**). Initially, an inexpensive and smaller nitrogen laser was used in MALDI,^{30,31} but the laser repetition and life span is limited.³⁴ The demands of higher repetition rate and longer lifetime lasers in MALDI applications such as imaging and high-throughput are fulfilled by neodymium-doped yttrium aluminum garnet (**Nd:YAG**) lasers (wavelength ~355 nm, repetition rate >1000 Hz).³⁴ As can be seen in the scheme above, the particles do not leave the target surface at the same time, resulting in time dispersion of ions. Delayed extraction reduces the velocity distribution.³⁵ Before the extraction voltage is applied, the generated ions first pass through a field-free region, and after a short delay (normally below a millisecond), the extraction voltage is turned on for subsequent time-of-flight (**TOF**) analysis.

Solid organic compounds (shown in **Scheme 1.4**) are used as traditional UV-MALDI matrices. α -Cyano-4-hydroxycinnamic acid (**CHCA**), 2,5-dihydroxybenzoic acid (**2,5-DHB**), and sinapinic acid are commonly used for peptides and proteins, 3-hydroxypicolinic acid is for oligonucleotides, dithronal for polymers, and 9-nitroanthracene for fullerenes. The aromatic rings in these MALDI matrices absorb light at UV wavelengths.

Scheme 1.4. Examples of common MALDI matrices. (A) α -Cyano-4-hydroxycinnamic acid (CHCA), (B) 2,5-dihydroxybenzoic acid (2,5-DHB), (C) sinapinic acid, (D) 3-hydroxypicolinic acid, (E) dithranol, (F) 9-nitroanthracene.



Traditional solvent-based MALDI sample preparation uses dried-droplet or layer method for sample preparation.^{31,32} Homogenous crystals are ideal for MALDI sample preparation to avoid the “hotspot” issue. If the laser beam strikes at the hotspot, more ions are generated, thus resulting in poor reproducibility from shot to shot. The analyte and matrix should be soluble in respective solvents that are compatible with each other.

A solvent-free sample preparation method has been reported³⁶ as an alternative to overcome the difficulties with insolubility of analyte, e.g. with membrane proteins³⁷ and synthetic polymers.³⁸ The matrix powder is mixed with dried analyte at higher molar ratio, homogenized and transferred to sample holders by a mini ball mill device.^{36,37} This approach overcomes the hurdles of the solubility restrictions for traditional MALDI, and in some cases yields even better mass spectra than solvent-based methods,^{39,40} without the hotspot issue, but generally with lower sensitivity.⁴¹

Photoionization⁴² and cluster models⁴³ are the most commonly accepted ion formation mechanisms in MALDI.⁴⁴ In the photoionization model, the laser energy is

absorbed by the matrix, producing a plume about 10 μm above the sample surface, and generating primary ions. Analyte molecules react with the primary ions in the hot plume and become ionized by a charge transfer mechanism. In the cluster model, charged matrix/analyte clusters are produced upon laser firing, and the clusters are desolvated to produce analyte ions.

Dominant singly charged ions are formed from the solid state. For larger peptides and proteins, multiply charged ions can be produced with the matrix CHCA.⁴⁵ However, the ions are metastable and dissociate during travel through the analyzer.⁴⁶ The production of singly charged ions simplifies data interpretation in a straight-forward fashion. MALDI is commonly coupled with a TOF mass analyzer and will be discussed in more details in **Section 1.4.1**. New developments have involved coupling MALDI to other mass analyzers, e.g. quadrupole-TOF for tandem MS,⁴⁷ or FT-ICR for ultrahigh mass accuracy.⁴⁸ More details on mass analyzer will be introduced in **Section 1.4**.

MALDI is applicable to the ionization of a wide range of biological compounds such as peptides and proteins, lipids, carbohydrates, oligonucleotides, bacteria, etc., directly from solid surfaces.⁴⁹⁻⁵⁴ This merit enables MALDI for mass spectrometric imaging applications,^{55,56} which is a technique to visualize the spatial distribution of compounds by their m/z values. MALDI imaging can provide spatial information of peptides and proteins, lipids, metabolites, etc. directly from surfaces like tissue sections.^{55,57,58} Sample preparation is critical in MALDI imaging, especially matrix application to the surfaces.^{57,59} Progress including applying small matrix droplets⁶⁰ and subliming dry matrix onto the surfaces⁵⁷ has been made to reduce sample delocalization. The spatial resolution achieved by MALDI is typically $\geq 25 \mu\text{m}$.⁵⁵ Development of lasers is also

reported to achieve improved spatial resolution. Ablation areas with diameters $<10\ \mu\text{m}$ can be achieved by sophisticated laser focusing setup⁶¹ and at the expense of long acquisition time.⁶² MALDI imaging not only provides the location of the analyte of interest, but also the relative amount by color-coded display. Quantification has been reported by spotting internal standard on the tissue sections.^{63,64}

2) *AP MALDI*

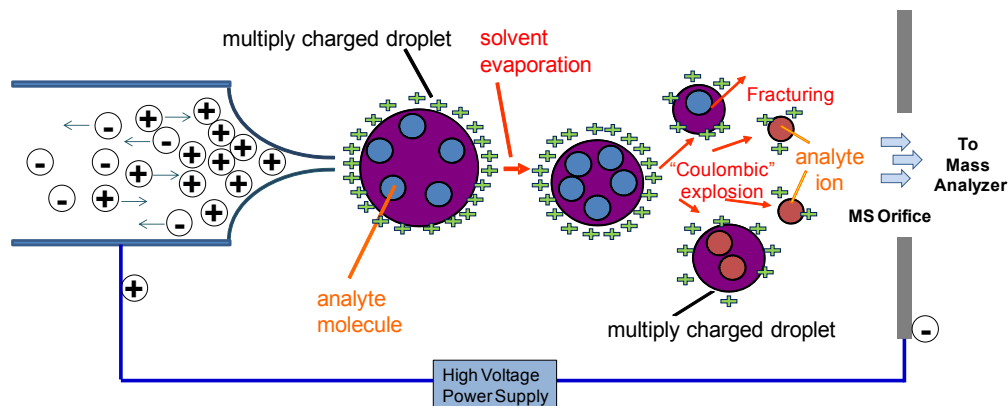
About one decade after the invention of vacuum MALDI, Burlingame and co-workers introduced MALDI to be operated at AP (**Scheme 1.3 B**).⁶⁵ With this configuration, common MALDI matrices (**Scheme 1.4**) and lasers can be used except that the target plate and laser ablation take place at AP.⁶⁶ AP MALDI greatly simplifies the operation procedure.⁶⁷ It is “softer” than vacuum MALDI because of the elimination of harsh vacuum conditions and lower acceleration voltage ($\sim 5\ \text{kV}$).⁶⁵ Galicia *et al.* have proposed laser ablation using transmission geometry to improve laser beam focusing and ion transmission.⁶⁸ The ionization efficiency of this approach was reported to be poor. In general, the ion efficiency and thus the sensitivity of AP MALDI is lower than vacuum MALDI because of the reduced ion transmission from AP to vacuum. It has been modeled that 99% of the ions formed are lost in AP MALDI.⁶⁹

The disadvantages of MALDI mainly include high chemical background resulted from the use of matrix in conjunction with a laser,⁷⁰ the production of singly charged ions limits the application of high-performance mass spectrometers, the high cost of commercial MALDI sources, and not being able to couple to online separation.

1.3.2 Electrospray Ionization (ESI)

In contrast to MALDI as a surface ionization method, ESI ionizes analyte from solution.^{33,71} **Scheme 1.5** presents the ionization process of ESI operating in positive ion mode. The analyte solution is sprayed through a metal capillary on which high voltage (a few kV) is applied. A “Taylor cone” is formed at the capillary tip and ejects charged droplets. The charged droplets undergo solvent evaporation and Coulombic explosion, producing bare analyte ions.^{33,72} The mechanisms for ion production currently accepted are the ion evaporation⁷³ and charge residue models.⁷⁴ The ion evaporation model suggests that ions are ejected from evaporating charged droplets.⁷³ The charge residue model suggests that the solvent evaporates from the charged droplets producing smaller charged droplets, leaving bare analyte ions after a few cycles.⁷⁴ The ions are subsequently extracted into the inlet of the mass spectrometer where a few volts of extraction voltage is applied. Negative ion mode is applicable by switching the potential on the spray capillary and extraction cone. Multiply charged ions are dominantly produced (from all but small molecules) by ESI that are beneficial for extending the mass range of high-performance mass spectrometers⁷⁵ and efficient intentional fragmentation for improved structural characterization.⁷⁶

Scheme 1.5. Schematic representation of ESI.



Because ESI directly ionizes analyte in solutions, it can be interfaced with separation techniques such as LC for online separation and analysis. The eluent eluting from the LC column is pushed through the electrospray capillary and the resulting gas-phase ions are introduced into the mass spectrometer. This coupling requires the solvent of the eluent to be “sprayable”. Proteomics is one of the most important applications to which LC-ESI can be applied.⁷⁷ After enzymatic digestion, large proteins are converted to peptides and smaller proteins. The peptide/protein mixture is separated by LC and then subsequently ionized by ESI. Tandem MS (CID and ETD) are commonly used to obtain sequence information.

Quantification of small molecules is another application typically achieved by LC-ESI-MS or tandem MS. The calibration curve is usually obtained by injecting a series of standard solutions at different concentrations, and the peak area of the ion of interest is plotted against concentration.

In some cases only very limited amounts of samples are available, e.g. a few μg protein can be obtained for mammalian proteomics.⁷⁸ LC and ESI⁷⁹ at nanoliter per minute flow rates are necessary for better separation and sensitivity when less material is consumed.⁸⁰ Ion efficiency is improved by nanoESI mainly due to the fact that smaller charged droplets are produced at the needle tip from which the solvent evaporates more rapidly in the time available. Therefore, the tip can be placed closer to the mass spectrometer orifice, resulting in higher ion transmission efficiency.⁸¹ However, the low flow rate will increase the time for analysis, and the fragile emitters for use in nanoESI with smaller diameters are considerably more expensive.⁸² The nanoESI capillary requires more user expertise for proper alignment and is prone to clogging.

1.3.3 Ambient Ionization

A variety of “ambient ionization” techniques have been developed that ionize samples from their original states, with little or no sample preparation.⁸³⁻⁸⁹ To name a few, direct analysis in real time (**DART**)⁸³ and atmospheric solids analysis probe (**ASAP**)⁸⁸ rapidly ionize materials by vaporizing them in the environment of heated gas (e.g. N₂ or He). Surface analysis methods based on desorption, e.g. desorption electrospray ionization (**DESI**)⁸⁵ and nanoDESI⁸⁹, ionize a large variety of compounds by spraying ESI solvent onto the surface while collecting the desorbed and ejected ions. Direct surface liquid-extraction has also been used for sampling followed by ESI.⁸⁶ Laser-based approaches⁹⁰⁻⁹³ have been introduced to combine the advantages of ESI and MALDI using solvent to collect laser-ablated materials from surfaces, and producing multiply charged ions. However, these AP ionization methods are subject to lower ion transfer efficiency due to the rim and dispersion losses as in ESI and MALDI.⁶⁹

1.4 Mass Analyzers for Mass Spectrometry

Once the molecules are converted to gas-phase ions, they are guided into the mass analyzer and separated according to their m/z . Vacuum is critical in mass analyzers to provide a longer mean free path. Better vacuum means less collision occurring between ions before they reach the detector. Currently oil based rotary and turbo pumps are commonly used to provide high vacuum in mass spectrometers ($<10^{-7}$ mbar).

Common mass analyzers are sorted by their principle of operation as follows: 1) TOF used to separate pulsed ion beams; 2) scanning mass analyzers such as magnetic sector and quadrupole to separate continuous ion beams; 3) linear ion trap (**LIT**) and triple quadrupole separate continuous ion beams and can also trap ions; 4) trapped-ion mass

analyzers such as Orbitrap, and Fourier transform ion cyclotron resonance (**FT-ICR**). These mass analyzers have different duty cycles, providing mass analysis with different mass accuracy and resolution, sensitivity, analysis speed, and mass range. But there is no “ideal” mass analyzer for all applications. The principle of operation, resolving power (defined as the minimum mass difference between two peaks is calculated as $m/\Delta m$ at the half-maximum peak height), mass range, and applications of several different analyzers that are used later in this dissertation, along with examples of hybrid mass spectrometers, will be discussed in more details in the following sections.

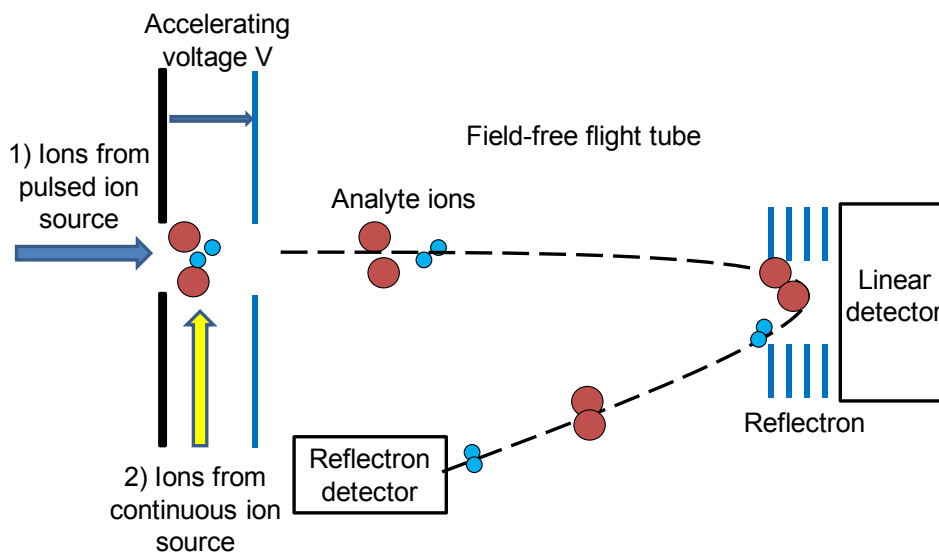
1.4.1 Time-of-Flight (TOF)

TOF analyzers use an electric field to accelerate ions, and the ions fly through a field-free tube to the detector (**Scheme 1.6**). The ions are accelerated based on their m/z with approximately the same kinetic energy. The time it takes for the ions to fly through the field-free tube and reach the detector is measured and converted to m/z of the ions. The heavier ions take longer time to reach the detector. It is necessary to let the ions start their flight at the same time, therefore TOF is usually coupled with a pulsed ionization method (e.g. MALDI). The continuous ion methods (e.g. ESI) employ orthogonal extraction to interface to TOF.⁹⁴ The orthogonal extraction uses a “pusher” to accelerate ions perpendicularly to their original direction and push them into the flight tube, so that a pulsed beam is produced from the continuous ion production.

In principle, the mass range for TOF is unlimited as eventually all of the ions get to fly through the flight tube.⁹⁵ TOF was introduced as a linear tube for ions to fly through a certain distance before being detected. Shown in **Scheme 1.6** is the TOF in both linear and reflectron ion detection modes, with the reflectron mode to achieve better mass

resolution of the smaller ions. The reflectron works as an ion mirror and is made of a set of grids on which potential is applied to change the directions of the ions. The use of a reflectron not only extends the distance for ions to fly, but also corrects the slightly different positions and velocity of ions with the same m/z . As a result, the mass resolving power of the TOF mass spectrometer is improved. It has been reported the mass resolving power of 80,000 at $m/z=2500$ was achieved by spiral TOF instrument.⁹⁶

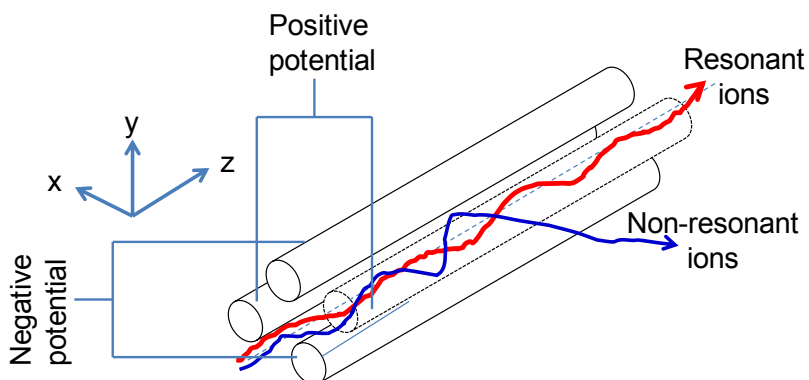
Scheme 1.6. Schematic representation of TOF analyzer in both linear and reflectron detection modes. The red circles represent “heavier” ions, and the blue ones are “lighter” ions. Ions are introduced through either 1) pulsed ion source or 2) a continuous ion source and are accelerated by orthogonal extraction.



1.4.2 Quadrupole

A quadrupole analyzer consists of four rods on which DC and AC voltages are applied (**Scheme 1.7**). Positive and negative potential is applied on the opposite pairs of rods, respectively. When ions enter the quadrupole analyzer in the z direction, only the ions with certain m/z that resonate with the RF voltage will oscillate and pass through the rods (red line), while others are filtered out (blue line).

Scheme 1.7. Schematic representation of a quadrupole analyzer. The red line represents the path of ions that pass through the rods, and the blue line represents the ions that do not pass through.



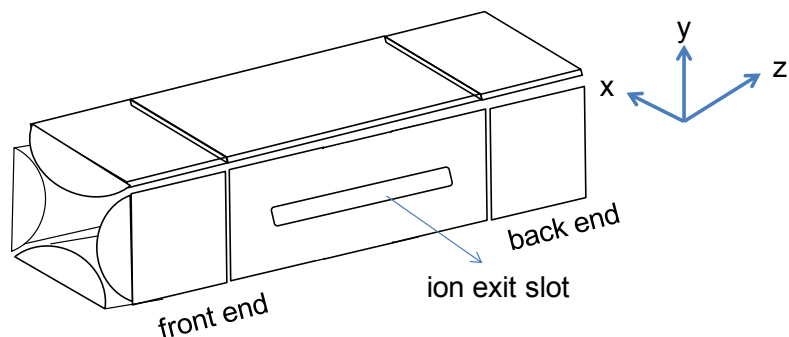
The quadrupole is a scanning mass analyzer thus it is not well suited to pulsed ionization method. The duty cycle for full scan is very low because only the ions at a certain m/z can be projected at a given time.⁹⁷

Three sets of quadrupole rods in a series (triple quadrupole mass spectrometer) can be used in tandem mass spectrometers. The first and third quadrupole serve as mass filters, and the center quadrupole works as the collision cell. The ions of interest are selected in the first quadrupole, fragmented in the second quadrupole, and the fragments are mass analyzed in the third quadrupole. Selected ion monitoring is achieved by fixing the RF and can provide 100% duty cycle. Therefore these are more sensitive and suitable for targeted analysis.⁹⁸

1.4.3 Linear Quadrupole Ion Trap (LIT)

An LIT consists of three sets of hyperbolically shaped rod electrodes similar to the quadrupole analyzer. The front and back ends are applied with higher potential that can trap ions within the quadrupole region (**Scheme 1.8**).

Scheme 1.8. Schematic representation of a linear quadrupole ion trap mass analyzer.



The LTQ Velos (Thermo, Bremen, Germany) is a commercial linear ion trap mass spectrometer used in most of the studies in this thesis. The scanning linear ion trap instrument offers fast scanning speed (typically 33000 amu/s) and improved sensitivity,⁹⁹ at the expense of mass resolving power⁹⁷ (e.g. 6000 at m/z 609¹⁰⁰). The mass range is up to m/z 4000 on the LTQ Velos.

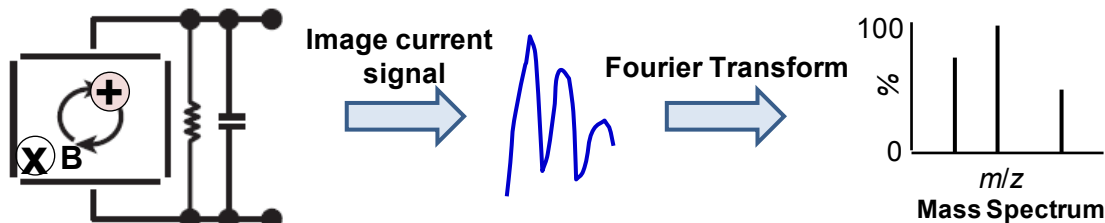
The capability of trapping ions enables LIT to be used for tandem MS. Collision gas for CID or radical anions for ETD can be introduced to the trap and react with analyte ions during gas-phase collisions for MS². Multiple stages of ion selection and fragmentation can take place in the trap, therefore ion trap can achieve MSⁿ for more thorough structural analysis.

1.4.4 Fourier Transform Ion Cyclotron Resonance (FT-ICR)

When an ion enters a magnetic field perpendicular to its original velocity direction, it will move in a circle by Lorentz force. The angular frequency is only dependent on the ion's mass, charge, and the magnetic field. The ions therefore will circulate in the cyclotron cell. The FT-ICR detects the ions based on the image currents the ions produce when they approach the electric plates. The time-domain current image is converted to

frequency-domain spectrum by Fourier transform, and the frequencies are subsequently converted to m/z values (**Scheme 1.9**).¹⁰¹

Scheme 1.9. Schematic representation of the principle of FT-ICR MS. Image current signals are obtained when the ions approach the electrode plate, and the signals are converted to a mass spectrum by Fourier transformation.



The FT-ICR mass spectrometer has the highest resolving power by far. The mass resolving power is over 400,000 at m/z 1000.¹⁰¹ However, the mass range is limited (e.g. m/z 400-2000 for optimal response) and it takes longer (~ 1 s) than other instruments to measure ions.¹⁰¹

1.4.5 Hybrid Mass Spectrometer

Quadrupole time-of-flight (**Q-TOF**) is an example of a hybrid mass spectrometer that combines mass analyzers for better performance and tandem MS capability. Q-TOF couples a quadrupole with a TOF analyzer. TOF has a higher duty cycle than the full-scan quadrupole, therefore Q-TOF is more sensitive than triple quadrupole except in the selected ion monitoring mode, and the reflectron TOF increases the mass resolving power at the same time.¹⁰²

The SYNAPT G2 (Waters, Manchester, UK) is a commercial hybrid quadrupole/ion mobility spectrometry (**IMS**)/orthogonal TOF mass spectrometer also used in the work reported herein. The configuration is similar to Q-TOF, but adds an IMS device between the quadrupole and TOF. Unlike MS, ions are separated according to their number of

charges, size, and shape.^{103,104} IMS-MS has advantages for extended dynamic range and the ability to separate isomeric compounds.^{105,106} The TriWave region also consists of a trap before the IMS cell and a transfer after it. Fragmentation for tandem MS is applicable in both trap and transfer regions.

1.6 Motivation

In all cases described in the previous section, ionization methods should be efficient to produce ions and simple to interface with mass spectrometers to utilize these advanced mass analyzer features. Advancement of MS towards the goal of more efficient ionization and simpler operation may be achieved through the development of new ionization methods. Ionization methods are discovered before and during my PhD period for which I contributed in some cases during the initial discovery phase and helped mass measurements, but will not be the main focus of this thesis. More details of the development, summary of the schemes, and fundamental understandings of these methods will be introduced in **Chapter 3**.

ESI-like ions can be produced by novel *inlet* and *vacuum* ionization methods. *Inlet* ionization methods include laserspray ionization *inlet* (**LSII**),^{75, 107, 108} matrix assisted ionization *inlet* (**MAII**),^{109, 110} and solvent assisted ionization *inlet* (**SAII**).^{111 - 114} Ionization process occurs in the heated inlet tube linking AP and the first stage of vacuum in a mass spectrometer. Solid matrix/analyte (LSII and MAII) or liquid analyte solution (SAII) is introduced into the heated inlet tube of the mass spectrometer with (LSII) or without (MAII and SAI) laser ablation. ESI-like multiply charged ions are produced by either method with sufficient ion abundance for MS and tandem MS analysis, without the use of voltage or nebulizing gas. *Vacuum* ionization, in analogy to LSII and MAII,

includes laserspray ionization *vacuum* (LSIV)^{115, 116} and matrix assisted ionization *vacuum* (MAIV).¹¹⁷⁻¹²⁰ Heat is not required in *vacuum* ionization. With the assistance of proper matrix and “softer” instrument settings (e.g. low or no laser power, sample plate voltage removed), multiply charged ions can be produced from surfaces in vacuum.

By the time I started my PhD research, multiply charged ions from peptides/proteins had already been observed by laser ablating a mixture of proper matrix and analyte from the solid state without using any voltage, but the mechanism of LSII was not yet clear. Predominantly solvent-based sample preparation was used, solvent-free preparation was only attempted with a vortexer that did not provide efficient homogenization.¹⁰⁸ Other new ionization methods were developed along the way with some limitations at the initial discovery stage. For example, the use of a silica tube to infuse analyte solution at the hotspot in the capillary tube is not applicable for fast and simple operations. The *inlet* ionization methods are beneficial to mass spectrometers equipped with heated inlet (e.g. LTQ Velos), but many high performance mass spectrometers (e.g. Apex II FT-ICR) do not have this feature. Fabrication of a heated capillary has been reported by attaching a copper tube to the skimmer cone of a SYNAPT G2 but is less analytically useful.¹²¹ No new ionization methods have been used for quantification. These limitations will be overcome or at least reduced as reported in this thesis.

1.7 Scope of This Dissertation

This dissertation presents the instrumental development, fundamental insights, and initial applications of the new ionization method developed by my colleagues and me, towards the potential to employ the novel ionization process for their rapid, robust, and simple-operated analyses during the course of the work described here.

Chapter 2 describes the general experimental procedures including materials, sample preparation, instrumentation, data acquisition, software, etc. used during this research. More detailed experimental sections relevant to each chapter are included in individual chapters.

Chapter 3 briefly states the history of novel ionization method development. *Inlet* and *vacuum* ionization is introduced in more detail in this chapter, along with mechanistic discussions. Our initial understanding of the unprecedented mechanisms of ion production will be revealed in this chapter.

Chapter 4 presents a total solvent-free analysis approach using LSII-IMS-MS to analyze both hydrophobic and hydrophilic compounds. The total solvent-free analysis consists of solvent-free sample preparation and solvent-free gas-phase separation using IMS coupled with MS. This chapter reports the first example of highly charged peptide/protein ions to be produced in MS from solid state without using solvent during either sample preparation or separation. TissueLyzer and grinding beads are utilized to homogenize dry matrix compounds with dried analytes. Factors such as temperature, and homogenization frequency during sample preparation, and thermal requirements for different matrices, are investigated to discuss the multiple charging results.

Chapter 5 reports the construction of a simple and convenient instrumental setup to couple LC at very low flow rates (as low as 400 nL min^{-1}) with SAI. In contrast to ESI, it was demonstrated that no voltage or extra connection is required to interface LC to MS. Data dependent tandem MS is also shown in this chapter for rapid sequence analysis of BSA digested peptides achieved by SAI-CID. Comparable sensitivity to ESI is achieved by this SAI method with much less effort.

Chapter 6 reports the development of instrumentation and methods that allow multiplexing of a variety of molecules, including small drugs to larger protein. With the assistance of heat applied to the inlet tube, 42 samples of 7 analyte solutions in 6 cycles were analyzed within 5 min under the same inlet temperature. As a proof of principle, the sample holder was carried by an x,y-stage for automation. For convenient observation and fast analysis, the sample locations were mapped using the m/z of the ions by imaging software so that the content of each solution and relative abundance can be visually displayed. The map can provide the m/z for signal identity, tandem MS for specificity, and signal intensity for relative amounts of certain compounds in different wells of the 96-well sample holder.

Chapter 7 presents the development of matrix assisted ionization *vacuum* to FT-ICR mass spectrometer to establish the capability of ultrahigh performance mass measurements. Over 400,000 mass resolving power was achieved for proteins at m/z 800. Both the MALDI and ESI source on the commercial dual-source instrument were used. Multiply charged ions of peptides and proteins are produced in the MALDI source without firing the laser, and on the ESI source without voltage, sheath gas, or heat.

Chapter 8 describes the development of simple and rapid surface assessment methods to quantify a schizophrenia drug from brain tissue sections of a drug-treated mouse. The material can be extracted either by solvent and subsequently transferred to the heated inlet (SAII), or by proper matrix when exposing the partially matrix-covered tissue section to vacuum (MAIV). Compared to the traditional quantification method, LC-ESI-MS/MS, similar results were obtained by SAII but at a much faster speed (a few minutes for SAII and over an hour for LC-ESI-MS/MS). MAIV is slower but is

independent of a heated inlet and more reproducible due to the continuous ion production.

Both sampling methods demonstrate that only the material from the surface was extracted, independent of the tissue thickness.

CHAPTER 2

MATERIALS AND INSTRUMENTATIONS

2.1 Materials and Sample Preparation

The analytes and matrices were purchased from Sigma Aldrich (St. Louis, MO) unless otherwise noted. Angiotensin I and non- β -amyloid component of Alzheimer's disease (NAC) were obtained from American Peptide Co. (Sunnyvale, CA), trypsin-digested BSA MS standard (CAM-modified) was purchased from New England BioLabs Inc. (Ipswich, MA, USA), sphingomyelin was from Avanti Polar Lipids, Inc. (Alabaster, AL), clozapine and clozapine-d8 were from Santa Cruz Biotechnology (Santa Cruz, CA). Leucine enkephalin was provided by Waters Co. (Milford, MA). N-acetylated myelin basic protein fragment from Anaspec (Fremont, CA), and phosphopeptide standard I was from Protea Biosciences (Morgantown, WV). 3-NBN was from Tokyo Chemical Industry Co., Ltd. (Portland, OR). Solvents were obtained from Fisher Scientific Inc. (Bremen, Germany) unless otherwise stated. HPLC grade water was purchased from EMD Chemicals (Gibbstown, NJ). Microscopy glass slides were obtained from Gold Seal Products (Portsmouth, NH).

Stock solutions of peptides and proteins were prepared by dissolving them in water as 1 mg mL⁻¹ concentrations. The stock solution of bovine insulin was in a 49.5:49.5:1 MeOH:water:acetic acid solution. Lipids were in methanol, and clozapine was in ethanol. Peptides and proteins were diluted to desired concentration by water or 50:50 ACN:water, with or without 0.1% formic acid. Lipids were diluted by MeOH with 1% acetic acid. Clozapine was diluted by water. The matrices were prepared by dissolving 5 mg of each matrix in 100 μ L 50:50 ACN:water unless otherwise stated.

For solvent-based analysis, the samples were prepared by either the droplet method or layer method. In the droplet method, the analyte and matrix solutions were mixed in 1:1 volume ratio, and 1 μL was spotted on the sample holder (glass slide or MALDI plate) and allowed air dry. In the layer method, 1 μL analyte solution was spotted on the sample holder first, followed by 1 μL matrix solution and mixed with the pipet tip. For solvent-free analysis, 10 μL analyte solution was dried overnight in a PCR tube placed in the Biodryer, containing 3 stainless steel beads; a spatula tip-full (amount not critical) 2,5-DHAP powder was added to the dry analyte. Then the dry mixture was homogenized and transferred onto the glass slide by TissueLyzer using frequencies 5-25 Hz for 2-10 min. More details about solvent-free sample preparation can be found in **Chapter 4**.

Mouse Brain Tissue – Mouse brain tissue sections were provided by Prof. Ken Mackie and Dr. James Wager-Miller from Indiana University. They were cut with a cryostat and mounted on microscopy glass slides. Briefly, mice were injected intraperitoneally with 50 mg kg^{-1} clozapine and sacrificed 60 minutes post-dosing with isoflurane overdose followed by perfusion of 20 mL of ice cold phosphate buffered saline. Brains were rapidly removed and frozen. Tissue sections were sliced on a Cryostat (Leica) to 10 or 20 μm thicknesses and sections were stored at $-80\text{ }^{\circ}\text{C}$ prior to analysis. All animal procedures were approved by the Indiana University Bloomington Institutional Animal Use and Care Committee.

2.2 Instrumentation

2.2.1 Mass Spectrometers

LTQ Velos. On the mass spectrometers that are commercially equipped with an inlet tube, e.g. LTQ Velos (Thermo Scientific Inc., Bremen, Germany), the temperature of the

inlet was directly heated from 50 °C to 450 °C. The ESI source housing was removed and the interlock was overridden so that free access to the inlet orifice was available. Helium gas was used for collision induced dissociation (**CID**), and a mixture of ultrapure helium and nitrogen (25% helium and 75% nitrogen; purity ~99.995%) was used as the reaction gas for electron transfer dissociation (**ETD**). Fluoranthene was used as electron reagent for ETD. Both positive and negative ion mode were used with the following settings: the Auto Gain Control was on, maximum injection time was 20 ms, and each mass spectrum was obtained by summing up 5 microscans. The sheath gas, aux gas, sweep gas, and capillary voltage were all set at 0. S-lense was 65%. Mass range was set to 'normal', scan rate was 'normal', and scan time was 'full'. Xcalibur 2.1.0 was used for data analysis.

For ESI, the commercial housing was used. The capillary voltage was set at 2.5-4 kV, depending on the solvent system. Sheath gas around 10. CID was performed for ESI-MS/MS experiments.

SYNAPT G2. On those mass spectrometers that are not equipped with an inlet tube that can be heated, e.g. SYNAPT G2 (Waters, Manchester, UK), the skimmer cone can only be heated up to 150 °C and is not efficient for *inlet* ionization methods. Therefore, a capillary was attached to the skimmer cone to help desolvation. The source temperature was held at 150 °C, and the nichrome wire which wrapped the copper tube around was connected to a Variac for additional heat. More details about fabricating the inlet capillary can be found in **Chapter 4**.

The SYNAPT G2 was operated in positive and resolution modes. The sample cone was set at 40 V and the extraction cone was 4 V. The scan time was set at 1 sec. Nitrogen gas was used for drift time separation at a flow of 22 mL min⁻¹. The IMS wave velocity

was 650 m s^{-1} and wave height of 40 V. The pressure of the drift cell was 3.2 mbar. MassLynx 4.1 and DriftScope ver. 2.1 (Waters Corp., Manchester, UK) were used for data analysis.

FT-ICR. An Apex II FT-ICR mass spectrometer (Bruker, Bremen, Germany) was used for MAIV and LSIV as the application of novel ionization methods on high-performance instruments to take advantage of its ultra-high mass resolving power. The dual MALDI/ESI source was used. For MAIV measurements, the laser fluence was set to 0, and the laser beam was blocked with paper. Voltage on the sample plate (240 V-300 V) was applied to assist lifting up ions. For LSIV measurements on the FT-ICR mass spectrometer, ubiquitin was combined with 2-NPG. The arbitrary laser fluence was 50%, and the plate voltage was 400 V.

MAIV from AP was performed on the dual MALDI/ESI source. The ESI source, the cover, and the cap over the ESI capillary were removed for direct access to the orifice of the ESI capillary. The capillary voltage, spray shield, nebulizing gas flow, and dry gas flow were all set to 0, and no override was necessary for operation. No added heat was applied to the ESI capillary.

2.2.2 Ultrahigh Performance Liquid Chromatography (UPLC)

A Waters Corporation NanoAcquity UPLC was used. Columns used include a Waters $100 \mu\text{m} \times 100 \text{ mm}$ BEH130 C18 column with $1.7 \mu\text{m}$ particles, and a Waters $1 \text{ mm} \times 100 \text{ mm}$ BEH 130 C18 column with $1.7 \mu\text{m}$ particles.

Water and ACN were used as mobile phase, the gradient can be found in more details in **Chapters 5 and 8**.

2.2.3 Other Equipments

Microscopy. Optical microscopy (Nikon Eclipse LV100) was performed to observe droplet production upon LSII, and to determine the analyzed area in surface SAI for clozapine quantification. The microscope was operated at 5x magnification.

Automated x,y-stage. A computer-controlled automated x,y-stage (Newmark Systems, Mission Viejo, CA) was used to carry and move sample holders in front of the mass spectrometer.

2.2.4 Other Software

BioMap 3.7.5.6 imaging software (Novartis Institution for Biomedical Research, Basel, Switzerland), typically used for imaging applications, was incorporated to map in which solution analyte was present as determined by the m/z ratio values obtained by MS or MS/MS. Besides mapping the location of analyte, the software allows relative concentrations to be displayed by color code. Thermo XCalibur .RAW files were converted to .IMG files using customized imaging software.

CHAPTER 3

FUNDAMENTAL UNDERSTANDING

Ionization methods are discovered before and during my PhD period. In some cases I have contributed during the initial discovery phase. This chapter focuses on a brief history of new ionization methods development and our current understanding of the mechanistic aspects of the novel ionization process. The experiments I participated in which led to the discovery and understanding so the relevant mechanism are included in this chapter. Figures and schemes are adopted from my co-authored publications from my contribution as follows:

Inutan, E.D.; **Wang, B.**; Trimpin, S. Commercial Intermediate Pressure MALDI Ion Mobility Spectrometry Mass Spectrometer Capable of Producing Highly Charged Laserspray Ionization Ions. *Anal. Chem.* **2010**, *83*, 678-684.

Trimpin, S.; **Wang, B.**; Inutan, E.D.; Li, J.; Lietz, C.B.; Harron, A.; Pagnotti, V.S.; Sardelis, D.; McEwen, C.N. A Mechanism for Ionization of Nonvolatile Compounds in Mass Spectrometry: Considerations from MALDI and Inlet Ionization. *J. Am. Soc. Mass Spectrom.* **2013**, *23*, 1644-1660.

Trimpin, S.; **Wang, B.**; Lietz, C.B.; Marshall, D.D.; Richards, A.L.; Inutan, E.D. Inroads to New Ionization Processes for Use in Mass Spectrometry. *Crit. Rev. Biochem. Mol. Biol.* **2013**, *48*, 409-429.

Chakrabarty, S.; Pagnotti, V.; **Wang, B.**; Trimpin, S.; McEwen, C.N. Ionization from Ice in Mass Spectrometry and a Possible Connection to Thunderstorms, *Anal. Chem.* **2014**, *86*, 7343-7350.

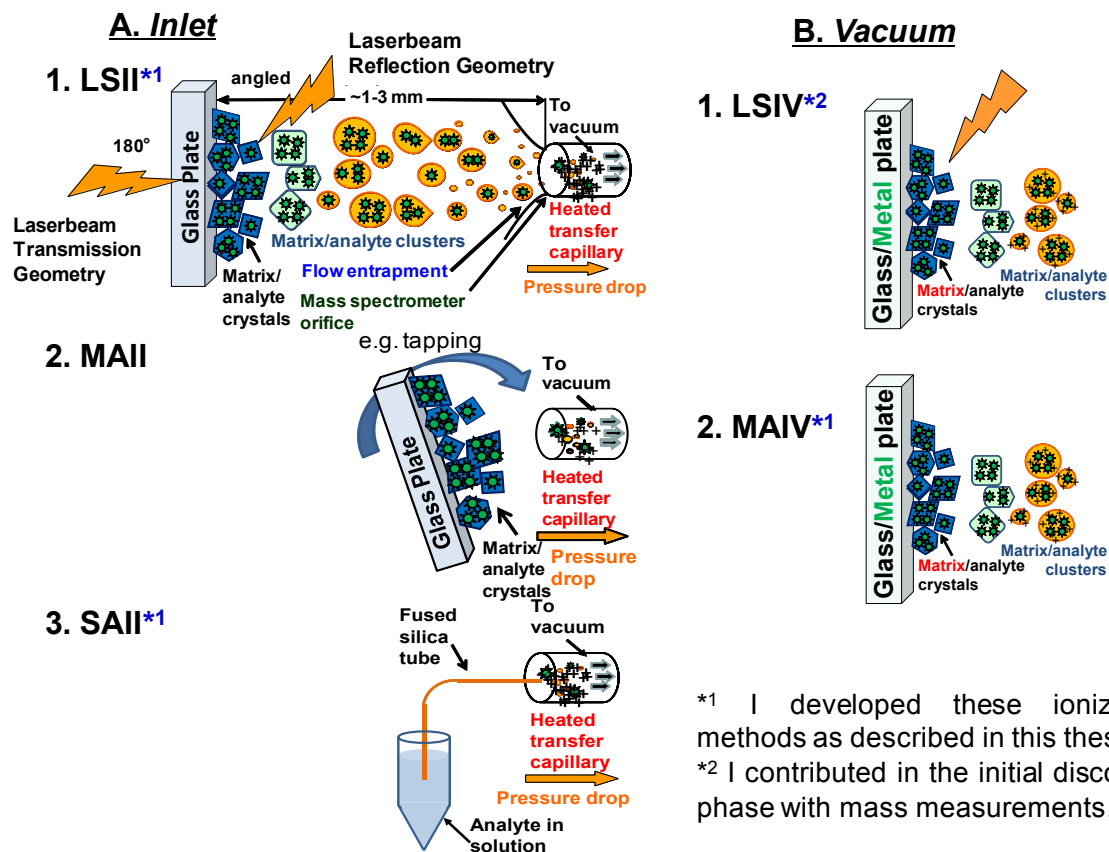
Trimpin, S.; Lutomski, C. A.; El-Baba, T. J.; Woodall, D. W.; Foley, C. D.; Manly, C. D.; **Wang, B.**; Liu, C.; Harless, B. M.; Kumar, R.; Imperial, L. F.; Inutan, E. D. Magic matrices for ionization in mass spectrometry. *Int. J. Mass Spectrom.* **2014**, doi: 10.1016/j.ijms.2014.07.033.

Trimpin, S.; **Wang, B.** Inlet and Vacuum Ionization from Ambient Conditions, in: *Ambient Ionization Mass Spectrometry*, Royal Society of Chemistry, by Eds. Marek Domin and Robert Cody, **2015**, 423-444.

Reprinted with permissions from American Chemical Society, Springer Science and Business Media, Informa Healthcare, Royal Society of Chemistry, and Elsevier.

Newly discovered ionization methods at their initial developed phase are summarized in **Scheme 3.1**. The left column represents *inlet* ionization and right column for *vacuum* ionization. These methods will be introduced respectively in the following sections.

Scheme 3.1. Schematic representation of: **(A)** *Inlet* ionization methods that produce ions with the assistance of heat and vacuum drop, ionization occurs in the inlet tube of the mass spectrometer **(B)** *Vacuum* ionization methods the utilize proper matrix occurring by exposing to vacuum. **(1)** Laserspray ionization that employs laser ablation to remove matrix/analyte mixtures from sample holder such as a glass slide; **(2)** matrix assisted ionization of which samples are introduced by mechanical force or matrix sublimation; **(3)** solvent assisted ionization that utilizes solvent instead of organic compounds as matrix. [Modified from 18]



3.1 Inlet Ionization

LSII was developed to use a UV laser to dislodge the solid analyte/matrix mixture from the sample plate and transfer it into the heated inlet.^{75,107,108} The matrices were first thought to have similar features in MALDI that they require an aromatic benzene ring to absorb UV laser energy. However, if the same matrix/analyte mixture (e.g. 2,5-DHAP/ubiquitin mixture) is ablated by UV, visible, and infrared laser respectively (**Figure 3.1**), similar mass spectra are produced indicating that LSII operates with a different mechanism than MALDI.¹²²

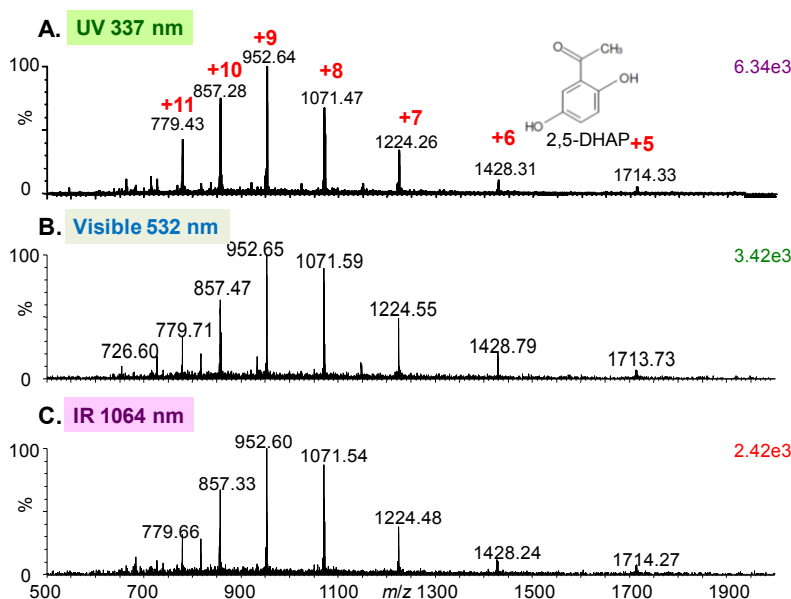


Figure 3.1. LSII-MS spectrum of ubiquitin (MW 8570) using 2,5-DHAP matrix. The matrix/analyte mixture was ablated by (A) ultraviolet (B) visible and (C) infrared laser at different wavelengths and produced similar ions. The numbers on the right top corner denote ion abundances. [Adopted from 122]

Based on this observation, mechanical force, instead of laser ablation, can be employed to introduce analyte/matrix mixture to the heated inlet.^{109,110} SAI is a liquid sample introduction method that does not require organic compound as matrix and directly infuses analyte solution into the heated inlet.¹¹¹ In all cases, the super heating of

the inlet tube is required as well as the pressure drop from AP to the first stage of vacuum of the mass spectrometer.¹²² Depending on the matrix (solid or solvent), up to 450 °C may be required for good analyte ionization.^{110,122} In contrary to traditional ionization methods such as MALDI and ESI as described in **Chapter 1**, no voltage is used in *inlet* ionization. The ionization source of *inlet* ionization is the heated inlet tube in the mass spectrometer.¹⁸ Gas-phase ions are produced when compounds, preferably in a matrix or solvent, pass through a heated tube linking the first vacuum stage of a mass analyzer with AP.¹²²

A unified mechanism was proposed for all three *inlet* ionization methods shown in **Scheme 3.2**.¹²² When matrix/analyte (organic matrix/analyte droplets or particles for LSII and MAII, solvent/analyte solution for SAII) enter the heated inlet tube, heat and the pressure drop result in charge separation that may be caused by superheating and bubbling carrying away surface charge into small droplets.¹²³ Millions of charges can be generated from charge separation. In this mechanism, the progeny droplets will have opposite charge from the remaining parent droplet. The charged droplets undergo solvent evaporation and coulombic fission. They also collide with the inner walls of the inlet tube and with each other, and finally matrix/solvent evaporation producing bare gas-phase analyte ions.¹²² It was proposed by Vestal in 1983, before the invention of MALDI or ESI, that ions are produced from charged clusters.¹²⁴ This solvent removing process is similar to ESI after the analyte solution is sprayed from the ESI capillary, but in *inlet* ionization ions are produced without applying any voltage or nebulizing gas.

Therefore, similar ions can be produced as long as the mixture of matrix (solid or liquid) and analyte are transferred into the heated inlet tube, and it does not matter if a

laser or organic matrix is used.¹²⁵ **Figure 3.2** shows the mass spectra of the myelin basic protein fragment peptide introduced to the instrument by LSII, MAII, and SAII, respectively. Identical mass spectra were produced. ETD was performed to the quadruply charged ions, and similar sequence coverage was obtained with all three methods (**Figure 3.2.B**).

Scheme 3.2. Schematic representation of the fundamental understanding of *inlet* ionization. SAII is displayed in the scheme by pipetting analyte solution right in front of the heated inlet tube linking AP and vacuum of the mass spectrometer.

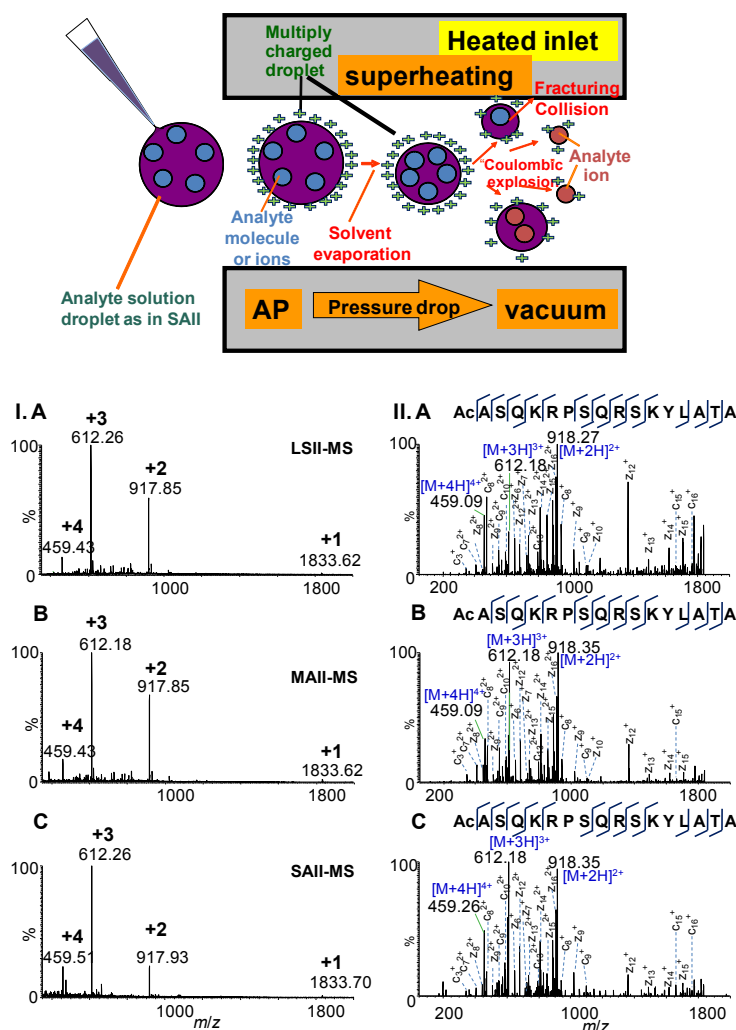


Figure 3.2. MS and MS/MS spectra of myelin basic protein fragment (MW 1832) by (A) LSII and (B) MAII using 2,5-DHAP as matrix, and (C) SAII using water with 0.1% formic acid as solvent. In all cases, the inlet temperature was held at 250 °C. [Adopted from 125]

Charge separation also occurs from freezing water droplet (**Figure 3.3**).¹²⁶ Charged particles are produced and ejected from frozen droplet surfaces by surface splintering. The sublimation of dry ice helps surface splintering and can produce highly charged protein ions directly from a frozen droplet of analyte aqueous solution. An extended inlet was used and wrapped by ice bags to assist cold ionization. Up to +10 charge state was observed from ubiquitin in aqueous solution.

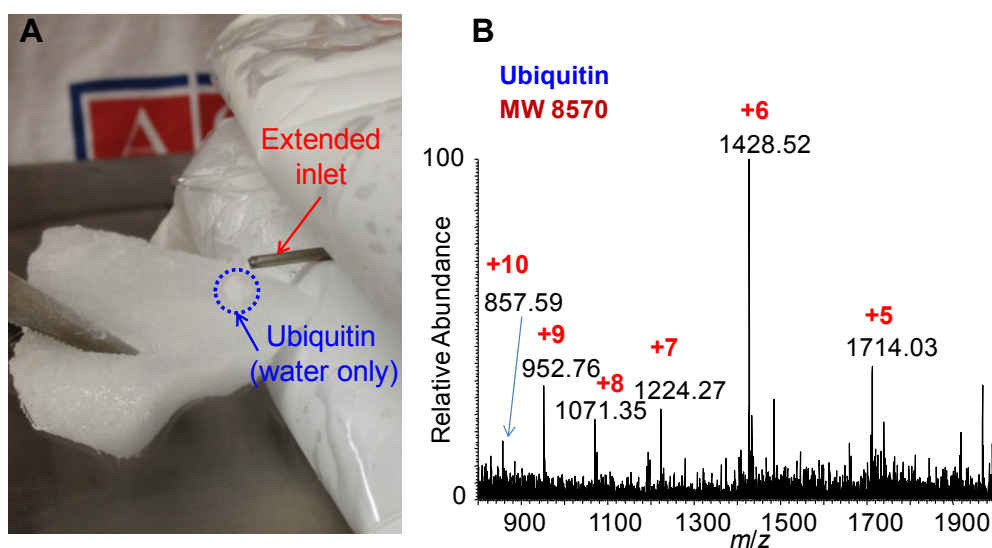


Figure 3.3. Analysis of ubiquitin aqueous solution by cold ionization. (A) Picture of a 10 μL ubiquitin aqueous solution spotted on dry ice and introduced into the cold extended inlet assisted by dry ice sublimation. (B) Mass spectrum of ubiquitin.[Adopted from 126]

Instruments such as the LTQ Velos have a heated inlet that benefits *inlet* ionization, but many high-performance mass spectrometers are not equipped with commercial heated inlet. If the proposed mechanism is correct – that ions are produced from charged analyte/matrix clusters, more volatile matrix compounds will efficiently evaporate or sublime from charged analyte/matrix droplets or particles in the presence of vacuum and without added heat. With such a matrix, it would be necessary to have a means of producing the charged particles.

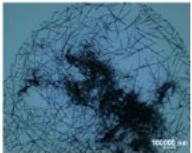
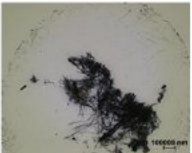
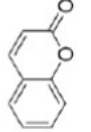
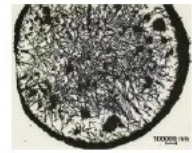
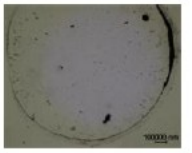
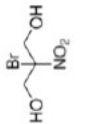
3.2 Vacuum Ionization

With the proper matrix with a low thermal requirement to produce LSII ions, e.g. 2,5-DHAP, and “soft” instrument parameters (low laser power and no plate voltage), ESI-like ions were first produced from a mixture of lipids, peptides, and proteins employing laser ablation on a commercial intermediate pressure (10^{-2} mbar) MALDI-IMS-MS instrument.¹¹⁵ Although there is no heated inlet or external thermal energy, a pressure drop is present inside the mass spectrometer, and absorption of the laser beam provides heat. In analogy to laserspray ionization *inlet*, the ionization occurring in the vacuum source is termed laserspray ionization *vacuum* (**LSIV**). More volatile matrices, e.g. 2-nitrophenol (2-NPG), can be used in high vacuum MALDI-TOF-TOF mass spectrometers of which the source is at even lower pressure (10^{-6} mbar).¹¹⁶

Among the volatile matrices, 3-nitrobenzotrile (**3-NBN**) sublimes in vacuum. When the analyte is exposed to the matrix and vacuum, multiply charged ions from peptides and proteins are produced without employing the laser or applying extraction voltage.¹¹⁷⁻¹²⁰ This method is termed matrix assisted ionization *vacuum* (**MAIV**) and produces ESI-like ions from a wide range of compounds such as drugs, peptides, lipids, and proteins. A number of novel matrices with different functionalities have been discovered to produce ions.¹²⁷ Interestingly, the crystal morphologies vary a lot according to the microscopy images. Their sublimation capabilities are quite different, too. Shown in **Table 3.1** are representative microscopy images of 3-NBN, coumarin, and 2-bromo-2-nitro-1,3-propanediol (bronopol) that sublime differently over 24 hour period. 3-NBN sublimed at room temperature and pressure in 3 h; coumarin was partially sublimed after a 24 h, but no observable sublimation occurred for bronopol. This method has been extended to

operate on slightly or non-modified ESI source to simplify the operation and improve throughput.¹¹⁹

Table 3.1. Microscopic images of 3-NBN, coumarin and bronopol showing the sublimation of these matrices at room temperature and atmospheric pressure. Images were taken right after spotting, 3 h, 6 h, and 24 h. [Adopted from 127]

Matrix	0 h	3 h	6 h	24 h
3-NBN 				Not observable after 24 h
coumarin 				
bronopol 				

CHAPTER 4

PRODUCING HIGHLY CHARGED IONS WITHOUT SOLVENT USING LASERSPRAY IONIZATION: A TOTAL SOLVENT-FREE ANALYSIS APPROACH AT ATMOSPHERIC PRESSURE

First examples of highly charged ions in mass spectrometry (**MS**) produced from the solid state without using solvent during either sample preparation or mass measurement are reported. Matrix material, matrix/analyte homogenization time and frequency, atmospheric pressure (**AP**) to vacuum inlet temperature, and mass analyzer ion trap conditions are factors that influence the abundance of the highly charged ions created by laserspray ionization (**LSI**). LSI, like matrix-assisted laser desorption/ionization (**MALDI**), uses laser ablation of a matrix/analyte mixture from a surface to produce ions. Preparing the matrix/analyte sample without the use of solvent provides the ability to perform total solvent-free analysis (**TSA**) consisting of solvent-free ionization and solvent-free gas-phase separation using ion mobility spectrometry (**IMS**) MS. Peptides and small proteins such as non- β -amyloid components of Alzheimer's disease and bovine insulin are examples in which LSI and TSA were combined to produce multiply charged ions, similar to electrospray ionization, but without the use of solvent. Advantages using solvent-free LSI and IMS-MS include simplicity, rapid data acquisition, reduction of sample complexity, and the potential for an enhanced effective dynamic range. This is achieved by more inclusive ionization and improved separation of mixture components as a result of multiple charging.

B. Wang, C. B. Lietz, E. D. Inutan, S. M. Leach, S. Trimpin, *Anal. Chem.*, **2011**, *83*, 4076-4084. Reprinted with permission from Copyright (2011) American Chemical Society.

4.1 Introduction

Mass spectrometry (**MS**) at atmospheric pressure (**AP**) is of analytical interest for reasons ranging from rapid data acquisition to sample analysis of biological materials under more physiologically relevant conditions.^{39,84,128} Unfortunately, the observation of high-mass singly charged ions is limited by the mass-to-charge (m/z) range of most high-performance mass spectrometers, a major drawback of AP matrix-assisted laser desorption/ionization (**MALDI**).⁶⁵ Laserspray ionization (**LSI**) MS is a newly introduced method capable of soft ionization of small and large molecules such as lipids, peptides, proteins, and other high-mass compounds by laser ablation at AP.^{75,107,108,121, 129 - 135} Advantages include small ablation areas/volumes, AP conditions, speed of analysis, and the production of multiply charged ions to extend the mass range of high-performance mass spectrometers. The ability to obtain multiply charged ions also provides enhanced fragmentation important for structural characterization. For example, sequence analysis by electron transfer dissociation (**ETD**) was obtained on a Thermo LTQ-ETD mass spectrometer providing nearly complete sequence coverage of ubiquitin and identified an endogenous peptide directly from mouse brain tissue.^{107,134}

LSI ions have been generated on commercial atmospheric pressure ionization (**API**) sources directly,^{75,107,129,130,131,133-135} after retrofitting with a home-built LSI desolvation tube,^{121,130,132} and by introducing LSI conditions on a commercial AP-MALDI source.¹⁰⁸ Initial solvent-free gas-phase separation results enabled by the ion mobility spectrometry (**IMS**) dimension showed the utility and benefits for the analysis of protein mixtures, even when isomeric, directly from surfaces.^{121,132} Recently, LSI has been extended to intermediate pressure (**IP**) MS applications, producing highly charged and high abundant

peptide and protein ions.¹¹⁵ These ions, especially in mixtures as complex as mouse brain tissue, are notably well-separated by IMS-MS using a solvent-based LSI approach.

Solvent-free sample preparation/ionization operates independent of analyte solubility,³⁸ a key advantage over any solvent-based MS method. Combined with solvent-free gas-phase separation using IMS-MS, this provides total solvent-free analysis (TSA) by MS.^{39,136} Potential advantages using solvent-free LSI and IMS-MS in a TSA approach include simplicity, rapid data acquisition, reduction of sample complexity, and enhanced effective dynamic range. Justifications for exploring solvent-free approaches relate to a number of factors that can be broadly defined as (i) the need to perform chemical analysis on molecules that are difficult or impossible to solubilize, known collectively as the “insolubelome”;¹³⁷ (ii) the need to avoid chemical reactions that can spontaneously change the structures of certain types of molecules when they are in solution; (iii) the need to address problems associated with extreme loss of certain analytes in solution during sample preparation; and (iv) the need to address diffusion of analytes within a complex matrix such as tissue sections for mass spectrometric imaging, where spatial distribution of analytes is a major variable in the analysis. The poorly soluble constituents of living organisms, such as membrane proteins, as well as hydrophobic compounds, such as lipids, metabolites, synthetic polymers, crude oil, and biofuels, need new analytical methods for their analysis.

Solvent-based LSI, similar to ESI, forms singly charged ions of lipids and low molecular weight peptides but for higher molecular weight biological and synthetic macromolecules produces highly charged ions.^{75,107,108,115,121,129-135} Using a laboratory vortexer¹³⁸ and 2,5-dihydroxybenzoic acid (**2,5-DHB**) as matrix, LSI was reported to

exclusively produce singly charged ions with solvent-free sample preparation and employing 350 °C on the heated inlet capillary of a Thermo Scientific Orbitrap Exactive mass spectrometer.⁷⁵ We show here the first examples that matrix/analyte materials combined in the solid state can produce abundant highly charged peptide and protein ions and, when in mixtures, are well-separated in the solvent-free gas-phase dimension provided by IMS because of the successful introduction of multiple charging. Further, pictorial “snapshots” of this TSA experiment using the dimensions of drift time and m/z suggest usefulness for rapid observation of changes in relative sample composition even in complex samples such as crude oil without the need of extensive optimization of sample preparation and separation.

4.2 Materials and Methods

Materials. Besides the general chemicals stated in **Chapter 2**, oils were obtained from a local store. Stainless steel beads (1.2 mm) were obtained from BioSpec Products, Inc., Bartlesville, OK, USA.

LSI Sample Preparation. Stock solutions were prepared as described in **Chapter 2**. For the peptide/lipid mixture, angiotensin I and sphingomyelin were premixed to a 1:1 volume ratio using the stock solutions.

Solvent-Free Sample Preparation. The matrix/analyte samples were simultaneously homogenized and transferred to the glass microscopy slide using the TissueLyser II (Qiagen Inc., 27220 Turnberry Lane, Valencia, CA, USA), similar to published procedures.^{139,140} Solutions of 10 μL of 772 $\text{pmol } \mu\text{L}^{-1}$ angiotensin I in water, 10 μL of peptide/lipid mixture in MeOH/H₂O, 3.26 μL of 307 $\text{pmol } \mu\text{L}^{-1}$ NAC in water, and 5.73 μL of 174 $\text{pmol } \mu\text{L}^{-1}$ bovine insulin in MeOH/H₂O with 1% acetic acid were used.

Identical to previous solvent-free preparation,^{37,41} the respective analyte samples were transferred to individual 0.2 mL PCR tubes containing three stainless steel beads and then evaporated in the Biodryer (BioSpec Products Inc., PO Box 788, Bartlesville, OK, USA) for 3 h to ensure complete dryness of the samples. The oil samples were prepared without solvent by pipetting 1 or 2 μ L of the liquid directly to the vial to be used for homogenization; waxy and oily materials were previously studied by solvent-free sample preparation protocols.^{36,138} After the samples were completely dry, except for the crude oil, a spatula tip amount (this is not a critical parameter) of 2,5-DHAP matrix was added into each tube, identical to the previously published procedures.^{139,140} The top opening of the tube was then covered by the microscopy glass slide and was firmly and securely placed in the TissueLyser II sample holder. Each set of sample was homogenized with the desired frequency and time. The matrix/analyte mixtures of angiotensin I, NAC, and peptide/lipid mixture were homogenized for 10 min at 25 Hz, while bovine insulin and oils were ground at 30 Hz.

Specific Study of Frequency and Time. Angiotensin I was homogenized with the 2,5-DHAP matrix for time periods of 2, 5, 10, and 20 min at grinding frequencies of 15, 20, and 25 Hz. To ensure the most identical matrix/analyte ratio composition, the mixture was ground for 2 min so that a reasonably homogeneous powder was obtained before removing the glass slide cover with matrix/analyte powder attached. The powdered matrix/analyte sample on the glass surface was then analyzed by LSI-IMS-MS. The remaining matrix/analyte sample in the tube was covered with a new glass slide and rehomogenized for another 3 min to prepare the sample with the second time point (5 min), and so on.

Specific Study of Temperature. Angiotensin I was homogenized with the 2,5-DHB matrix for 2 and 10 min and with 2,5-DHAP matrix for 10 min with a grinding frequency of 25 Hz. The homogenized matrix/analyte sample was initially analyzed by LSI-IMS-MS (SYNAPT G2) at 150 °C on the skimmer cone with and without additional heat applied on the home-built desolvation device described previously.¹²¹ To gain more accurate temperature values, we also analyzed the homogenized matrix/analyte sample on the Thermo LTQ Velos instrument equipped with the commercial desolvation device with accurate temperature readings. Temperatures of 40, 150, 275, and 400 °C were applied.

Solvent-Based Sample Preparation. The solvent-based sample preparation was carried out for comparison. To ensure the most direct comparison, homogenized matrix/analyte powder mixture that remained in each tube from the respective TSA experiment was used by adding 5 µL of 50:50 ACN/H₂O. The powder and solvent were stirred by a micropipet tip. Only some of the analyte/matrix mixture was dissolved, and approximately 4 µL of the saturated solution was transferred to the glass slides. After complete evaporation of the solvent, LSI-IMS-MS analysis was performed identical to the solvent-free prepared samples. Solvent-based crude oil sample was prepared by dissolving crude oil in 2:1 toluene/methanol mixture¹⁴¹ and then was premixed with 2,5-DHAP solution with a 1:4 volume ratio. Two times 2 µL of the crude oil/matrix mixture was spotted without drying between on the microscopy glass slide and then blow-dried at low heat. NAC and bovine insulin were prepared by solvent-based layer method similar to previous studies.¹³²

Laserspray Ionization. The nitrogen laser (Spectra Physics VSL-337ND-S, Mountain

View, CA, USA) was focused and aligned to the ion entrance of the SYNAPT G2 and LTQ Velos mass spectrometers as previously described.^{121,135} The fabrication of the desolvation device for the SYNAPT G2 was also described previously.¹²¹ Briefly, the exit end of a 3.175 mm o.d., 1.5875 mm i.d., 19.05 mm copper tube, which was wrapped with 24 gauge nichrome wire (Science Kit and Boreal Laboratories, Division of Science Kit, Inc., Tonawanda, NY, USA) and coated with Saureisen P1 cement (Inso-lute Adhesive Cement Powder no. P1) was securely attached to the ion entrance skimmer cone of the Waters Z-spray source by Saureisen cement. The source temperature was held at 150 °C, indirectly heating the copper desolvation device. To supply additional heat to the desolvation device, the nichrome wire was connected to a Variac (Powerstat, the Superior Electric Co., Bristol, CT, USA). With analyte/matrix samples facing the mass spectrometer, the glass slide was placed in front of the ion entrance of the desolvation device using the x,y,z stage of the nanolockspray source (SYNAPT G2) or manually (LTQ Velos) and was slowly moved through the focused laser beam aligned with the orifice in transmission geometry (180° with the ion entrance capillary) and focused ~2 mm from the orifice. For all studies using the laser, gloves and laser safe goggles were worn.

IMS-MS Instrumentation. The SYNAPT G2 HDMS (Waters Corporation, Manchester, UK) with a quadrupole having a high mass limit of m/z 8000 was used to perform LSI-IMS-MS analysis. The first generation of this instrument has been previously described.¹⁴² The instrument was operated in resolution mode at a cone voltage of 0 to 40 V and extraction cone of 4 V. The total acquisition time was set at 1 min, acquiring 1 mass spectrum per second. The flow rate of nitrogen, which was used

for drift time separation, was 22 mL min⁻¹. The IMS cell pressure was 3.13 mBar and in the Triwave region, wave velocity ranged from 450 to 650 ms⁻¹, and wave height from 30 to 40 V. DriftScope version 2.1 (Waters Corp., Manchester, UK) was used to plot and process the two-dimensional (2-D) data of drift time versus *m/z* using emerald forest and hot metal color backgrounds. For acquisitions without IMS, only the source and trap gases were on. Other parameter settings used were the same excluding the IMS settings.

LTQ-MS Instrumentation. The LTQ Velos (Thermo Fisher Scientific Inc., Fitchburg, WI, USA) was used to perform LSI-MS for the ion entrance capillary temperature-dependent studies. The API source housing of the instrument was removed.¹³³⁻¹³⁵ For the temperature-dependent studies, the total acquisition time was 1 min, summing three microscans using a maximum injection time of 50 ms for each acquired mass spectrum. The matrix/analyte produced by ablation directly enters the heated capillary of the mass spectrometer. The capillary temperature was set to 40, 150, 275, and 400 °C for the respective studies.

Microscopy. An optical microscope (Nikon, ECLIPSE, LV 100) was used to study the formation of liquid droplets in the LSI plume during the ablation of 2,5-DHAP and 2,5-DHB. Samples were prepared with the TissueLyser II as previously described in solvent-free sample preparation,^{139,140} but with the omission of analyte. The matrix was ground using 1.2 mm stainless steel beads and transferred to a glass slide using the TissueLyser II at a grinding frequency of 25 Hz. One batch of samples was ground for 30 s, and a second batch was ground for 10 min. The ablated plume from a single pulse of the 337 nm UV laser was collected on a separate glass slide for microscopy analysis. Additionally, a third batch of sample was created by a vortexer (Vortex-Genie 1 Touch

Mixer, Scientific Industries, Inc., Bohemia, NY, USA). Each matrix was ground in a PCR tube with three stainless steel beads for 30 s on the vortexer similar to published procedures.¹³⁸ The matrix was pressed onto a glass slide using a metal spatula to provide a thin coverage similar to previous protocols used with MALDI.^{36-38,41,138}

4.3 Results and Discussion

Method Development for the Production of Multiply Charged Ions of Peptides and Proteins by a Total Solvent-Free Analysis (TSA) Approach. Shown in Figure 4.1 is the analysis of angiotensin I using a TSA approach consisting of solvent-free sample preparation/ionization coupled to solvent-free gas-phase separation by IMS. In the extracted mass spectrum (**Figure 4.1A**), abundant signal intensities for both the doubly and triply charged ions are observed. There are no notable differences in the relative intensities of the charge state distribution of the multiply charged ions as compared to the

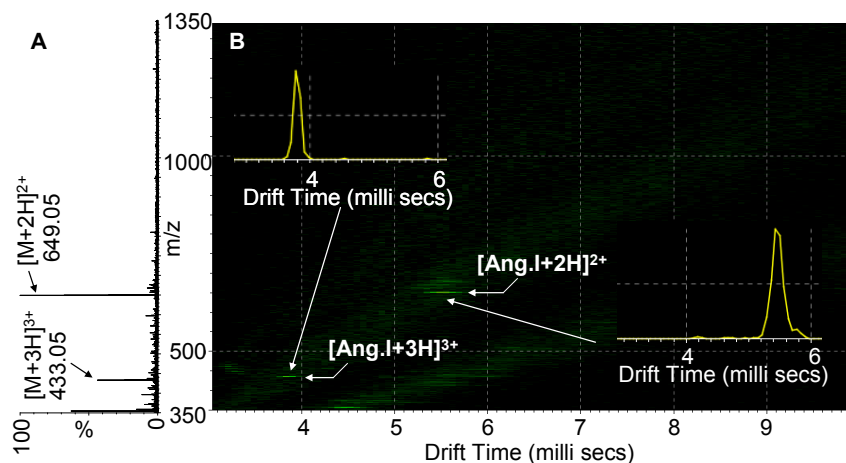


Figure 4.1. LSI-IMS-MS of angiotensin I (Ang. I) with 2,5-DHAP matrix using solvent-free sample preparation, a TSA approach: left panel (A) mass spectrum and right panel (B) 2-D plot of drift time versus m/z with insets displaying extracted drift time distributions for charge state +2 and +3. Reference data for solvent-based ESI-IMS-MS are included in Figure S4.1 in Appendix A.

solvent-based LSI analysis (**Figure S4.1A** in Appendix A) of the identical 2,5-

DHAP/angiotensin I mixture. Singly charged ions were not produced by either solvent-free or solvent-based LSI-MS. However, the total abundance of the angiotensin I ions produced using solvent-free preparation is lower than when solvent was used. Similar observations of relative intensities of soluble, more hydrophilic peptides using solvent-free sample preparation/ionization for analysis of peptides and proteins with a MALDI time-of-flight (TOF) mass spectrometer have been reported.^{37,41}

Figure 4.1B displays the dataset in a 2-D plot of drift time versus m/z with false color plot for the ion intensity showing that the multiply charged ions of angiotensin I obtained by solvent-free sample preparation/ionization undergo solvent-free gas-phase separation according to the number of charges and cross section (size and shape). This is best seen when viewing the extracted drift time distributions of +2 and +3 displayed in the respective insets of Figure 4.1B. The TSA results are essentially identical to those obtained by the solvent-based LSI-IMS-MS method, as shown by the respective 2-D plot and extracted drift time distributions (**Figure S4.1B** in Appendix A).

With increasing molecular weight (MW) of the analytes, ions with increasing number of charges are produced by TSA. Again, singly charged ions are not observed. Examples are shown in **Figure 4.2** for the non- β -amyloids component of Alzheimer's disease (NAC) and bovine insulin. The extracted mass spectra are displayed in the left panel, and 2-D plots are shown in the right panel. NAC (MW 3260) produces multiply charged ions ranging from +2 to +5 (**Figure 4.2A.1**) and bovine insulin (MW 5731) from +3 to +7 (**Figure 4.2.B.1**). Unexpectedly, with increasing charge state, an increasing degree of metal adduction of sodium cations (e.g., BI charge state +6 has 0-2 Na^+ ions replacing H^+ ions) is observed. Previous LSI studies using solvent-based sample preparation primarily

showed protonation of peptides and proteins.^{75,107,108,115,121,130-134} Solvent-free sample preparation in conjunction with MALDI-TOF analysis also produces a higher degree of metal cation adduction to the analyte, a key benefit for hydrophobic ionization retarded molecules.^{39,41,143} Furthermore, oxidation has been described for ESI and solvent-based MALDI approaches and was diminished using solvent-free sample preparation employing a mini-ball-mill approach with short homogenization times of about 1 min using CHCA matrix.⁴¹ Here, however, in order to have precise control of sample transfer to the vial, solvent was used, followed by evaporation of the solvent, allowing oxidation processes to take place. We, therefore, tentatively assign one of the adduct species to $[\text{NAC}_{\text{oxidized}} + 2\text{H} + \text{Na}]^{3+}$ instead of $[\text{NAC} + 2\text{H} + \text{K}]^{3+}$.

The TSA results were also compared with conventional solvent-based analysis approaches. Solvent-based LSI-IMS-MS analysis was obtained by adding 4 μL of 2,5-DHAP matrix solution on top of 1 μL of sample spotted on a glass slide, mixed, and blow-dried similar to previous procedures.¹³² This procedure was applied to NAC (in 50:50 ACN/H₂O with 0.1% TFA) and bovine insulin sample (in 50:50 MeOH/H₂O with 1% acetic acid). The solvent-based LSI and the ESI-IMS-MS results for NAC also show protonation, metal ion adduction, and the proposed oxidation (**Figure S4.2** in Appendix A). In contrast, the solvent-based LSI and ESI-IMS for bovine insulin only show protonation (**Figure S4.3** in Appendix A). Most likely, for NAC, the sample is already partially oxidized as purchased.

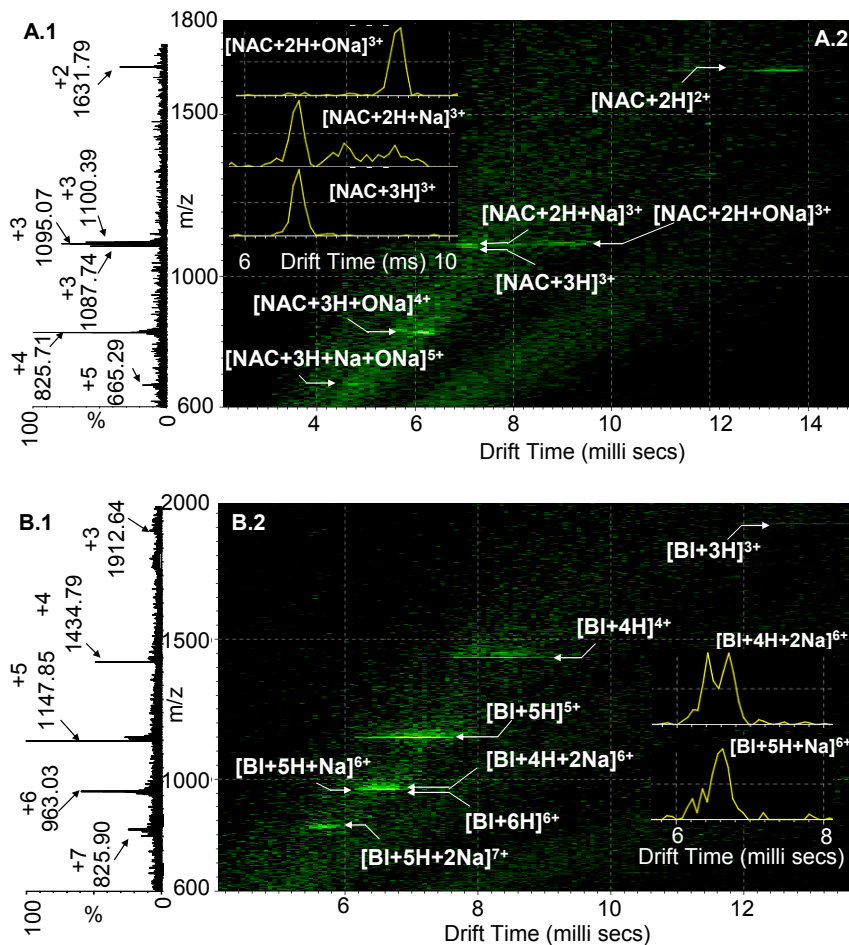


Figure 4.2. LSI-IMS-MS of (A) non- β -amyloid component of Alzheimer's disease (NAC) and (B) bovine insulin (BI) with 2,5-DHAP matrix using solvent-free sample preparation, a TSA approach: left panel (1) mass spectrum and right panel (2) 2-D plot of drift time versus m/z with insets displaying extracted drift time distributions of different ionizations for charge states +3 (NAC) and +6 (BI). Reference data for solvent-based ESI- and LSI-IMS-MS are included in Figures S4.2 and S4.3 in Appendix A.

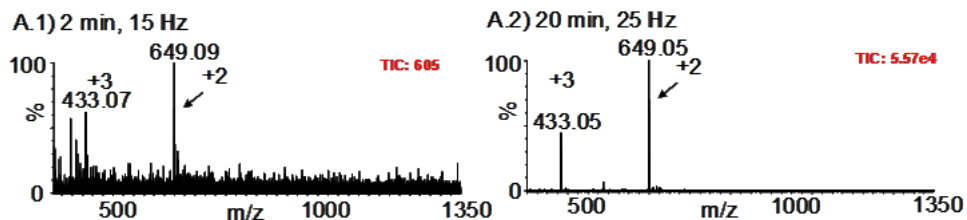
The relatively high degree of sodiation and oxidation are observed starting at +3, as seen by $[M + 3H]^{3+}$, $[M + 2H + Na]^{3+}$, and $[M_{\text{oxid}} + 2H + Na]^{3+}$, suggesting a specific structural change in the peptide to enhance metal cation adduction. It is therefore interesting to examine the drift time distributions (insets in **Figure 4.2.A.2**) for the different adducts at charge state +3 to provide some insight into the structures of NAC ions formed by protonation and sodiation. The charge state +3 ions of $[NAC + 2H +$

$[\text{Na}]^{3+}$ and $[\text{NAC}_{\text{oxidized}} + 2\text{H} + \text{Na}]^{3+}$ are significantly separated in the drift time dimension. The sodiated ion shows drift times very similar to the protonated ion $[\text{NAC}_{\text{oxidized}} + 3\text{H}]^{3+}$, while the oxidized ion shows a significantly slower drift time indicating a more elongated structure. The extent of the IMS gas-phase separation of ~ 7.0 (non-oxidized) and ~ 8.9 ms (oxidized) indicates a large difference in shape. Similarly, the bovine insulin ions with higher charge states show metal adducted ions (**Figure 4.2.B.2**) without a significant change in drift time (insets in **Figure 4.2.B.2**). This is in good agreement with previous investigations using an ESI-IMS-MS instrument with high drift time resolution¹⁰⁶ that demonstrated that the drift time distributions of lipid ions with different metal adduction frequently fall into families with nearly identical drift times (isodrifts), indicating that the cation attached to the molecule has little structural influence.

A motivation for producing multiply charged LSI ions from solid-state solvent-free preparation of the matrix/analyte is its potential application to tissue imaging. The results of Figures 4.1 and 4.2 show the relative abundance and ease with which the formation of the highly charged LSI ions can be achieved using a solvent-free approach. Compared to the production of exclusively singly charged LSI ions using 2,5-DHB without the use of solvents as described before,⁷⁵ the important conditions for forming and increasing the abundance of multiply charged LSI ions without the use of solvents are described below. First, the homogenization conditions of the matrix/analyte were examined in terms of the duration and frequency of the grinding process (**Figure S4.3A** and **Figure S4.4** in Appendix A). The abundances of the multiply charged ions of angiotensin I are low after homogenization for 2 min with 15 Hz frequency using 2,5-DHAP and increase

significantly with 20 min, 25 Hz homogenization (**Figure 4.3.A1** versus **A2**). The abundance of multiply charged ions of angiotensin with 2,5-DHB shows the same trend, comparing intensity after homogenization for 10 and 2 min (**Figure S4.5A** versus **B** in Appendix A). Thus, the abundances of highly charged ions are enhanced when more vigorous conditions for the matrix/analyte homogenization are applied. These homogenization conditions are well beyond those that can be achieved with a simple vortex device.⁷⁵

A. Increasing Grinding Time and Frequency: DHAP



B. Increasing Temperature in Desolvation Device: for DHB and DHAP matrixes

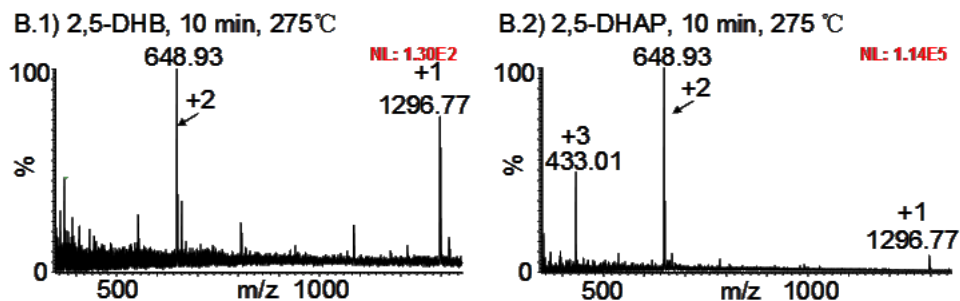


Figure 4.3. Solvent-free mass spectra of angiotensin I obtained from (A) SYNAPT G2, a TSA approach, using a home-built desolvation device and 150 °C source temperature after using different grinding times and frequencies during homogenization of 2,5-DHAP matrix/angiotensin I: (1) 2 min at 15 Hz and (2) 20 min at 25 Hz; (B) LSI-LTQ-Velos at 275 °C desolvation temperature homogenized at 25 Hz and 10 min using (1) 2,5-DHB and (2) 2,5-DHAP matrixes. More details are included in Figures S4.4 and S4.5 in Appendix A.

It is of interest to obtain more detailed information by investigating the LSI plume of different matrixes and grinding conditions by collecting the ablated matrix on a nearby glass slide. Optical microscopy of the ablated material collected from the solvent-free

prepared 2,5-DHB and 2,5-DHAP matrixes on a second microscope slide held at ~2 mm distance from the matrix is shown in **Figure 4.4** and **Figure S4.6** in Appendix A. After grinding for 30 s using the TissueLyser II, both matrixes produce liquid droplets upon ablation (**Figure 4.4**). Larger droplets (~5 to 7 μm diameter) are observed for 2,5-DHB compared to 2,5-DHAP (~1 μm diameter). The differences in volume of these molten droplets correlate with the observed lower temperature required to produce the highly charged LSI ions from 2,5-DHAP versus 2,5-DHB matrixes.

Increasing the grinding time to 10 min, 2,5-DHAP's liquid droplets maintained the same relative size, but 2,5-DHB's droplets became smaller (**Figure S4.6** in Appendix A). The third set of matrix samples were ground in a vortexer for 30 s, similar to the method introduced by Hanton and Parees¹³⁸ and used previously for solvent-free LSI.⁷⁵ The liquid droplets collected for both matrixes are notably less abundant than the droplets seen in the TissueLyser II sample (**Figure S4.7** in Appendix A). While multiply charged ions of angiotensin I were observed in all samples using 2,5-DHAP, samples using 2,5-DHB and 30 s vortexer grinding times produced predominantly singly charged ions on the LTQ Velos, similar to previous observations.⁷⁵

For the study of the thermal requirements within the atmospheric pressure to the vacuum transfer region on the formation of highly charged LSI ions of solvent-free prepared matrix/analyte samples, a LTQ Velos is used that has a commercial heated inlet capillary providing the ability to accurately control the desolvation temperatures (**Figure 4.3.B**). We find for angiotensin I that the production of multiply charged LSI ions can be enhanced with 2,5-DHB, as is shown for a temperature range from 40 to 400 °C (**Figure S4.5A,B** in Appendix A). Only low abundance signal of singly charged ions can be

observed at 40 °C using 2,5-DHB (**Figure S4.5B** in Appendix A), and high abundance of both doubly and singly charged ions was produced when the capillary temperature was increased to 275 °C (**Figure 4.3B.1**). In contrast, 2,5-DHAP provides abundant highly charged angiotensin I ions at temperatures as low as 40 °C (**Figure S4.5C** in Appendix A). Increasing the capillary temperature up to 400 °C did not have a significant effect on the charge state distribution but did on the abundance (ion count increased from 5.10×10^3 to 1.95×10^5) using 2,5-DHAP (**Figure 4.3B.2** and **Figure S4.5C** in Appendix A). The 2,5-DHAP matrix shows significantly lower thermal requirements than the 2,5-DHB using a solvent-free approach.

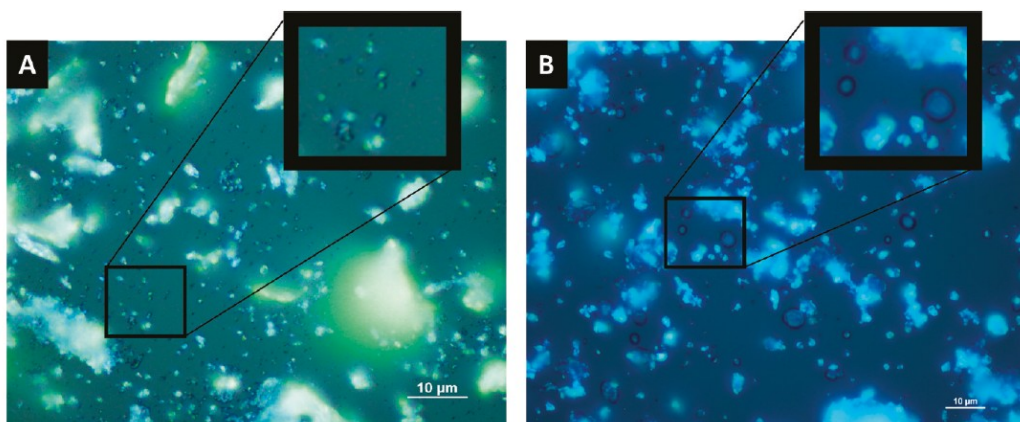


Figure 4.4. Microscopy images of liquid droplets produced by laser (N₂) ablation of (A) 2,5-DHAP and (B) 2,5-DHB matrixes after the material was ground for 30 s in the TissueLyser II. Reference data for optical microscopy of ablated 2,5-DHB and 2,5-DHAP after being ground for 10 min in the TissueLyser II (Figure S4.6 in Appendix A) and 30 s in the vortexer (Figure S4.7 in Appendix A) are included.

Interestingly, with all of the studies performed with angiotensin I using 2,5-DHAP, the SYNAPT G2 provides highly charged ions, increasing in abundance with increasing time and frequency of matrix/sample homogenization. Singly charged ions are not observed, as can be seen in Figures 4.1 and 4.3A. The LTQ Velos, however, frequently provides some degree of low abundant singly charged ions along with abundant multiply

charged ions as observed in Figure 4.3B. Because enhancement in multiply charged ion formation is observed with longer grinding times, higher grinding frequency, and higher temperature, the LTQ Velos (Thermo) results displaying both multiply and singly charged ions (**Figure 4.3B**) compare well, considering the conditions used, with the previously obtained Orbitrap Exactive results showing singly charged ion formation.⁷⁵ The SYNAPT G2 was used with and without the IMS dimension by controlling the helium gas (Figure S8 ion count increased from). Only low abundant singly charged ions are observed without the use of the IMS dimension (no helium), and abundant highly charged ions are observed with the use of the IMS dimension (helium on). This unexpected result may be related to the unique and delayed ionization phenomena occurring inside the ion transfer region¹⁰⁹ or in the Triwave of the SYNAPT G2 with the IMS “on”.¹¹⁵ This could also involve an ion transmission issue.

Applications of TSA to Mixtures of Peptides/Lipids and Crude Oil. Similar to ESI, under LSI conditions, lipids produce singly charged ions, thus, mixing a lipid with a peptide should produce both singly and multiply charged ions. The analysis of a mixture of angiotensin I and sphingomyelin using a TSA approach is shown in **Figure 4.5**. In the extracted mass spectrum (**Figure 4.5.A**), the doubly and triply charged ions of angiotensin I are observed in abundances similar to the pure sample along with abundant singly charged ions of sphingomyelin. In comparison, when the solvent ACN/H₂O (50:50) was added to the same homogenized matrix/analyte powder, lipid ions were no longer detected and the signal intensity for the peptide increased (**Figure S4.9A** in Appendix A). Without the TSA analysis, this would incorrectly suggest that the lipid component is not present in the mixture. This result has implications for the analysis of

biological materials, such as tissue imaging, in which lipids and peptides (proteins) are present and may be analyzed simultaneously. It also demonstrates that, with the IMS “on”, singly charged LSI ions are transferred to the MS detector.

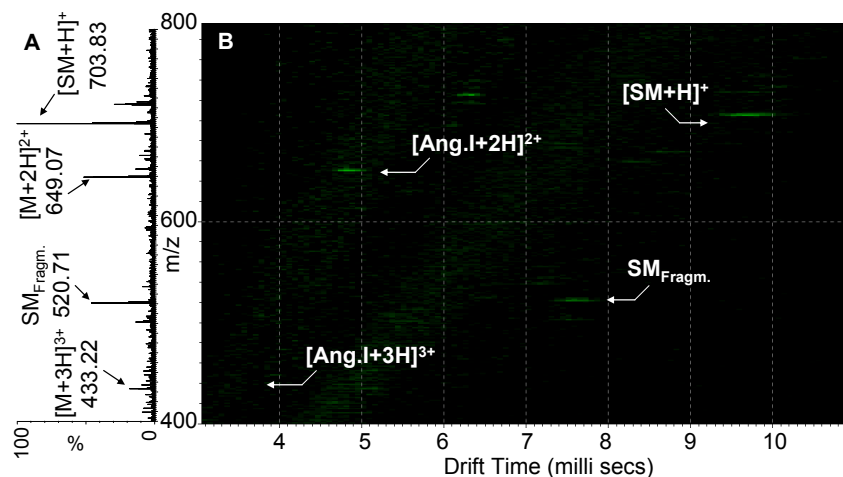


Figure 4.5. LSI-IMS-MS of a mixture of angiotensin I and sphingomyelin with 2,5-DHAP matrix using the solvent-free sample preparation method, a TSA approach: left panel (A) mass spectrum and right panel (B) 2-D plot of drift time versus m/z .

In the 2-D plot of drift time versus m/z (**Figure 4.5.B**), well-separated singly charged lipid (8.3 ms) and multiply charged peptide ions (4.2 ms for +2, 2.9 ms for +3) are observed. Previous IMS-MS studies using MALDI showed that lipid and peptide ions fall into respective charge state families (trend lines) with some separation.¹⁴⁴ Further, the solvent-based LSI-IMS-MS study (**Figure S4.9B** in Appendix A) shows in the 2-D plot abundant doubly charged angiotensin I ions and a low abundant feature in the area where sphingomyelin singly charged ion and doubly charged ion of metal adducted dimer are expected based on the results observed in **Figure 4.5.B**. Without a prior knowledge of the sample composition, these ions would not be noticed in the mass spectrum (**Figure S4.9A** in Appendix A). More detailed DriftScope analysis of the solvent-based results verifies the identity of the singly charged sphingomyelin ions, demonstrating the

enhanced effective dynamic range achieved by incorporating the drift time separation in an IMS-MS experiment. The comparison of results of solvent-free and solvent-based LSI-IMS-MS analyses of this model mixture demonstrates the more inclusive ionization without the use of solvents during sample preparation/ionization.

Additional samples known to ionize exclusively by singly charged ion formation in LSI were used to compare the relative ability of the SYNAPT G2 using the IMS dimension versus the LTQ or Orbitrap mass spectrometers to determine if ion transmission discrimination by charge state exists. Here, the applicability of TSA by LSI for oil samples is examined. These samples are notoriously sticky and of extreme complexity and therefore prone to sample loss.¹⁴⁵ Furthermore, the ionization of crude oil samples is frequently limited to ESI, atmospheric solids analysis probe (**ASAP**), or atmospheric pressure photoionization (**APPI**).¹⁴⁶⁻¹⁴⁸ MALDI performs poorly because of the chemical background introduced with the matrix in the mass range of the oil sample and, most notably, the tendency of gas-phase aggregation and coalescence due to use of higher laser fluence, as shown with these and similar systems.^{146,149-154} Additionally, solvent-based separation approaches for the reduction of sample complexity are difficult, so the analyses are predominantly obtained using ultrahigh mass resolution Fourier transform ion cyclotron resonance (**FT-ICR**) instrumentation^{145,146,148,153} and more recently by IMS-MS.^{146,147}

The analyses of liquid oils from various origins were prepared and analyzed by the TSA approach using LSI with 2,5-DHAP as matrix. Typical examples are shown in **Figure 4.6** and Figure S4.10 in Appendix A. The 2-D plot of drift time versus m/z shows abundant signals in the expected mass range of m/z 200 and 800 and demonstrates that

laser-induced aggregates are not observed, even though the laser fluence is higher using LSI compared to MALDI. Aggregation and “clustering” have

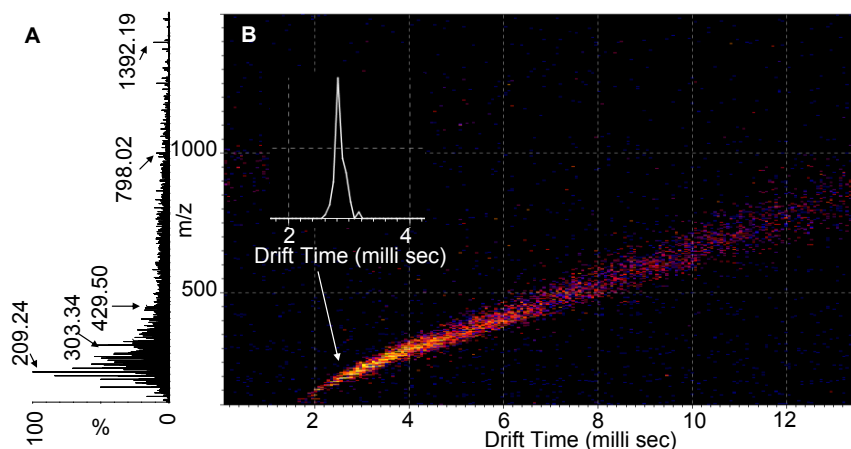


Figure 4.6. LSI-IMS-MS of crude petroleum oil with 2,5-DHAP matrix using solvent-free sample preparation, a TSA approach: left panel (A) mass spectrum and right panel (B) 2-D plot of drift time versus m/z with insets displaying extracted drift time distributions of m/z 205.18 and 205.24. Reference data for other oily and sticky materials are included in Figure S4.10 in Appendix A.

been reported for laser-based analyses such as MALDI and LDI of crude oil and similar materials.^{146,149-152} The LSI-TSA approach does not show aggregation or clustering. The chemical background introduced by the matrix is also insignificant using the LSI-TSA approach. The lower chemical background has been described for solvent-free ionization approaches for a number of low molecular weight systems including efficient ionization of fatty acids, pigments, and polycyclic aromatic hydrocarbon compounds.^{36,143,154} A comparison with solvent-based LSI-IMS-MS shows some chemical background related to the use of solvent (Figure S4.11 in Appendix A). Again, the observation of singly charged ions under LSI conditions with the IMS “on” suggests that transmission discrimination is not a detrimental issue. The solvent-free gas-phase separation of small structures of isobaric composition is delineated by the extracted drift time distributions of m/z 205.18 and 205.24 in the inset of **Figure 4.6.B**. An initial study on TSA using a

MALDI approach delineated isobaric tissue composition at m/z 863.3 to 863.7.¹³⁶ When comparing the different oil samples relative to each other, the differences are evident (**Figure 4.6** and **Figure S4.10** in Appendix A). Both the pure vegetable oil and the motor oil exhibit the presence of more low mass species, while crude oil shows a more complex nature with more abundant high mass species. This indicates the useful nature of the 2-D plots when using the snapshot approach as previously indicated for the analysis of synthetic polymers.¹⁵⁵

4.4 Discussion

The preparation of supersaturated 2,5-DHAP solution is crucial for the success of LSI, though the solubility of 2,5-DHAP is low in most solvents.¹³² As shown here, the solvent-free sample preparation is more streamlined, and the solubility of 2,5-DHAP or deposition procedure to the sample holder is no longer a setback for obtaining similar and in some cases improved mass spectra as compared to solvent-based sample preparation.

The ability and simplicity of preparation and ionization of even sticky oil samples relates well with previous studies of sticky and liquid polymeric samples using a solvent-free MALDI approach.^{36,138,154} The disadvantage of the solvent-free sample preparation used here as well as other solvent-free sample preparation methods developed for surface analysis¹³⁶ is the larger sample requirement relative to solvent-based LSI sample preparation, which showed sensitivities in the low femtomole range for insulin and mid-attomole range for peptides.⁷⁵ The ability to produce highly charged ions without the use of a voltage^{75,107,108,121,129-135} is of analytical utility but is also of fundamental importance. Previous work showed that the ion production occurs inside the capillary in the AP vacuum pressure drop region and that desolvation processes of the matrix occur, leaving

behind the multiply charged ions similar to ESI-like processes at AP.^{107,131} Multiply charged ions were previously obtainable only by using ionization methods that involve a solution state such as in ESI¹⁵⁶ or solvent-based sample preparation for LSI.^{75,107,108,115,121,130-134} Interestingly, adding a drop of solvent to a sample prepared solvent-free using a vortexer for homogenization of matrix/analyte converts the singly charge ionization observed using that procedure to the sole production of multiply charged ions, suggesting that analyte incorporation in MALDI might be important in forming multiply charged LSI ions.⁷⁵ Here, we show that solvent is also not a necessity to produce multiply charged ions of peptides and proteins. The solid matrix/analyte mixture prepared and homogenized without employing solvent when ablated from a surface forms molten droplets upon the absorption of the laser energy similar to solvent-based LSI observations.¹³¹ Garrison et al. modeled matrix droplets in vacuum laser ablation of solid matrix.^{157,158}

Initial solvent-free results show that multiply charged ions from solvent-free sample preparations are easily obtained on the SYNAPT G2 (Figures 4.1 and 4.2), but that the reproducibility between instruments and relative to published work⁷⁵ on the Orbitrap is low. Exploring different preparation (e.g., grinding time and frequency) and instrument parameters (e.g., orifice temperature, IMS gas) on two different mass spectrometers (LTQ Velos, SYNAPT G2) elucidated a number of important mechanistic aspects to solvent-free and multiply charged ion formation (**Figure 4.3**). 2,5-DHAP solvent-free sample preparations are readily obtained and reproducible on the LTQ Velos and SYNAPT G2, but the DHB results notably vary between instruments. To elucidate the differences, an approach similar to that of published work¹³¹ on solvent-based LSI-MS was used that

showed that significant amounts of matrix/analyte materials are transformed by the impact of the laser on the solid matrix/analyte to liquid droplets collected on a glass slide 2 mm distant from the matrix holding glass slide and visualized by microscopy. Here (**Figure 4.4**, **Figure S4.6** and **S4.7** in Appendix A), ablating solid matrix material from the surface shows that both the DHAP and the DHB matrixes produce droplets, though not to as large of an extent as with solvent-based sample preparation, and that the droplet sizes are significantly different for both matrixes prepared solvent-free. DHAP produces small droplets under all tested preparation methods that do not significantly change in size using various grinding conditions. However, the size of DHB's droplets are large relative to the droplets formed from DHAP and are inversely proportional to grinding time in the ball-mill device. The smaller droplets likely require less energy for efficient desolvation in the ion transfer region and consequently enhance the ease and thus the abundance for forming multiply charged ions. The always small sized DHAP droplets (**Figure 4.4A**) also offer a sound argument for the reproducibility of the solvent-free experiment using DHAP. Microscopic results are in agreement with our mass spectrometric observations. We cannot assert a causal relationship between smaller matrix/analyte droplets and the formation of more abundant multiply charged ions, but there is a correlative connection. A correlation appears to exist between the production of multiply charged LSI ions and the abundance of small liquid droplets formed from ablated matrixes. In the case of the DHB matrix, this is achieved with longer grinding times (10 min) on the Velos at a temperature of 275 °C for which the doubly charged ion is now the base signal relative to the singly charged ion (**Figure 4.3**).

Relating the microscopy data to the mass spectrometric results of DHB and DHAP

matrixes seems to suggest that the production of highly charged ions is more efficient from materials that form smaller droplets. A droplet of $\sim 2 \mu\text{m}$ (DHAP) versus $\sim 8 \mu\text{m}$ (DHB) diameter has 64 times more matrix material. The difficulty of desolvation of the larger droplets may explain the higher temperature requirements in the transfer capillary of the mass spectrometer for DHB. It is possible that the thermal energy requirement for producing the multiply charged ions is only sufficient for the smaller droplets. Small droplets can be achieved from appropriate matrix material by laser ablation at AP from samples that were not “incorporated” into the matrix in a conventional way but by the grinding forces. Extended grinding times (SYNAPT G2; Velos) and high desolvation temperatures (Velos) allow highly charged LSI ions to be formed in the source region as well as downstream of the mass spectrometer (SYNAPT G2).

LSI is a subset of MAII¹⁰⁹ in which a laser is used to transfer the matrix/analyte material to the ion transfer capillary for ionization. Other means of MAII are the use of, for example, a center punch or simply a spatula giving identical results as compared to LSI. Clearly not all MAII methods start with small molten droplets but produce multiply charged ions. Important to success is efficient heating (**Figure 4.3.B1** and Figure S4.5A,B in Appendix A), low thermal requirements (**Figure 4.3.B2** and Figure S4.5C in Appendix A), and homogeneity (**Figure 4.3A** and **Figure S4.4** in Appendix A). The singly charged ions previously produced using a solvent-free LSI approach are a result of non-incorporating vortexing conditions.⁷⁵

Previous MALDI studies discussed ionization, incorporation of analyte into the matrix, morphology changes in solvent-free and solvent-based sample preparation/ionization for analysis,^{36,39,159-166} with some indication that the solvent-free

method enhances the efficiency of MALDI ion production of compounds difficult to protonate because the analyte and metal cations get close in the solid state through the grinding process.^{39,41,143,154,157} Solvent-based LSI-MS and LSI-IMS-MS provides little evidence for producing Na⁺ adduction to peptides or proteins similar to MALDI or ESI-MS, probably because of segregation that occurs upon crystallization on removal of solvent. It seems possible that the more aggressive homogenization in solvent-free MALDI produces smaller and better mixed matrix/analyte(/metal cation) particles which produce the desired “incorporation” and molten state, thus accounting for the observation of multiply charged ions formed by proton and metal cation attachment. In contrast to MALDI and LDI, the chemical background in TSA by LSI is relatively low and analyte aggregation^{146,149-152} is not observed, similar to ESI-IMS-MS, but provides the ability for fast, solvent-free, and surface analyses independent of analyte or matrix solubility.

The structural changes observed in the IMS dimension for protonation versus sodiation are small based on the drift time separation, whereas the structural changes of oxidized and non-oxidized NAC are significant, demonstrating the potential of structural differentiation of ions directly from the solid state. Because ESI-IMS-MS gives the same results, the oxidation or structural changes are not related to one ionization method. Morphology changes during sample preparation to produce small molten droplets and the absence of sodiation in ESI and LSI-IMS-MS measurements lead us to conclude that the attachment of metal cation(s) is a direct result of the homogenization process of the matrix/analyte.

4.5 Conclusion

We report the first observation of multiply charged ions produced from the solid state

using solvent-free matrix/analyte sample preparation. Combined with IMS-MS, this TSA approach provides greatly improved IMS separation of compound classes that differ by charge states (e.g., lipids and peptides). Other advantages of a TSA approach include one-step sample preparation and deposition on the target plate, rapid data acquisition for simplifying sample complexity relative to ESI and LC-MS, reduction of sample artifacts caused by the use of solvents, and enhancement of the effective dynamic range by the IMS dimension. The ability to observe multiply charged ions using LSI from solvent-free sample preparation will have immense benefits if it can be translated to solvent-free matrix deposition for tissue imaging where the use of solvent is detrimental to retaining spatial integrity of the more soluble compounds.

CHAPTER 5

A NEW APPROACH TO HIGH SENSITIVITY LIQUID CHROMATOGRAPHY-MASS SPECTROMETRY OF PEPTIDES USING NANOFLOW SOLVENT ASSISTED INLET IONIZATION

Liquid chromatography (LC) solvent assisted *inlet* ionization (SAII) mass spectrometry (MS) was previously reported to give good chromatographic resolution and MS detection injecting 66 ng of a BSA tryptic digest. In analogy to nano-electrospray ionization (nESI), we extend SAII LC/MS to nano-SAII (nSAII) operating at nL min⁻¹ flow rates and demonstrate good quality ion chromatograms and mass spectra from injection of as little as 0.7 ng of BSA digest onto a capillary LC column. Data dependent fragmentation is demonstrated for injection of 7 ng of a BSA digest. This method has advantages over nESI in ease of use and low cost as it requires no voltage and is operational without the necessity of connectors or fragile nESI emitters, although similar constricted tips can be helpful in nSAII to stabilize the signal at low nanoliter flow. At a flow rate of 0.8 μL min⁻¹, the only requirement for nSAII is that the exit-end of the capillary LC column be adjusted near the aperture of the heated inlet of the mass spectrometer.

B. Wang, E. D. Inutan, S. Trimpin, *J. Am. Soc. Mass Spectrom.* **2012**, *23*, 442-445.

Reprinted with permission from Springer Science and Business Media.

5.1 Introduction

Modern liquid chromatography/mass spectrometry (**LC/MS**) almost exclusively uses electrospray ionization (**ESI**) except for low polarity compounds which use atmospheric pressure chemical ionization (**APCI**).^{167,168,169} For analyses where sample amount is limited, ESI LC/MS is performed at nanoliter (**nL**) min^{-1} mobile phase flow rates.^{78,170,171,172} This approach, called nano-ESI (**nESI**),¹⁷³ is especially important for peptide and protein analyses. Because ESI is a concentration sensitive method, lower flow rates produce similar signal to higher flow but with consumption of less material.⁸⁰ However, the low flow condition also enhances ionization, presumably by producing smaller solvent droplets with increased charge, thus reducing ion suppression and ionizing a wider range of compounds. Because of the importance of nESI, ion sources are commercially available. Recently, Smith and coworkers^{174,175} reported on nESI at subambient pressure using ion funnel technology. However, nESI has a number of shortcomings. The low solvent flow greatly increases the time for a complete LC run relative to higher flow rates, and achieving a stable ion current is notoriously difficult. Special spray emitters are available to help address this issue,⁸² but the emitter tips are fragile and add considerable cost to nESI. The sharp tips also reduce the voltage range over which a stable ESI spray is observed: too high voltage produces a corona discharge. Technical issues generally limit the use of nESI to problems that need its additional capabilities.

Recently, *inlet* ionization methods have been introduced that have the potential to compete with both matrix assisted laser desorption/ionization (**MALDI**) and ESI. Methods that utilize a solid phase matrix similar to those used in MALDI are laserspray ionization inlet (**LSII**)^{75,107,121,129,132,135} and matrix assisted *inlet* ionization (**MAII**).¹⁰⁹

Solvent assisted *inlet* ionization (**S_{AI}I**) is the equivalent of ESI in that similar mass spectra are produced from solvent/analyte solutions introduced into the mass spectrometer inlet and ionized.¹¹¹ Just as in ESI, S_{AI}I can be used for ionization in LC/MS.¹¹² It was shown that introducing the LC mobile from a 1 mm i.d. LC column directly into a heated inlet transfer tube of the mass spectrometer produced a high quality ion chromatogram and corresponding mass spectra with injection of ca. 70 ng of bovine serum albumin (BSA) tryptic digest. Here, we extend the applicability of *inlet* ionization to nanoliter flow rates by positioning the LC effluent just outside of the mass spectrometer inlet aperture and demonstrate similar results from injection of just 0.7 ng of BSA digest.

5.2 Materials and Methods

Materials. Chemicals were stated in **Chapter 2**.

Methods.

S_{AI}I-MS. One end of a 40 cm length of 25 μm i.d. fused silica tubing (Polymicro Technologies, Phoenix, AZ, USA) was connected to a syringe and the exit end taped on an x,y,z-stage to control the alignment and distance of the exit end relative to the inlet aperture of the heated atmospheric pressure (**AP**) to vacuum inlet tube of the mass spectrometer. A study of the optimum distance of the fused silica exit from the inlet orifice was performed by pumping a 1:1 ACN:water 0.1 % FA 1 pmol μL^{-1} angiotensin I solution through the fused silica tube at a flow rate of 1.2 $\mu\text{L min}^{-1}$. The x,y,z-stage was used to adjust the exit end of the fused silica from 0.4 mm on the AP side to 0.2 mm on the vacuum side of the mass spectrometer inlet aperture.

NanoS_{AI}I and nanoESI LC-MS and MS/MS. A Waters Corporation NanoAcquity

UPLC was used with a Waters 100 $\mu\text{m} \times 100 \text{ mm}$ BEH130 C18 column with 1.7 μm particles. Water and ACN both containing 0.1% FA was used as the mobile phases in all studies. A 35 min gradient of 1 to 85% ACN was used at mobile phase flow rates varying from 0.4 to 0.8 $\mu\text{L min}^{-1}$, and a 12 min gradient at a flow rate of 1.2 $\mu\text{L min}^{-1}$. For 0.4 $\mu\text{L min}^{-1}$ flow rate, a 6.35 cm long 360 $\mu\text{m o.d.} \times 20 \mu\text{m i.d.}$ (with 10 $\mu\text{m i.d.}$ at the tip) pre-cut PicoTip emitter (Waters) was employed as an extension to the end of LC capillary column and mounted on the x,y,z-stage to be positioned about 0.1–0.2 mm outside of the mass spectrometer inlet for optimum results. At flow rates of 0.8 $\mu\text{L min}^{-1}$ and higher, the exit-end of the LC capillary column (100 $\mu\text{m i.d.} \times 360 \mu\text{m o.d.}$) was used without need of a special emitter or any tubing connections. A Thermo LTQ-Velos mass spectrometer with the inlet tube heated to 300 $^{\circ}\text{C}$ was used for LC-nSAII-MS and MS/MS. Data dependent MS/MS was obtained using collision induced dissociation (CID) with 35 V collision energy. A three point boxcar smoothing was used for the LC chromatogram display. A Waters SYNAPT G2 mass spectrometer^{109,112,121,132} was used for LC-nESI-MS for relative comparison. The skimmer cone was heated to 150 $^{\circ}\text{C}$. The voltage applied on the nESI capillary is 3.06 kV. BSA tryptic digest solution, 1 μL of a 100 fmol μL^{-1} , was analyzed using the same LC gradient at a mobile phase flow of 0.8 $\mu\text{L min}^{-1}$ and 0.4 $\mu\text{L min}^{-1}$.

5.3 Results and Discussion

SAII was recently interfaced with LC/MS at a mobile phase flow rate of 55 $\mu\text{L min}^{-1}$ with chromatographic resolution comparable to ESI LC/MS and produces good signal-to-noise with injection of 1 pmol of a BSA digest.¹¹² This work was accomplished on a LTQ-Velos, which has a heated inlet tube linking AP with the first vacuum region of

the mass spectrometer. The higher flow rates used in the previous study requires that the exit-end of the fused silica capillary be stripped of its polyimide coating and inserted into the heated inlet tube of the mass spectrometer to a ‘sweet spot’ for ion production. Here, we demonstrate, in analogy to nESI, that nanoliter mobile phase flow rates are also compatible with SAI. The initial ‘tuning’ for the low flow rate was achieved by delivering an angiotensin I solution using an infusion pump to the exit end of the fused silica tube (25 μm i.d.) so that it could be adjusted (Figure S5.1 in Appendix B) for the best stability and abundance of the signal from the triply charged angiotensin I ion (m/z 433). For flow rates of a few microliters and lower, the best position of the fused silica capillary exit-end was found to just at the inlet entrance aperture, and no longer requiring the removal of the coating. A stable signal with good sensitivity was achieved with the mass spectrometer inlet tube temperature set to 300 °C. The flow of air into the vacuum region of the heated mass spectrometer entrance inlet is sufficient to nebulize the solution at the tip of the fused silica, sweeping the ensuing mist of solvent droplets into the inlet where ions are generated with the assistance of heat and vacuum.

Laserspray ionization (**LSII**), potentially useful for imaging at high spatial resolution,^{75,107,121,129,134,135} is a subset of matrix assisted *inlet* ionization (**MAII**)¹⁰⁹ in which a laser is used to transfer the matrix/analyte mixture to the mass spectrometer inlet where ions are produced in the heated pressure drop region having similar charge states to ESI. We hypothesize that ion formation is vacuum and thermal assisted.^{107,110,121,122,131} SAI^{111,112} is similar to the other *inlet* ionization methods of LSII^{75,107,121,129,134,135} and MAII¹⁰⁹ in which any means of introducing matrix/analyte into the heated inlet produces ions similar to ESI. In the case of SAI¹¹¹ where the matrix is a solvent, it can be shown

(**Figure S5.2** in Appendix B) that ions are not produced by a sonic spray mechanism as is evident by the requirement that the inlet be heated to produce ions: heat is not a requirement for sonic spray.^{176,177} There are also significant differences between *inlet* ionization with a solvent and thermospray ionization¹²⁴ in addition to the high charge states, low flow rates and the high sensitivity achievable with SAI, as was recently pointed out.¹¹²

Without the need to place the fused silica inside the heated mass spectrometer inlet, it is possible to use the exit of the capillary LC column and eliminate all connections, unlike in our previous LC-SAI study.¹¹² By attaching the exit of the LC column to an x,y,z-stage with tape, the end of the LC column capillary tubing is visually adjusted near the entrance of the mass spectrometer inlet for optimum ion current stability (Figure 5.1A and Figure S5.3 in Appendix B). This procedure can be accomplished in a couple of minutes. This arrangement provides stable ion current at flow rates from 0.8 $\mu\text{L min}^{-1}$ (**Figure S5.4A** in Appendix B) to at least 1.2 $\mu\text{L min}^{-1}$ (Figure S5.4B in Appendix B). However, the signal is not sufficiently stable with this arrangement at 0.4 $\mu\text{L min}^{-1}$ for good quality LC/MS. Observationally, it appears that the instability is the result of larger droplets exiting the fused silica tubing rather than a fine spray. A stable signal is achieved by attaching the LC column to a Waters PicoTip emitter (**Figure 5.1B**), as is done in nESI. Because SAI operates without the requirement for a voltage and at high nanoliter flow rates without the necessity of a fragile emitter, it is exceptionally easy to implement.

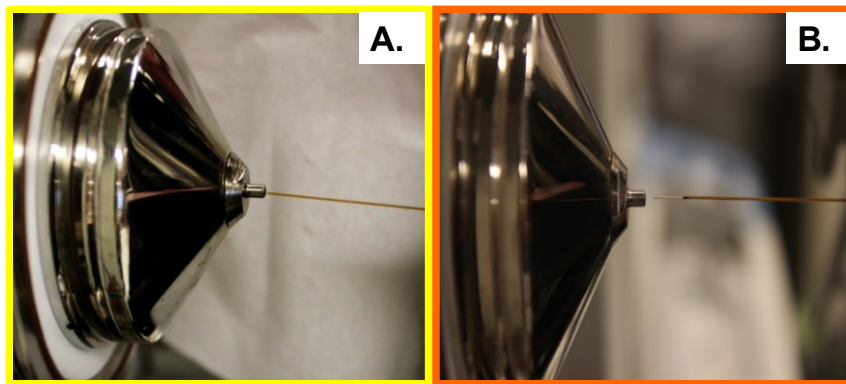


Figure 5.1. Pictures showing the setup for LC-nSAII. Side view of MS inlet in which the tip of the fused silica capillary tube of the LC column is placed about 0.1 mm out of the orifice inlet entrance of the mass spectrometer (A) directly or (B) by use of a “PicoTip” attached to the end of the fused silica capillary tube. Front view of the LC and mass spectrometer setup is displayed in Figure S5.3 in Appendix B.

Using the simple set-up (**Figure 5.1A** and **Figure S5.3** in Appendix B) requiring no emitter connected to the LC column and a mobile phase flow rate of $0.8 \mu\text{L min}^{-1}$, injection of 100 fmol (7 ng) of BSA digest produces roughly equivalent results to those reported¹¹² for ca. 70 ng injected at $55 \mu\text{L min}^{-1}$. The base peak chromatogram for the 100 fmol injection is shown in **Figure S5.5A** in Appendix B. The mass spectrum from the peak eluting at 17.8 min shows doubly and singly charged analyte ions (**Figure S5.5B** in Appendix B). In order to have a relative comparison, nESI LC/MS was acquired using the commercial nESI source on the SYNAPT G2 mass spectrometer at a mobile phase flow rate of 0.8 and $0.4 \mu\text{L min}^{-1}$ using the same gradient and injecting 100 fmol of the same BSA digest used in the SAII study (**Figures S5.4** and **S5.6** in Appendix B).

Additionally, data dependent fragmentation for the 100 fmol SAII injection on LTQ Velos also produces excellent LC/MS/MS fragmentation as is demonstrated by the high sequence coverage using MASCOT for the BSA peptide fragment at m/z 740 having the sequence LGEYGFQNALIVR (**Figure 5.2**). MASCOT identified the protein as BSA from this single MS/MS spectrum with a score of 103. The first nSAII LC/MS and

MS/MS results, without the necessity of special connections, tips, or voltage, produce roughly equivalent results to nESI and in much less set-up time for the experiment.

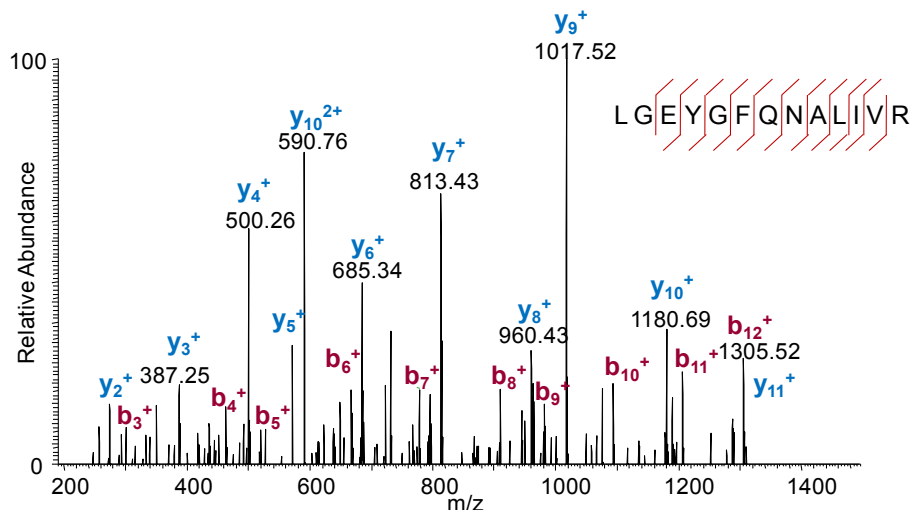


Figure 5.2. LC-nSAII-MS/MS mass spectrum of 100 fmol μL^{-1} BSA tryptic digest with 1 μL injection at a flow rate of 800 nL min^{-1} using the setup shown in Figure 5.1(A). The sequence shows the Mascot coverage providing a MASCOT score of 103.

Injection of just 10 fmol (0.7 ng) of BSA digest using SAII at 0.8 $\mu\text{L min}^{-1}$ produces the base peak chromatogram in which only the most abundant ions are observed. However, connecting the exit of the LC column to a 20 μm i.d. PicoTip with 10 μm i.d. on the tip allows a stable signal to be obtained at a flow rate of 0.4 $\mu\text{L min}^{-1}$. Under these conditions, injection of 0.7 ng of BSA digest produced the base peak chromatogram shown in **Figure 5.3**. The signal-to-noise was calculated by the data system for the peak eluting at m/z 582 is 277.

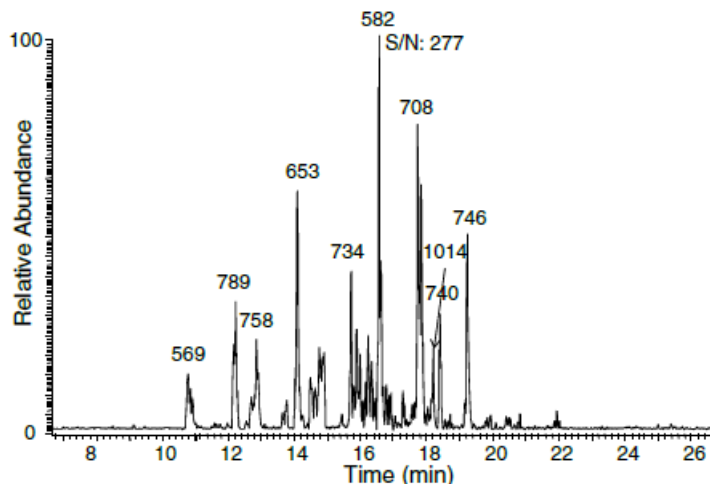


Figure 5.3. nSAII-LC/MS base peak chromatograms of 10 fmol μL^{-1} BSA tryptic digest with 1 μL injection at a flow rate of 400 nL min^{-1} using the “PicoTip” extension shown in Figure 5.1(B).

5.4 Conclusion

Inlet ionization is a new method for producing mass spectra equivalent in charge state to those produced by ESI but from solid (LSI or MAII) or solution (SAII) states without the need for a laser or voltage for ionization. The sensitivity of *inlet* ionization is demonstrated by the production of good quality base peak chromatograms and clean mass spectra with high signal-to-noise with injection of as little as 0.7 ng of a BSA digest using nSAII LC/MS. Data-dependent fragmentation was shown for injection of just 7 ng of BSA digest using a mobile phase flow rate of 800 nL min^{-1} . These results suggest the potential of SAI for proteomics and most likely other areas where sample amounts are limited. Detailed mechanistic discussion relative to *inlet* ionization is addressed in a forthcoming paper.¹²²

CHAPTER 6

HIGH THROUGHPUT SOLVENT ASSISTED IONIZATION *INLET* (SAII) FOR USE IN MASS SPECTROMETRY

In this work we developed a multiplexed analysis platform providing a simple high-throughput means to characterize solutions. Automated analyses, requiring less than 5 s per sample without carryover and 1 s per sample, accepting minor cross contamination, was achieved using multiplexed solvent assisted ionization *inlet* (SAII) mass spectrometry (MS). The method involves sequentially moving rows of pipet tips containing sample solutions in close proximity to the inlet aperture of a heated mass spectrometer inlet tube. The solution is pulled from the container into the mass spectrometer inlet by the pressure differential at the mass spectrometer inlet aperture. This sample introduction method for direct injection of solutions is fast, easily implemented, and widely applicable, as is shown by applications ranging from small molecules to proteins as large as carbonic anhydrase (molecular weight ca. 29 000). MS/MS fragmentation is applicable for sample characterization. An x,y-stage and common imaging software are incorporated to map the location of components in the sample wells of a microtiter plate. Location within an x,y-array of different sample solutions and the relative concentration of the sample are displayed using ion intensity maps.

B. Wang, S. Trimpin, *Anal. Chem.* **2014**, *86*, 1000-1006.¹ Reprinted with permission from Copyright (2014) American Chemical Society.

¹ This publication has been converted to a provisional patent and later to a patent application, pending. "Multiplexing system used to allow high throughput analysis of samples using solvent assisted ionization inlet comprises ionizing system for solvent assisted ionization inlet, x,y-stage or x,y,z-stage, and software program at maps samples" US2014166875-A1, Trimpin, S.

6.1 Introduction

High-throughput screening is an important need of the pharmaceutical industry including drug design and clinical applications.¹⁷⁸⁻¹⁸⁰ Commonly used technologies are fluorescence,¹⁸¹ electrophoresis,¹⁸² and mass spectrometry (**MS**).¹⁸³ While electrospray ionization (**ESI**) has a number of advantages, matrix-assisted laser desorption/ionization (**MALDI**) is the faster ionization method by simply increasing the frequency of the laser used for desorbing/ionizing the matrix/analyte (e.g., 20 kHz).¹⁸⁴ Work on increasing the speed of ESI technology is based on using multiple inlets,^{185,186} an automated chip-based work flow (e.g., Nanomate),¹⁸⁷⁻¹⁹¹ or segmented flow.^{192,193} Recent years have seen a renaissance for ionization approaches used in MS. One result has been many clever ways to analyze materials under ambient conditions,⁸⁴ thus providing a convenient and direct means of sample analysis.^{89, 194} The novel methods that are capable of ionizing nonvolatile compounds are frequently based on ESI.^{33,156}

A series of *inlet* ionization methods^{107,109,111} have been discovered recently that produce ESI-like mass spectra from the solution or solid state. Ionization occurs in a heated pressure drop region linking atmospheric pressure (**AP**) with the first vacuum stage of a mass spectrometer. The simplicity of *inlet* ionization methods is that neither a high voltage nor a laser is required, and the natural gas flow through the inlet replaces the necessity of a nebulizing gas. Multiply charged ions produced by these methods extend the mass range of high performance mass spectrometers,¹⁰⁷ enhance separations by charge states in ion mobility spectrometry (**IMS**),¹³² and allow advanced fragmentation using electron-transfer dissociation (**ETD**).¹³⁴ Several modes of analyzing surfaces and solutions are available with *inlet* ionization, some providing high spatial resolution or

high-speed imaging.¹⁹⁵ These ionization methods, even in their early development, are highly sensitive as has been shown for bovine insulin and steroids.^{111,196}

Solvent assisted ionization inlet (**SAII**) is the liquid introduction variant of the family of *inlet* ionization operating without a laser or a voltage and capable of coupling with a liquid chromatography (**LC**)^{112,196} and nano-LC/MS/MS¹⁹⁷ with high sensitivity (7 ng of bovine serum albumin (**BSA**) tryptic digest injected on column,¹⁹⁷ and low femtograms for steroids¹⁹⁶). Because in SAI, the exit end of a fused-silica capillary is placed inside the inlet, a pressure differential drives the flow of solvent into the mass spectrometer without the need of a pump.¹¹¹ The best sensitivity was achieved in the initial approach by aligning the fused-silica tube to a “hot spot” within the inlet tube.¹¹¹ Subsequent SAI work showed that for nanoliter flow, good sensitivity (e.g., 10 fmol of a BSA digest by LC/MS), is achieved simply by placing the LC outlet in front of the inlet aperture of the mass spectrometer.¹⁹⁷ Solution is swept into the inlet in the flow of air, and analyte is ionized in the inlet.

Here, we present a flexible SAI approach based on direct injection and use of disposable pipet tips for the analyses of compounds independent of molecular weight and volatility. This method can be used to conveniently map solution content, location, and relative quantities in a high-throughput manner.

6.2 Materials and Methods

Materials and Sample Preparation.

Clarithromycin tablet (500 mg) was obtained from local pharmacy and ground to fine powder by mortar and pestle. Other general chemicals were stated in **Chapter 2**. For the experiments using directly pipetting, the phosphorylated peptide mixture was prepared in

50:50 acetonitrile:water with 0.1% formic acid for positive mode acquisition at 150 °C, and in 0.5% ammonia for negative mode acquisition at 400 °C. Myoglobin and carbonic anhydrase were diluted in water with 0.1% formic acid and analyzed at inlet temperature of 250 °C. In the pH study, bovine insulin and lysozyme solutions at pH of about 3, 4.5, 6, and 9 were tested. Bovine insulin stock solutions were prepared in 50:50 methanol:water with 1% acetic acid and 50:50 methanol:water with 1% ammonia. Then the acidic solution was diluted with methanol:water with acetic acid or water, and the basic solution was diluted with methanol:water with ammonia or water. Lysozyme was prepared by dissolving lysozyme in 1% formic acid, 50:50 acetonitrile:water with 0.1% formic acid, 50:50 acetonitrile:water with 0.05% formic acid, water, and 0.1% ammonia, respectively. Carbonic anhydrase was diluted in water with 0.1% formic acid.

For the experiments using the 8-channel pipette, leucine enkephalin and galanin were prepared in water with 0.1% formic acid, and ubiquitin was in 50:50 acetonitril:water with 0.1% formic acid. Clozapine was diluted by methanol to desired concentrations. For the analysis of tablets, 8 wells in the first row of the 384-well microtiter plate (Greiner Bio-One Inc., Monroe, NC) were filled with 100 μ L methanol. A pipette tip was used to dip into the tablet powder, transferred random amount of the powder and swirled them into the second, fifth, and eighth well (**Scheme S6.2** in Appendix C). The tablet solutions were then diluted 100 fold by methanol in the second row of the microtiter well plate, and the diluted tablet solutions were diluted again 100 fold in the third row (**Scheme S6.2.A** in Appendix C).

For experiments using the 96-well plate, analytes were diluted from their stock solutions using the following solvent systems: clozapine was in methanol, sphingomyelin

was in methanol with 1% acetic acid, bovine insulin in 50:50 methanol:water with 1% acetic acid, and all the others were in 50:50 acetonitrile:water with 0.1% formic acid.

Methods.

The SAII-MS and SAII-MS/MS experiments were carried out on an LTQ Velos mass spectrometer (Thermo Fisher Scientific, Bremen, Germany), from which the ESI source was removed and interlocks overridden as described previously.¹³⁵ The inlet of the mass spectrometer was heated between 150 to 450 °C depending on solvent and its pH. To avoid cross contamination, pipet tips filled with only solvent, used for dissolving the analyte in the previous pipet tip, were added to alternate pipet tips. Mass spectra were displayed as a single acquisition, generally by acquiring 1 microscan and with the maximum injection time of 100 ms for pipetting, 1 microscan and 300 ms maximum injection time for multiplexing, unless otherwise stated. Collision induced dissociation (**CID**) and electron transfer dissociation (**ETD**) were employed for characterization of certain analytes by selecting the parent ion using a mass tolerance of 1 m/z unit. Similar to a previous study,¹⁹⁸ the CID MS/MS spectra were obtained using a normalized collision energy setting between 20 to 30 depending on the analyte, and ETD using an activation time of 100 ms.

For these experiments, pipet tips (10 μL micropipet tips, Fisher Scientific, Pittsburgh, PA) are aligned with the MS inlet by having them held in an 8-channel pipet holder or the 96-pipet tip holder in which new pipets are shipped. Solutions containing sample, or blank, were loaded by simultaneously dipping the pipet tips into a 96 multivial or well plate containing the various analyte solutions; ~ 3 μL of each solution is drawn into the pipet tip by capillary action (based on acetonitrile/water solution). The holder was affixed

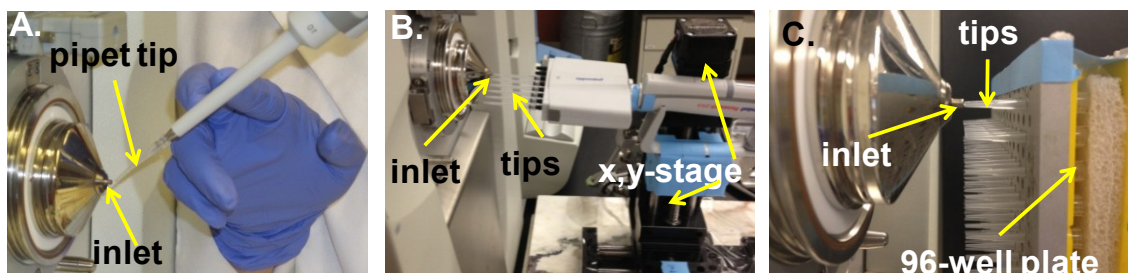
on the x,y-stage with the first pipet tip (typically empty) placed in close proximity (~ 0.1 mm at low inlet temperatures and ~ 0.5 mm at high inlet temperature) to the inlet aperture. Using the control of the x,y-stage, rows of pipet tips were moved automatically in front of the inlet aperture so that the solution containing the analyte exits the pipet tip under the influence of the pressure differential when the tip is in close proximity with the inlet aperture of the mass spectrometer. The x,y-stage movement was continuous, and rate of movement was controlled from 1.5 to 18 mm s⁻¹. Data were acquired in the mass-to-charge (m/z) range of 150–2000, unless otherwise stated. Mass spectra were displayed as a single acquisition, generally by acquiring 1 microscan and with a maximum injection time of 100 ms for pipetting, 1 microscan and 300 ms maximum injection time for multiplexing, and 1 microscan and 500 ms maximum injection time for quantitative studies. Biomap imaging software (Novartis Institution for Biomedical Research, Basel, Switzerland), typically used for imaging applications,^{135,195,199} was incorporated to map in which solution analyte was present as determined by the m/z ratio values obtained by MS or MS/MS. Besides mapping the location of analyte, the software allows relative concentrations to be displayed by color code.

6.3 Results and Discussion

Initial results were obtained using a single pipet and purchased standards. Sample solution was introduced for mass analysis from a pipet tip held close to the inlet aperture of the mass spectrometer. For ease of operation, the source housing was removed and interlocks overridden. Analyte ions were observed as soon as the pipet tip was close, but not touching, the heated (150 °C) inlet tube entrance of the LTQ Velos and solution was

drawn into the inlet (**Scheme 6.1A**). Standards, and standard mixtures, of varying concentrations were run to acquire initial benchmark results for ongoing improvements.

Scheme 6.1. Pictures of the SAII source setup using (A) a single pipet, (B) an 8-channel pipet, (C) a 96-pipet array; loading of the samples through use of the 96 sample plate is displayed in **Scheme S6.1** in Appendix C. (B) and (C) are automated by mounting the pipet holder on a xy-stage and mapping of the location is achieved through inclusion of the Biomap program.



With phosphorylated peptides, both positive (**Figure 6.1A**) and negative (**Figure 6.1B**) ions were produced using this method without the loss of phosphorylation. Fragmentation using collision-induced dissociation (**CID**) provides good sequence coverage of each phosphorylated peptide dispensing 1 μL of a 2.5 pmol μL^{-1} solution (**Figure S6.1** in Appendix C). Proteins as large as myoglobin and carbonic anhydrase are efficiently ionized and detected using this approach (**Figure S6.2** in Appendix C). The angle of the pipet relative to the inlet had little effect so long as solution was drawn into the inlet. Results from this study demonstrated that SAII is operationally simple and tolerant of a wide range of solvents, such as 100% water (**Figure S6.3A** in Appendix C), chloroform (**Figure S6.3B** in Appendix C), or 90% acetonitrile (**Figure S6.3C** in Appendix C).

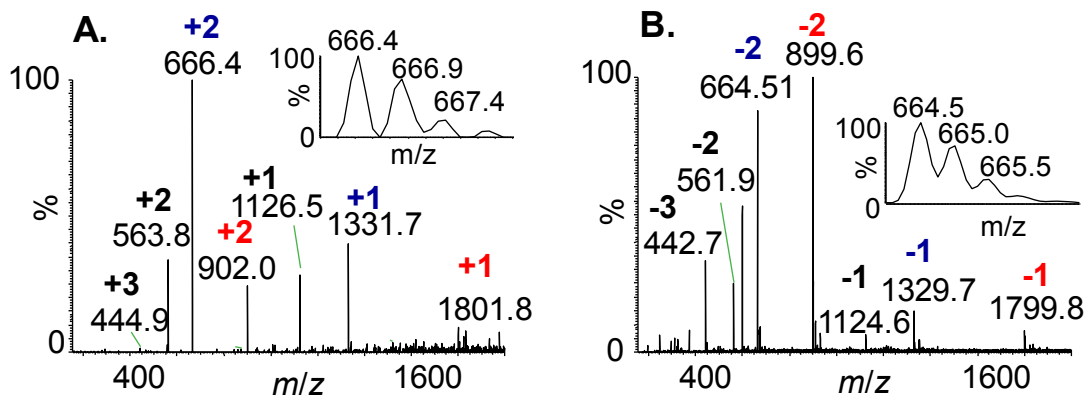


Figure 6.1. A mixture of phosphorylated peptides (angiotensin II, molecular weight (MW) 1125; cholecystokinin (10-20), MW 1330; and calcitonin (15-29), MW 1800) was pipetted into the inlet (**Scheme 6.1A**). 1 μL of 2.5 pmol μL^{-1} solution was used for each acquisition. Mass spectra of the mixture were obtained in (A) positive acquisition mode at 150 $^{\circ}\text{C}$ and (B) negative acquisition mode at 400 $^{\circ}\text{C}$. The MS/MS spectra (CID) of each peptide are shown in **Figure S6.1** in Appendix C. Data were acquired in the m/z range of 50-2000 for positive mode and 155-2000 for negative mode.

A pH study using bovine insulin and lysozyme was carried out at an inlet temperature of 250 $^{\circ}\text{C}$ showing higher charge state ions were obtained in acidic solutions and that the highest intensity for the most abundant charge state was obtained at pH \sim 4.5 for lysozyme (**Figure S6.4** in Appendix C). Basic pH decreased the charge states of bovine insulin. A temperature study using bovine insulin and lysozyme solutions is shown in **Figure S6.5** in Appendix C. Similar charge states but increasing ion abundance are observed at higher temperatures (100 $^{\circ}\text{C}$ increments from 150 to 450 $^{\circ}\text{C}$) as expected from previous SAIL studies on an Orbitrap with the solution introduced inside the inlet tube.¹¹¹ Over a wide range of temperatures, the method shows analytical utility. Higher temperature is required to produce abundant ions when less volatile solvent, e.g., water, is used (**Figure S6.6** in Appendix C). However, “signal tailing” is observed using pure water and at high temperature indicating the undesired adduction of sodium cations to the

protein. Metal adduction is prevented through the addition of acids (**Figure S6.5II** in Appendix C), as noted in previous SAI studies.^{111,114} The accumulation of results show that, although the optimum inlet temperature is somewhat different for certain analytes and sample preparation methods, sufficient ion abundance for analytical utility is obtained over a wide range of conditions. As is the case with the traditional methods of ESI and MALDI, smaller molecules are more easily detected than the larger nonvolatile molecules. The optimal inlet temperature of the LTQ Velos is lower than those reported for an Orbitrap Exactive in which solution was introduced inside the mass spectrometer inlet.¹¹¹

An advantage of the approach used here is that the volume of solution introduced to the inlet can be better controlled using pipet tips relative to using fused-silica tubing, and because the tips are disposable, cross contamination caused by sample adhering to the walls of the fused silica is eliminated. The initial automation experiment with pipet tips used an 8-channel pipet. The setup, designed to operate with the capillary inlet source of the LTQ Velos, is shown in Scheme 6.1B. Three microliters of solutions containing leucine enkephalin ($2.5 \text{ pmol } \mu\text{L}^{-1}$), galanin ($1 \text{ pmol } \mu\text{L}^{-1}$), and ubiquitin ($1 \text{ pmol } \mu\text{L}^{-1}$) were simultaneously drawn from multisample well plates into alternate pipet tips with pure solvent between each solution. The dispenser was fastened to an x,y-stage, and each tip was sequentially moved in front of the inlet of the mass spectrometer. The setup was previously aligned so that all plotting the total ion chromatogram (TIC) (**Figure 6.2A**), from which mass spectra of leucine enkephalin, galanin, and ubiquitin were extracted. Good ion abundance was observed for each sample without cross contamination (**Figure 6.2B.1–D.1**). The Biomap software displays the location of any selected m/z in the

sampled multisample well plate, as is commonly performed with imaging of tissue sections.^{135,195,199} This is exemplified in Figure 6.2B.2–D.2 for leucine enkephalin (+1, m/z 556), galanin (+3, m/z 1053), and ubiquitin (+7, m/z 1224) using 150 °C inlet temperature. The mass spectra from the same set of analytes tested at different inlet temperatures (250, 350, and 450 °C) are similar (Figure S6.7 in Appendix C).

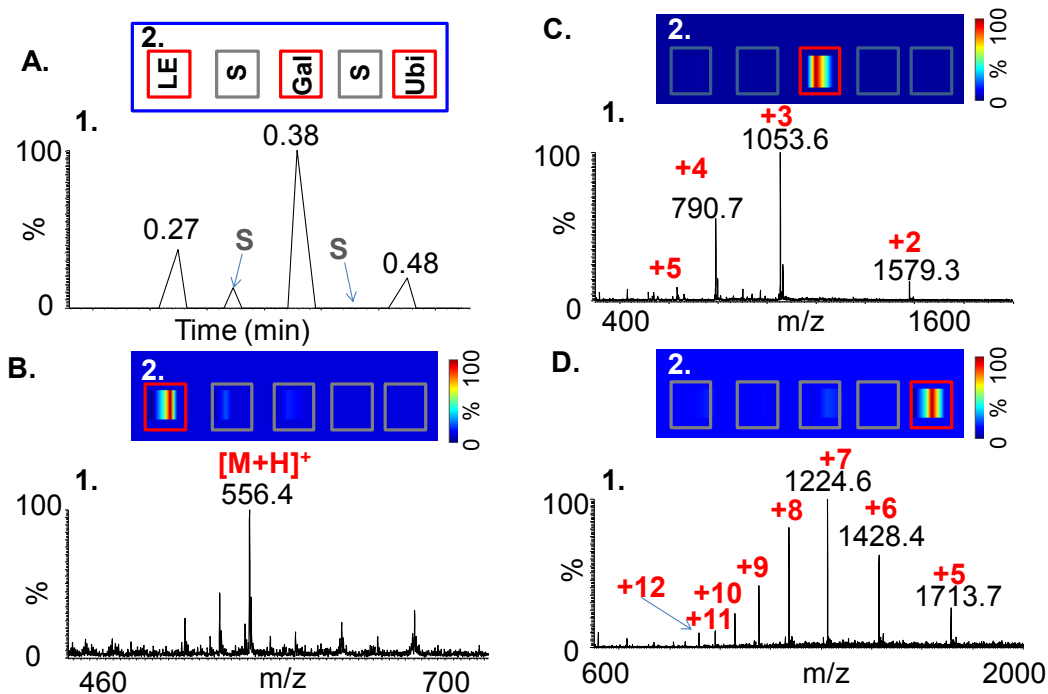


Figure 6.2. Multiplexing SAII-MS using the 8-channel pipet (Scheme 6.1B) at an inlet temperature of 150 °C. The analysis of 5 tips filled (3 μL) with 3 different samples with solvent (S) between each two samples. (A) Total ion chromatogram (TIC): (1) Mass spectra and (2) mapping of the location of individual analytes: (B) 2.5 $\text{pmol } \mu\text{L}^{-1}$ leucine enkephalin (LE, m/z 556), (C) 1 $\text{pmol } \mu\text{L}^{-1}$ galanin (Gal, m/z 1053), and (D) 1 $\text{pmol } \mu\text{L}^{-1}$ ubiquitin (Ubi, m/z 1224). Data were acquired in the m/z range of 300-2000.

However, split peaks are observed in the TIC at 350 and 450 °C because the pipet tips needed to be further from the inlet to prevent pipet melting which caused the solutions to be drawn inconsistently and slowly so that, instead of a liquid stream, droplets are drawn into the inlet. The pipet tip size is not critical, but with the present setup, the smaller tips

are more difficult to align properly with the inlet. It is interesting to note that the speed of the x,y-stage has little impact for any given size of pipet tips tested. As soon as the solution is exposed to the vacuum, it is drawn into the mass spectrometer and analyte rapidly ionized. However, even smaller size tips than explored here are expected to slow the speed of solution exiting the pipet, as has been demonstrated for the picotips using nano-ESI.¹⁹⁷

The rate of analyses can be paced by adjusting the movement of the x,y-stage and can be as short as one sample/s, accepting some cross contamination between samples. In principle, one could also actively stop the x,y-stage movement at the expense of time requirements. Figure S6.8 in Appendix C displays the analysis of three analytes (angiotensin I, bovine insulin, and ubiquitin) in only 2 s with some acceptable carryover between samples. For high-throughput screening this performance may already be sufficient. Using this construction, three solutions of an antipsychotic drug clozapine at 25, 250, and 500 fmol μL^{-1} were mapped for relative amounts (**Figure 6.3I**). Two solvents were used between each two analyte solutions. Different clozapine solutions or pure methanol solvent were filled in the tips as indicated in Figure 6.3IA. MS/MS was used to enhance the specificity of the experiment. The protonated ion (m/z 327) was selected and fragmented by CID. The mass spectral data of the transition, $327 \rightarrow 270$,^{23,200} is visualized by a mapping display using Biomap (**Figure 6.3IB**). The color trace correctly displays the location of the analytes with little or no carryover in the methanol acquisitions. The color code also reflects the relative analyte concentration, with blue at lower concentrations and red at higher concentrations. **Figure 6.3II** shows

the TIC (**Figure 6.3IIA**) and mass spectra with ion abundances (**Figure 6.3IIB**) for each of the samples.

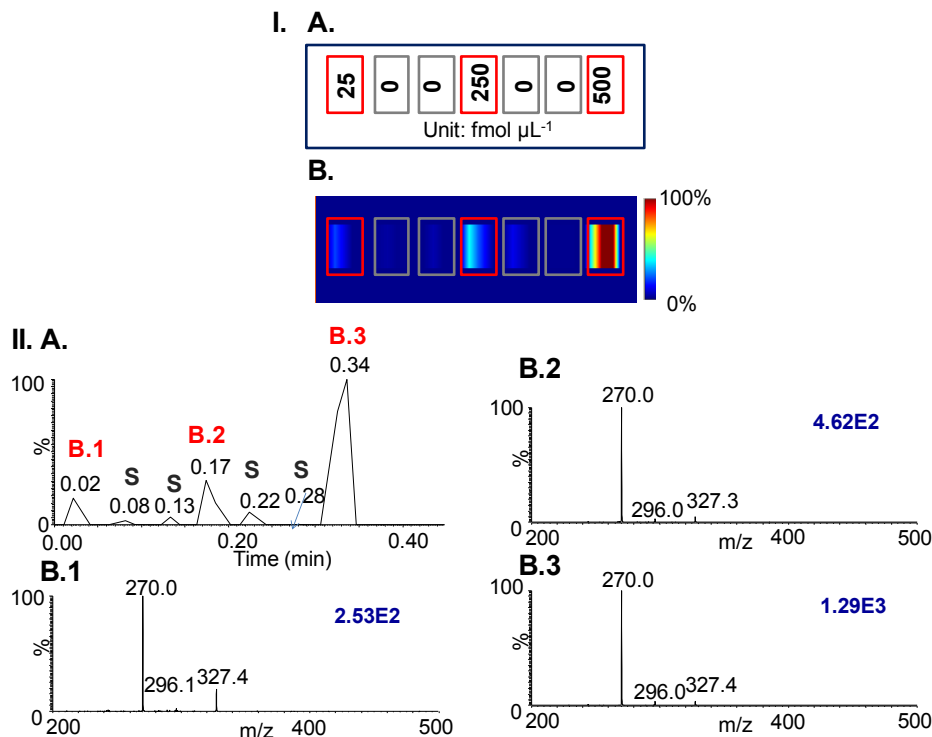


Figure 6.3. Mapping using the 8-channel pipette (**Scheme 6.1B**). **(I)**: **(A)** Schematic representation of content in each pipette tip. Red boxes indicate tips filled with 2 μL clozapine solutions at 25 fmol μL^{-1} , 250 fmol μL^{-1} , and 500 fmol μL^{-1} , respectively; grey boxes represent pure solvent methanol; **(B)** The mapping of m/z 270 peak. **(II)**: **(A)** TIC and **(B)** Mass spectra extracted from **(1)** 0.02 min, **(2)** 0.17 min, and **(3)** 0.34 min of the TIC. Data were acquired in the m/z range of 200-500.

Using the same approach and concentrations, the more concentrated analyte may have an effect on the less concentrated samples as is seen in the mapping display of the methanol solutions (**Figure S6.9** in Appendix C). If necessary, more tips containing methanol blank solutions can be employed to reduce cross contamination between samples for quantitative analyses. Using this approach, a 1 μL solution of 1 fmol μL^{-1} clozapine was readily detected (**Figure S6.10** in Appendix C). This automated method is

therefore sensitive, rapid, simple, and robust and can characterize small and large molecules.

The comparison of introducing the same amount of ubiquitin (3 μL) by either manually injecting or vacuum drawing (**Figure 6.4**) shows that both methods produce nearly identical results. A tip-to-inlet distance of ca. 0.5 mm allows solution transfer without concern for the tip melting at higher inlet temperature, but increasing distance beyond this makes drawing the entire content of each pipet problematic. The ability for the sample to be dispensed for ionization only when the tip of the pipet is close to the entrance aperture, to make use of the mass spectrometer vacuum for sample introduction, suggests a simple means for high-throughput sampling.

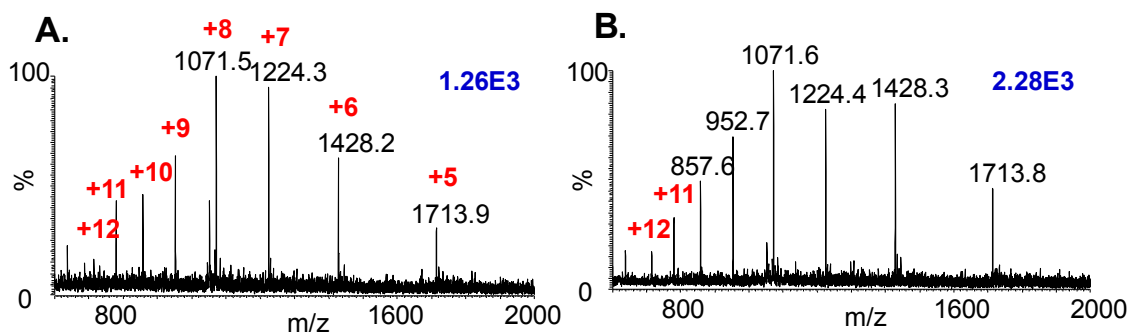


Figure 6.4. SAIL mass spectra of ubiquitin at inlet temperature of 250 $^{\circ}\text{C}$. Solutions of 3 μL of 1 pmol μL^{-1} were introduced by (A) manually pipetting and (B) vacuum drawing (**Scheme 6.1A**). Data were acquired in the m/z range of 150-2000.

The number of samples which can be analyzed in a single automated analysis was therefore extended using a commercial 96-pipet holder (**Scheme 6.1C**) to affix the pipet tips for sampling 96-well plates. Because of the physical limitations of our x,y-stage relative to the mass spectrometer inlet, only 84 samples of the possible 96 positions were in the range of the x,y-stage motion. Sample loading is straightforward because the pipet tips only need to be placed into the well of a multisample plate containing the various

solutions and capillary action loads the pipet tips with approximately the same volume of each solution/solvent (**Scheme S6.1** in Appendix C) providing the solvents used are of approximately the same composition, especially in water content. On the basis of a 1:1 acetonitrile:water solution, and the pipet tips used in the experiment, ca. 3 μL are drawn into each of the pipet tips. Different pipet tips are expected to load different volumes, and higher viscosity solvents, such as water, are more problematic using this approach so that organic solvents such as acetonitrile or methanol were added to lower viscosity. Again, to avoid the possibility of carryover, solvent was placed between any two samples.

A typical TIC is shown in Figure 6.5I in which 42 tips out of 84 were analyzed with seven different analyte solutions providing six analyses of each solution. This corresponds to 1 sample per 5 s for the analyses of liquid samples using this approach. Individual mass spectra of clozapine, leucine enkephalin, sphingomyelin, galanin, bovine insulin, ubiquitin, and lysozyme (**Figure 6.5II**) are observed with little or no cross contamination. Because of multiply charging, proteins can also be analyzed on a limited m/z mass spectrometer. The minimal chemical background allows small and large molecules to be characterized at subpicomole concentration using an inlet temperature of 250 $^{\circ}\text{C}$. All six mass spectra for bovine insulin extracted from each cycle are displayed in Figure S6.11 in Appendix C showing poor reproducibility as indicated by the ion intensity. We attribute this to the difficulty with our home-built approach to properly align all 84 pipet tips in the same position relative to the inlet aperture.

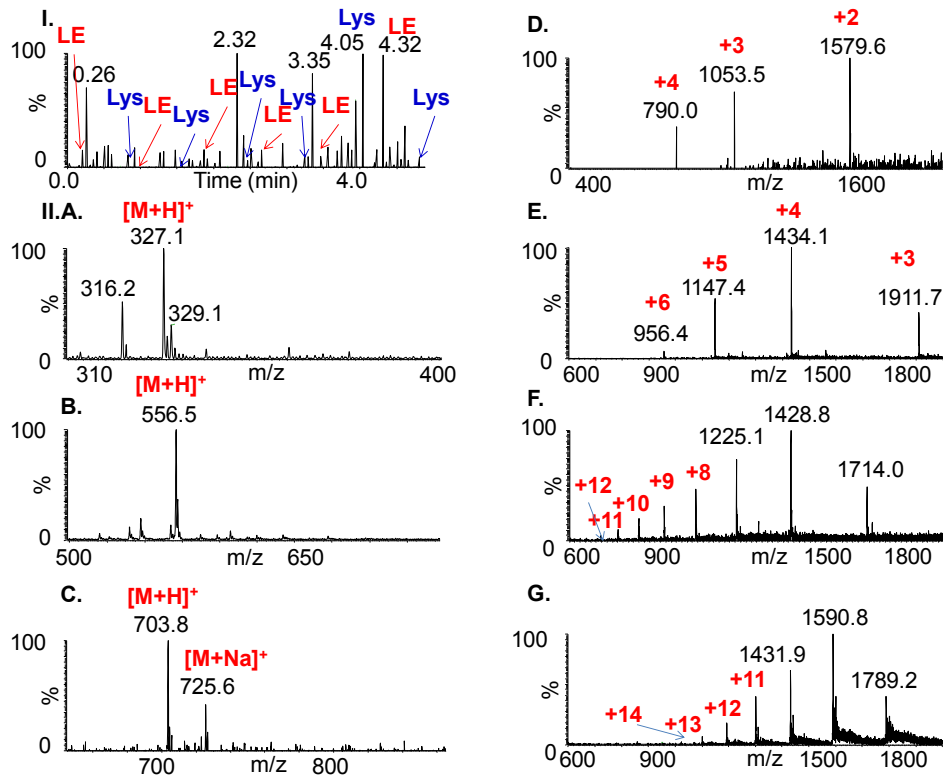


Figure 6.5. SAI-MS using 84 tips mounted on a 96-well pipet tip holder (Scheme 6.1C) with the inlet temperature at 250 °C acquired in ~5 min. (I) Total ion current. (II) Mass spectra of (A) 1 pmol μL^{-1} clozapine (in methanol), (B) 2.5 pmol μL^{-1} leucine enkephalin (in acetonitrile:water with formic acid), (C) 1 pmol μL^{-1} sphingomyelin (in methanol with acetic acid), (D) 1 pmol μL^{-1} galanin (in acetonitrile:water with formic acid), (E) 5 pmol μL^{-1} bovine insulin (in methanol:water with acetic acid), (F) 1 pmol μL^{-1} ubiquitin (in acetonitrile:water with formic acid), and (G) 10 pmol μL^{-1} lysozyme (in acetonitrile:water with formic acid). Data were acquired in the m/z range of 150-2000.

Figure S6.12 in Appendix C provides the TIC and mass spectra of the same set of samples at lower speed. All 84 pipet tips (42 samples) were analyzed in ~10 min by reducing the x,y-stage movement to 1.5 mm s^{-1} . No cross contamination was observed, but at the expense of longer analysis time. This approach is also less reproducible for larger molecules. However, in these experiments we used compounds ranging in molecular weight from 326 to ~14300. In practice, better reproducibility and higher sensitivity is obtained if one only needs to look at a specific mass range for certain

compound types such as drugs or peptides. For example, analyzing for the drug clozapine in four different substantially lower concentrations (0.5–30 fmol μL^{-1}) using MS/MS and mapping m/z 270, the location and the relative amount present are correctly displayed for each vial (**Figure S6.13** in Appendix C).

Higher capacity microtiter plates are widely used in pharmaceutical industry. A 384-well plate was used to analyze the drug clarithromycin in form of a tablet obtained from a local pharmacy. Random amounts of tablet powder were dissolved and diluted in the microtiter plate wells (**Scheme S6.2** in Appendix C) and analyzed using CID with solution introduction using the 8-channel pipet approach (**Figure 6.6I**). The major fragment ion at m/z 590²⁰¹ was mapped using Biomap software. The map correctly displays the locations where drug was present (**Figure 6.6II**). The first well with the first sample contains the highest amount of tablet and the fourth well with the second sample contains the least based on the color code of the map.

For the pipet tips used in this study, the speed of sample introduction is greatly influenced by the exposure to the vacuum, and thus on the distance of the pipet exit to the inlet aperture of the mass spectrometer, the scanning nature of the mass spectrometer, and little if at all on the speed of movement of the x,y-stage. With increasing numbers of samples, reproducibility becomes more challenging to achieve because of alignment issues with the current method. Another possible issue is the pulsed nature of the ionization, which may be improved using the appropriate analyzer with ion trapping synchronized with the ionization event similar to the challenges previously observed with MALDI.^{202,203} It is expected that this can be optimized using shorter ion trapping and

multiple microscans. Narrower scan windows will increase reproducibility as is the case for any targeted ESI analyses approach.^{204,205}

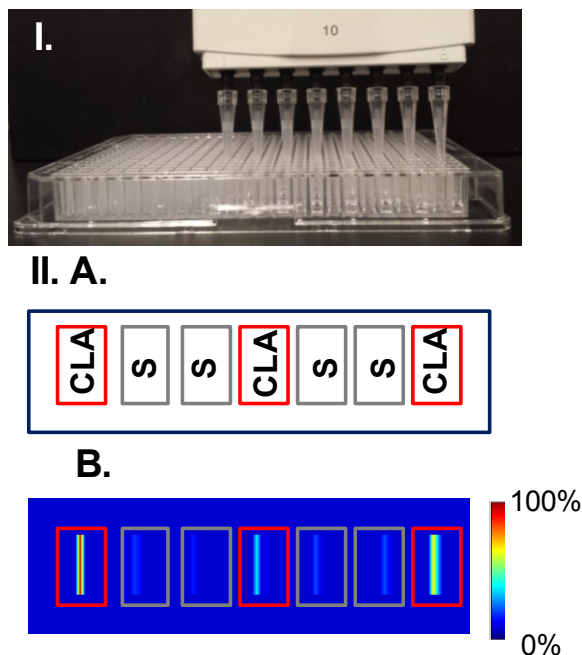


Figure 6.6. Mapping of clarithromycin from tablet in a 384-microtiter plate using the 8-channel pipette (**Scheme 6.1B**). **(I)** Picture of loading tablet solution and pure solvent from microtiter plate to pipette. **(II)(A)** Schematic representation of content in each pipette tip. Red boxes indicate tips filled with solutions containing clarithromycin tablet (**CLA**); grey boxes represent pure solvent methanol (**S**); **(B)** The mapping of a major fragment at m/z 590.3. Data were acquired in the m/z range of 205-1000.

At the current stage of development, automation of the SAI method provides a simple high-throughput analysis approach for compounds regardless of mass, volatility, or “sprayability”. With this approach potentially 4000 samples that can be analyzed per day per instrument using profile mode without significant cross contamination. Such an achievement will require more reproducible control of sample position relative to the mass spectrometer inlet. Higher throughput is envisioned with larger well plate numbers.

6.4 Conclusion

Mapping of select compounds in microtiter plate wells is an obvious application of this new technology, but any area in which fast analyses are valued such as proteomics, metabolomics, and lipidomics could be impacted. It is our expectation, based on current performance, that some of these new ionization technologies in conjunction with IMSMS,²⁰⁶⁻²⁰⁸ ETD,^{209,210} and LC,²¹¹⁻²¹⁴ will have considerable advantages relative to current analytical methods. The potential of these methods for direct analyses of complex mixtures will be achieved using high mass resolution available with Fourier transform instruments.²¹⁵

CHAPTER 7

MATRIX ASSISTED IONIZATION VACUUM FOR HIGH RESOLUTION FOURIER TRANSFORM ION CYCLOTRON RESONANCE MASS SPECTROMETERS

Matrix-assisted ionization vacuum (**MAIV**) produces charge states similar to electrospray ionization (**ESI**) from the solid state without requiring high voltage or added heat. MAIV differs from matrix-assisted laser desorption/ionization (**MALDI**) in that no laser is needed and abundant multiply charged ions are produced from molecules having multiple basic sites such as proteins. Here we introduce simple modifications to the commercial vacuum MALDI and ESI sources of a 9.4 T Fourier transform-ion cyclotron resonance (**FTICR**) mass spectrometer to perform MAIV from both intermediate and atmospheric pressure. The multiply charged ions are shown for the proteins bovine insulin, ubiquitin, and lysozyme using 3-nitrobenzonitrile as matrix. These are the first examples of MAIV operating at pressures as low as 10^{-6} mbar in an FT-ICR mass spectrometer source, and the expected mass resolving power of 100000 to 400000 is achieved. Identical protein charge states are observed with and without laser ablation indicating minimal, if any, role of photochemical ionization for the compounds studied.

B. Wang, E. Tisdale, C. L. Wilkins, S. Trimpin, *Anal. Chem.* **2014**, *86*, 6792-6796.

Reprinted with permission from Copyright (2014) American Chemical Society.

7.1 Introduction

High-field Fourier transform ion cyclotron resonance (**FT-ICR**) mass spectrometry (**MS**) is an important tool used in the analyses of biological materials because of the high mass resolving power.²¹⁶ Frequently FT-ICR mass spectrometers are coupled with electrospray ionization (**ESI**)⁹¹ to take advantage of multiply charged analyte ions which bring the mass-to-charge (m/z) within instrumental limits. ESI requires analyte to be desolved in a “sprayable” solvent and hundreds of volts applied to achieve analyte ionization.³³ Vacuum matrix-assisted laser desorption/ionization (**MALDI**) produces gas-phase ions from the solid state using a vacuum stable matrix that has absorption at the laser wavelength.^{31,35,217-219} An advantage of ionization at vacuum is that ion transmission losses^{65,220} common with atmospheric pressure ionization (**API**) methods is mitigated.

Inlet ionization is an alternative method producing ESI-like multiply charged gas-phase ions from the solid state with the assistance of a matrix (e.g., 2,5-dihydroxybenzoic acid, 2,5-DHB), vacuum, and heat.^{18,107,109} Ionization is initiated in the heated inlet tube without use of voltage or laser ablation.¹²¹ The first examples of coupling laserspray ionization inlet (**LSII**) and matrix-assisted ionization inlet (**MAII**) to high field FT-ICR MS were achieved on a home-built LTQ 14.5 T FT-ICR mass spectrometer by heating a ~10 cm long inlet capillary to 350 °C.²¹⁵ Myoglobin (17 kDa) was detected by MAII. The need for applicability on mass spectrometers that do not use a heated inlet tube, initiated a quest for more volatile matrix compounds that might operate at lower inlet temperature.¹¹⁰

The discoveries of more volatile matrices led to *vacuum* ionization, which unlike *inlet* ionization, is dependent on matrices that do not require a heated inlet tube to produce ions

having ESI-like charge states. The ability to produce highly charged ions by laser ablation of the matrix 2,5-dihydroxyacetophenone (**2,5-DHAP**) was first developed on a commercial intermediate pressure (0.21 mbar) MALDI ion source of an ion mobility spectrometry-mass spectrometer (SYNAPT G2).¹¹⁵ The more volatile matrix, 2-nitrophenol (**2-NPG**), was later shown to produce multiply charged ions from proteins upon laser ablation on a high vacuum (10^{-6} mbar) MALDI-TOF mass spectrometer.¹¹⁶ Charge states observed at high vacuum are lower than at intermediate and atmospheric pressure. A similar vacuum (10^{-6} mbar) is used on MALDI sources coupled to FT-ICR mass spectrometers.²²¹

One of the more volatile matrix compounds discovered, 3-nitrobenzonitrile (**3-NBN**), produces ions having ESI-like charge states when used as a matrix and introduced with incorporated analyte into the intermediate pressure vacuum MALDI source of a SYNAPT G2 mass spectrometer without laser ablation.¹¹⁷ This method, which eliminates the need of a laser, is termed matrix-assisted ionization vacuum (**MAIV**). MAIV ionizes a wide range of compounds, including bovine serum albumin (66 kDa). 3-NBN is amenable to sample introduction from atmospheric pressure with tube or skimmer inlets and produces ions at atmospheric pressure simply using mild heat.^{119,222} Working from atmospheric pressure, proteins such as lysozyme (14.3 kDa) and carbonic anhydrase (28 kDa) are ionized, and the method's tolerance of salts enables direct analysis of urine and blood.^{117,120}

MAIV matrices are hypothesized^{117,118} to require sublimation as well as charge separation through the fracturing process that produces triboluminescence; 3-NBN fulfills both of these proposed requirements.²²³⁻²²⁵ Here, we describe the implementation of

MAIV using both the vacuum MALDI and atmospheric pressure ESI sources of a 9.4 T FT-ICR mass spectrometer and discuss the role of vacuum in the ionization process.

7.2 Materials and Methods

Materials and Sample Preparation. Chemicals were obtained and stock solution prepared as stated in **Chapter 2**. The peptide mixture was prepared by mixing leucine enkephalin, angiotensin I, bombesin, allatostatin, and bovine insulin with the volume ratio of 3:3:1:1:1. The angiotensin mixture contains 1 mg mL⁻¹ of angiotensin I, angiotensin II, and angiotensin (1–9) fragment in water solution. The MAIV matrix 3-nitrobenzonitrile (**3-NBN**) was prepared by dissolving 5 mg in 50 μ L (concentrated) identical to the previous study,¹¹⁷ or 500 μ L (diluted) acetonitrile with 0.1% formic acid. The LSIV matrix 2-nitrophenol (2-NPG) was prepared by dissolving 5 mg in 100 μ L 50:50 acetonitrile:water identical to previous work.¹¹⁶ For MAIV experiments on the MALDI source, angiotensin I and bovine insulin were prepared by spotting 1 μ L of analyte on a AnchorChip plate (Bruker, Bremen, Germany) followed by adding 1 μ L concentrated matrix solution; 3 μ L ubiquitin was spotted on 384 ground steel plate (Bruker, Bremen, Germany), and 1 μ L diluted matrix solution was added. Samples were allowed to air-dry before loading the plate to the vacuum source. For LSIV experiments, all analytes were premixed with the matrix 2-NPG in a 1:1 volume ratio on AnchorChip target plates. For MAIV experiments from atmospheric pressure using the ESI source inlet aperture, angiotensin, bovine insulin, ubiquitin, and lysozyme were premixed with the concentrated 3-NBN matrix solution in a 1:1 volume ratio and stir-mixed using a pipet tip. The matrix:analyte mixture, 2 μ L, was drawn into a pipet tip and allowed to air-dry at its tip.

Vacuum Ionization on FT ICR Mass Spectrometer. The commercial high vacuum MALDI and ESI sources on a 9.4 T Apex FT-ICR mass spectrometer (Bruker, Bremen, Germany) were used for MAIV and LSIV studies. The source pressure of the high vacuum MALDI source was $2.0\text{E}-6$ mbar. Bruker DataAnalysis was used to determine resolving power.

MAIV from High Vacuum. The sample plate was loaded after the samples were air-dried. The laser fluence was set to 0, and the laser beam was blocked with paper. The plate voltage was optimized at 240 V for angiotensin I, and 300 V for bovine insulin and ubiquitin. Acquisition was started once the matrix:analyte mixture spotted on the target plate was loaded. The acquisition size was 2 million points, and the mass spectra are 100 acquisitions summed for angiotensin I and bovine insulin. For ubiquitin, acquisition was stopped when the background started to increase; in this case, about 20 acquisitions were averaged.

LSIV from High Vacuum. Ubiquitin solution was mixed with 2-NPG matrix solution and spotted on a target plate. The sample plate was loaded after the samples were air-dried. For LSIV of ubiquitin, the arbitrary laser fluence was 50%, and the plate voltage was 400 V. The acquisition size was 512 K points for higher signal abundance. Twenty acquisitions were averaged to obtain a mass spectrum.

MAIV from Atmospheric Pressure. The commercial ESI source housing was removed, as well as the cover and the cap on the ESI capillary so that direct access to the capillary orifice was obtained. The capillary voltage, spray shield, nebulizing gas flow, and dry gas flow were all set to 0. On this dual ESI/MALDI source, the voltage on the MALDI plate was set at 300 V and the MALDI source was disabled. The capillary temperature was

kept at room temperature without additional heat. The dried matrix:analyte crystals on the pipet tip were introduced into the vacuum of the mass spectrometer by gently contacting the capillary opening. Acquisition lasted for about 2 min until the crystals were consumed from the pipet tip.

7.3 Results and Discussion

Inlet ionization methods were previously demonstrated on a high field FT-ICR mass spectrometer having a home-built heated inlet tube.²¹⁵ Meanwhile, matrix compounds were discovered that produce multiply charged gas-phase ions spontaneously without a laser or heat, other than the ambient heat available in the matrix and target plate, when exposed to low pressure conditions. Furthermore, the matrix, 3-NBN, produces abundant analyte ions when introduced from atmospheric pressure to the subambient pressure inlet aperture of a mass spectrometer without the necessity of a heated inlet tube.¹¹⁹ Previous studies have suggested that pressure may be an important variable in MAIV. The Bruker Apex 9.4 T FT-ICR mass spectrometer MALDI source operates at 2E^{-6} mbar, well below the source pressure of previous MAIV studies¹¹⁸ and provides the opportunity to determine if MAIV is compatible with high vacuum and ultrahigh mass resolving power.

The mass spectrum of ubiquitin (**Figure 7.1A**), with 3-NBN as matrix, produces a measured resolving power of 403000 at +9 (m/z 952.5206) using the vacuum MALDI FT-ICR source. The +4 charge state (m/z 1434.1586) of bovine insulin had a mass resolving power of 254000, and the +2 charge state of the peptide angiotensin I (m/z 648.8432) had a resolving power of 185000. The MAIV mass spectra acquired using the MALDI source produce the high resolving power characteristic of this FT-ICR mass spectrometer.²²⁶

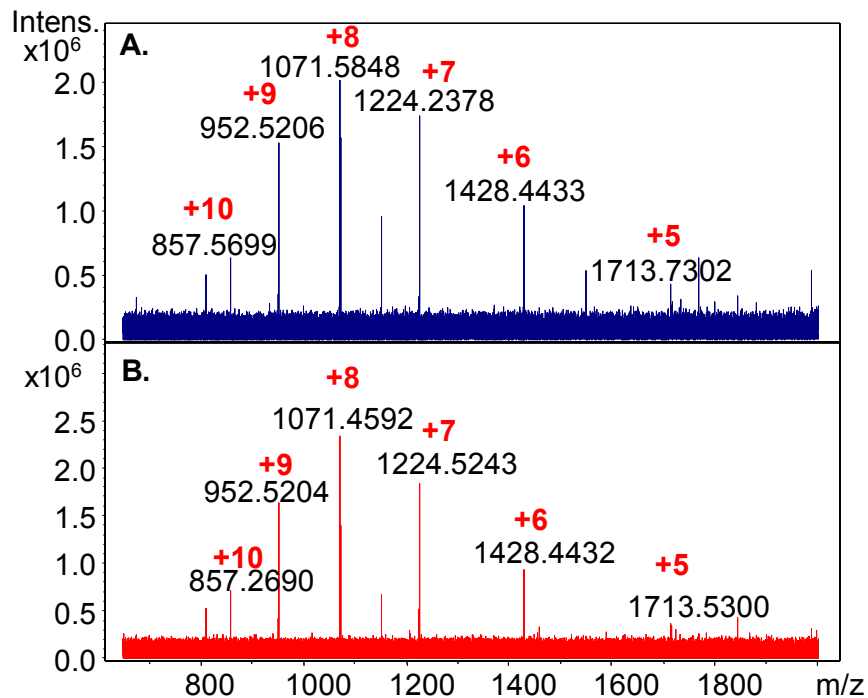


Figure 7.1. Mass spectra of ubiquitin using 3-NBN as matrix obtained on the high vacuum MALDI source of the Apex FT-ICR mass spectrometer (A) without (MAIV) and (B) with the use of a laser (LSIV) for matrix:analyte ablation.

In similar experiments using the intermediate pressure (0.21 mbar) MALDI source of a SYNAPT G2 mass spectrometer, the 3-NBN matrix produced analyte ions for ca. 2 min after the sample was loaded (3 min, including loading time).¹¹⁷ The time over which ionization is observed relates to the rate of sublimation of the matrix. In the lower pressure MALDI source ($2E^{-6}$ mbar) coupled to the Apex FT-ICR mass spectrometer, sublimation of the matrix occurred over a 30 min period. Ions could be observed during this time but in lower abundance.

In contrast to the SYNAPT G2 vacuum MALDI source in which the protein bovine serum albumin (66 kDaA) was analyzed using MAIV,¹¹⁷ ubiquitin was the largest molecule analyzed on the FT-ICR vacuum MALDI source. The most abundant and highest charge state ions for ubiquitin were lower on the FT-ICR than SYNAPT G2 for

the same compound. The most abundant ion shifts from +10 to +8, and the highest charge state shifts from +12 to +10.

The differences observed with the MAIV analysis using the MALDI source of a SYNAPT G2 and Apex FT-ICR logically relates to the pressure difference the sample experiences in the two instruments. Under vacuum conditions, sublimation cools the surface and at lower pressure heat transfer from the ambient environment is inefficient. Thus, an ionization process dependent on sublimation will be inhibited under cooling conditions. The higher pressure of the SYNAPT G2 MALDI source counters the cooling effect of sublimation through heat transfer to the matrix surface from the residual gas. A means of adding thermal energy is therefore expected to reduce the time over which ionization occurs, increase the ion abundance, and expand the compounds that act as matrices without need of a laser. This concept is supported by three independent studies. In the first study, the target plate of the SYNAPT intermediate pressure source was cooled, simultaneously inhibiting sublimation and ionization,¹¹⁸ but second, warming the inlet used with atmospheric pressure sample introduction reduces the time of ionization.¹²⁷ In a third study, a warmed gas flow (75 °C) was used to dislodge the matrix/analyte from the substrate holder to initiate analyte ionization.²²² Under the current conditions of the high vacuum source of the FT-ICR, proteins larger than ubiquitin may not be observed because they cannot be removed from the surface under the cooler conditions, or once removed they are not able to shed the matrix that accompanies them into the gas phase.¹²²

Although the 3-NBN matrix absorbs 355 nm photons poorly, a Nd:YAG laser was used to ablate the matrix crystals over several minutes. Even though the rate of removal

of the matrix was increased, no change in charge states and only a small increase in ion abundance was observed for ubiquitin (**Figure 7.1B**). The minimal influence of the laser fluence on ionization strongly suggests that the nitrogen discharge related to triboluminescence of this matrix^{224,225} is not directly involved with ionization. In other words, it is the charge separation that causes triboluminescence that is important and not the dinitrogen discharge.

The 2-NPG matrix was previously shown to produce ESI-like charge states of analyte by UV laser ablation using the SYNAPT G2 MALDI source.¹¹⁶ This matrix, however, performs poorly relative to the more volatile 3-NBN matrix on the FT-ICR MALDI source. Both the charge state and ion abundance are lower with the less volatile 2-NPG than with the most volatile 3-NBN matrix. For example, FT-ICR of ubiquitin in 2-NPG using laser ablation produced up to the +4 charges with +2 as the most abundant (**Figure S7.2** in Appendix D), while MAIV of the same analyte solution and mass spectrometer using 3-NBN as matrix with or without the laser provided up to +10 charges (**Figure 7.1**) and with higher ion abundance and signal-to-noise ratio. The vacuum Apex FT-ICR results are similar to high vacuum laser ablation on a MALDI TOF mass spectrometer of ubiquitin using the 2-NPG matrix where the most abundant charge state is +3.¹¹⁶ The experimental observation of dependence of matrix and volatility has been proposed to be related to the inability to evaporate matrix from the charged matrix:analyte clusters in the time available before mass separation.^{110,122} These results relate well with the observations that chemical structure of the matrix is not critical¹²⁷ so long as volatility of the matrix is sufficient to remove the matrix from the charged matrix/analyte clusters.^{110,122} As observed with *inlet* ionization,²²⁷ less energy is needed to remove

matrix from smaller compounds which agrees with the ability to readily analyze peptides using MAIV on the FT-ICR as shown for a mixture in Figure S7.1 in Appendix D. However, for the FT-ICR, the time available for desolvation is much longer than with MALDITOF and suggests that pressure may be a more important parameter in producing bare ions.

In the present experiments, different plate voltages (240 and 300 V) and data acquisition sizes (2 million and 512 thousand) were examined for MAIV. Nearly identical charge state distributions and ion intensities were obtained for bovine insulin (**Figure S7.2** in Appendix D). Angiotensin I showed some plate voltage dependence (**Figure S7.3** in Appendix D), with 240 V being optimal forming +2 charge state ions with +3 being observed in low abundance (**Figure S7.3.II.C** in Appendix D). With 200 (**Figure S7.3.I.C** in Appendix D) and 500 V (**Figure S7.3.I.E** in Appendix D) no ions were observed for this peptide. Interestingly, at 400 V (**Figure S7.3.I.D** in Appendix D), an abundant singly charged ion is observed. The voltage dependence is in agreement with intermediate and atmospheric pressure LSI studies in which the charge states can be altered by instrument parameters; lower charge states correspond to increased energy input.^{108,122}

Although the continuous ion formation of over 30 min using MAIV with the FT-ICR mass spectrometer may benefit some applications (e.g., fragmentation methods for characterization),²²⁷ the inefficiency in ionization at the low source pressure as well as the ~1 min sample plate loading time are not favorable for many analytical applications. Directly introducing the MAIV matrix from atmospheric pressure into the inlet aperture of a mass spectrometer has been shown to be an effective means for rapidly analyzing

samples using MAIV matrices.^{119,222} Therefore, introducing the matrix:analyte sample from atmospheric pressure on the FT-ICR mass spectrometer provides an intermediate pressure region to produce ions and a direct comparison with MAIV on the high vacuum MALDI source of the same instrument. **Figure 7.2** illustrates the approach.

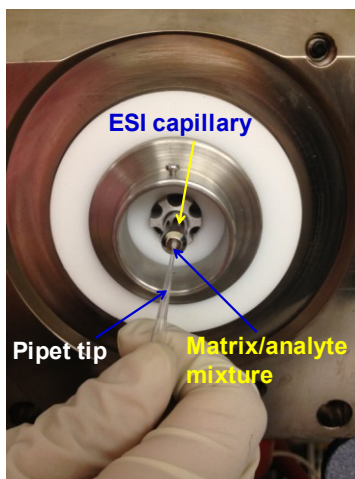


Figure 7.2. Picture of MAIV operating on the ESI source of the Apex FT-ICR mass spectrometer.

Shown in **Figure 7.3** are representative isotopic distributions of ubiquitin (**Figure 7.3A**) and lysozyme (**Figure 7.3B**) obtained when the individual 3-NBN:analyte crystals were introduced to the source by gently touching the capillary orifice so the vacuum of the mass spectrometer can draw the matrix:analyte into the glass inlet tube held at room temperature. Each mass spectrum was obtained in less than 2 min until the crystals were consumed from the pipet tip. Similar to MAII on an LTQ FTICR instrument using the matrix 2,5-DHAP,²¹⁵ the most abundant charge state for ubiquitin using 3-NBN is +8. In MAIV, the matrix:analyte introduced into the inlet experiences decreasing pressure as well as the natural airflow from atmospheric pressure to the first vacuum region. Under these conditions, the charge states and ion abundance of peptides and small proteins are ESI-like. This increase in charge state makes larger proteins applicable (e.g., lysozyme,

14303 Da, Figure 7.3B as compared to ubiquitin, 8560 Da Figure 7.1A on the high vacuum MALDI source) using the same solutions. Further, MAIV from atmospheric pressure provides equivalent mass resolving power for insulin (255000, +5 at m/z 1147.5279) and ubiquitin (376000, +9 at m/z 952.6316) to vacuum conditions, and 206900 for the +10 charge state of lysozyme (m/z at 1431.4889). Because of multiply charging in MAIV, the mass range of the mass spectrometer is extended or compounds analyzed from the solid state, as is the case with ESI from solution.

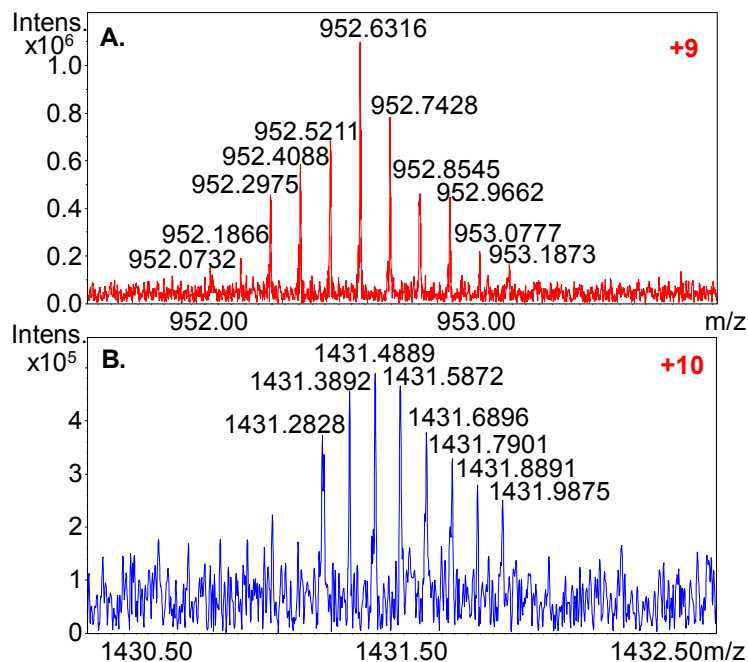


Figure 7.3. MAIV mass spectra of (A) +9 charge state of ubiquitin and (B) +10 charge state of lysozyme using 3-NBN as matrix obtained on the ESI source of the Apex FT-ICR mass spectrometer.

7.4 Conclusion

This study indicates the potential utility of MAIV and its applicability to high-performance FT-ICR mass spectrometers. The results presented here indicate that this simple and easy to use ionization method can be widely adapted with a minimum effort.

The importance of pressure conditions using MAIV is demonstrated. Because of the multiply charging, electron capture dissociation (**ECD**)^{228, 229} and electron transfer dissociation (**ETD**)^{107,117,134, 230} of ions sublimed directly from a surface should be possible with FT-ICR. Because of the high resolving power, these methods are potentially useful in the analysis of complex materials such as tissue and blood.^{117,120} While the experiments reported here used the standard ESI inlet and MALDI vacuum sources, adaptation specifically for MAIV is expected to greatly improve sensitivity.

CHAPTER 8

DRUG DETECTION AND QUANTIFICATION DIRECTLY FROM TISSUE USING NOVEL IONIZATION METHODS FOR MASS SPECTROMETRY

Solvent assisted ionization *inlet* (SAII) and matrix assisted ionization *vacuum* (MAIV) were used to rapidly quantify an antipsychotic drug, clozapine, directly from surfaces with minimal sample preparation. This simple surface analysis method based on SAI- and MAIV-mass spectrometry (MS) was developed to allow detection of endogenous lipids, metabolites, and clozapine directly from mouse brain tissue sections. Rapid surface assessment was achieved by SAI with the assistance of heat on the mass spectrometer inlet, and MAIV showed capability on heat-limited instruments with better reproducibility. In addition, isotope dilution and standard addition were used without sample clean-up, and the results correlate well to liquid chromatography (LC)-tandem MS with sample work-up. Using the simple surface methods, standard solutions containing clozapine and deuterated internal standard (clozapine-d8) at different concentration ratios were used to extract and quantify clozapine from brain tissue sections of a drug-treated mouse at different thicknesses. The amount of clozapine extracted by these surface methods was independent of tissue thickness.

8.1 Introduction

An ideal analytical method should be fast, simple, able to quantify material with minimal effort, and provide spatial resolution. However, those ideals are difficult to achieve in combination. Characterization methods based on mass spectrometry (**MS**) have gained popularity in pharmaceutical industry for speed of analysis, sensitivity, selectivity, and the ability to be coupled with separation methods such as liquid chromatography (**LC**).^{231,232} In addition to identification, rapid quantification of drugs is important in drug discovery. Quantifying drugs and their metabolites in biological tissue is an even more arduous task. MS alone is a semi-quantitative method, since ion intensity values can vary significantly during acquisition.²³³ However, the signal ratio with an isotopically labeled internal standard is reasonably reproducible.²³³ Isotope dilution is commonly used in MS-based quantification methods^{234,235} (e.g. LC tandem MS^{236,237}). The traditional LC-MS method requires sample work-up,^{238,239} which can be time and labor-intensive, and removes the analyte from its native environment, such as a surface.

MS has been used to provide chemical information directly from surfaces.^{55,240} Information on relative amount of analytes from surfaces is achieved by MS imaging^{241,242} using the mass to charge ratio (m/z) and a heat map of the ion abundances detected. In addition, MS imaging provides location of compounds within a surface. Quantification has been reported by spotting internal standard on the tissue section.^{63,64}

Matrix-assisted laser desorption/ionization (**MALDI**) is widely used in molecular imaging, providing relative amount and spatial information for peptides, proteins,^{56,243} lipids,⁵⁷ and metabolites,⁵⁸ etc. from surfaces such as tissue sections. Critical to the success in MALDI-MS is the matrix sample preparation which may result in sample

adulteration²⁴⁴ and potential chemical delocalization if the surface wets during matrix application.²⁴⁵ Ambient surface analysis methods, such as desorption electrospray ionization (DESI)⁸⁵ and nanospray desorption electrospray ionization (nanoDESI)⁸⁹ operate without the use of matrix compounds, allowing surface samples to be analyzed at atmospheric pressure with no or minor sample preparation and less chemical background.²⁴⁶⁻²⁴⁸ For example, the antipsychotic drug clozapine from mouse brain tissue has been imaged using DESI^{23,233} with a typical spatial resolution of $\sim 200 \mu\text{m}$.²⁴⁹ Notable exceptions are those that make use of a laser providing improved spatial resolution measurements and some with ease in instrumental setup.^{24,61,135,195, 250} Hours and sometimes days are required for MS imaging especially at high spatial resolution using sophisticated laser focusing setups.^{62,251}

Spatial resolution can be useful, but is often not required. If the exact location of surface analytes is not required, a liquid microjunction surface sampling probe can be used to extract analytes employing a liquid junction formed between a probe and the surface in a more rapid manner.¹⁸⁹ A solid-phase tissue sampling method achieved by thermal evaporation provided rapid volatile analyte identification capabilities.²⁵² Some of the ionization methods involve critical connections and precise alignments of the ionization apparatuses, requiring considerable user expertise to obtain reliable performance.¹⁶

The recently developed solvent assisted ionization *inlet* (**SAII**)¹¹¹ and matrix assisted ionization *vacuum* (**MAIV**)¹¹⁷ produce mass spectra similar to electrospray ionization (**ESI**) without the use of any external voltage or a laser. SAII has sensitivity comparable to ESI when the position of the capillary, which introduces samples to the mass

spectrometer inlet, is at the “hot spot” inside of the heated inlet.^{111,112,114} A recent study showed ESI-like ions can be produced when the analyte solution was pipetted near the entrance aperture of a heated mass spectrometer inlet tube.^{197,253} MAIV was demonstrated to produce ESI-like ions directly from a surface, e.g. mouse brain tissue sections, by simply spotting a MAIV matrix on tissue and exposing it to vacuum without the requirements of additional heat, voltage, or a laser.^{117,120}

Here, we report the development of SAI and MAIV for rapid surface analysis of the drug clozapine from brain tissue sections of drug-treated mice along with endogenous lipids and other small molecules. Isotope dilution and standard addition were employed for quantification.

8.2 Materials and Methods

Materials

All chemicals and mouse brain tissue sections were obtained as stated in **Chapter 2**.

Instrumentation

The LTQ Velos mass spectrometer (Thermo, Bremen, Germany) was used for SAI and LC-ESI studies. For ESI, the voltage was 3 kV, sheath gas was 8, and inlet temperature at 275 °C.²⁵⁴ For SAI, the ESI source of the LTQ Velos instrument was removed for direct access to the inlet as previously described.¹³⁵ The temperature of the inlet can be adjusted through the commercial temperature control of the inlet. In this study the inlet tube was operated at 200 °C to avoid peak broadening while ensuring sufficient ion intensity. The sheath gas, auxiliary gas, sweep gas, and capillary voltage were all set at 0. The mass spectra were acquired with automatic gain control on, with 5 microscans maximum injection time of 20. For tandem mass MS, collision energy of 35

was applied for collision induced dissociation (CID) to fragment the isolated molecular ion.

The SYNAPT G2 (Waters, Manchester, UK) mass spectrometer was used for MAIV study. For MAIV on the MALDI source, the commercial intermediate pressure MALDI was used with “LSIV” settings as previously reported.¹¹⁵ Briefly, the sample plate voltage was set to 0, the laser power was 0 and was not initiated. An extraction voltage of 10 V was applied. For MAIV operating at atmospheric pressure, the LockSpray ESI source was removed and overridden.¹¹⁷ A modified skimmer cone was used as previously introduced to provide better vacuum, with a notch to allow air flow.²⁵⁵

A nanoAcquity UPLC system (Waters, Milford, MA) equipped with a 1 mm x 50 mm column packed with 1.7 μm C18 BEH particles was used for LC-ESI-MS/MS quantification. A 3 min gradient using ACN/H₂O/0.1% formic acid (organic composition from 40% to 95%) was employed similar to a previous study using the same system.¹¹²

An optical microscope (Nikon, ECLIPSE, LV 100) was used to determine the diameters of the surface areas analyzed. Luxol fast blue was doped into extracting solvent and matrix solution to enhance the optical microscopic image by leaving the blue color on the extraction area.

Sample Preparation

Sample Preparation and Clozapine Quantification using LC-ESI-MS/MS

Half of a tissue section was scraped from the glass slide holding the tissue and dissolved in 50 μL MeOH. The mixture was vortexed for 1 min before being loaded in centrifuge for 5 min. The supernatant was used for quantification. The other half was reserved for surface analysis (**Scheme 8.1.I and II.C**).

The calibration curve was obtained by LC-ESI-MS/MS using clozapine standard solutions at concentration of 10, 25, 50, 100, and 200 fmol μL^{-1} plotted against peak area. For sample work-up, 1 μL supernatant was diluted by 20-fold and 1 μL was injected onto the UPLC column. For the comparison with surface SAI quantification, 1 μL MeOH was used to extract material from the tissue section from drug-treated mouse. The 1 μL solution was diluted by 147-fold before injected into UPLC system. All the LC-MS/MS analyses were performed in triplicates.

Surface Sample Introduction Methods based on SAI

Surface SAI in discontinuous mode. Solution of 0.3 μL of MeOH hanging from a pipet tip was touched to a control mouse brain tissue section to allow the droplet to extract material from the surface (**Scheme 8.1. II.A**). The MeOH droplet was held still touching the surface of the mouse brain tissue for about 3 seconds before it was drawn back into the tip. The solvent-containing extracted material was subsequently directly transferred into the heated inlet capillary of the LTQ Velos by placing the pipet tip near the entrance aperture where the droplet was drawn immediately into the inlet by the vacuum of the mass spectrometer, inducing ionization in the inlet tube.

Surface SAI in continuous mode. Two pieces of 20 cm long fused silica tube (75 μm i.d., 360 μm o.d., Polymicro Technologies, Phoenix, AZ) were taped near the ends at $\sim 90^\circ$ to keep a distance of about 1 mm between the two ends. Methanol was pumped through one piece of fused silica tube by a syringe pump (Fusion 400, Chemyx Inc., Stafford, TX) at 5 $\mu\text{L min}^{-1}$ flow from the non-taped end. The non-taped end of the other piece of fused silica tube was inserted about 0.2 mm inside the mass spectrometer inlet. A liquid junction bridge of the solvent was formed between the tips of the silica tubes with

the assistance of the vacuum in the mass spectrometer. A constant flow of MeOH was created between the tips so that the formed liquid junction droplet touched against the drug-treated mouse brain tissue section. Material from the surface was continuously extracted by the liquid junction, and the solvent containing the extracted material was transferred to the mass spectrometer through the second fused silica tube (**Scheme 8.1. II.B**).

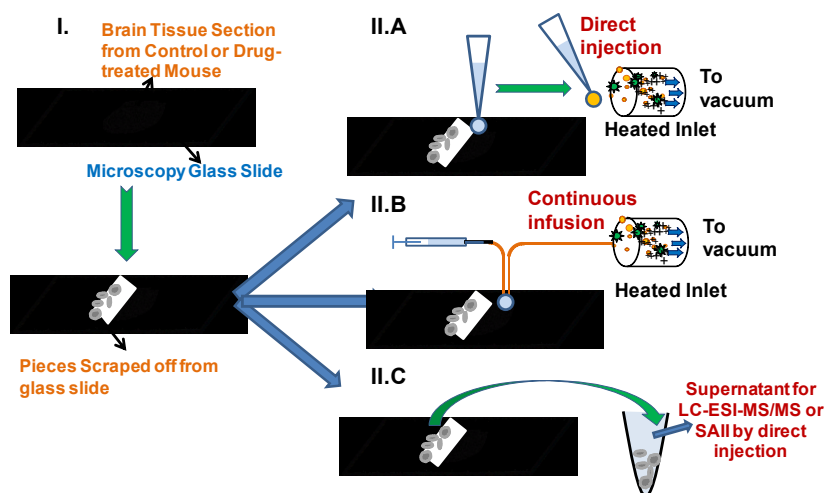
Quantification by SAI

Isotope dilution and standard addition were used to quantify clozapine from drug-treated mouse brain tissue. Stock solutions of clozapine and clozapine-d8 were prepared in EtOH and acetone at 1 mg mL^{-1} , respectively. The stock solution was diluted to $20 \text{ pmol } \mu\text{L}^{-1}$ by water, and MeOH was used for further dilutions. Five standard solutions were prepared. In each single solution, the concentration of clozapine-d8 was held constant at $2 \text{ pmol } \mu\text{L}^{-1}$ and the concentration of clozapine was varied. The final clozapine:clozapine-d8 molar ratios were 0:1, 0.5:1, 1:1, 1.5:1, and 2:1.

For the quantification from solution, $0.5 \text{ } \mu\text{L}$ of each solution was drawn into the $20 \text{ } \mu\text{L}$ pipet tip (Fisher Scientific, Pittsburgh, PA) and directly introduced into the heated inlet tube of the LTQ Velos. Eight repetitive measurements were performed from each clozapine/clozapine-d8 standard and the ion intensities of the singly charged protonated ions from clozapine (m/z 327) and clozapine-d8 (m/z 335) were recorded. The intensity ratio at m/z 327:335 was calculated for each measurement and averaged. The average intensity ratio at m/z 327:335 is plotted versus the concentration ratio of m/z 327:335, and the standard deviation was used to represent the error bar.

For the quantification from mouse brain tissue, 1 μL of each solution was drawn into a long-tailed ultra micro gel tip (Genesee Scientific, San Diego, CA) and carefully deposited on the sample surface. About 0.8 μL of the standard solution was picked up by the same pipet tip after ~ 3 seconds and introduced into the heated inlet. The signals were plotted the same way as using solution directly from the vial. The amount of clozapine extracted from the surface is determined by extending the calibration curve to find the intersection with the X-axis. Both the vehicle and drug-treated mouse brain tissue sections were analyzed with the vehicle mice serving as the control.

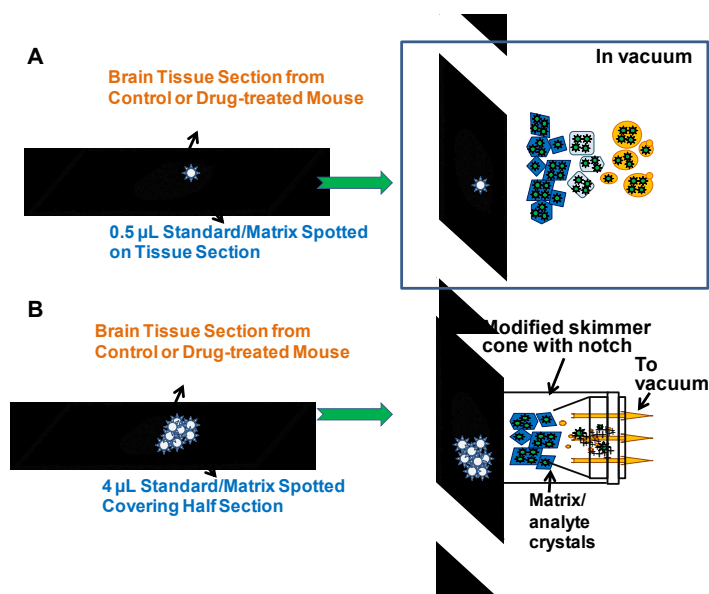
Scheme 8.1. Schematic representation of the workflow of SAII and typical LC-tandem MS methods. **(I)** Half of the brain tissue section from drug-treated mouse was scraped off from the glass slide, the other half was preserved for surface analysis. **(II)** From the preserved tissue section, surface SAII was performed in **(A)** discontinuous mode – extracting materials by solvent-droplet hanging at the pipet tip, and **(B)** continuous mode – extracting by liquid junction formed at the end of two pieces of silica tube. MS and MS/MS were performed in continuous mode. **(C)** Typical sample work-up was performed with the scraped tissue, the supernatant after vortex and centrifugation was analyzed by either LC-ESI-MS/MS or SAII direct injection.



Surface Analysis and Quantification by MAIV

MAIV operating from intermediate pressure vacuum: A series of standard mixtures of clozapine:clozapine-d8 at different concentration ratios were used. The concentration ratios were the same as in SAI (0:1, 0.5:1, 1:1, 1.5:1, 2:1), but at double the concentration. The standard clozapine:clozapine-d8 mixture was pre-mixed with a 3-NBN solution made by dissolving 5 mg in 100 μL ACN at 1:1 volume ratio. A solution of 0.5 μL matrix/clozapine:clozapine-d8 mixtures was spotted on the tissue section. The tissue section was loaded into the vacuum of the MALDI source after spotting each standard, and data acquisition was started as soon as the sample plate was indexed in the source. The mass spectrum was acquired for about 2 min. Brain tissue sections from both control and drug-treated mice were analyzed the same way.

Scheme 8.2. Schematic representation of workflow of MAIV methods. (A) The solution of 0.5 μL 3-NBN/clozapine:clozapine-d8 mixture was spotted on tissue surface and loaded into the vacuum of an intermediate pressure MALDI source. (B) Four 1 μL 3-NBN/clozapine:clozapine-d8 solutions were spotted on the tissue surface covering half of the tissue section, and exposed to vacuum of a modified skimmer cone of the overridden ESI source.



MAIV operating from atmospheric pressure: The calibration curve was obtained using control mouse brain tissue sections. A series of standard solutions of clozapine:clozapine-d8 were prepared at the concentration ratio of 0:1, 1:1, 2:1, 3:1, with the concentration of clozapine-d8 held at $4 \text{ pmol } \mu\text{L}^{-1}$. The standard clozapine:clozapine-d8 solution was also pre-mixed with the 3-NBN solution. Four $1 \text{ } \mu\text{L}$ matrix/clozapine:clozapine-d8 mixtures were spotted on the tissue surface. Half of the tissue section was covered by this procedure. The tissue with half of it covered by the matrix/clozapine:clozapine-d8 mixture was exposed to vacuum. This was accomplished by holding the glass slide against the modified skimmer cone where it was held by the vacuum for 10 minutes. For the quantification from the brain tissue section of drug-treated mouse, half of the tissue section was covered by the mixture of 3-NBN and $4 \text{ pmol } \mu\text{L}^{-1}$ clozapine-d8 at 1:1 volume ratio. The signal intensity ratio at m/z 327:335 was recorded and the amount of clozapine was quantified by standard addition method from the calibration curve.

8.3 Results and Discussion

SAII has been reported to produce ESI-like ions by injecting analyte solution into a heated inlet of a mass spectrometer.^{197,253} For analytes on a surface, such as tissue sections, liquid extraction using proper solvents can be employed prior to SAI. The material on the surface of a $20 \text{ } \mu\text{m}$ -thick brain tissue section of a drug-treated mouse was extracted by a MeOH droplet hanging from the pipet tip followed by transfer to the heated inlet tube (**Scheme 8.1.II.A**). Data acquisition of the software was initiated before surface extraction, therefore the total ion chromatogram (**TIC**) reflects the entire duration of sample analysis from exposure of solvent to surface to the ionization in inlet, which was

only about 25 seconds as shown in **Fig. 8.1A**. The mass spectrum having good ion abundances is dominated by phosphatidylcholines along with protonated clozapine and alkali-adducted cholesterol (**Fig. 8.1B**). The lipid peaks were assigned according to previously published data²⁵⁶ and no phosphocholine head group fragment (m/z 184) was observed, unlike MALDI.²⁵⁷ Tandem MS using CID was performed on the most abundant lipid peak at m/z 798. MS^2 on the parent ion produced mainly a loss of 59, and MS^3 on the major fragment ion at m/z 739 generated a fragment with a loss of 183 (**Figure S8.1** in Appendix E). The loss of trimethylamine ($\Delta m/z=59$) and phosphocholine head group ($\Delta m/z=183$) are characteristic for sodiated phosphatidylcholines.²⁵⁸ The inset spectrum shows clozapine with its characteristic isotopic distribution. Brain tissue section from a drug-treated mouse, which was from the same batch but had been stored frozen for months at -80 °C, was analyzed in the same manner. The protonated clozapine ions were observed at lower ion abundance, likely because the drug has degraded over time (**Figure S8.2** in Appendix E). One of the major clozapine metabolites, clozapine N-oxide,²⁵⁹ was also observed having the characteristic chlorine isotopic distribution. Sodiated and potassiated cholesterol were assigned similar to an ambient infrared MALDI surface study.²⁶⁰

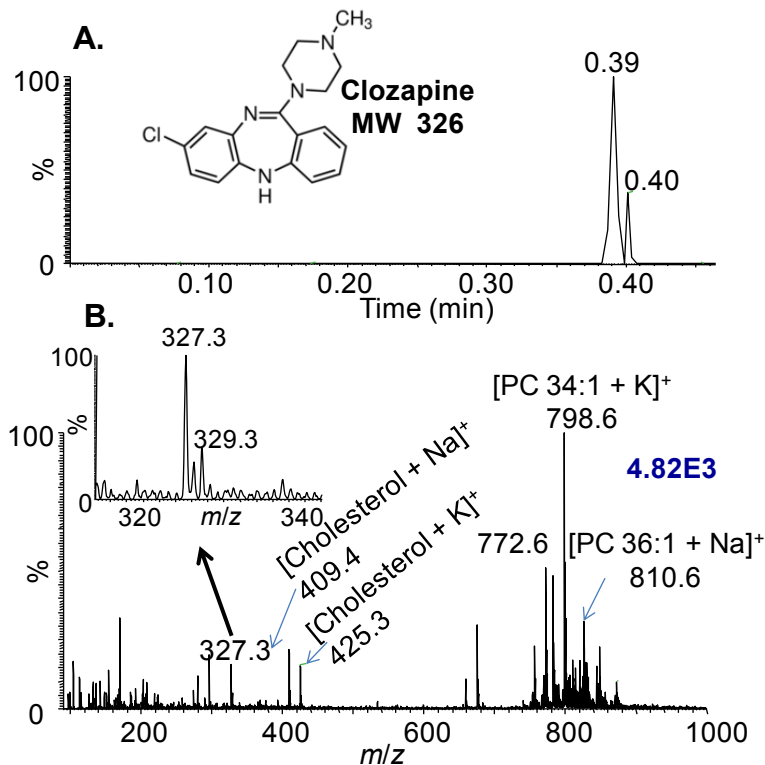


Figure 8.1. Fast surface assessment using a SAIL method employing surface extraction by 1 μ L of MeOH in discontinuous mode as shown in **Scheme 8.1. II.A.** (A) TIC of the entire duration of sample analysis including exposure of solvent to surface to ionization in inlet. (B) Mass spectrum extracted from the TIC with the inset showing the isotopic distribution of protonated clozapine ions. The blue number on the top right corner denotes ion abundance.

The material was sampled directly from the tissue surface at ambient conditions, and the mass analysis was obtained without the requirement of any voltage or extra connections between surface sampling and sample introduction. The analysis was soft enough to maintain the intact analyte structures with less chemical background. Neither cholesterol fragment with the loss of water nor water clusters was detected as observed with ionization methods employing matrix and/or a laser.^{240,260} This method is discontinuous as solvent/lipid droplets are analyzed individually, yet it is a very simple sampling and ionization approach.

A continuous surface SAI sampling method was achieved by the configuration shown in **Scheme 8.1. II.B**. A liquid junction is formed at the mouse brain tissue surface by interfacing two pieces of fused silica tubing. Here, the glass plate containing the mouse brain tissue section was hand held and manually moved over the surface to analyze different areas. The TIC in **Figure 8.2A** shows the constant ion production for about 1 min acquisition time. The mass spectrum from time point 0.37-0.86 min was extracted from the TIC (**Figure S8.3** in Appendix E) showing similar ions from lipids and clozapine as discussed above, but at lower ion abundance. This may be due to the shorter time the liquid remains on the surface, so that less material is extracted. Structural characterization of clozapine present in the drug-treated mouse brain tissue was confirmed by fragmenting the peak at m/z 327 (**Figure 8.2B.1**) using CID. The fragment ions produced at m/z 270 and 296 were identical to those of a purchased standard (**Figure 8.2B.2**).²³

The method development using direct pipetting SAI for quantification of drugs was first established using standard clozapine:clozapine-d8 solutions from vials. The solution of 0.5 μ L clozapine and clozapine-d8 mixture at a certain concentration ratio was directly introduced into the inlet of the mass spectrometer. As shown in **Figure S8.4** in Appendix E, at a concentration ratio of 0.5:1, the protonated peak height of clozapine (m/z 327) versus clozapine-d8 (m/z 335) is approximately 0.54 (**Figure S8.4A** in Appendix E), while a 1:1 concentration ratio results in the ion intensity ratio of approximately 1.08 (**Figure S8.4B** in Appendix E).

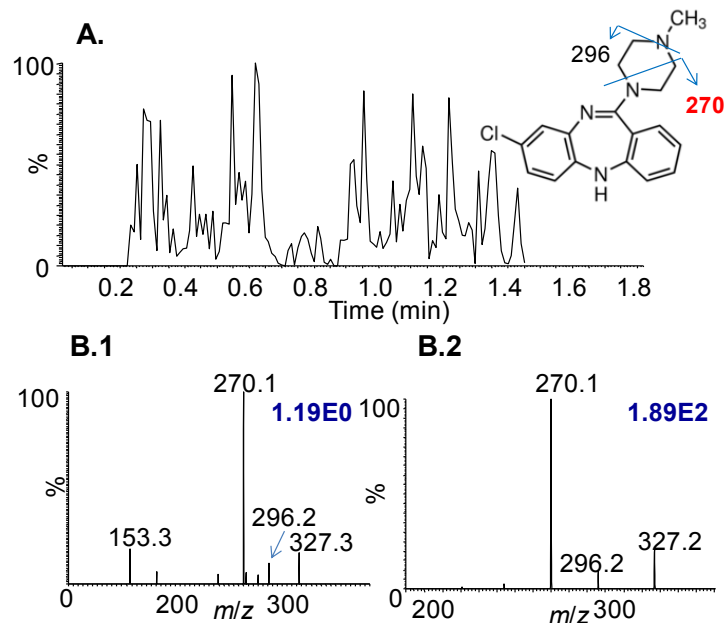


Figure 8.2. Fast surface assessment using the SAI method employing surface extraction by 1 μL of MeOH in continuous mode as shown in **Scheme 8.1. II.B.** (A) TIC of the whole analysis for ~ 1.4 min. (B) SAI-CID-MS of the protonated clozapine ions (1) directly extracted from tissue surface and (2) from synthesized clozapine chemical solution. The blue numbers on the top right corner denote ion abundances.

The average of the signal intensity ratio from 8 repetitive measurements of each standard was plotted against the concentration ratio of clozapine:clozapine-d8 in **Figure 8.3A**. The high regression coefficient ($R^2=0.9929$) and small error bars demonstrate the reproducibility of the SAI method for quantification. Using this calibration curve, an unknown sample from a tissue section of a drug-treated mouse was analyzed. One μL supernatant from half of the tissue section scraped off the glass slide was mixed with 1 μL of 4 $\text{pmol } \mu\text{L}^{-1}$ clozapine-d8 solution producing a mixture containing 2 $\text{pmol } \mu\text{L}^{-1}$ clozapine-d8. This solution was injected into the heated inlet. A signal intensity ratio of 0.694:1 at m/z 327:335 was obtained, reflecting the concentration of clozapine in the 1 μL extraction solution to be 1.27 $\text{pmol } \mu\text{L}^{-1}$. In comparison, another 1 μL of the same supernatant was further diluted by 20-fold and quantified by LC-MS/MS (**Figure 8.3B**).

The concentration of the supernatant was determined to be $1.33 \text{ pmol } \mu\text{L}^{-1}$. The total analysis time spent on the SAI approach was only about 1 min for 5 replicates, where the LC-MS/MS method took more than 30 min for triplicate analyses.

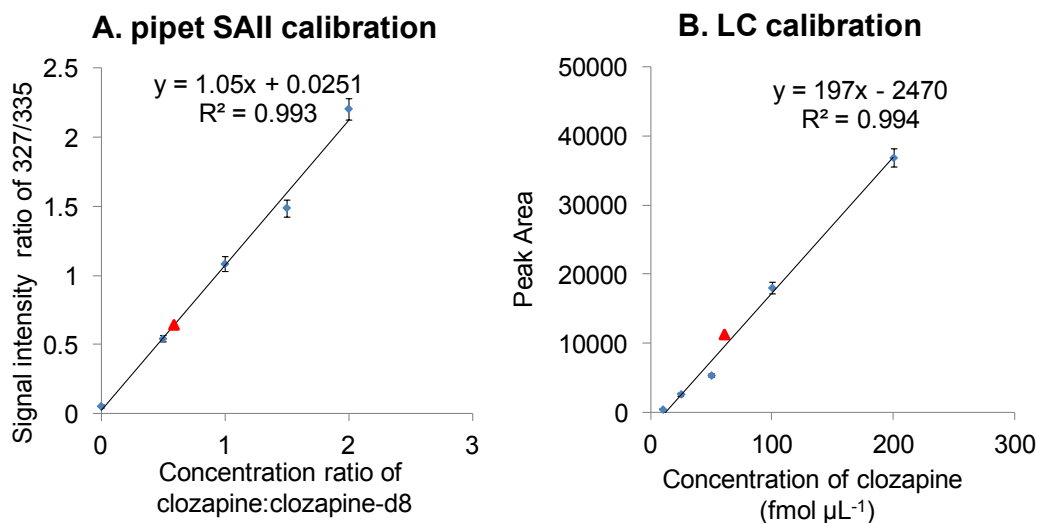


Figure 8.3. Calibration curves of clozapine (A) using SAI by pipetting standard clozapine:clozapine-d8 solutions at different concentration ratio with clozapine-d8 at $2 \text{ pmol } \mu\text{L}^{-1}$, signal intensity ratio is plotted against concentration ratio; and (B) using LC-ESI-MS/MS with standard clozapine solutions at different concentration, peak area of the fragment ion at m/z 270 is plotted against concentration.

The other half of the $20 \text{ } \mu\text{m}$ -thick tissue section was analyzed by surface analysis methods. The same series of standard solutions of clozapine:clozapine-d8 were used to extract material from the surface instead of pure MeOH solvent. As a control experiment, the control tissue, for which the mouse was not treated with clozapine before sacrificing, was analyzed first. When the solution of $1 \text{ } \mu\text{L}$ clozapin:clozapine-d8 mixture at the concentration ratio of 0.5:1 was used to extract material by contacting the surface for ~ 3 s and then transferred to the mass spectrometer inlet, the signal intensity ratio at m/z 327:335 obtained was 0.52:1 (**Figure S8.5A** in Appendix E), indicating no external clozapine was detected after extraction. When the tissue section from drug-treated mouse

was extracted by the same standard clozapine:clozapine-d8 mixture, the signal intensity ratio increased to 2.20:1 (**Figure S8.5B** in Appendix E). The concentration ratio (X) was plotted against the ion intensity ratio (Y) (**Figure 8.4**) with control tissue (red square) and drug-treated tissue (blue triangle). The curve from drug-treated tissue has a significant increase, indicating clozapine was extracted from the surface by the standard solutions. Although only one measurement was taken from each standard solution, the linearity ($R^2=0.9374$) was confirmed by the high reducibility of this method (**Figure 8.3A**). The amount of clozapine extracted by 1 μL solution was calculated by extending the calibration curve to the x-axis. The intersection shows 2.68 pmol of clozapine was extracted from the surface area of about 1.5 mm in diameter (**Figure 8.4** inset) as determined using optical microscopy. For a comparison with the LC-MS/MS method, one μL pure MeOH was used to extract clozapine from the surface and analyzed by LC-MS/MS after a 147-fold dilution. The amount of clozapine extracted by the 1 μL MeOH was calculated as 2.58 pmol from the calibration curve.

The amount of clozapine quantified from surface extraction of the right half of the tissue section is similar between SAII-MS and LC-MS/MS methods (2.68 pmol using SAII vs. 2.58 pmol using LC-MS/MS from surface extraction), indicating the reliability of the SAII method but at much faster analysis speed. However, the amount from 1 μL solvent extraction on the right half is not reflective of the results obtained from the 1 μL supernatant using traditional sample work-up and LC-MS/MS of the left half of the section (2.68 pmol using SAII from surface extraction vs. 1.33 pmol using LC-MS/MS from supernatant). We hypothesize that only the clozapine on the surface of the tissue section was extracted by the surface extraction method. In contrast, when tissue section

was scraped off, vortexed and centrifuged, the extracted clozapine is not limited to the surface. To test our hypothesis, another set of tissue sections that were 10 μm -thick from a drug-treated mouse were analyzed in the same manner.

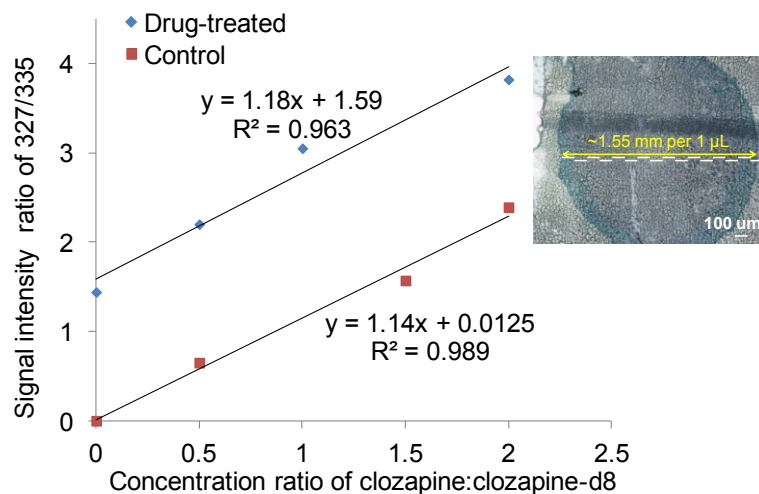


Figure 8.4. The right half of a 20 μm brain tissue section from drug-treated mouse was quantified by SAI method in discontinuous mode as shown in **Scheme 8.1. II.A.** Solution of 1 μL of each of the four standard clozapine:clozapine-d8 mixtures at different concentration ratios was used for surface extraction and then pipetted into the heated inlet of the mass spectrometer. Calibration curves were obtained by plotting the signal intensity ratio against the concentration ratio. A brain tissue section from a normal mouse was used as control. The inset shows an optical microscopy image to illustrate the extracted area. For enhanced image, 1 μL MeOH was doped with Luxol fast blue and the droplet was not removed from surface.

Table 8.1 shows the comparison of 10 μm and 20 μm -thick tissue sections, using both the typical sample work-up and the novel surface SAI method. Thicker tissue results in more clozapine extracted by vortex and centrifugation. The amount obtained from the 20 μm -thick tissue is approximately twice that of the 10 μm tissue as determined by LC-MS/MS using the traditional tissue work-up. In contrast, the amount of clozapine extracted from the surface was not significantly different (2.84 pmol for 10 μm and 2.68 pmol for 20 μm). This result indicates that the amount of clozapine determined by surface

SAII is the amount per unit area that was extracted, and was not limited by tissue thickness, at least for sections of 10 μm or greater.

Table 8.1. Amounts of clozapine quantified by typical LC-ESI-MS/MS (**Scheme 8.1. II.C**) and surface SAII in discontinuous mode (**Scheme 8.1. II.A**). 10 μm and 20 μm tissue sections were analyzed. For LC-ESI-MS/MS, the left half of the tissue section was scraped off, dissolved in 50 μL MeOH, vortexed and centrifuged, results showed the amount in pmol per μL supernatant. For surface SAII, results showed the amount in pmol per μL solution used for surface extraction.

Thick-ness	LC-ESI-MS/MS from scraped tissue Amount of clozapine in 1 μL supernatant	Surface SAII Amount of clozapine extracted by 1 μL standard solution
10 μm	0.725 pmol	2.84 pmol
20 μm	1.33 pmol	2.68 pmol

SAII used in surface analysis and quantification is a simple and fast assessment but limited to mass spectrometers equipped with a heated inlet tube. On instruments without a commercially available heated inlet, MAIV has been demonstrated to produce ESI-like ions directly from surfaces, including mouse brain tissue sections.^{117,120} The quantification of clozapine using MAIV was first achieved on the intermediate pressure vacuum MALDI source of a SYNAPT G2 instrument. The mixture of individual standard clozapine:clozapine-d8 solutions mixed with 3-NBN matrix solution was spotted on the control and drug-treated tissue sections and loaded into the vacuum using a MALDI plate loader but without use of the laser. From each single matrix/clozapine:clozapine-d8 spot, the mass spectrum was extracted over the sublimation period of time (ca. 2 min). An area of about 1 mm^2 covered by 3-NBN matrix was analyzed: matrix uncoated parts of the tissue do not produce ions. The signal intensity ratio at m/z 327:355 was plotted against

the concentration ratio of clozapine:clozapine-d8 from the standard solution (**Figure 8.5**). The amount of clozapine from each spotted area was determined as 1.48 pmol from the plots. Miniaturization of the tissue area covered by the matrix can be employed to improve the spatial resolution of the analysis.¹¹⁷

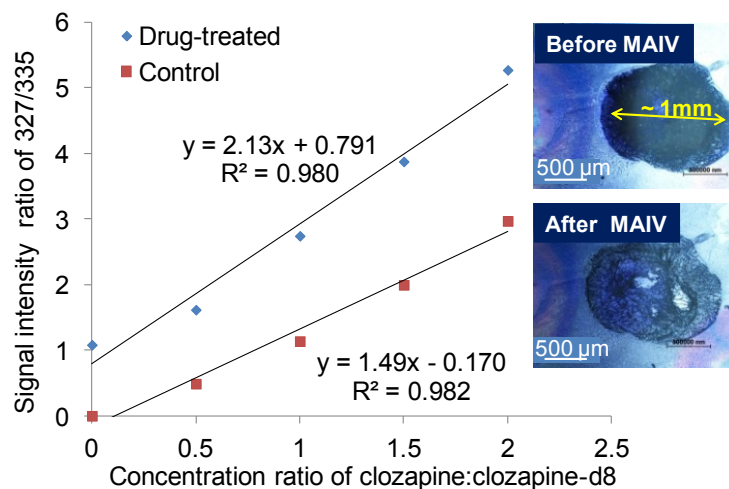


Figure 8.5. 20 μm brain tissue sections from drug-treated and control mice were analyzed by MAIV operating at intermediate pressure. Solution of 0.5 μL 3-NBN/clozapine:clozapine-d8 mixture was spotted on the tissue section and the sample was loaded into the commercially available vacuum chamber (**Scheme 8.2.A**). The matrix sublimed in approximately 2 min. The ion intensities of clozapine and clozapine-d8 were averaged over the 2 min acquisition, and the intensity ratio was plotted against concentration ratio. Insets show the microscopy images of the matrix/clozapine:clozapine-d8 spotted on tissue section before and after MAIV analysis.

MAIV on the vacuum source produced better linearity ($R^2=0.9797$) than SAIL, because the average ion intensity summarized over a longer period of time provides better reproducibility. However, the operation of MAIV on the commercial vacuum MALDI source is time consuming and a significant amount of analyte is potentially wasted in the 2 min loading time.¹¹⁷ Only one matrix/clozapine:clozapine-d8 mixture can be spotted for each loading, otherwise all the spots would sublime simultaneously. To achieve the goal of simpler assessment from the surface, the ESI source was overridden

and employed for MAIV operating from atmospheric pressure as described previously.¹¹⁹ The source temperature was held at 80 °C, and a sealed vacuum outer skimmer cone with a notch¹¹⁵ to allow air flow was used for operation. Four 1 μ L clozapine:clozapine-d8 solutions mixed with 3-NBN were spotted on a tissue section (control and drug-treated, respectively) and covered half of the tissue section completely. The glass slide tissue holder was sealed to the notched cone by the vacuum for a 10 min analysis. The total analysis results of the 10 μ m-thick brain tissue from drug-treated mouse are shown in **Figure S8.6** in Appendix E as an example. The matrix sublimed over this 10 min period of time as shown in the TIC (**Figure S8.6.I** in Appendix E). Extracted clozapine, the standard clozapine-d8, cholesterol, and lipids were observed from the total mass spectrum and the two-dimensional plot of drift time *vs.* m/z (**Figure S8.6.II** in Appendix E). Particularly, lipids were not directly observed from mouse brain tissue sections in positive mode and the same heat-limited mass spectrometer.¹⁹⁵ The nested dataset¹⁰⁶ extracted from the two-dimensional plot (**Figure S8.6.II.B insets** in Appendix E) allows the identification of clozapine and clozapine-d8 without additional time requirement. The calibration curve was obtained using four standard clozapine:clozapine-d8 mixtures of different concentration ratios on control tissue sections (**Figure 8.6**). The amount of clozapine was determined by the standard addition method by spotting four 1 μ L 3-NBN/clozapine-d8 mixture on half of the tissue section. The quantification of this method from 10 μ m- and 20 μ m-thick tissue sections did not show much difference (20.0 pmol for 10 μ m and 19.4 pmol for 20 μ m), indicating that the same amount of matrix also extracts similar amount of clozapine only from the surface, regardless of the tissue thickness.

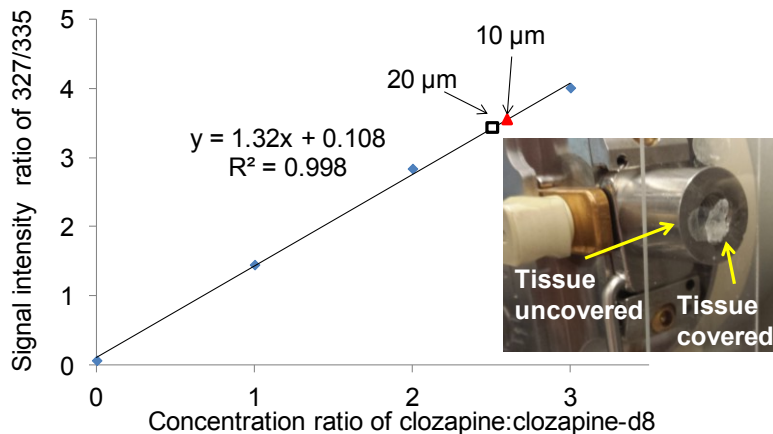


Figure 8.6. Calibration curve obtained by spotting 4 μL 3-NBN/clozapine:clozapine-d8 mixture on control mouse brain tissue sections. The glass slide holding the half-covered tissue was then sealed to the vacuum on a modified skimmer cone and let sublime for 10 min (**Scheme 8.2.B**). Ion intensity ratio was plotted against concentration ratio. The red triangle and hollow square show the results obtained from 10 μm and 20 μm tissue sections, respectively, from the drug-treated mouse using standard addition method. The inset shows a picture of the modified skimmer cone and a half-covered tissue section.

In comparison to SAI using liquid extraction, the amount of clozapine extracted by MAIV is much higher. This is not only due to the fact that larger area was covered by matrix, but also that more material was extracted for the same unit area when matrix was employed. To further confirm our observation, the tissue, after surface extraction by SAI and MAIV, was cut through the center breaking the glass slide, and the cross section was examined under the microscope to determine the depth of droplet and matrix penetration (**Figure S8.7** in Appendix E). SAI on the 20 μm -thick tissue section, only ~ 3 μm had the color from the doped Luxol fast blue dye indicating the wet area indicating the surface extracted area in SAI (**Figure S8.7.A** in Appendix E). MAIV provides a result with larger amount of clozapine than SAI, indicating that the matrix/clozapine:clozapine-d8 mixture went deeper into the tissue than solvent-extraction. Previous studies have shown that MAIV can be destructive to tissue sections,¹¹⁷ and blue color in the microscopy

image shows a deeper extraction for about 7 μm (**Figure S8.7.B** in Appendix E), more than twice as deep compared to SAI liquid extraction.

8.4 Conclusion

Rapid and efficient surface assessment is achieved by surface SAI and MAIV ionization methods. The surface quantification methods demonstrated in this work are potentially useful where fast analysis is valued, e.g. disease diagnosis or drug screening; one just needs to have the criterion of amounts of analyte per unit area of the surface (instead of per unit weight tissue, or volume) from healthy and diseased/treated tissue. In this case the thickness of the sample ($>10 \mu\text{m}$) has little impact on the analysis. With this approach, the tissue need not be sectioned to a certain thickness for quantification.

Chapter 9

CONCLUSION AND FUTURE PROSPECTUS

Novel ionization methods have been developed to produce ESI-like ions of biological materials from AP and vacuum conditions for use in MS. The newly developed ionization methods have been interfaced to a variety of commercially available mass spectrometers from different vendors to utilize their features.

Inlet ionization methods operate from AP and are beneficial for the instruments equipped with a heated inlet capillary. Ionization occurs in the heated inlet, with the assistance of the pressure drop from AP to the first vacuum stage of the mass spectrometer, regardless how the analyte is introduced into the inlet, with or without the use of a laser, from the solid or solution state. The first example of total solvent-free analysis by LSI-IMS-MS showed the production of multiply charged ions from solid state. Insoluble compounds, e.g. membrane proteins from brain tissue, could benefit from the solvent-free sample preparation.

For solution samples, the independence of any extra connection or voltage greatly simplified the sample introduction method. Comparable sensitivity can be achieved by nanoLC-SAI as by nanoESI, with much less labor force and expense. NanoLC-SAI could potentially be employed for e.g. mammalian proteomics where the amount of proteins that can be obtained is limited. The automated analysis by multiplexing SAI and the mapping approach may potentially advance in any field that fast analyses are valued, e.g. pharmaceutical or clinical analyses, for the merit of its simple of use, low consumables cost, and little expertise required.

Although a liquid sample introduction method, SAI also shows its application in fast surface assessment by incorporating liquid-surface extraction. This ionization method is not only fast but also softer than traditional ionization techniques. The typical isotope dilution and external addition methods were well suited in this SAI approach to quantify the drug from drug-treated tissue surface. Comparable results were obtained by SAI and typical LC-ESI, but SAI takes much shorter time.

Vacuum ionization methods operating at AP or vacuum makes use of proper matrix and the vacuum which any mass spectrometer has to produce ESI-like ions from solid state. High performance mass spectrometer was used to obtain multiply charged ions from solid state while maintaining the high mass resolving power. The mass resolution achieved by FT-ICR is beneficial for e.g. proteomics by this hyphenated method with MAIV, especially for those the solubility in sprayable solvent is restricted. The instantaneous and continuous ion formation is favored by electron capture dissociation that is currently available on FT-ICR instruments, too.

In summary, new ionization methods have shown advantages such as simple of use, low cost, and ready to be coupled with other analytical techniques, etc. that provide the potential for real world application. As listed in the “Holy Grail” in **Scheme 1.1**, for example, sensitivity and dynamic range should be extended, so that some component in low abundance from a complex environment, such as proteins from brain tissue, can be detected besides the dominant lipids. The hyphenation of novel ionization methods with other analytical techniques and high performance instrument is valuable for the analysis of complex materials, e.g. interfacing UPLC with IMS-MS by MAIV could also free the ionization from the restriction of spray conditions. Coupling the mentioned techniques

with high mass resolution instrument and tandem MS could be greatly advantageous for proteomics. Reproducibility should be improved for direct quantifications, ideally without the need to add external standards. The spatial resolution of the surface analysis approaches should be improved by employing a laser or miniaturizing solvent/matrix deposition, so that the methods could be utilized for diagnoses of diseased tissue from the healthy. The speed, simplicity, robustness, automation, low-cost will always be favorable for e.g. pharmaceutical industry and drug discovery. With these being said, we have just begun scratching the surface, there are a lot more needed to be studied.

Scheme 1.1 Technology development needed to expand the use of MS for clinical applications [Adopted from Reference 18]. Points highlighted in blue will need further investigation.

- | |
|--|
| <p>A. Sensitivity and dynamic range: to observe <i>all</i> components (e.g., lipids and proteins, hydrophilic and hydrophobic, low and high abundance) directly from native and complex environment (e.g., tissue, plasma, serum, urine), improvements needed include:</p> <ol style="list-style-type: none">1. Separation: to deal with complexity and isoforms (LC, mass resolution, IMS)2. Specificity: fragmentation (MS/MS: CID, ETD) for confirmation and ID (bottom up, top down)3. Reproducibility: for quantitation4. Spatial resolution: for location (with and without a laser) <p>B. Speed: of data acquisition and interpretation</p> <p>C. Robust, simple and cheap: automation, disposables</p> |
|--|

APPENDIX A

TOTAL SOLVENT-FREE ANALYSIS SUPPLEMENTAL INFORMATION

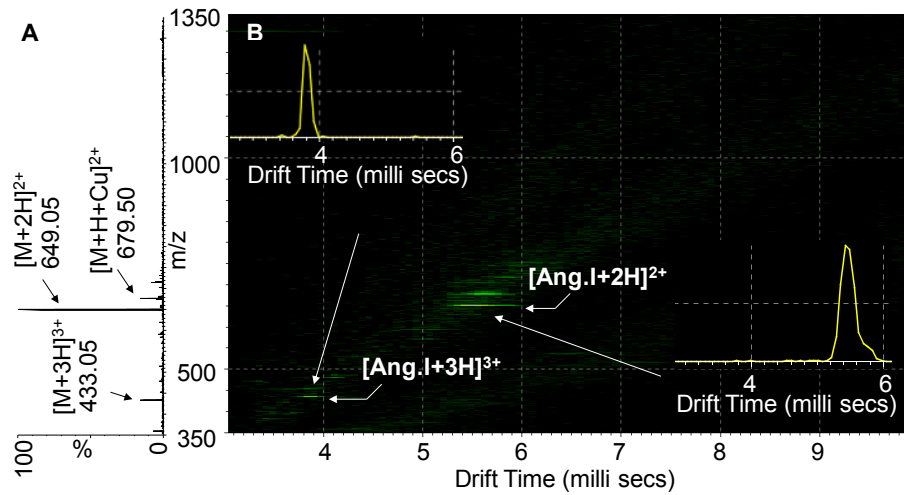


Figure S4.1. Solvent-based LSI-IMS-MS analysis of angiotensin I. **(A)** Total mass spectrum and **(B)** 2-D plot of drift time versus m/z .

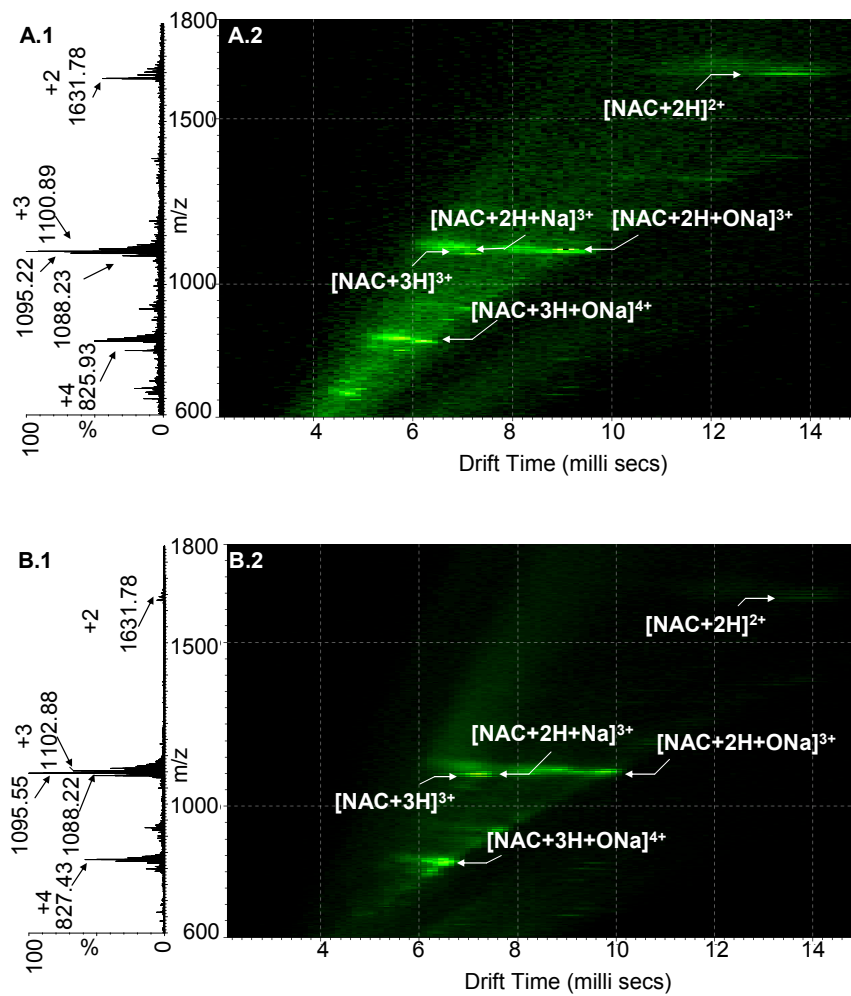


Figure S4.2. (A) Solvent-based LSI-IMS-MS analysis and (B) ESI-IMS-MS of NAC. (1) Total mass spectrum and (2) 2-D plots of drift time versus m/z .

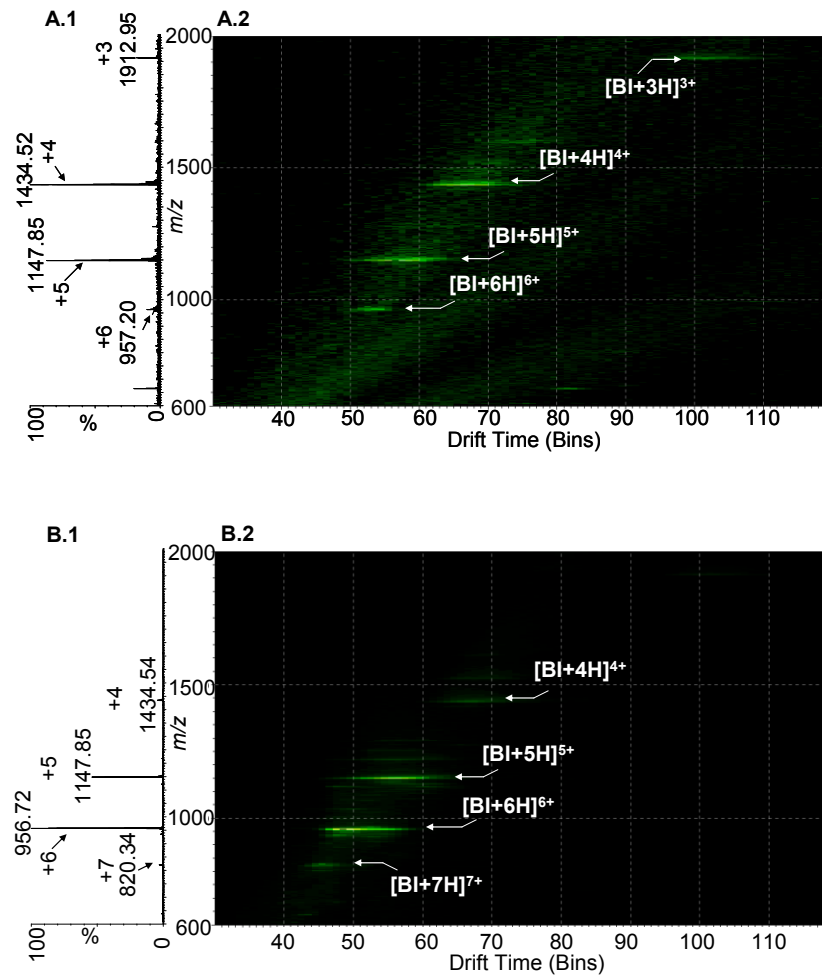


Figure S4.3. (A) Solvent-based LSI-IMS-MS analysis and (B) ESI-IMS-MS of BI. (1) Total mass spectrum and (2) 2-D plots of drift time versus m/z .

Figure S4.4. Total solvent-free analysis spectra of angiotensin I using 2,5-DHAP matrix under different grinding time and frequency on SYNAPT™ G2 instrument.

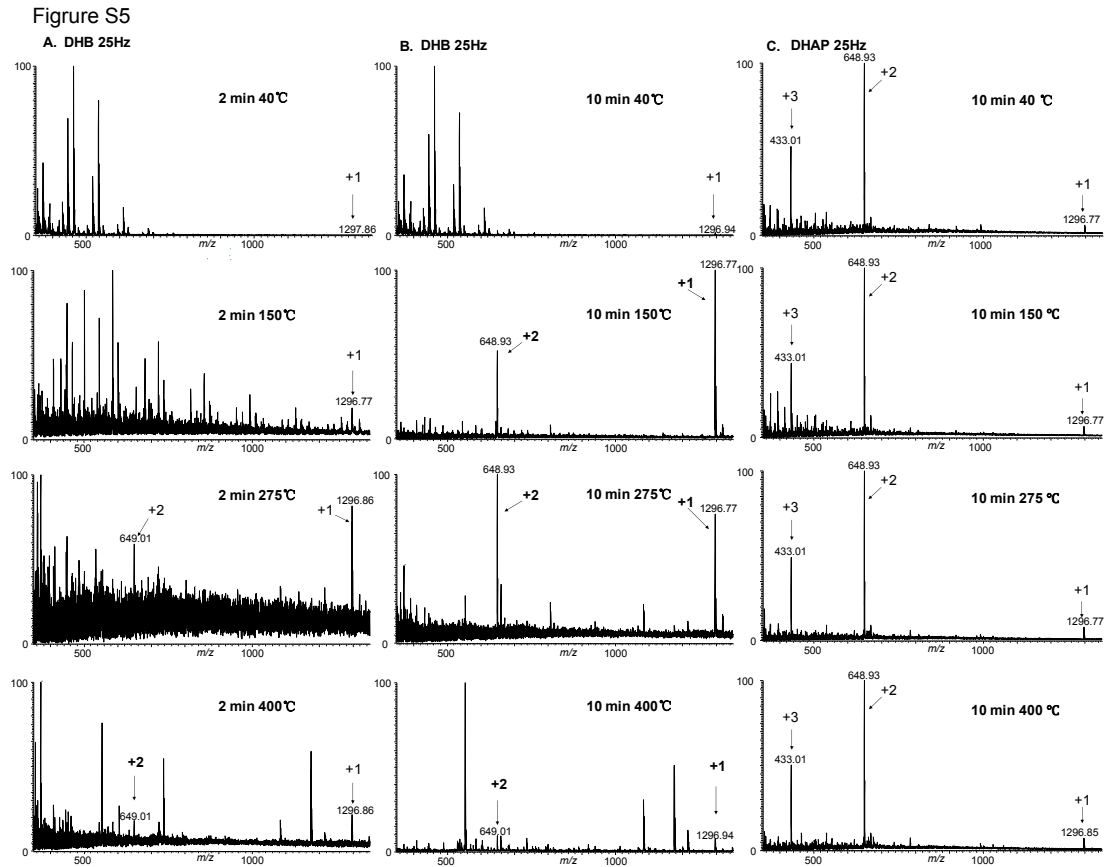


Figure S4.5. Total solvent-free analysis spectra of angiotensin I using (A) and (B) 2,5-DHB matrix, (C) 2,5-DHAP under 25 Hz, different grinding times and capillary temperature on LTQ-Velos instrument.

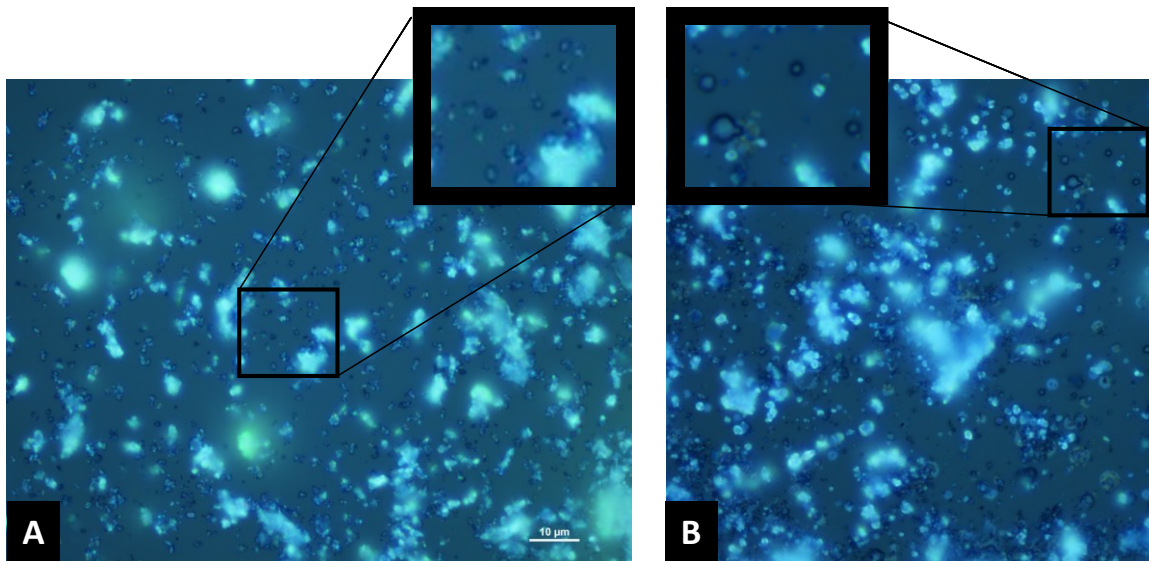


Figure S4.6. Microscopy of liquid droplets produced by the ablation of (A) 2,5-DHB and (B) 2,5-DHAP after the matrix had been ground for 10 minutes in TissueLyser II.

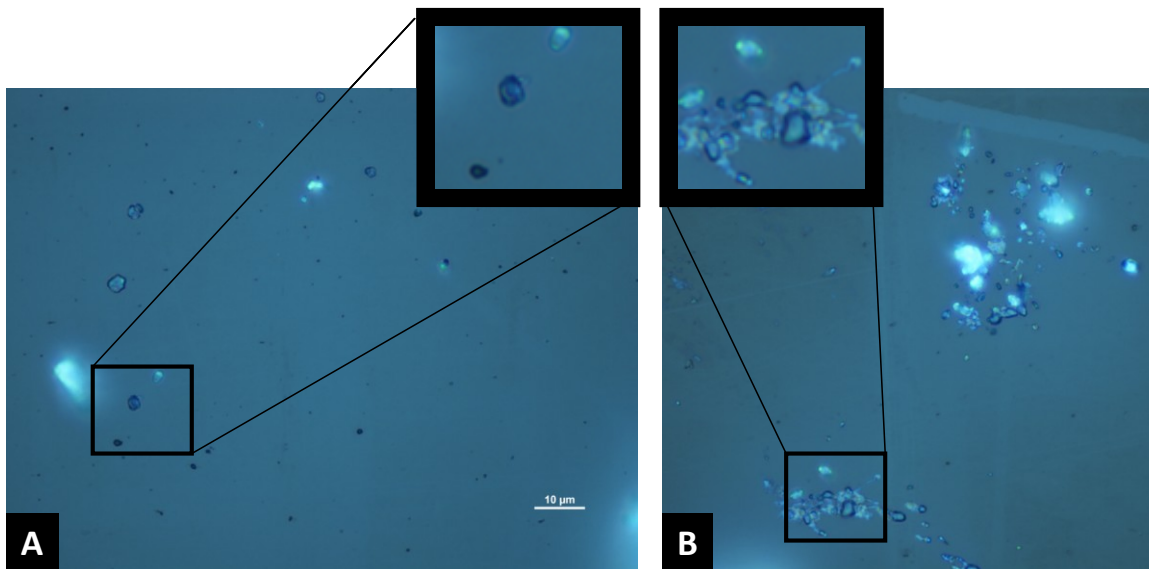


Figure S4.7. Microscopy of the ablation plume from 2,5-DHB after the matrix was ground for 30 seconds in (A) TissueLyser II and (B) Vortexer.

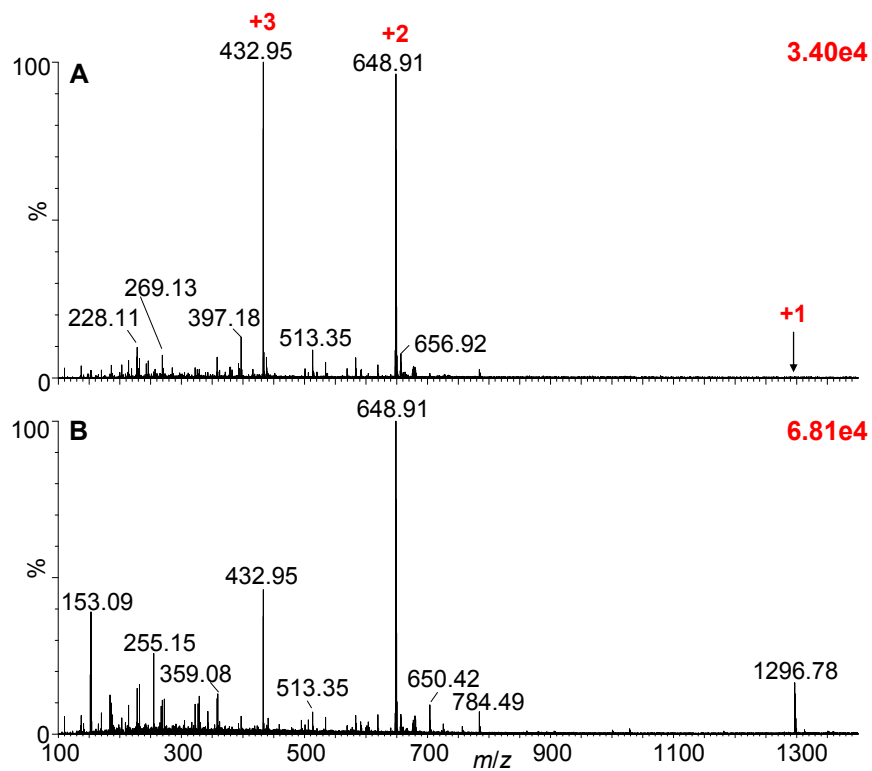


Figure S4.8. Solvent-free LSI-MS mass spectrum of angiotensin I acquired (A) with IMS and (B) using TOF mode only (without IMS).

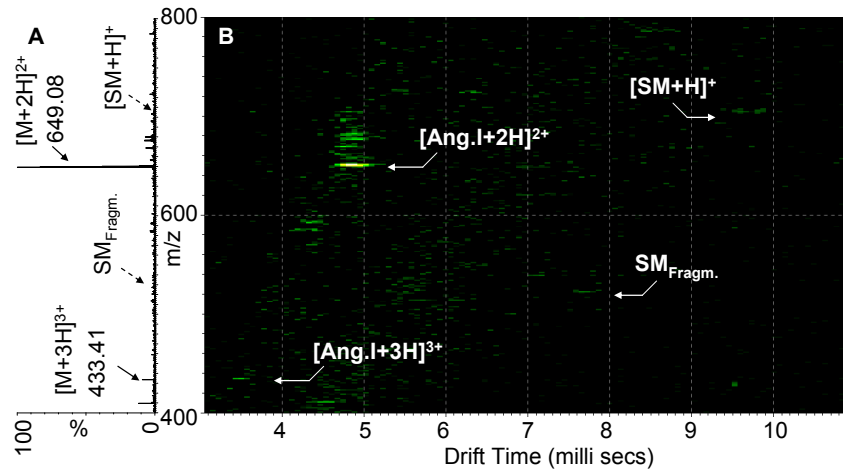


Figure S4.9. Solvent-based LSI-IMS-MS analysis of a lipid (sphingomyelin, SM) and a peptide (angiotensin I) mixture. **(A)** Total mass spectrum and **(B)** 2-D plots of drift time versus m/z .

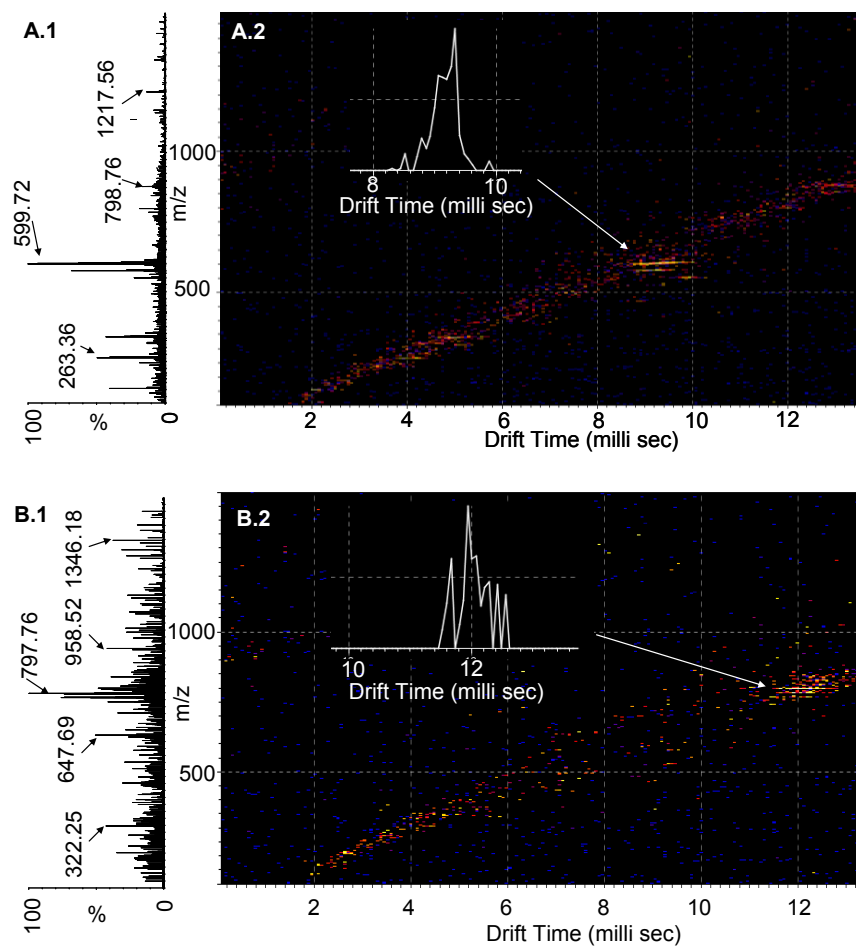


Figure S4.10. Solvent-free LSI-IMS-MS analysis of (A) vegetable oil and (B) motor oil.

(1) Total mass spectrum and (2) 2-D plots of drift time versus m/z .

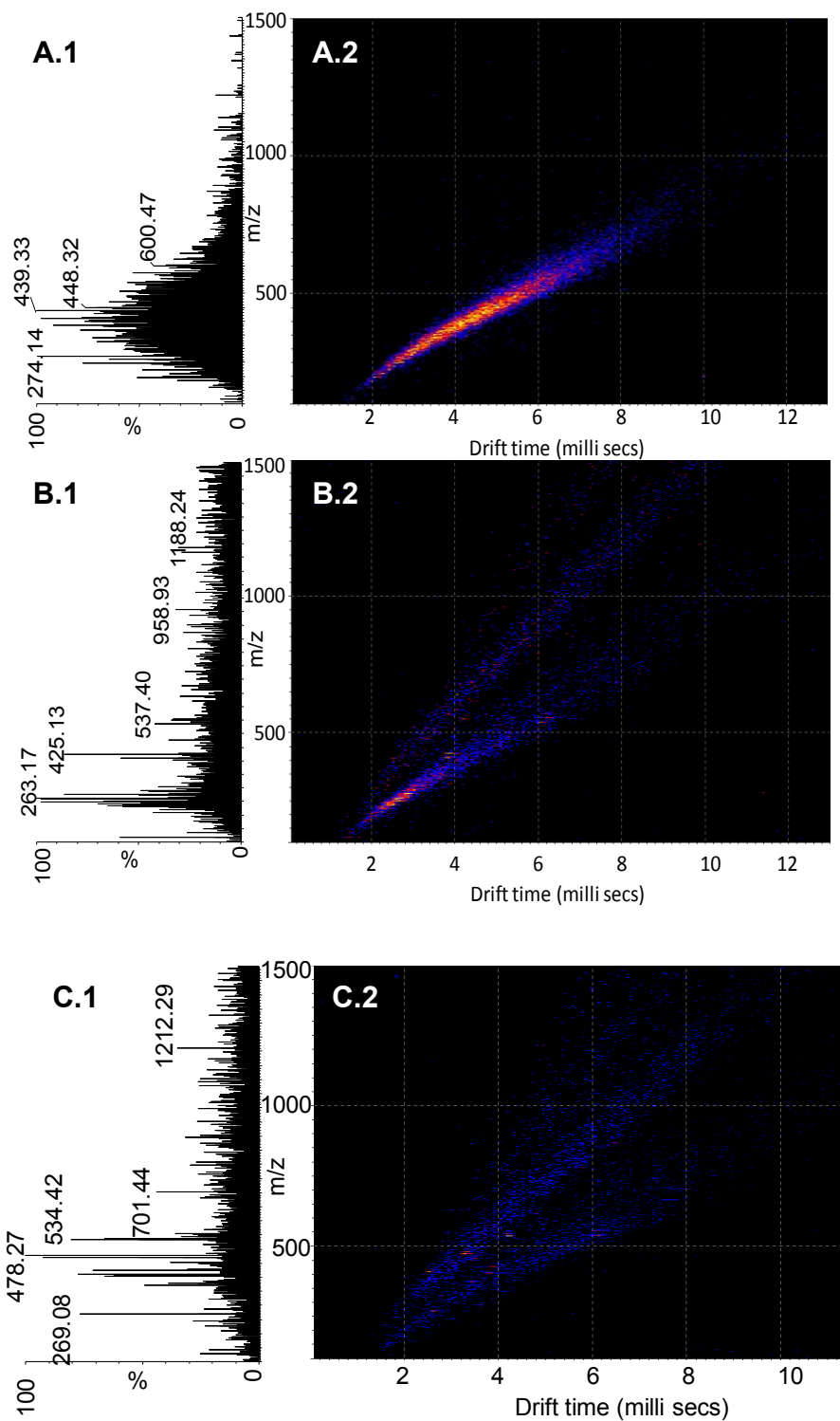


Figure S4.11. LSI-IMS-MS of (A) crude petroleum oil using solvent-free sample preparation with 2,5-DHAP matrix; (B) crude oil using solvent-based sample preparation

with 2,5-DHAP matrix and (C) 2:1 toluene/methanol solvent with 2,5-DHAP matrix; left panel **(1)** Total mass spectra and right panel **(2)** 2-D plots of drift time versus m/z .

APPENDIX B

LC-SAI SUPPLEMENTAL INFORMATION

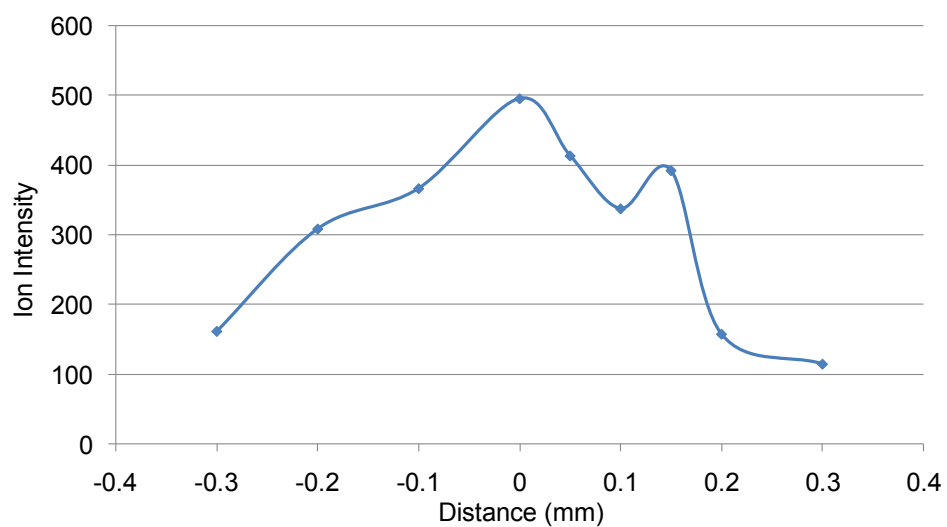


Figure S5.1. Ion intensity changes with the distance between the silica tube tip and the entrance of the inlet to the mass spectrometer.

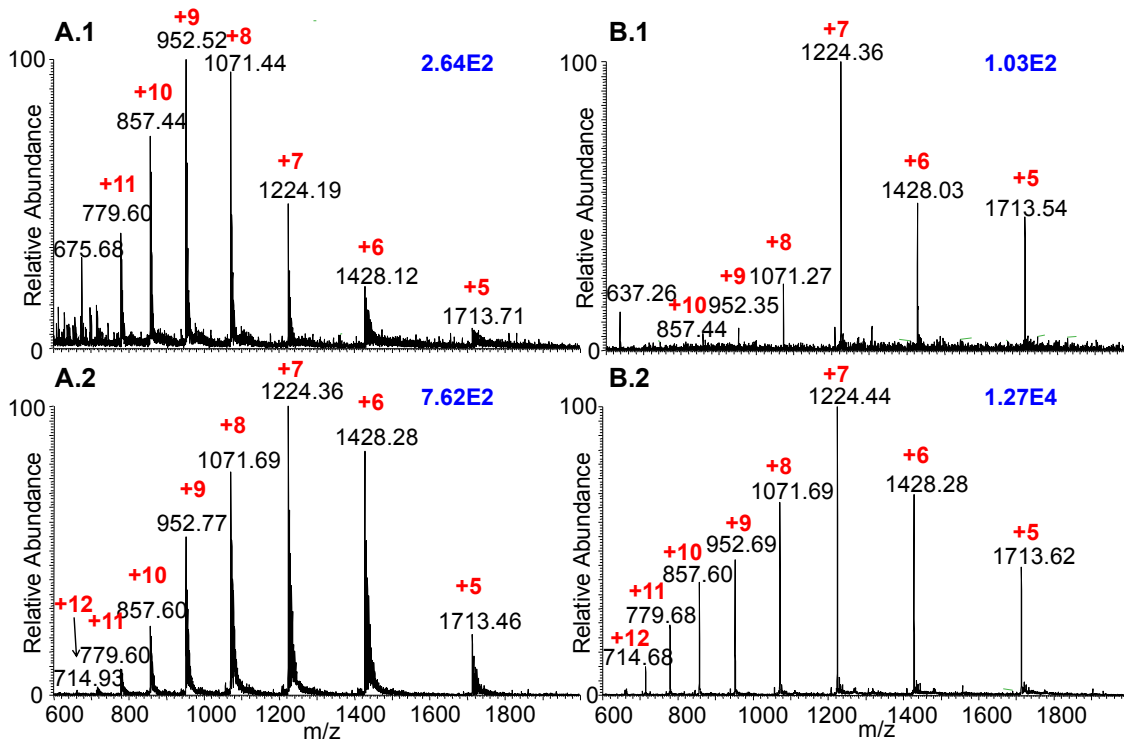


Figure S5.2. SAI-MS of ubiquitin. The liquid solvent/analyte droplet is placed with a pipette tip (10 μ L plastic tip) vertically just outside of the mass spectrometer inlet and slowly pipetted off. The droplets formed are vacuum drawn into the inlet of the mass spectrometer where *inlet* ionization of the analyte occurs. Solutions of 5 pmol ubiquitin (10 μ L) were used. Depending on the solution conditions and inlet temperature the abundance of the highly charged ubiquitin ions varies; less volatile solvent conditions require higher inlet temperatures: **(A)** ubiquitin in 100% water solution and **(1)** 300 °C and **(2)** 450 °C and **(B)** ubiquitin in 50:50 ACN/H₂O in 1% formic acid solution and **(1)** 50 °C and **(2)** 300 °C applied on the inlet of the mass spectrometer. In pure water, Na⁺ adducts are in high abundance lowering the overall intensity of any single peak. Addition of formic acid as shown in B almost eliminates the Na⁺ adducts.



Figure S5.3. Picture showing the setup for LC-nSAII: Front view of Waters NanoAcquity liquid chromatography, Thermo LTQ-Velos mass spectrometer and, here, an automated x,y,z-stage for alignment of tip (**Figure 1a**) and the “picotip” extension (**Figure 1b**) of the fused silica capillary tube of the LC column placed about 0.1 mm out of the orifice inlet entrance of the mass spectrometer.

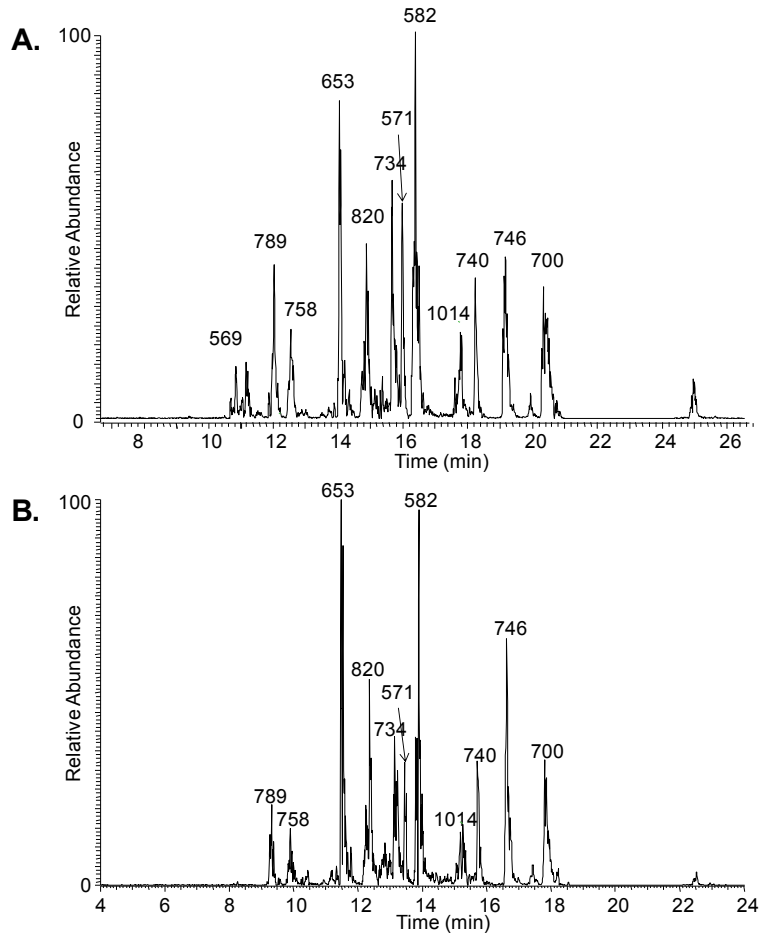


Figure S5.4. LC-SAII-MS of $100 \text{ fmol } \mu\text{L}^{-1}$ BSA tryptic digest acquired on the Thermo LTQ Velos mass spectrometer. **(A)** The base peak chromatogram of $1 \mu\text{L}$ injection at $0.8 \mu\text{L min}^{-1}$ flow rate; **(B)** the base peak chromatogram of $1 \mu\text{L}$ injection at $1.2 \mu\text{L min}^{-1}$ flow rate. The m/z of the most intense peak from the mass spectra of each LC chromatographic peak is labeled at the top of the peak. The mass range for MS data acquisition is 555-1600.

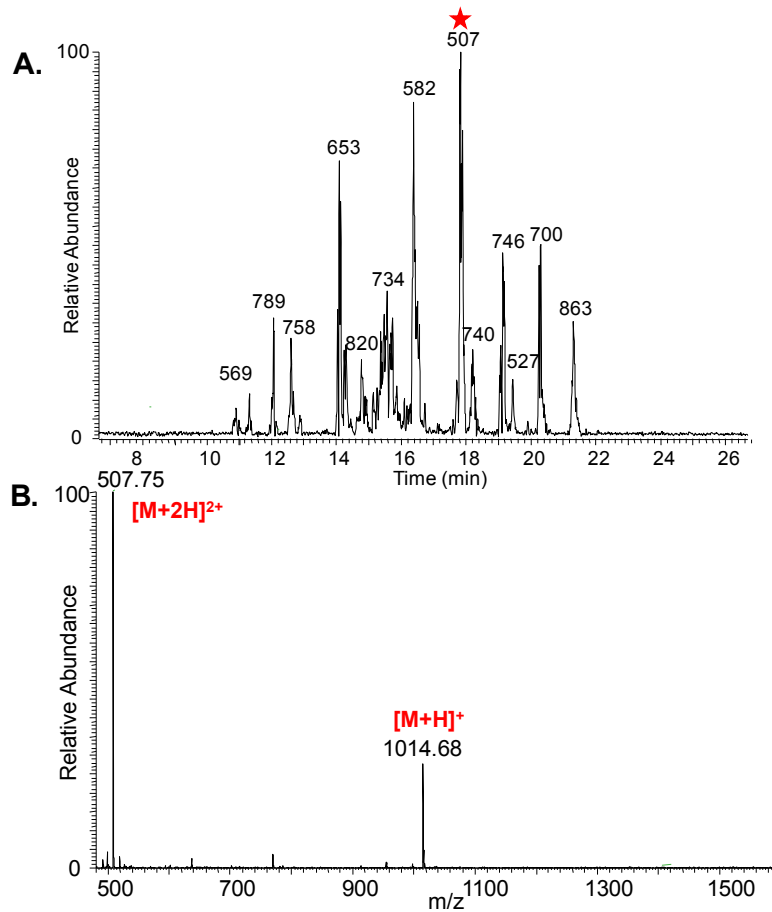


Figure S5.5. A 50 min LC run injecting 1 μL of a 100 $\text{fmol } \mu\text{L}^{-1}$ BSA tryptic digest solution analyzed by LC-nSAIL-MS at a mobile phase flow of 800 nL min^{-1} . **(A)** A section of the base peak chromatogram. The start trigger for the mass spectral acquisition was the same as for the LC so that the inject time is included in the X-axis. The most intense m/z obtained on the mass spectra for each chromatographic peak is labeled. **(B)** Mass spectrum of the chromatographic peak at 17.8 min.

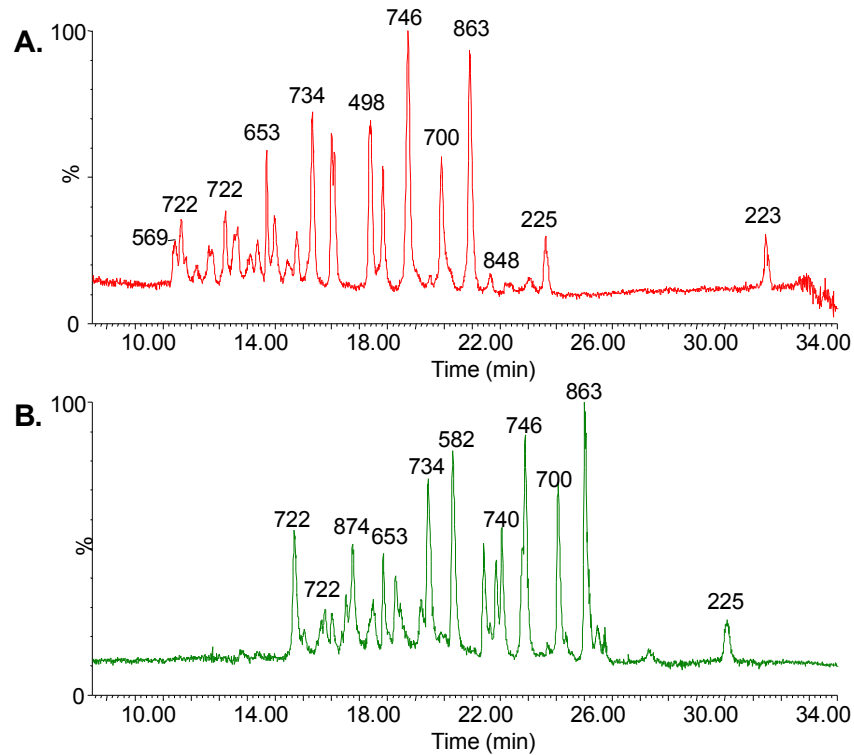
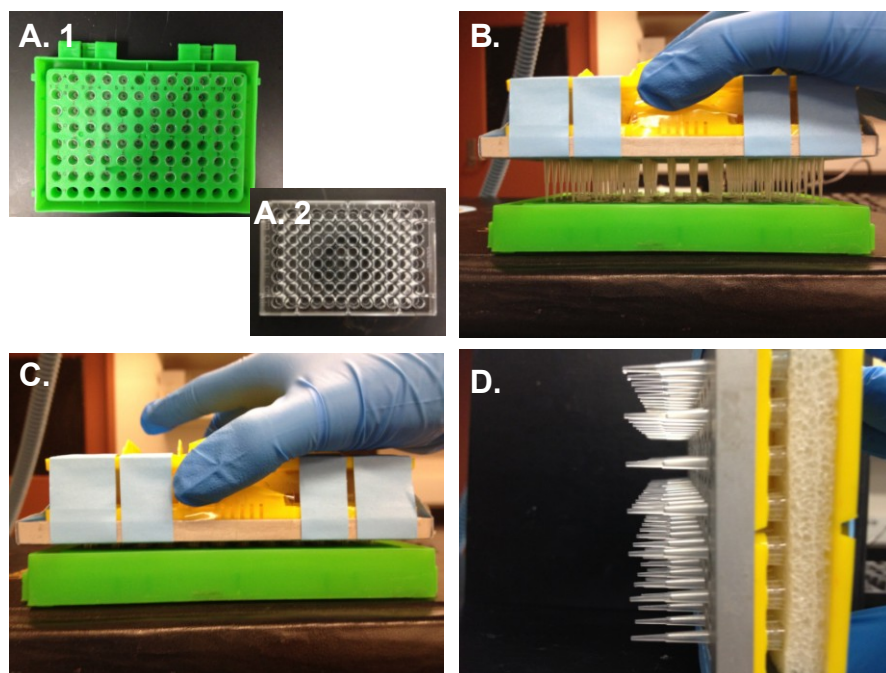
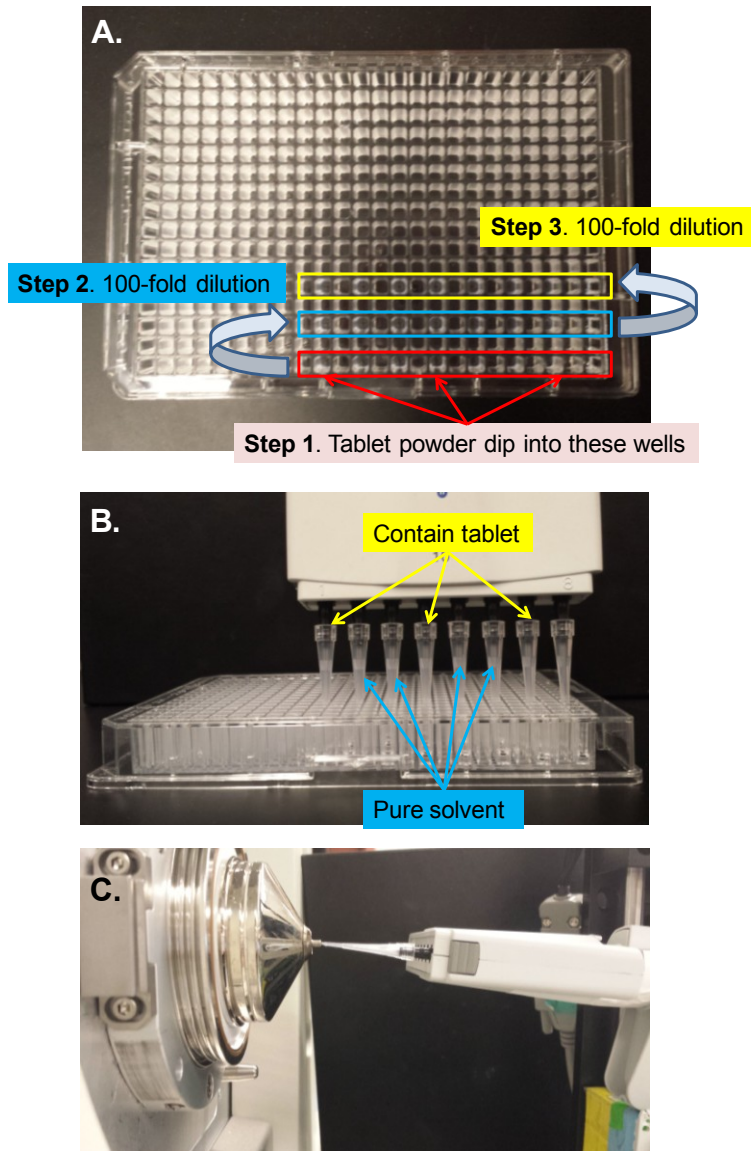


Figure S5.6. Base peak chromatogram of LC-nESI-MS of $100 \text{ fmol } \mu\text{L}^{-1}$ BSA tryptic digest on Waters SYNAPT G2 mass spectrometer. The skimmer temperature is held at $150 \text{ }^\circ\text{C}$. **(A)** The base peak chromatogram of $1 \text{ } \mu\text{L}$ injection at 800 nL min^{-1} flow rate; **(B)** the base peak chromatogram of $1 \text{ } \mu\text{L}$ injection at 400 nL min^{-1} flow rate. Peaks are labeled with m/z values.

APPENDIX C
HIGH THROUGHPUT MULTIPLEXING SAIL SUPPLEMENTAL
INFORMATION



Scheme S6.1. Pictures of sample loading for SAIL multiplexing using a 96-well plate. (A) Vials (1) or wells (2) filled with analyte solutions or pure solvents in a 96-well plate format. (B) Empty pipette tips mounted on another 96-vial plate (1). (C) Dip the tips into the sample vials. (D) Tips filled with about 3 μL solutions by capillary action and are ready to mount on the xy-stage.



Scheme S6.2. Pictures of sample loading for SAIH multiplexing using a 384-well microtiter plate. (A) The workflow of sample preparation of clarithromycin tablet in the microtiter well plate. (B) 1 μL of each tablet solution and pure solvent was drawn into the 8-channel pipette. (C) The pipette is mounted on the xy-stage with the tips aligned with the inlet orifice.

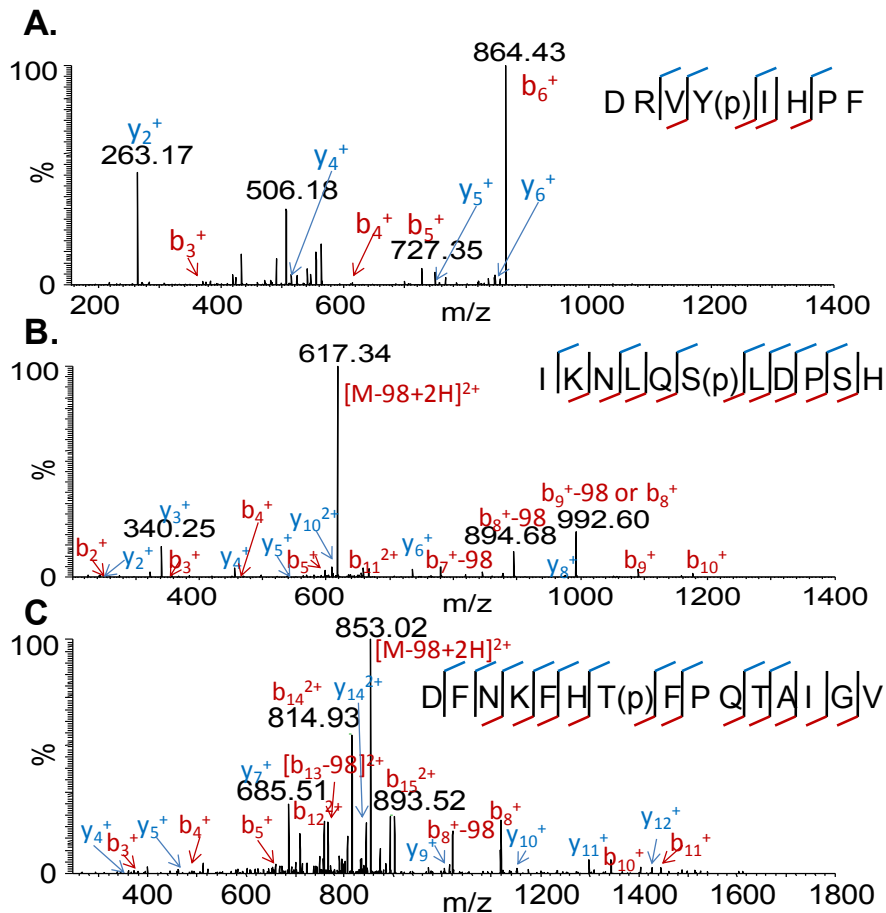


Figure S6.1. A mixture of phosphorylated peptides (angiotensin II, cholecystokin (10-20), and calcitonin (15-29)) was pipetted into the inlet (**Scheme 1A**) which was heated to 250 °C. MS/MS spectra from the mixture of the doubly charged ions using CID are shown in this figure. **(A)** phosphorylated angiotensin II at collision energy 30, data acquired in the mass range of 155-2000; **(B)** phosphorylated cholecystokin (10-20) at collision energy 20, data acquired in the mass range of 180-2000; and **(C)** phosphorylated calcitonin (15-29) at collision energy 20, data acquired in the m/z range of 245-2000;. 1 μL of 2.5 $\text{pmol } \mu\text{L}^{-1}$ solution was used for each acquisition.

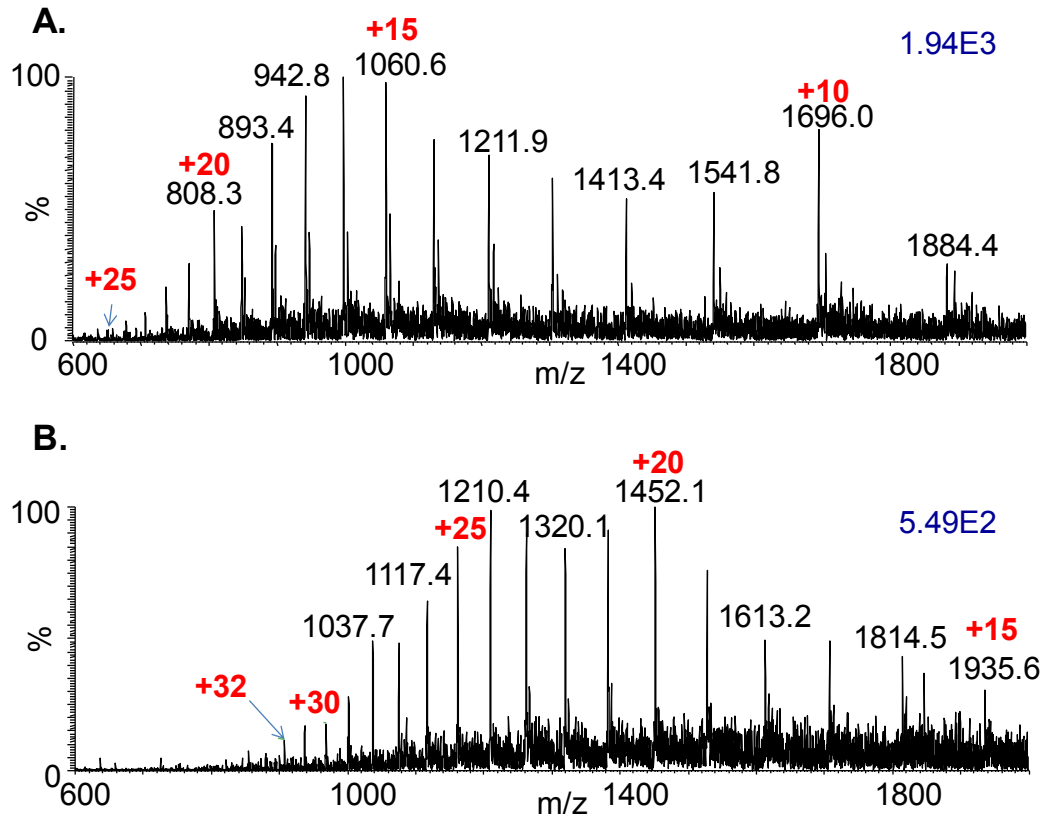


Figure S6.2. SAI mass spectra of (A) $1 \mu\text{L}$ $2.5 \text{ pmol } \mu\text{L}^{-1}$ myoglobin and (B) $1 \mu\text{L}$ $5 \text{ pmol } \mu\text{L}^{-1}$ carbonic anhydrase obtained by pipetting the solution into the inlet (**Scheme 1A**) at an inlet temperature of $250 \text{ }^\circ\text{C}$. The blue number in top right corner denotes the ion intensity. Data were acquired in the m/z range of 600-2000.

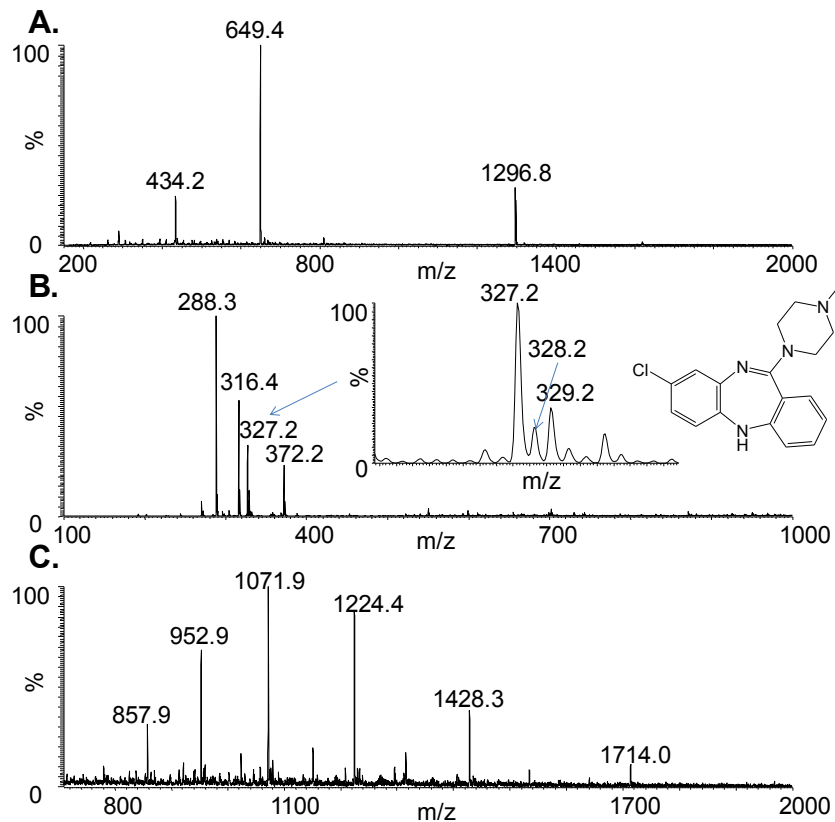


Figure S6.3. SAI mass spectra of (A) 5 pmol μL^{-1} angiotensin I in water at 150 °C, (B) 5 pmol μL^{-1} clozapine in chloroform at 250 °C with matching isotopic distribution, data acquired in the mass range of 100-1000 and (C) 1 pmol μL^{-1} ubiquitin in 90:10 acetonitrile:water at 400 °C inlet temperatures. 1 μL solution of each solution was pipetted into the inlet (Scheme 1A). Data were acquired in the m/z range of 150-2000.

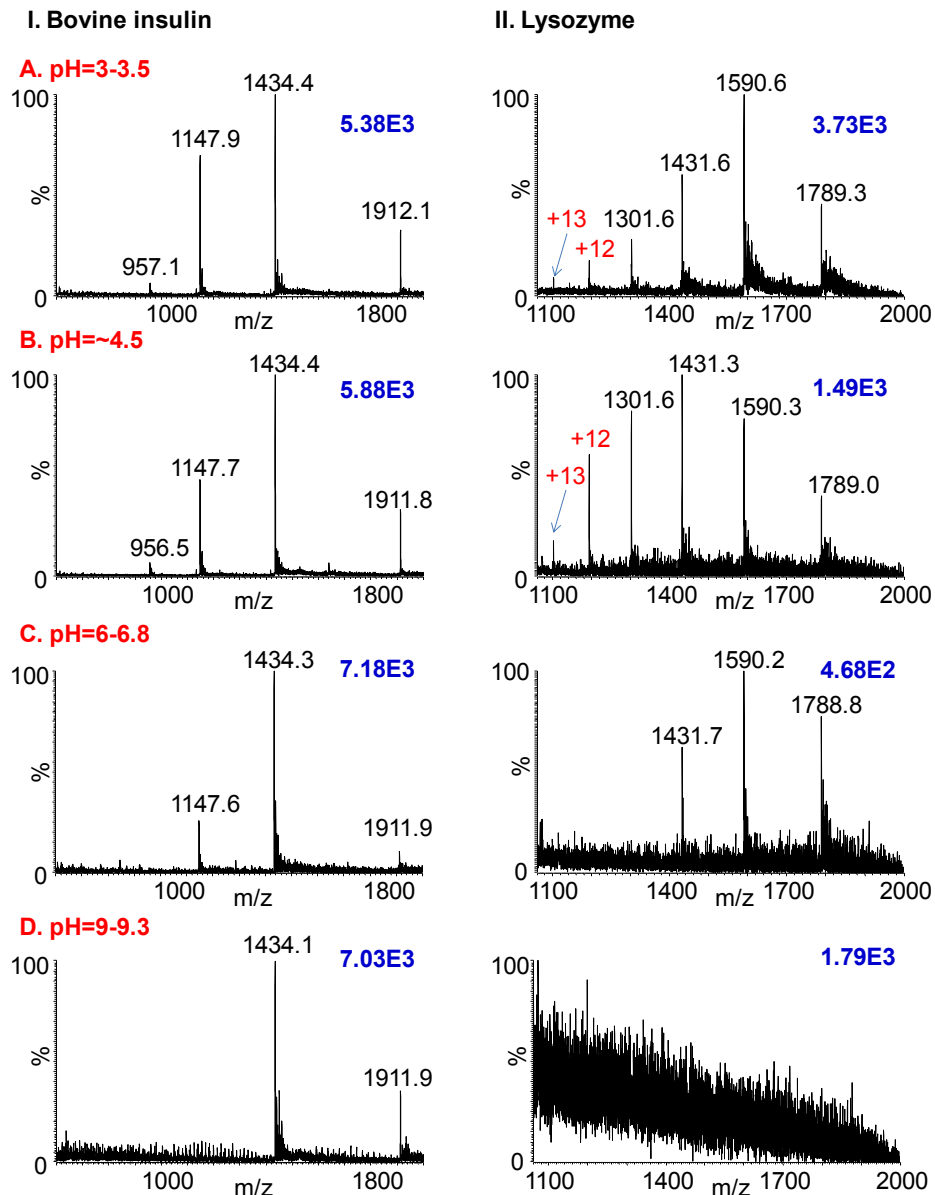


Figure S6.4. pH study of (I) 5 pmol μL^{-1} bovine insulin and (II) 10 pmol μL^{-1} lysozyme using SAIL-MS at an inlet temperature of 250 °C: pH: (A) 3 to 3.5, (B) ~4.5, (C) 6 to 6.8, (D) 9 to 9.3. 2 μL solution was pipetted into the inlet (Scheme 1A). Data were acquired in the m/z range of 150-2000.

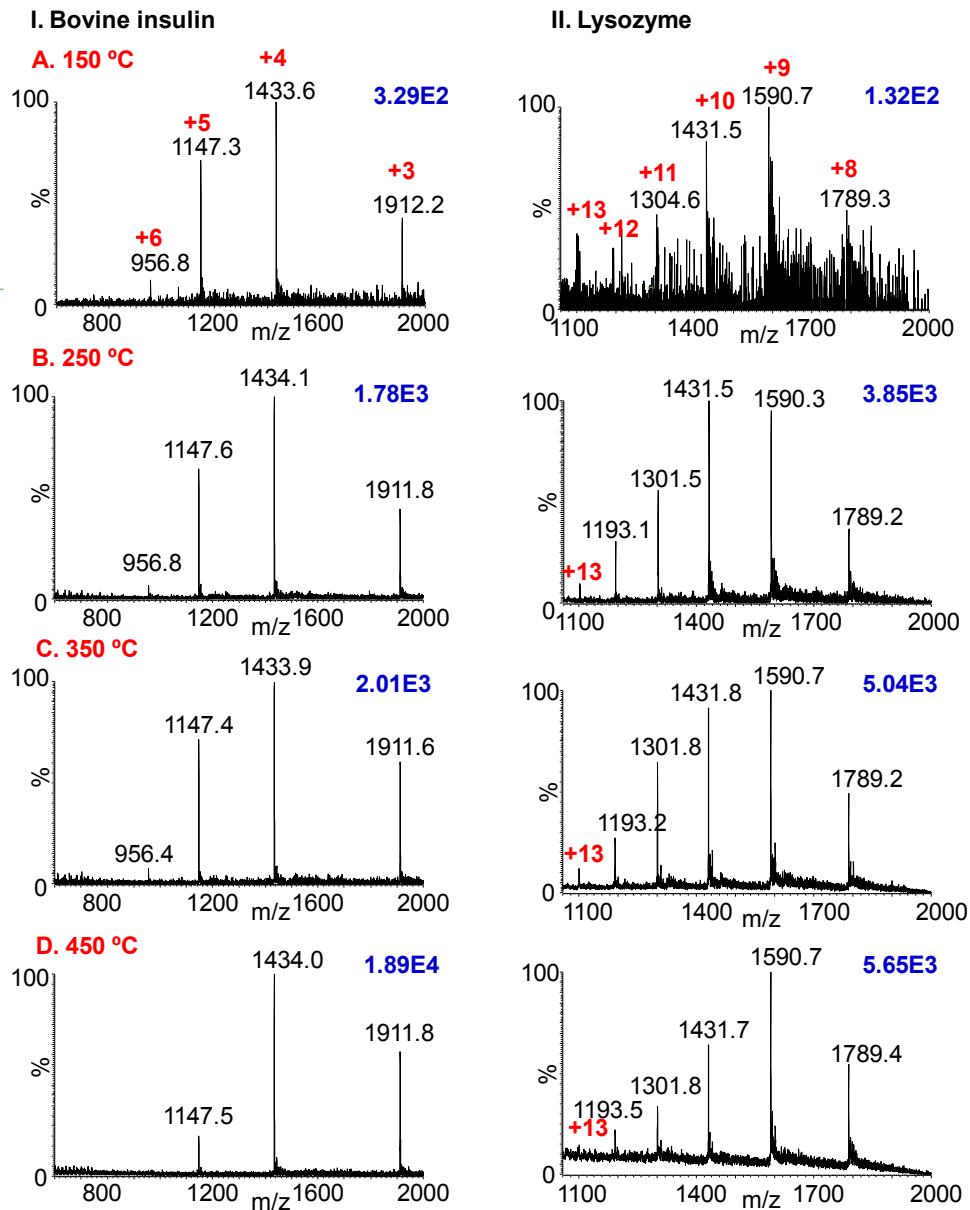


Figure S6.5. SAI mass spectra of (I) 5 pmol μL^{-1} bovine insulin in 50:50 methanol:water with 1% acetic acid and (II) 10 pmol μL^{-1} lysozyme in 50:50 acetonitrile:water with 0.1% formic acid at different inlet temperatures: (A) 150 °C, (B) 250 °C, (C) 350 °C, and (D) 450 °C. 2 μL solution was pipetted into the inlet (Scheme 1A). Data were acquired in the m/z range of 150-2000.

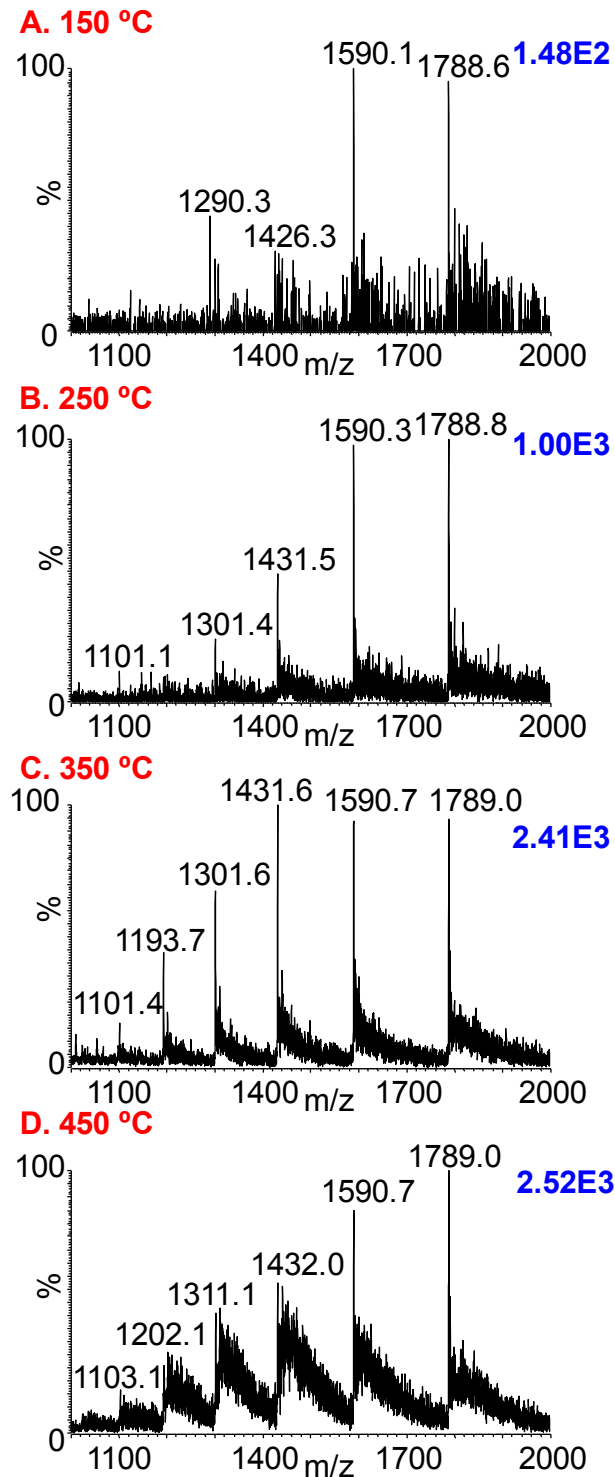


Figure S6.6. SAIL mass spectra of $10 \text{ pmol } \mu\text{L}^{-1}$ lysozyme in water at different inlet temperatures: (A) 150 °C, (B) 250 °C, (C) 350 °C, and (D) 450 °C. $2 \text{ } \mu\text{L}$ solution was pipetted into the inlet (Scheme 1A). Data were acquired in the m/z range of 150-2000.

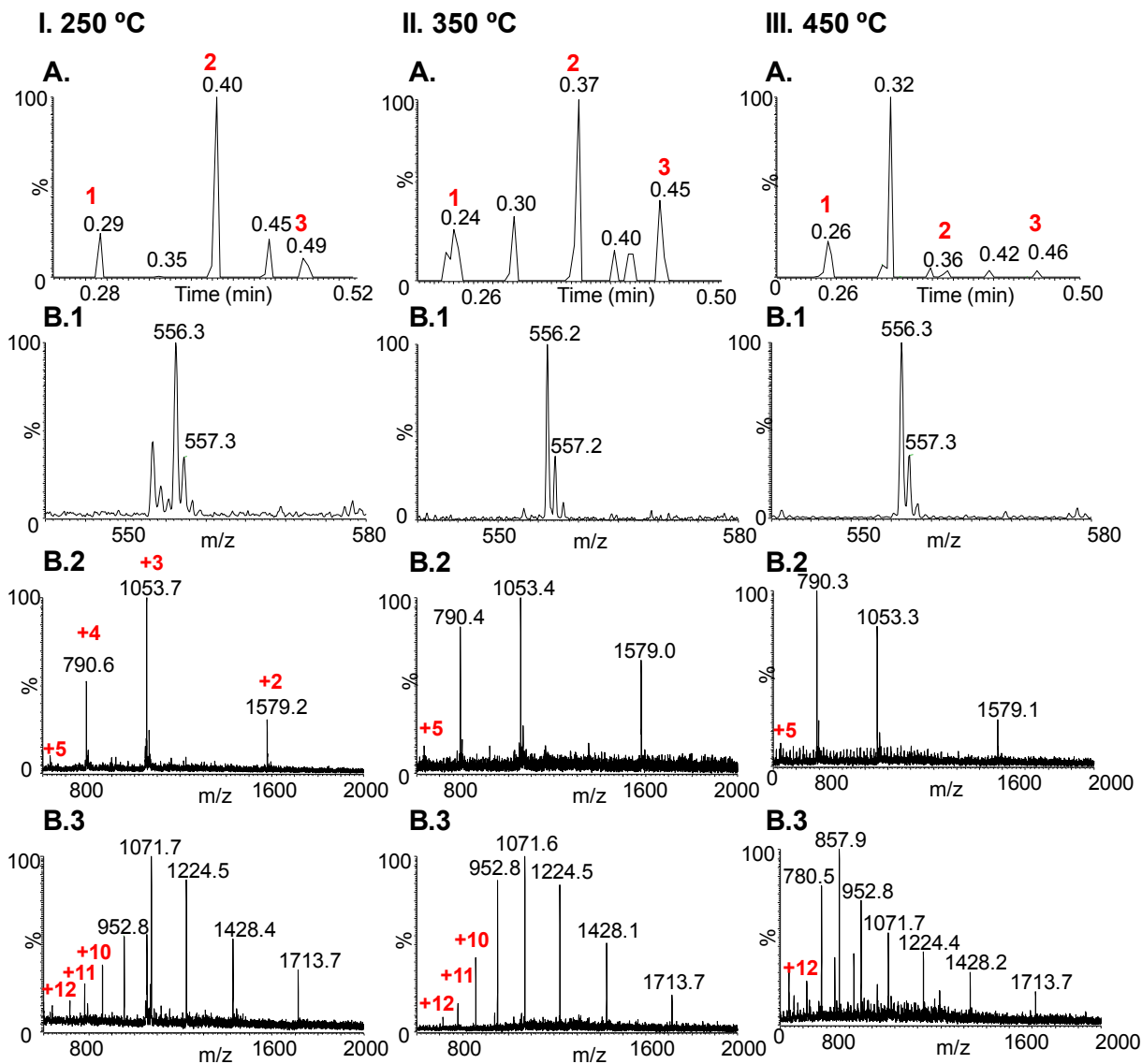


Figure S6.7. Multiplexing SAI-MS using the 8-channel pipette (**Scheme 1B**) at different inlet temperatures: **(I)** 250 °C, **(II)** 350 °C, and **(III)** 450 °C in a total of ~15 seconds. **(A)** The TIC and **(B)** mass spectra of the analysis of tips filled with **(1)** 2.5 pmol μL^{-1} leucine enkephalin, **(2)** 1 pmol μL^{-1} galanin, and **(3)** 1 pmol μL^{-1} ubiquitin with solvent between each two samples. 2 μL analyte/solvent was drawn into each pipet tip. The maximum injection time was 100 ms. Data were acquired in the m/z range of 150-2000.

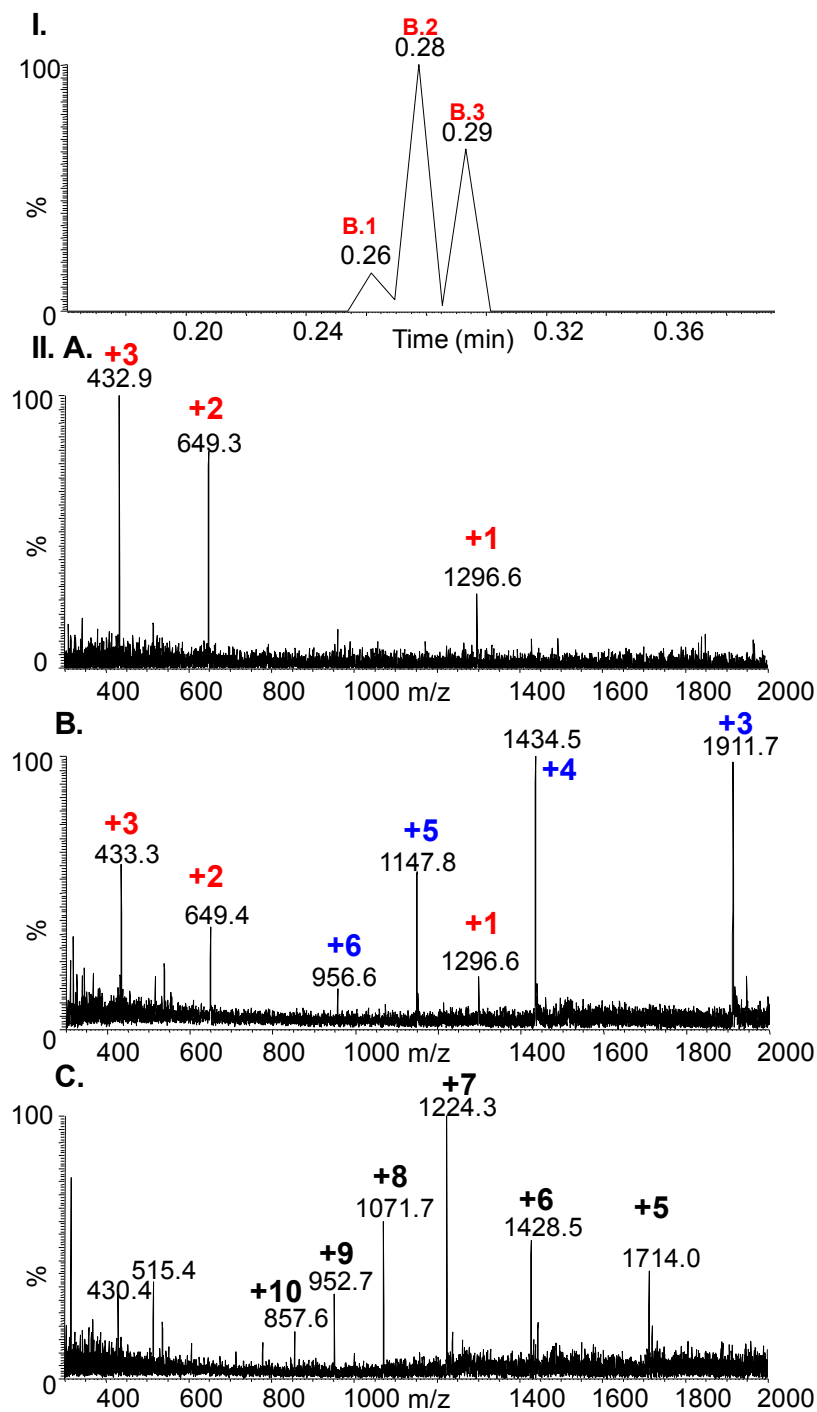


Figure S6.8. SAIL-MS using the 8-channel pipette (**Scheme 1B**) and an inlet temperature of 150 °C. All three analytes were analyzed in a total of ~2 seconds. **(I)** The TIC of 5 tips filled with angiotensin I, bovine insulin, and ubiquitin with pure solvent between each two analytes. **(II)** Mass spectra extracted from **(A)** 0.26 min for 1 pmol μL^{-1} angiotensin

I, **(B)** 0.28 min for 5 pmol μL^{-1} bovine insulin with some angiotensin I cross contamination, and **(C)** 0.29 min for 1 pmol μL^{-1} ubiquitin. 2.5 μL analyte/solvent was drawn into each pipet tip. The maximum injection time was 500 ms. Data were acquired in the m/z range of 150-2000.

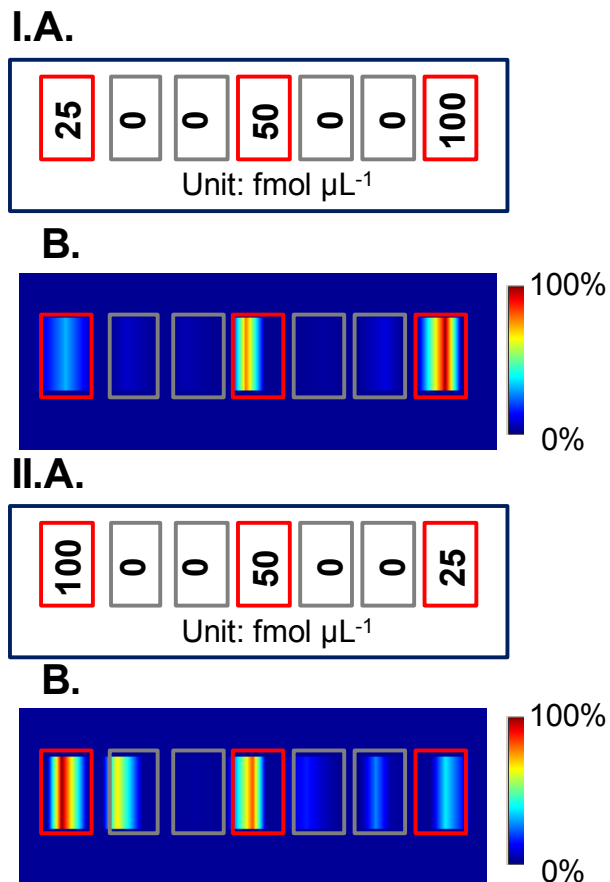


Figure S6.9. Mapping using the 8-channel pipette (**Scheme 1B**). The solutions were scanned from **(I)** low to high and **(II)** high to low concentrations. **(A)** Schematic representation of content in each pipette tip. Red boxes indicate tips filled with 2 μL clozapine solutions at 25 fmol μL^{-1} , 50 fmol μL^{-1} , and 100 fmol μL^{-1} , respectively; grey boxes represent pure solvent methanol. **(B)** The mapping of m/z 270 peak. Note that the methanol solutions (grey boxes) furthest to the right in **(I)** and **(II)** are more intense than the prior methanol solutions (second last) suggesting that carryover are neglectable in both cases for the sample (samples solutions furthest to the right, red boxes). Data were acquired in the m/z range of 90-345.

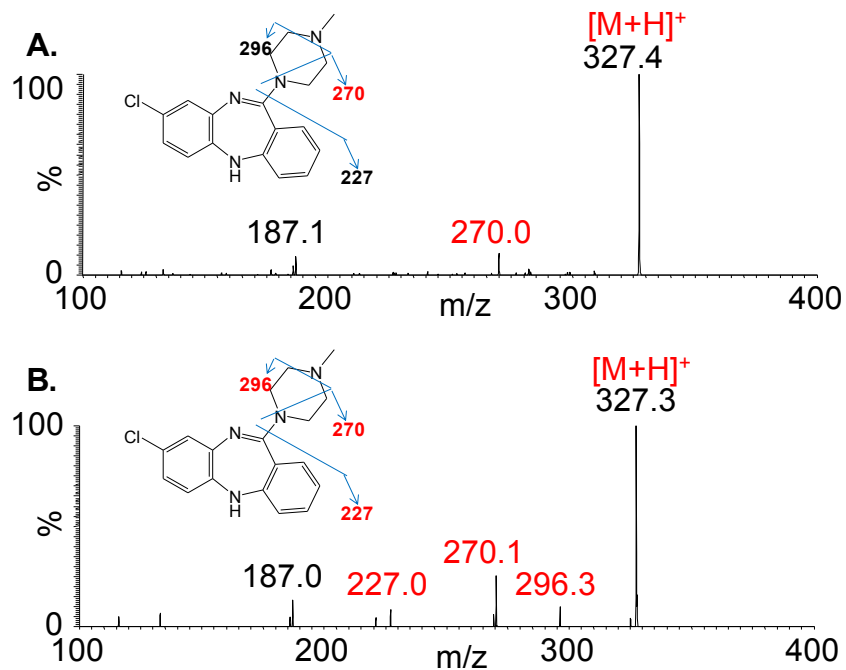


Figure S6.10. SAI-MS/MS of clozapine using the 8-channel pipette (**Scheme 1B**). The protonated ions were selected and fragmented by CID using normalized collision energy of 30. The maximum injection time was 100 ms. (**A**) 1 μL of 1 $\text{fmol } \mu\text{L}^{-1}$ clozapine and (**B**) 3 μL of 0.5 $\text{fmol } \mu\text{L}^{-1}$ clozapine was drawn into the pipette tip. The inlet temperature was 250 $^{\circ}\text{C}$. Data were acquired in the m/z range of 100-400.

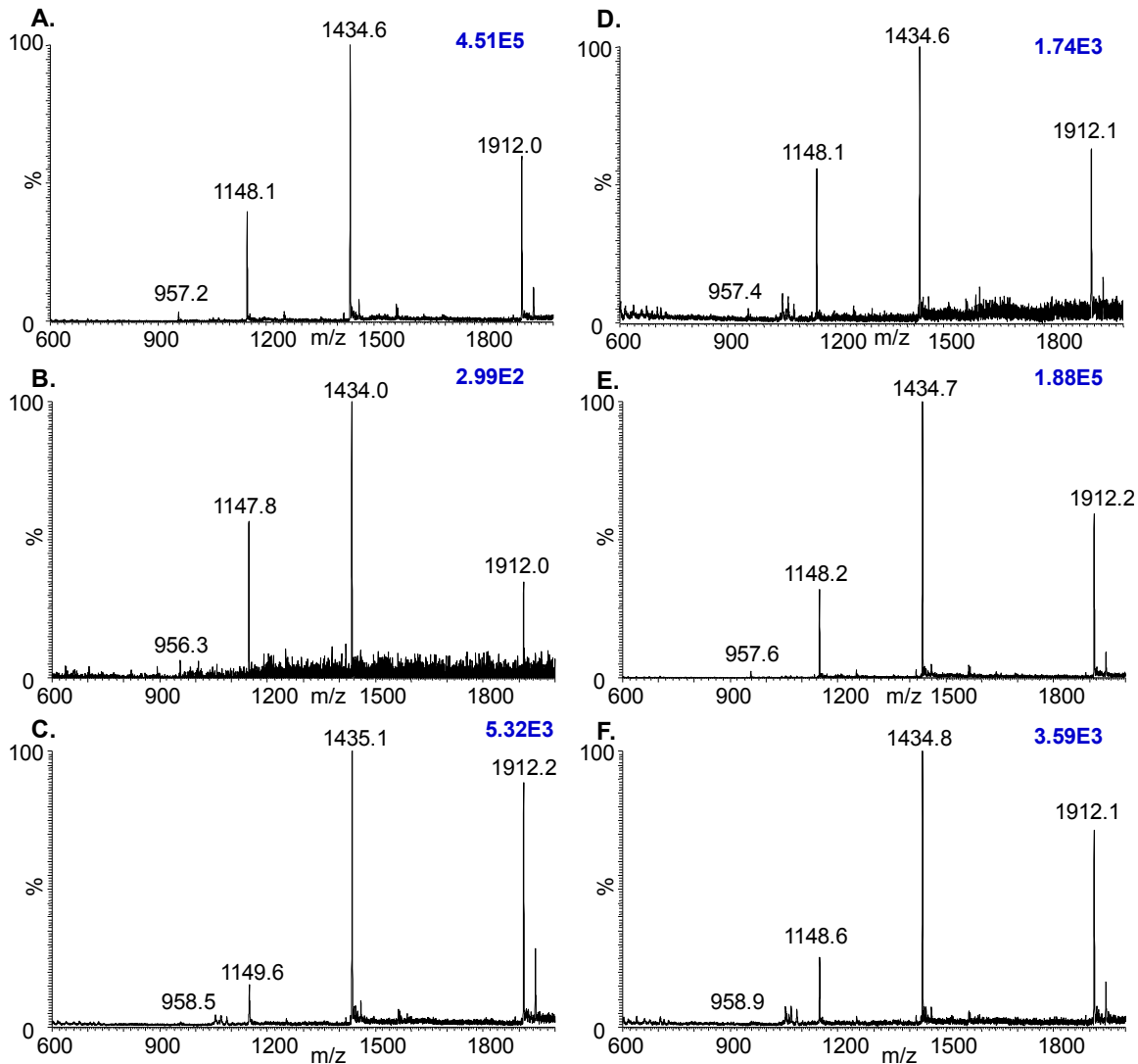


Figure S6.11. All six mass spectra (A to F) of 5 pmol μL^{-1} bovine insulin (in methanol/water with acetic acid) extracted from the repetitive six cycles of SAI multiplexing using a 96-vial plate (Scheme 1C) at the inlet temperature of 250 °C. The numbers in blue in the top right corner indicate the ion intensity. Data were acquired in the m/z range of 150-2000.

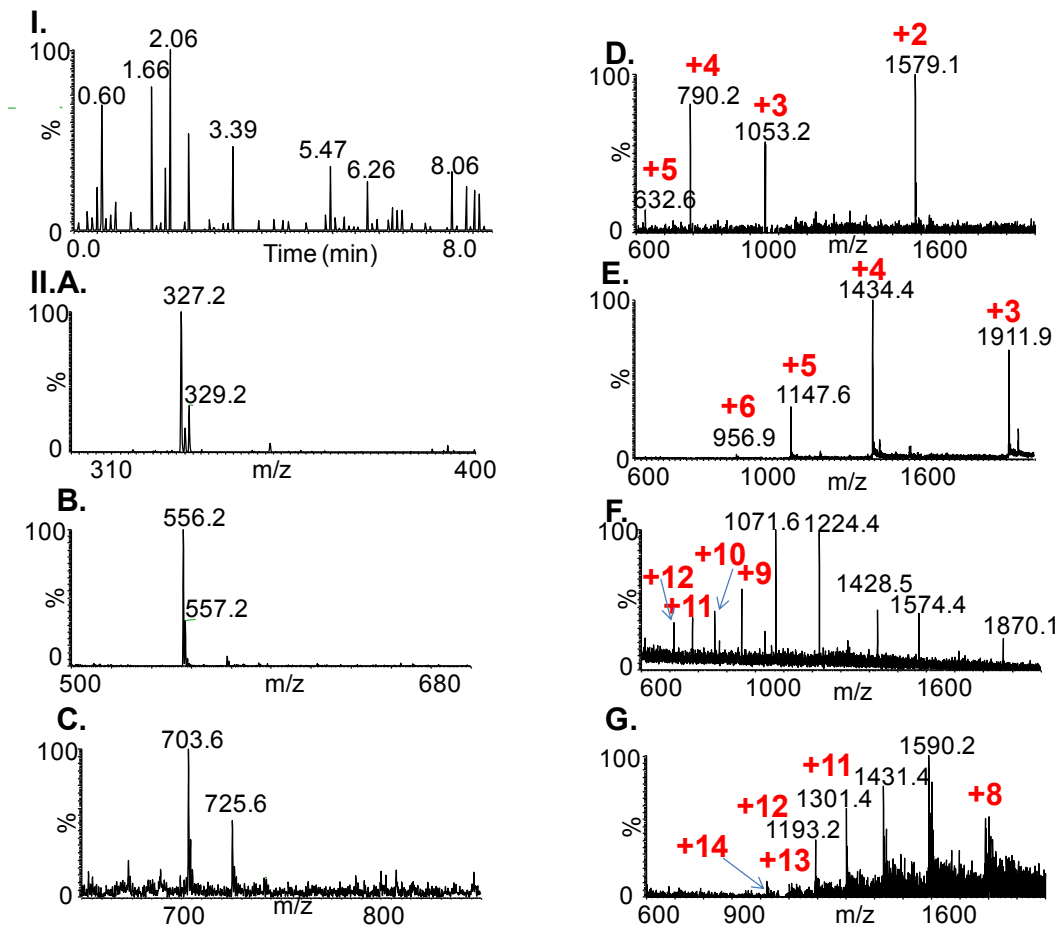


Figure S6.12. SAIL-MS using 84 tips mounted on a 96-vial plate (**Scheme 1C**) when the inlet temperature was held at 250 °C in a total of ~ 10 min. **(I)** Total ion current. **(II)** Mass spectra of **(A)** 1 pmol μL^{-1} clozapine (in methanol), **(B)** 2.5 pmol μL^{-1} leucine enkephalin (in acetonitrile:water with formic acid), **(C)** 1 pmol μL^{-1} sphingomyelin (in methanol with acetic acid), **(D)** 1 pmol μL^{-1} galanin (in acetonitrile:water with formic acid), **(E)** 1 pmol μL^{-1} bovine insulin (in methanol:water with acetic acid), **(F)** 1 pmol μL^{-1} ubiquitin (in acetonitrile:water with formic acid), and **(G)** 1 pmol μL^{-1} lysozyme (in acetonitrile:water with formic acid). Data were acquired in the m/z range of 150-2000.

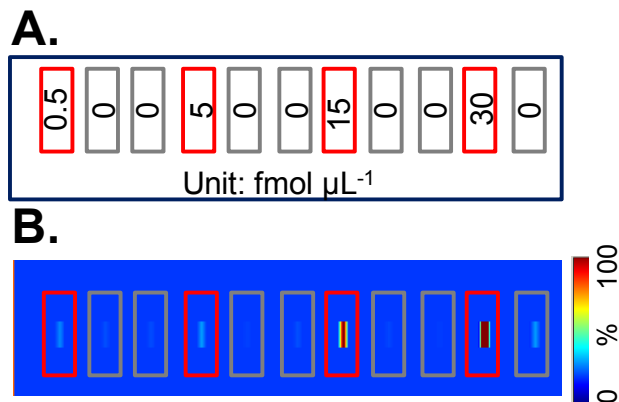


Figure S6.13. Mapping using the 96-sample plate shown in **Scheme 1C**. **(A)** Schematic representation of content in each pipet tip. Red boxes indicate tips filled with clozapine solutions at 0.5, 5, 15, and 30 fmol μL^{-1} , respectively; grey boxes represent pure solvent methanol. **(B)** The mapping of m/z 270 peak obtained by selecting the m/z 327 ($[\text{M}+\text{H}]^+$ ion) for CID fragmentation using normalized collision energy of 30. The maximum injection time was 100 ms. Data were acquired in the m/z range of 90-345.

APPENDIX D

MAIV ON FT-ICR SUPPLEMENTAL INFORMATION

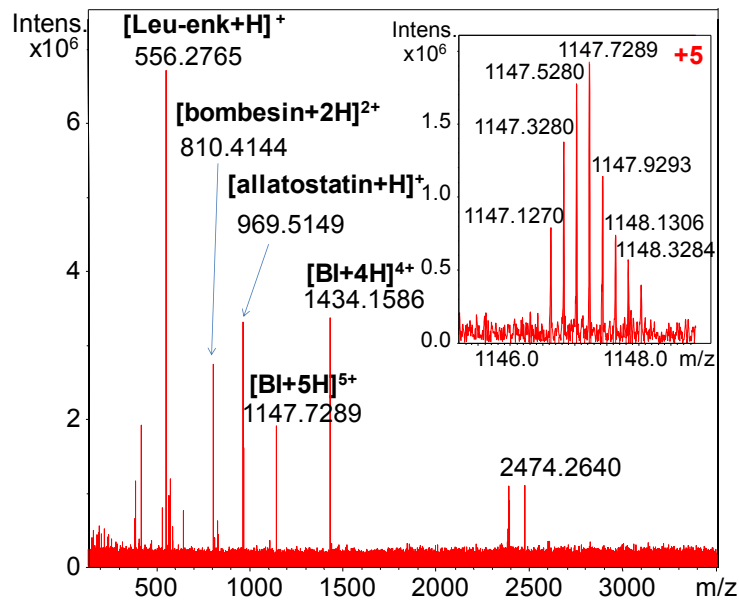


Figure S7.1. MAIV mass spectrum of a mixture of peptides and proteins including: leucine enkephalin (Leu-enk), bombesin, allatostatin, and bovine insulin (BI). The inset shows the +5 charge state of bovine insulin.

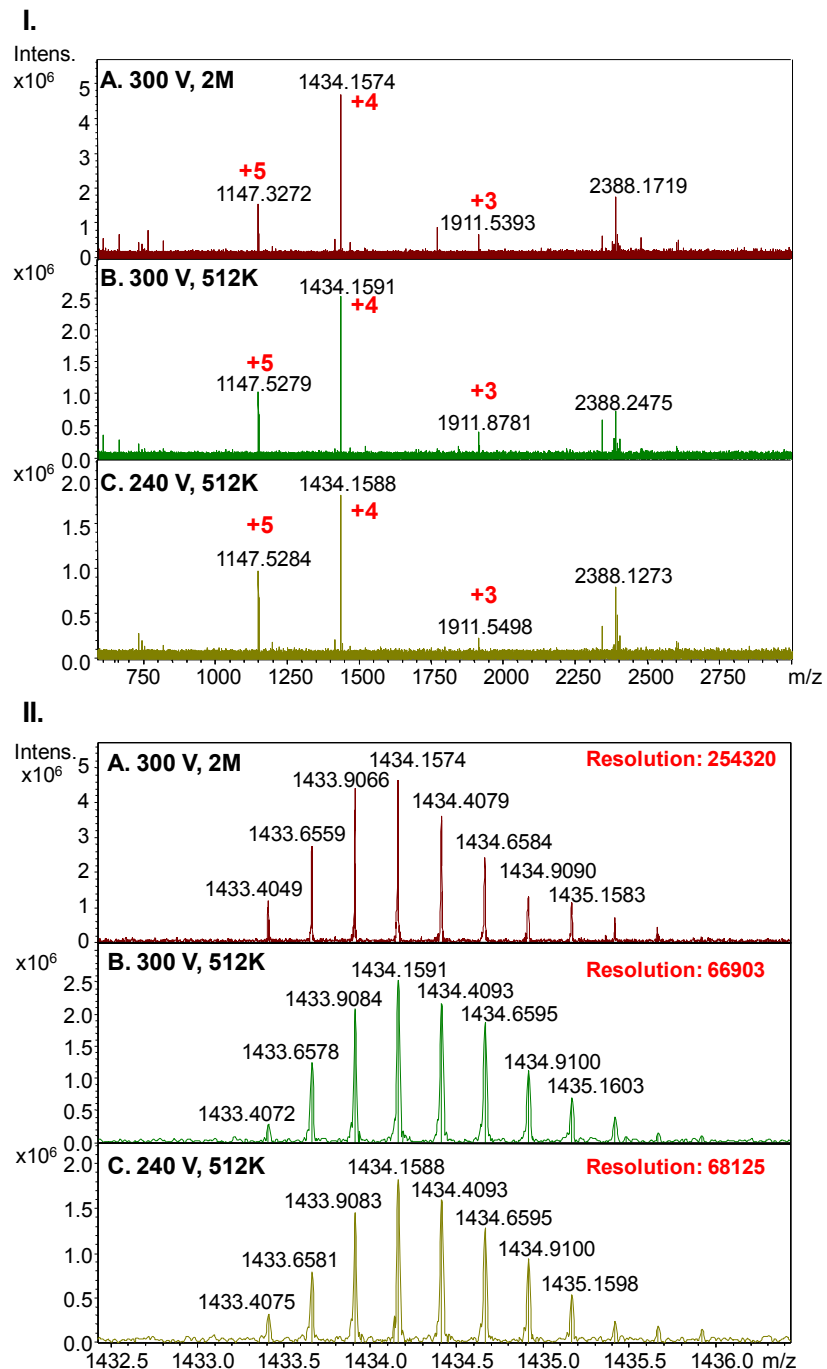


Figure S7.2. MAIV mass spectra (**I**) and the +4 inset (**II**) of bovine insulin using different plate voltages and data acquisition sizes. (**A**) 300 V plate voltage and 2 million acquisition size; (**B**) 300 V plate voltage and 512 thousand acquisition size; and (**C**) 240 V plate voltage and 512 thousand acquisition size.

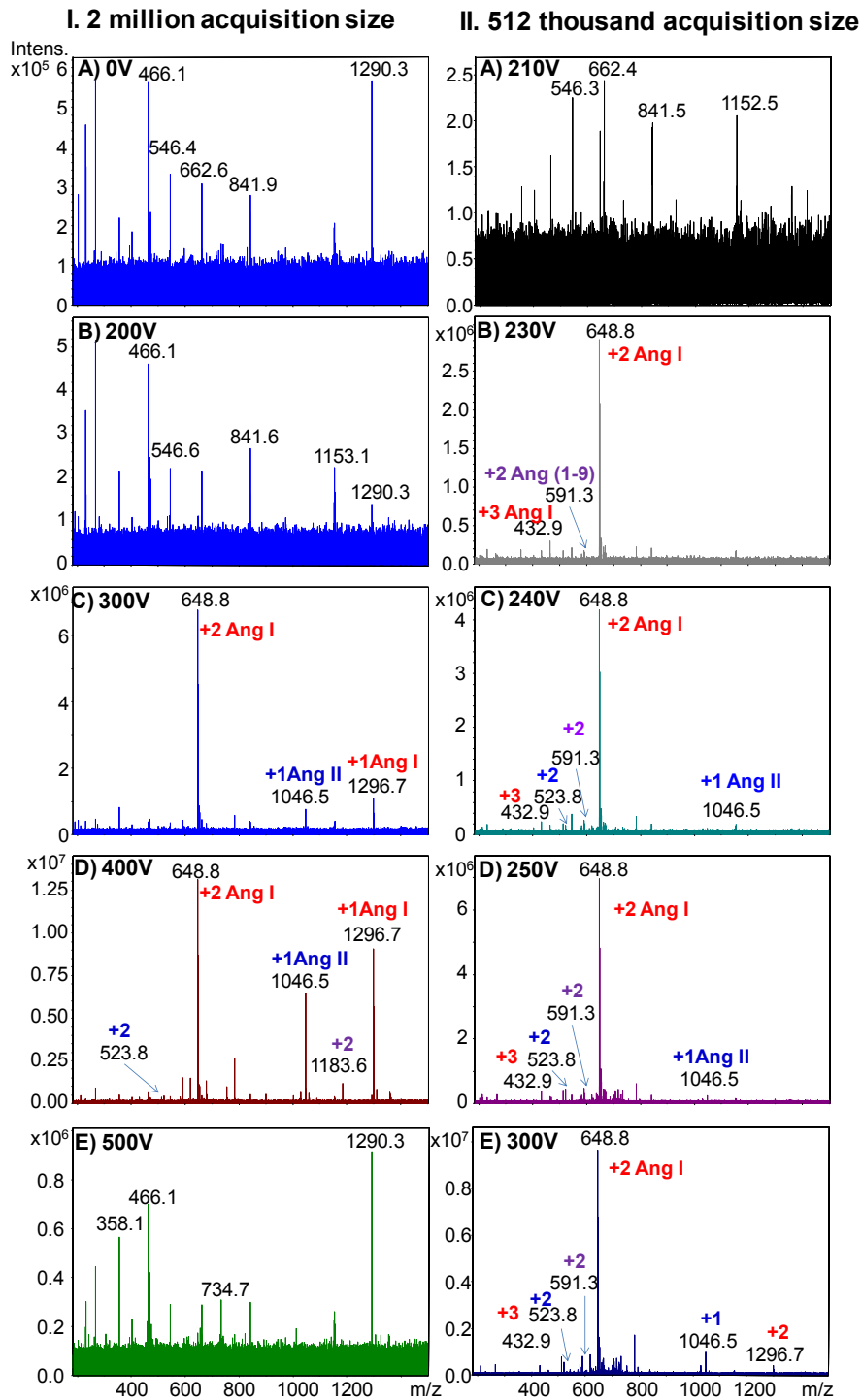


Figure S7.3. MAIV mass spectra of angiotensin mixture using different plate voltages and data acquisition sizes. **(I)** With 2 million acquisition size at **(A)** 0 V, **(B)** 200 V, **(C)**

300V, **(D)** 400 V, and **(E)** 500V; **(II)** with 512 thousand acquisition size at **(A)** 210 V, **(B)** 230 V, **(C)** 240 V, **(D)** 250 V, and **(E)** 300 V.

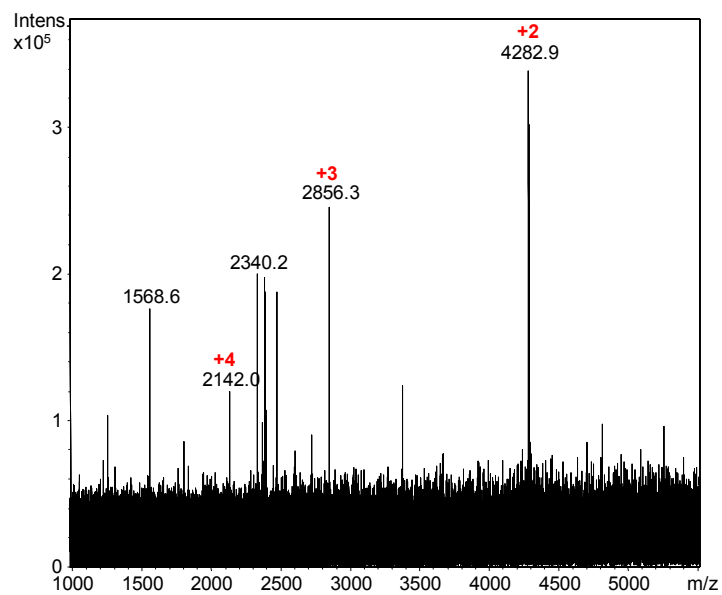


Figure S7.4. LSIV mass spectrum of 100 pmol ubiquitin using 2-NPG matrix summarizing 20 scans. The laser power was 50%, the voltage applied on the target plate is 400 V, and data acquisition size was 512 thousand.

APPENDIX E

QUANTIFICATION SUPPLEMENTAL INFORMATION

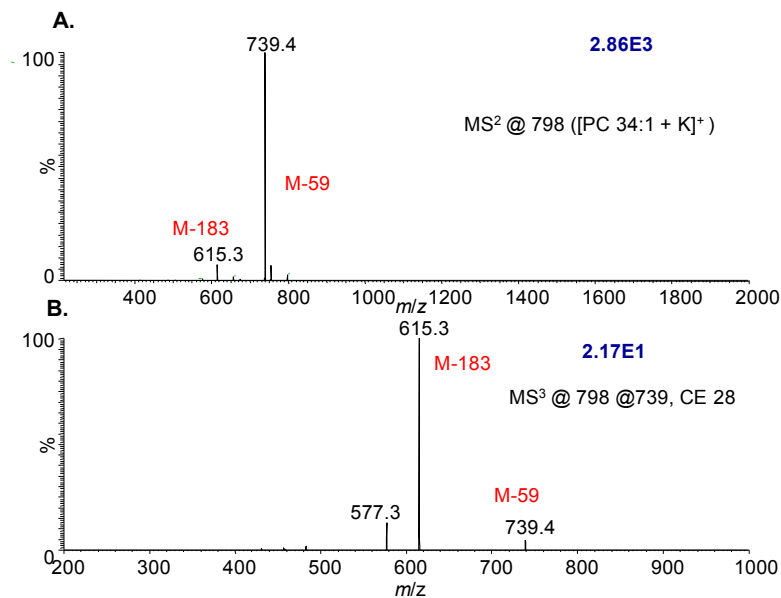


Figure S8.1. Characterization of phosphatidylcholine (34:1) extracted from the brain tissue section of a drug-treated mouse and pipetted into the heated inlet (**Scheme 8.1. II.A**). (**A**) MS² by fragmenting the most abundant peak from **Figure 8.1. B** ([PC 34:1 + K]⁺) and CID was performed with CE=28. (**B**) MS³ by fragmenting the most abundant product ion at *m/z* 739 using CID with CE=28. The blue numbers on the top right corner denote ion intensities.

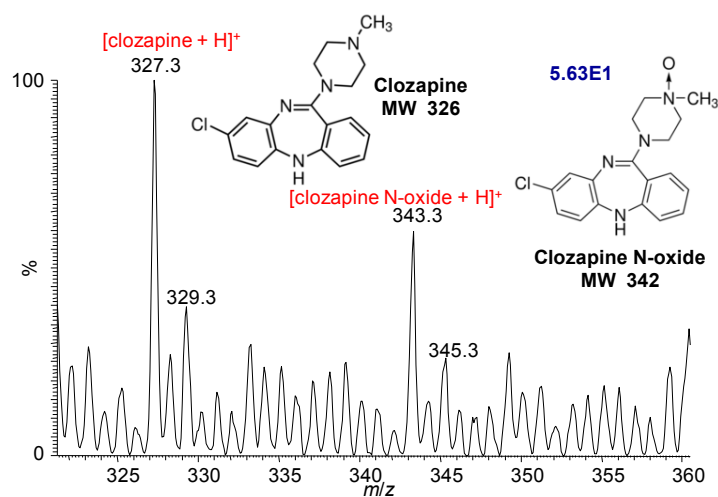


Figure S8.2. Inset mass spectrum showing clozapine and one major metabolite, clozapine N-oxide, obtained by surface extraction of an aged brain tissue section from drug-treated mouse followed by SAI method in discontinuous mode (**Scheme 8.1. II.A**). The blue number on the top right corner denotes ion intensities.

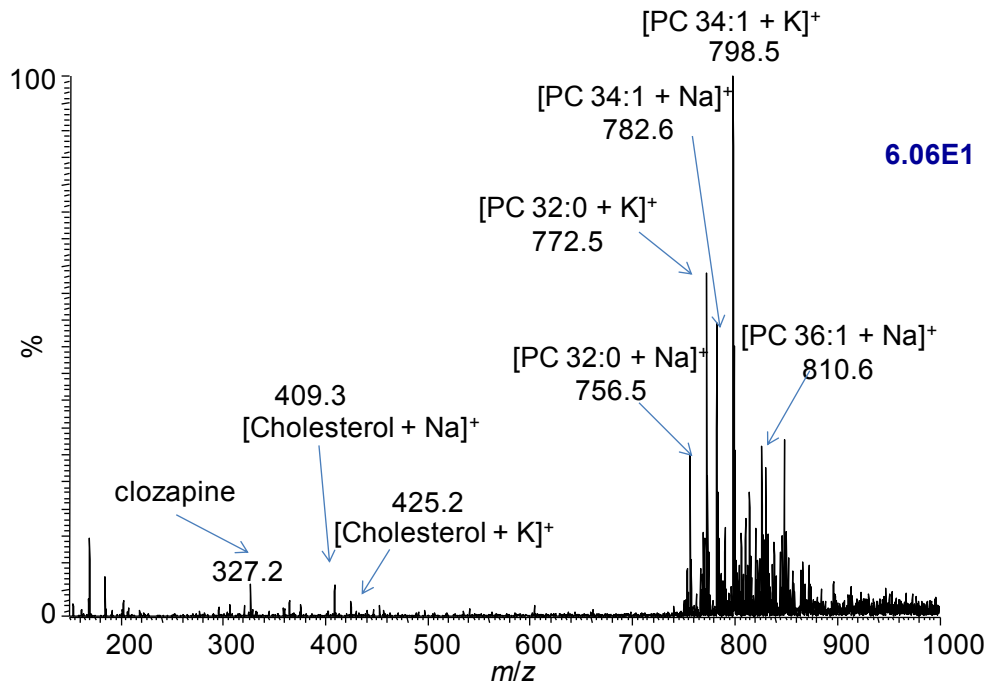


Figure S8.3. Mass spectrum obtained by SAIL in continuous surface extraction mode (**Scheme 8.1. II.B**). A brain tissue section of drug-treated mouse was analyzed. The mass spectrum was extracted from 0.37 to 0.86 min from the TIC shown in **Figure 8.2A**. The blue number on the top right corner denotes ion intensity. The peaks were assigned according to previous studies. No cholesterol fragment with the loss of water (at m/z 369) or water cluster background was detected as observed in typical MALDI analysis.

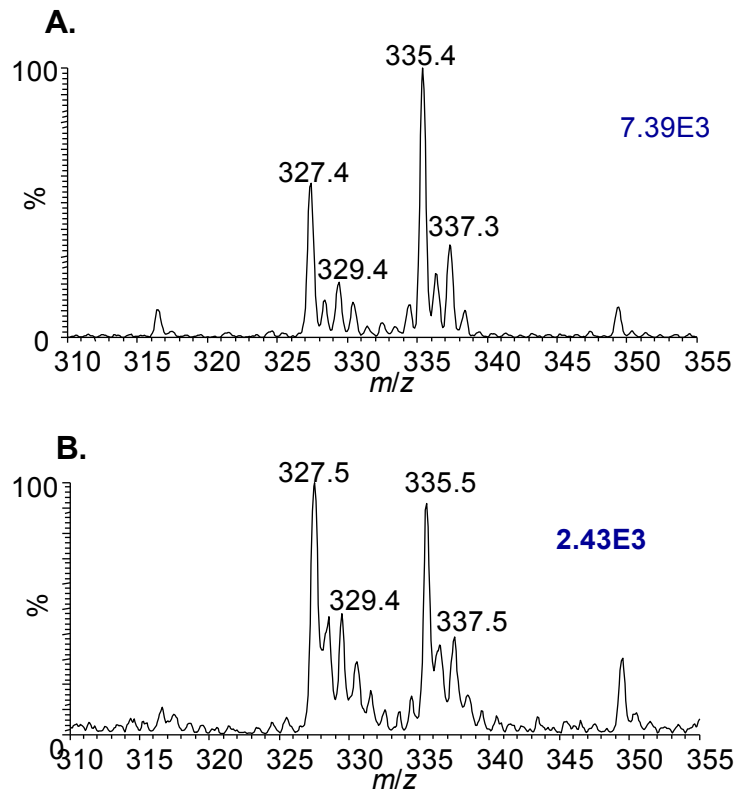


Figure S8.4. Mass spectra using SAI by pipetting 1 μL standard clozapine:clozapine-d8 solution from the vial into the heated mass spectrometer inlet. The concentration ratio of clozapine:clozapine-d8 is **(A)** 0.5:1 and **(B)** 1:1 with the clozapine-d8 at 2 pmol μL^{-1} . The ion intensity ratio at m/z 's 327:335 is approximately **(A)** 0.54:1 and **(B)** 1.08:1. The blue numbers on the top right corner denote ion intensities.

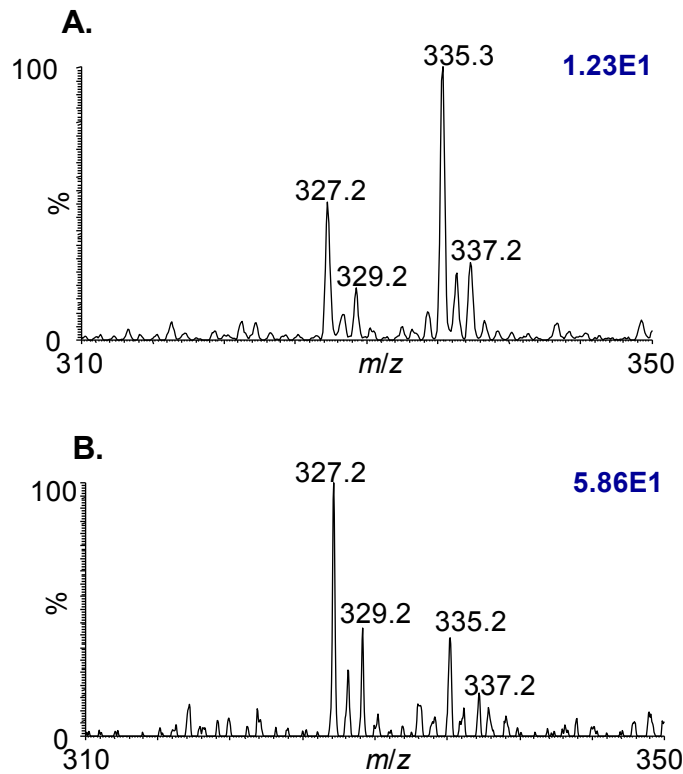


Figure S8.5. Mass spectra using SAI in discontinuous mode (**Scheme 8.1. II.A**). The material was extracted by using 1 μL standard solution (clozapine:clozapine-d8 at 0.5:1 with the clozapine-d8 at 2 $\text{pmol } \mu\text{L}^{-1}$) from tissue section surfaces of (A) control and (B) drug-treated mouse and pipette into the heated mass spectrometer inlet. The ion intensity ratio at m/z 's 327:335 is approximately (A) 0.52:1 and (B) 2.20:1. The blue numbers on the top right corner denote ion intensities.

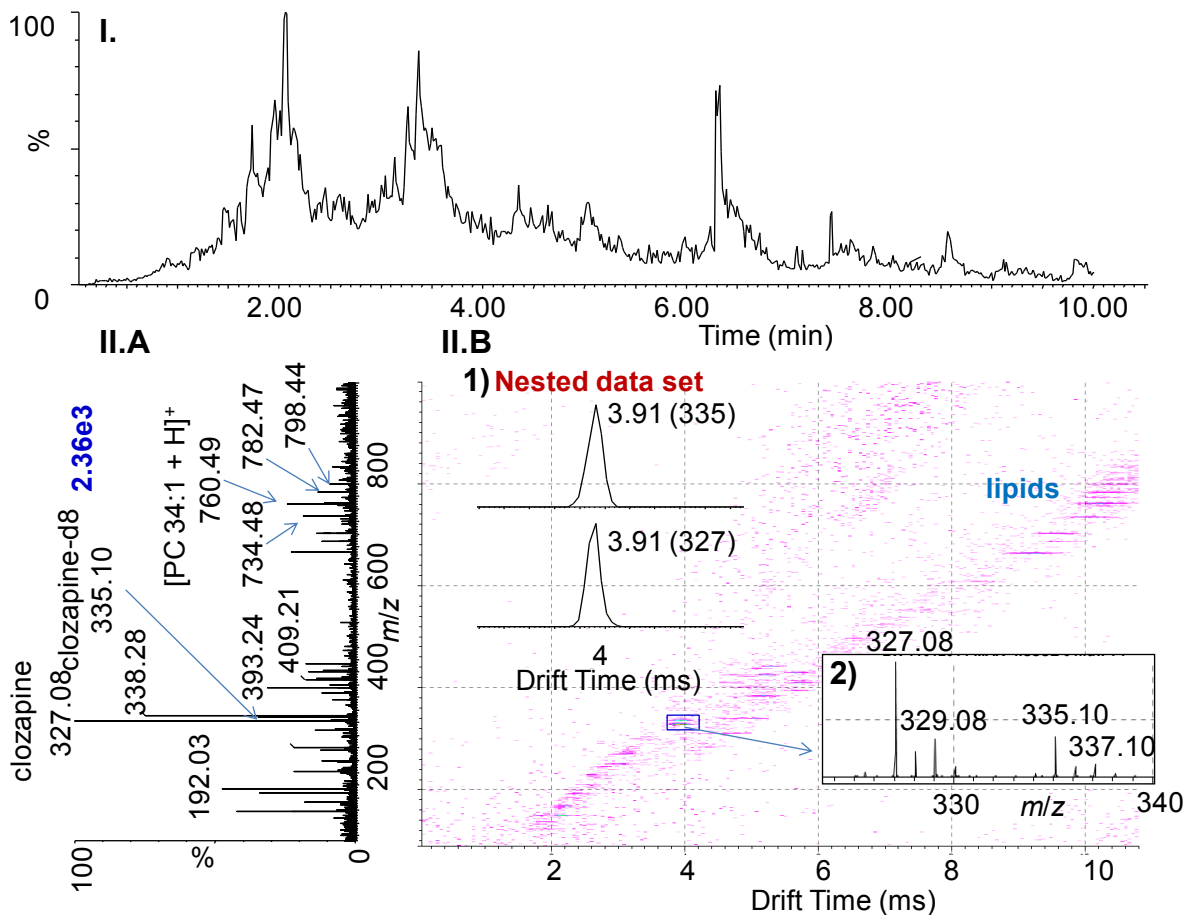


Figure S8.6. Half of a tissue section covered by four 1 μ L matrix/clozapine:clozapine-d8 mixture and analyzed by MAIV operating at atmospheric pressure (**Scheme 8.2.B**). The glass slide holding tissue section was sealed to the modified skimmer cone, and the matrix sublimed over 10 min. **(I)** TIC showing continuous ion formation from a MAIV analysis. **(II): (A)** Total mass spectrum, clozapine, clozapine-d8, cholesterol, and lipids were observed; **(B)** two dimensional plots of drift time vs. m/z with insets showing extracted **(1)** nested dataset and **(2)** mass spectrum from the blue-boxed area. The ion intensity ratio at m/z 's 327:335 is approximately 3.02:1.

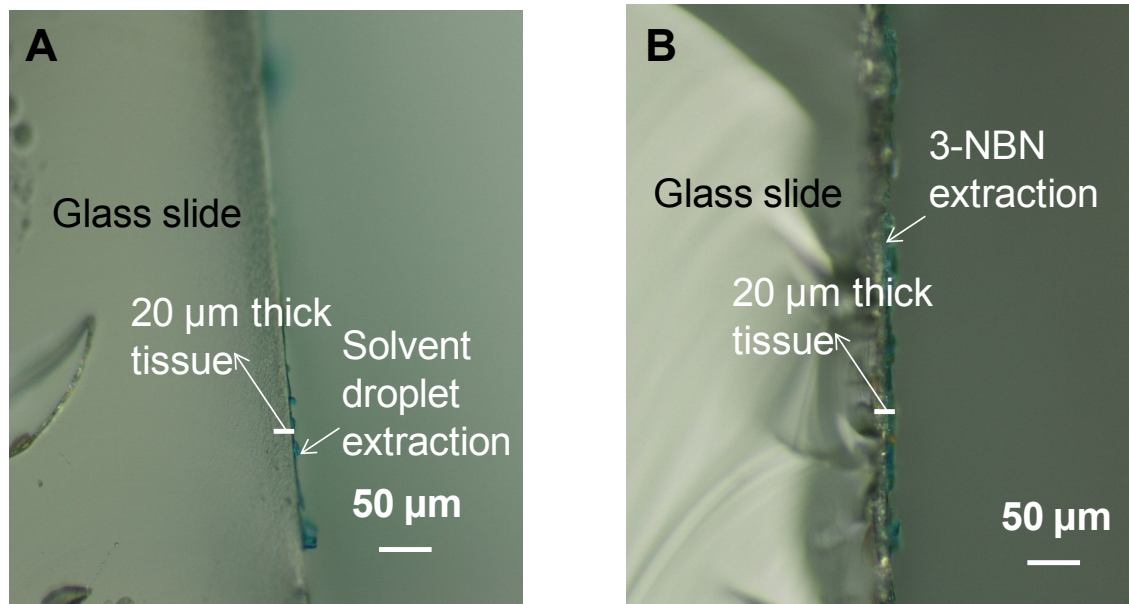


Figure S8.7. Microscopy images of the glass slides holding 20 μm-thick tissue section after (A) solvent-droplet extraction (**Scheme 8.1. II.A**) and (B) 3-NBN/clozapine:clozapine-d8 mixture sublimation for 10 min (**Scheme 8.2.B**). The tissue section and the glass slide were cut through the center, and the images show the cross section. The scale bar represents 50 μm, and a scale bar representing 20 μm is included to indicate the thickness of the tissue section.

BIBLIOGRAPHY

- ¹ Imami, K., Sugiyama, N., Kyono, Y., Tomita, M., & Ishihama, Y. (2008). Automated phosphoproteome analysis for cultured cancer cells by two-dimensional nanoLC-MS using a calcined titania/C18 biphasic column. *Analytical Sciences*, 24(1), 161-166.
- ² Mikesch, L. M., Ueberheide, B., Chi, A., Coon, J. J., Syka, J. E., Shabanowitz, J., & Hunt, D. F. (2006). The utility of ETD mass spectrometry in proteomic analysis. *Biochimica et Biophysica Acta (BBA)-Proteins and Proteomics*, 1764, 1811-1822.
- ³ Trimpin, S., Brizzard, B.L. (2009). Analysis of insoluble proteins. *Biotechniques* 46, 409-419.
- ⁴ Agranoff, B.W., Benjamins, J.A., Hajra, A.K. (1999) *Basic Neurochemistry Molecular, Cellular and Medical Aspects*, 6th ed, Siegel, G. J., Agranoff, B. W., Albers, R. W., Fisher, S. K., Uhler, M. D. Eds., Lippincott Williams & Wilkins: Philadelphia, pp 47-67.
- ⁵ McIlwain, H. and Bachelard, H.S. (1985) *Biochemistry and the Central Nervous System*, Edinburgh: Churchill Livingstone.
- ⁶ Durcan, M., Rigdon, G.C., Norman, M.H., Morgan, P.F. (1995) Is clozapine selective for the dopamine D4 receptor?. *Life Sciences* 57, PL275-283.
- ⁷ Farooqui, A. A., Horrocks, L. A., & Farooqui, T. (2000). Glycerophospholipids in brain: their metabolism, incorporation into membranes, functions, and involvement in neurological disorders. *Chemistry and Physics of Lipids*, 106, 1-29.
- ⁸ Fuchs, B., & Schiller, J. (2009). Application of MALDI-TOF mass spectrometry in lipidomics. *European Journal of Lipid Science and Technology*, 111, 83-98.

- ⁹ Dunn, W. B., Bailey, N. J., & Johnson, H. E. (2005). Measuring the metabolome: current analytical technologies. *Analyst*, *130*, 606-625.
- ¹⁰ Fiehn, O. (2002). Metabolomics—the link between genotypes and phenotypes. *Plant Molecular Biology*, *48*, 155-171.
- ¹¹ Prakash, C., Shaffer, C. L., & Nedderman, A. (2007). Analytical strategies for identifying drug metabolites. *Mass Spectrometry Reviews*, *26*, 340-369.
- ¹² Annesley, T. (2009). Mass spectrometry in the clinical laboratory: how have we done, and where do we need to be?. *Clinical Chemistry*, *55*, 1236-1239.
- ¹³ Saint-Marcoux, F., Sauvage, F. L., & Marquet, P. (2007). Current role of LC-MS in therapeutic drug monitoring. *Analytical and Bioanalytical Chemistry*, *388*, 1327-1349.
- ¹⁴ Diamandis, E. P. (2004). Mass spectrometry as a diagnostic and a cancer biomarker discovery tool opportunities and potential limitations. *Molecular & Cellular Proteomics*, *3*(4), 367-378.
- ¹⁵ Rifai, N., Gillette, M. A., & Carr, S. A. (2006). Protein biomarker discovery and validation: the long and uncertain path to clinical utility. *Nature Biotechnology*, *24*, 971-983.
- ¹⁶ Engwegen, J. Y., Gast, M. C. W., Schellens, J. H., & Beijnen, J. H. (2006). Clinical proteomics: searching for better tumour markers with SELDI-TOF mass spectrometry. *Trends in Pharmacological Sciences*, *27*, 251-259.
- ¹⁷ Meng, Q. H. (2013). Mass Spectrometry Applications in Clinical Diagnostics. *Journal of Clinic Experimental Pathology*, *S6*, 2161-0681.

- ¹⁸ Trimpin, S., Wang, B., Lietz, C. B., Marshall, D. D., Richards, A. L., & Inutan, E. D. (2013). New ionization processes and applications for use in mass spectrometry. *Critical Reviews in Biochemistry and Molecular biology*, *48*, 409-429.
- ¹⁹ Strathmann, F. G., & Hoofnagle, A. N. (2011). Current and future applications of mass spectrometry to the clinical laboratory. *American Journal of Clinical Pathology*, *136*, 609-616.
- ²⁰ Seeley, E. H., Oppenheimer, S. R., Mi, D., Chaurand, P., & Caprioli, R. M. (2008). Enhancement of protein sensitivity for MALDI imaging mass spectrometry after chemical treatment of tissue sections. *Journal of the American Society for Mass Spectrometry*, *19*, 1069-1077.
- ²¹ Goodwin, R. J. (2012). Sample preparation for mass spectrometry imaging: small mistakes can lead to big consequences. *Journal of Proteomics*, *75*, 4893-4911.
- ²² Mikesh, L. M., Ueberheide, B., Chi, A., Coon, J. J., Syka, J. E., Shabanowitz, J., & Hunt, D. F. (2006). The utility of ETD mass spectrometry in proteomic analysis. *Biochimica et Biophysica Acta (BBA)-Proteins and Proteomics*, *1764*, 1811-1822.
- ²³ Wiseman, J. M., Ifa, D. R., Zhu, Y., Kissinger, C. B., Manicke, N. E., Kissinger, P. T., & Cooks, R. G. (2008). Desorption electrospray ionization mass spectrometry: Imaging drugs and metabolites in tissues. *Proceedings of the National Academy of Sciences*, *105*, 18120-18125.
- ²⁴ El-Baba, T. J., Lutomski, C. A., Wang, B., Inutan, E. D., & Trimpin, S. (2014). Toward high spatial resolution sampling and characterization of biological tissue surfaces using mass spectrometry. *Analytical and Bioanalytical Chemistry*, *406*, 1-9.

- ²⁵ Coon, J. J., Syka, J. E., Shabanowitz, J., & Hunt, D. F. (2005). Tandem mass spectrometry for peptide and protein sequence analysis. *Biotechniques*, *38*, 519-523.
- ²⁶ Coon, J. J. (2009). Collisions or electrons? Protein sequence analysis in the 21st century. *Analytical chemistry*, *81*, 3208-3215.
- ²⁷ Mark, T. D. (1982). Fundamental aspects of electron impact ionization. *International Journal of Mass Spectrometry and Ion Physics*, *45*, 125-145.
- ²⁸ Munson, M. S. B., & Field, F. H. (1966). Chemical ionization mass spectrometry. I. General introduction. *Journal of the American Chemical Society*, *88*, 2621-2630.
- ²⁹ Barber, M., Bordoli, R.S., Sedgwick, R.D., Tyler, A.N. (1981). FAB of Solids as an Ion Source in Mass Spectrometry. *Nature* *293*, 270-275.
- ³⁰ Honig, R.E. (1985). The Development of Secondary Ion-MS (SIMS): a Restrospective. *International Journal of Mass Spectrometry and Ion Processes*. *66*, 31-54.
- ³¹ Karas, M., Bachmann, D., Bahr, U., Hillenkamp, F. (1987). Matrix-Assisted Ultraviolet-Laser Desorption of Nonvolatile Compounds. *International Journal of Mass Spectrometry and Ion Processes* *78*, 53-68.
- ³² Tanaka, K., Waki, H., Ido, Y., Akita, S., Yoshida, Y., Yoshida, T. (1988). Protein and polymer analyses up to m/z 100 000 by laser ionization time-of-flight mass spectrometry. *Rapid Communications in Mass Spectrometry* *2*, 151-153.
- ³³ Fenn, J. B., Mann, M., Meng, C. K., Wong, S. F., Whitehouse, C. M. (1989). Electrospray ionization for mass spectrometry of large biomolecules. *Science* *246*, 64-71.

- ³⁴ Holle, A., Haase, A., Kayser, M., Höndorf, J. (2006). Optimizing UV laser focus profiles for improved MALDI performance. *Journal of Mass Spectrometry* 41, 705-716.
- ³⁵ Vestal, M. L., Juhasz, P., & Martin, S. A. (1995). Delayed extraction matrix-assisted laser desorption time-of-flight mass spectrometry. *Rapid Communications in Mass Spectrometry*, 9, 1044-1050.
- ³⁶ Trimpin, S., Rouhanipour, A., Az, R., Räder, H.J., Müllen, K. (2001). New aspects in matrix-assisted laser desorption/ionization time-of-flight mass spectrometry: a universal solvent-free sample preparation. *Rapid Communications in Mass Spectrometry* 15, 1364-1373.
- ³⁷ Trimpin, S., Deinzer, M.L. (2007). Solvent-free MALDI-MS for the analysis of a membrane protein via the mini ball approach: Case study of bacteriorhodopsin. *Analytical Chemistry* 79, 71-78.
- ³⁸ Trimpin, S. Grimsdale, A.C., Räder, H.J., Müllen, K.(2002). Characterization of an insoluble poly(9,9-diphenyl-2,7-fluorene) by solvent-free sample preparation for MALDI-TOF mass spectrometry. *Analytical Chemistry* 74, 3777-3782.
- ³⁹ Trimpin, S. (2010). A perspective on MALDI alternatives – total solvent-free analysis and electron transfer dissociation of highly charged ions by laserspray ionization. *Journal of Mass Spectrometry* 45, 471-485.
- ⁴⁰ Trimpin, S., Deinzer, M.L. (2005). Solvent-free MALDI-MS for the analysis of biological samples via a mini-ball mill approach. *Journal of the American Society for Mass Spectrometry* 16, 542-547.

- ⁴¹ Trimpin, S., & Deinzer, M. L. (2007). Solvent-free MALDI-MS for the analysis of β -amyloid peptides via the mini-ball mill approach: Qualitative and quantitative advances. *Journal of the American Society for Mass Spectrometry*, *18*, 1533-1543.
- ⁴² Ehring, H., Karas, M., & Hillenkamp, F. (1992). Role of photoionization and photochemistry in ionization processes of organic molecules and relevance for matrix-assisted laser desorption ionization mass spectrometry. *Organic Mass Spectrometry*, *27*, 472-480.
- ⁴³ Karas, M., Glückmann, M., & Schäfer, J. (2000). Ionization in matrix-assisted laser desorption/ionization: singly charged molecular ions are the lucky survivors. *Journal of Mass Spectrometry*, *35*, 1-12.
- ⁴⁴ Knochenmuss, R. (2006). Ion formation mechanisms in UV-MALDI. *Analyst* *131*, 966-986.
- ⁴⁵ Beavis, R. C., Chaudhary, T., & Chait, B. T. (1992). α -Cyano-4-hydroxycinnamic acid as a matrix for matrixassisted laser desorption mass spectrometry. *Organic Mass Spectrometry*, *27*, 156-158.
- ⁴⁶ Karas, M., Bahr, U., Strupat, K., Hillenkamp, F., Tsarbopoulos, A., & Pramanik, B. N. (1995). Matrix dependence of metastable fragmentation of glycoproteins in MALDI TOF mass spectrometry. *Analytical Chemistry*, *67*, 675-679.
- ⁴⁷ Loboda, A.V. Krutchinsky, A.N., Bromirski, M. (2000). A tandem quadrupole/time-of-flight mass spectrometer with a matrix-assisted laser desorption/ionization source: design and performance. *Rapid Communications in Mass Spectrometry* *14*, 1047-1057.

- ⁴⁸ Easterling, M.L., Mize, T.H., Amster, I.J. (1999). Routine part-per-million mass accuracy for high-mass ions: Space-charge effects in MALDI FT-ICR *Analytical Chemistry* 71, 624-632.
- ⁴⁹ Li, L.J., Garden, R.W., Sweedler, J.V. (2000). Single-cell MALDI: a new tool for direct peptide profiling. *Trends in Biotechnology*. 18, 151-160.
- ⁵⁰ Chaurand, P., Luetzenkirchen, F., Spengler, B. (1999). Peptide and protein identification by matrix-assisted laser desorption ionization (MALDI) and MALDI-post-source decay time-of-flight mass spectrometry. *Journal of the American Society for Mass Spectrometry* 10, 91-103.
- ⁵¹ Schiller, J., Arnhold, J., Benard, S., Muller, M., Reichl, S., Arnold, K. (1999). Lipid analysis by matrix-assisted laser desorption and ionization mass spectrometry: A methodological approach. *Analytical Biochemistry* 267, 46-56.
- ⁵² Harvey, D.J. (1999). Matrix-assisted laser desorption/ionization mass spectrometry of carbohydrates. *Mass Spectrometry Reviews* 18, 349-450.
- ⁵³ Masuda, N., Ohnishi, T., Kawamoto, S. (1999). Analysis of chemical modification of RNA from formalin-fixed samples and optimization of molecular biology applications for such samples. *Nucleic Acids Research* 27, 4436-4443.
- ⁵⁴ Claydon, M.A., Davey, S.N., EdwardsJones, V., Gordon, D.B. (1996). The rapid identification of intact microorganism using mass spectrometry. *Nature Biotechnology* 14, 1584-1586.
- ⁵⁵ McDonnell, L.A., Heeren, R.M.A. (2007). Imaging mass spectrometry. *Mass Spectrometry Reviews* 26, 606-643.

- ⁵⁶ Caprioli, R.M., Farmer, T.B., Gile, J. (1997). Molecular imaging of biological samples: Localization of peptides and proteins using MALDI-TOF MS. *Analytical Chemistry* 69, 4751-4760.
- ⁵⁷ Hankin, J.A., Barkley, R.M., Murphy, R.C. (2007). Sublimation as a method of matrix application for mass spectrometric imaging. *Journal of the American Society for Mass Spectrometry*. 18, 1646-1652.
- ⁵⁸ Reyzer, M.L., Hsieh, Y.S., Ng, K., Korfmacher, W.A., Caprioli, R.M. (2003). Direct analysis of drug candidates in tissue by matrix-assisted laser desorption/ionization mass spectrometry. *Journal of Mass Spectrometry* 221, 1081-1092.
- ⁵⁹ Schwartz, S.A., Reyzer, M.L., Caprioli, R.M. (2003). Direct tissue analysis using matrix-assisted laser desorption/ionization mass spectrometry: practical aspects of sample preparation. *Journal of Mass Spectrometry*. 223, 699-708.
- ⁶⁰ Kruse, R., Sweedler, J.V. Spatial profiling invertebrate ganglia using MALDI MS. (2003). *Journal of the American Society for Mass Spectrometry* 14, 752-759.
- ⁶¹ Schober, Y., Guenther, S., Spengler B, Rompp, A. (2012). Single cell matrix-assisted laser desorption/ionization mass spectrometry imaging. *Analytical Chemistry* 84, 6293-6297.
- ⁶² Jun, J.H., Song, Z., Liu, Z., Nikolau, B.J., Yeung, E.S., Lee, Y.J. (2012). High-spatial and high-mass resolution imaging of surface metabolites of *Arabidopsis thaliana* by laser desorption-ionization mass spectrometry using colloidal silver. *Analytical Chemistry* 82, 3255-3265.

- ⁶³ Pirman, D. A., Reich, R. F., Kiss, A., Heeren, R. M., & Yost, R. A. (2012). Quantitative MALDI tandem mass spectrometric imaging of cocaine from brain tissue with a deuterated internal standard. *Analytical Chemistry*, *85*, 1081-1089.
- ⁶⁴ Pirman, D. A., Kiss, A., Heeren, R. M., & Yost, R. A. (2012). Identifying tissue-specific signal variation in MALDI mass spectrometric imaging by use of an internal standard. *Analytical Chemistry* *85*, 1090-1096.
- ⁶⁵ Laiko, V.V., Baldwin, M.A., Burlingame, A.L. (2000). Atmospheric pressure matrix assisted laser desorption/ionization mass spectrometry. *Analytical Chemistry* *72*, 652-657.
- ⁶⁶ Li, Y., Shrestha, B., Vertes, A. (2008). Atmospheric pressure infrared MALDI imaging mass spectrometry for plant metabolomics. *Analytical Chemistry* *80*, 407-420.
- ⁶⁷ Dorosheno, V.M., Laiko, V.V., Taranenko, N.I., Berkout, V.D., Lee, H.S. (2002). Recent developments in atmospheric pressure MALDI mass spectrometry. *International Journal of Mass Spectrometry* *221*, 39-58.
- ⁶⁸ Galicia M C, Vertes A, Callahan J H. (2002). Atmospheric pressure matrix-assisted laser desorption/ionization in transmission geometry. *Analytical chemistry*, *74*: 1891-1895.
- ⁶⁹ Sheehan, E.W.; Willoughby, R. C. (June 13, 2006) U. S. Patent 7,060,976.
- ⁷⁰ Krutchinsky AN, Chait BT. (2002). On the nature of the chemical noise in MALDI mass spectra. *Journal of the American Society for Mass Spectrometry* *13*, 129-34.
- ⁷¹ Fenn, J.B. Electrospray wings for molecular elephants. (2003). *Angewandte Chemie International Edition* *42*, 3871-3894.

- ⁷² Konermann, L., Ahadi, E., Rodriguez, A.D., Vahidi, S. (2013). Unraveling the Mechanism of Electrospray Ionization. *Analytical Chemistry* 85, 2-9.
- ⁷³ Iribarne, J. V., Thomson, B. A. J. (1976). On the evaporation of small ions from charged droplets. *Journal of Chemical Physics* 64, 2287-2294.
- ⁷⁴ Dole, M., Mack, L.L., Hines, R.L. (1968). Molecular beams of macroions. *Journal of Chemical Physics*. 49, 2240-2249.
- ⁷⁵ Trimpin, S., Inutan, E.D., Herath, T.N., McEwen, C.N. (2010). Matrix-Assisted Laser Desorption/Ionization Mass Spectrometry Method for Selectively Producing Either Singly or Multiply Charged Molecular Ions. *Analytical Chemistry* 82, 11-15.
- ⁷⁶ Pitt, J.J. Principles and Applications of Liquid Chromatography-Mass Spectrometry in Clinical Biochemistry. (2009). *Clinical Biochemist. Reviews* 30, 19-34.
- ⁷⁷ Elias, J. E., & Gygi, S. P. (2007). Target-decoy search strategy for increased confidence in large-scale protein identifications by mass spectrometry. *Nature Methods*, 4, 207-214.
- ⁷⁸ Shen, Y.F., Zhao, R., Berger, S.J., Anderson, G.A., Rodriguez, N., Smith, R.D. (2002). High-efficiency nanoscale liquid chromatography coupled on-line with mass spectrometry using nanoelectrospray ionization for proteomics. *Analytical Chemistry* 74, 4235-4249.
- ⁷⁹ Mann, W.M. (1996). Analytical properties of the nanoelectrospray ion source. *Analytical Chemistry* 68, 1-8.
- ⁸⁰ Smith, R.D. (2006). Future directions for electrospray ionization for biological analysis using mass spectrometry. *Biotechniques* 41, 147-148.

- ⁸¹ Kebarle, P., & Verkerk, U. H. (2009). Electrospray: from ions in solution to ions in the gas phase, what we know now. *Mass Spectrometry Reviews*, 28, 898-917.
- ⁸² Gibson, G.T.T., Mugo, S.M., Oleschuk, R.D. (2009). Nanoelectrospray emitters trends and perspective. *Mass Spectrometry Reviews* 28, 918-936
- ⁸³ Cody, R.B.; Laramée, J.A.; Durst, H.D. (2005). Versatile new ion source for the analysis of materials in open air under ambient conditions. *Analytical Chemistry* 77, 2297-2302.
- ⁸⁴ Venter, A.; Nefliu, M.; Cooks, R.G. (2008). Ambient desorption ionization mass spectrometry. *Trends in Analytical Chemistry* 27, 284-290.
- ⁸⁵ Takatz, Z.; Wiseman, J.M.; Gologan, B.; Cooks, R.G. (2004). Mass spectrometry sampling under ambient conditions with desorption electrospray ionization. *Science* 306, 471-473.
- ⁸⁶ Ford, M.J.; Van Berkel, G.J. (2004). An improved thin-layer chromatography/mass spectrometry coupling using a surface sampling probe electrospray ion trap system. *Rapid Communications in Mass Spectrometry*. 18, 1303-1309.
- ⁸⁷ Haapala M.; Pol, J.; Saarela, V.; Arvola, V.; Kotiaho, T.; Ketola, R.A.; Franssila, S.; Kauppila, T.J. Kostianen, R. (2007). Desorption atmospheric pressure photoionization. *Analytical Chemistry* 79, 7867-7872.
- ⁸⁸ McEwen C.N.; McKay R.G.; Larsen, B.S. (2005). Analysis of solids, liquids, and biological tissues using solid probe introduction at atmospheric pressure on commercial LC/MS instruments. *Analytical Chemistry* 77, 7826-7831.

- ⁸⁹ Roach, P.J.; Laskin, J.; Laskin, A. (2010). Nanospray desorption electrospray ionization: an ambient method for liquid-extraction surface sampling in mass spectrometry. *Analyst* 135, 2233-2236.
- ⁹⁰ Nemes, P.; Vertes, A. (2007). Laser ablation electrospray ionization for atmospheric pressure, in vivo, and imaging mass spectrometry. *Analytical Chemistry* 79, 8098-8106.
- ⁹¹ Sampson, J.S.; Hawkrigde, A.M.; Muddiman, D.C. (2005). Generation and detection of multiply-charged peptides and proteins by matrix-assisted laser desorption electrospray ionization (MALDESI) fourier transform ion cyclotron resonance mass spectrometry. *Journal of the American Society for Mass Spectrometry* 17, 1712-1716.
- ⁹² Shie, J.; Huang, M.Z.; Hsu, H.J. (2005). Electrospray-assisted laser desorption/ionization mass spectrometry for direct ambient analysis of solids. *Rapid Communications in Mass Spectrometry* 19, 3701-3704.
- ⁹³ Ovchinnikova, O.S.; Kertesz, V.; Van Berkel, G.J. (2011). Combining transmission geometry laser ablation and a non-contact continuous flow surface sampling probe/electrospray emitter for mass spectrometry based chemical imaging. *Rapid Communications in Mass Spectrometry* 25, 3735-3740.
- ⁹⁴ Chernushevich, I. V., Loboda, A. V., & Thomson, B. A. (2001). An introduction to quadrupole-time-of-flight mass spectrometry. *Journal of Mass Spectrometry*, 36, 849-865.
- ⁹⁵ Fuerstenau, S. D., Benner, W. H., Thomas, J. J., Brugidou, C., Bothner, B., & Siuzdak, G. (2001). Mass spectrometry of an intact virus. *Angewandte Chemie International Edition*, 40, 541-544.

- ⁹⁶ Satoh, T., Sato, T., & Tamura, J. (2007). Development of a high-performance MALDI-TOF mass spectrometer utilizing a spiral ion trajectory. *Journal of the American Society for Mass Spectrometry*, *18*, 1318-1323.
- ⁹⁷ Hopfgartner, G., Varesio, E., Tschäppät, V., Grivet, C., Bourgoigne, E., & Leuthold, L. A. (2004). Triple quadrupole linear ion trap mass spectrometer for the analysis of small molecules and macromolecules. *Journal of Mass Spectrometry*, *39*, 845-855.
- ⁹⁸ Lange, V., Picotti, P., Domon, B., & Aebersold, R. (2008). Selected reaction monitoring for quantitative proteomics: a tutorial. *Molecular Systems Biology*, *4*, 1-14.
- ⁹⁹ Pekar Second, T., Blethrow, J. D., Schwartz, J. C., Merrihew, G. E., MacCoss, M. J., Swaney, D. L., Jason D. Russell, Joshua J. Coon, & Zabrouskov, V. (2009). Dual-pressure linear ion trap mass spectrometer improving the analysis of complex protein mixtures. *Analytical Chemistry*, *81*, 7757-7765.
- ¹⁰⁰ Hager, J. W. (2002). A new linear ion trap mass spectrometer. *Rapid Communications in Mass Spectrometry*, *16*, 512-526.
- ¹⁰¹ Marshall, A. G., & Hendrickson, C. L. (2008). High-resolution mass spectrometers. *Annual Reviews of Analytical Chemistry I*, 579-599.
- ¹⁰² Steen, H., Küster, B., & Mann, M. (2001). Quadrupole time-of-flight versus triple-quadrupole mass spectrometry for the determination of phosphopeptides by precursor ion scanning. *Journal of Mass Spectrometry*, *36*, 782-790.
- ¹⁰³ Clemmer, D. E., & Jarrold, M. F. (1997). Ion mobility measurements and their applications to clusters and biomolecules. *Journal of Mass Spectrometry*, *32*, 577-592.

- ¹⁰⁴ Wytttenbach, T., & Bowers, M. T. (2003). Gas-phase conformations: The ion mobility/ion chromatography method. *Modern Mass Spectrometry* (pp. 207-232). Springer Berlin Heidelberg.
- ¹⁰⁵ Liu, X., Valentine, S. J., Plasencia, M. D., Trimpin, S., Naylor, S., & Clemmer, D. E. (2007). Mapping the human plasma proteome by SCX-LC-IMS-MS. *Journal of the American Society for Mass Spectrometry*, *18*, 1249-1264.
- ¹⁰⁶ Trimpin, S., Tan, B., Bohrer, B. C., O'Dell, D. K., Merenbloom, S. I., Pazos, M. X., Clemmer, D.E., & Walker, J. M. (2009). Profiling of phospholipids and related lipid structures using multidimensional ion mobility spectrometry-mass spectrometry. *International Journal of Mass Spectrometry*, *287*, 58-69.
- ¹⁰⁷ Trimpin, S., Inutan, E. D., Herath, T. N., McEwen, C. N., (2010). Laserspray ionization, a new atmospheric pressure MALDI method for producing highly charged gas-phase ions of peptides and proteins directly from solid solutions. *Molecular & Cellular Proteomics*, *9*, 362-367.
- ¹⁰⁸ McEwen, C. N., Larsen, B. S., Trimpin, S. (2010). Laserspray ionization on a commercial atmospheric pressure-MALDI mass spectrometer ion source: selecting singly or multiply charged ions. *Analytical Chemistry*, *82*, 4998-5001.
- ¹⁰⁹ McEwen, C. N., Pagnotti, V. S., Inutan, E. D., Trimpin, S. (2010). New paradigm in ionization: multiply charged ion formation from a solid matrix without a laser or voltage. *Analytical Chemistry*, *82*, 9164-9168.
- ¹¹⁰ Li, J., Inutan, E. D., Wang, B., Lietz, C. B., Green, D. R., Manly, C. D., Richards, A. L., Marshall, D. D., Lingenfelter, S., Ren, Y., Trimpin, S. (2012). Matrix assisted ionization: new aromatic and nonaromatic matrix compounds producing multiply

charged lipid, peptide, and protein ions in the positive and negative mode observed directly from surfaces. *Journal of the American Society for Mass Spectrometry*, 23, 1625-1643.

- ¹¹¹ Pagnotti, V. S., Chubatyi, N. D., McEwen, C. N. (2011). Solvent assisted inlet ionization: an ultrasensitive new liquid introduction ionization method for mass spectrometry[J]. *Analytical Chemistry*, 83, 3981-3985.
- ¹¹² Pagnotti, V. S., Inutan, E. D., Marshall, D. D., Trimpin, S., McEwen, C. N. (2011). Inlet ionization: a new highly sensitive approach for liquid chromatography/mass spectrometry of small and large molecules. *Analytical Chemistry*, 83, 7591-7594.
- ¹¹³ Pagnotti, V. S., Chakrabarty, S., Harron, A. F., McEwen, C. N. (2012). Increasing the sensitivity of liquid introduction mass spectrometry by combining electrospray ionization and solvent assisted inlet ionization. *Analytical Chemistry*, 84, 6828-6832.
- ¹¹⁴ Pagnotti, V. S., Chakrabarty, S., McEwen, C. N. (2013). Carbonation and other super saturated gases as solution modifiers for improved sensitivity in solvent assisted ionization inlet (SAII) and ESI. *Journal of the American Society for Mass Spectrometry*, 24, 186-192.
- ¹¹⁵ Inutan, E. D., Wang, B., Trimpin, S. (2010). Commercial intermediate pressure MALDI ion mobility spectrometry mass spectrometer capable of producing highly charged laserspray ionization ions. *Analytical Chemistry*, 83, 678-684.
- ¹¹⁶ Trimpin, S., Ren, Y., Wang, B., Lietz, C. B., Richards, A. L., Marshall, D. D., Inutan, E. D. (2011). Extending the laserspray ionization concept to produce highly charged ions at high vacuum on a time-of-flight mass analyzer. *Analytical Chemistry*, 83, 5469-5475.

- ¹¹⁷ Inutan, E. D., Trimpin S. (2013). Matrix assisted ionization vacuum (MAIV), a new ionization method for biological materials analysis using mass spectrometry. *Molecular & Cellular Proteomics*, 12, 792-796.
- ¹¹⁸ Trimpin, S., Inutan, E. D. (2013). Matrix assisted ionization in vacuum, a sensitive and widely applicable ionization method for mass spectrometry. *Journal of The American Society for Mass Spectrometry*, 24, 722-732.
- ¹¹⁹ Trimpin, S., Inutan, E. D. (2013) New ionization method for analysis on atmospheric pressure ionization mass spectrometers requiring only vacuum and matrix assistance. *Analytical Chemistry*, 85, 2005-2009.
- ¹²⁰ Inutan, E.D., Wager-Miller, J., Narayan, S.B., Mackie, K., Trimpin, S. (2013). The potential for clinical applications using a new ionization method combined with ion mobility spectrometry-mass spectrometry. *International Journal for Ion Mobility Spectrometry* 16, 145-159.
- ¹²¹ Inutan, E., & Trimpin, S. (2010). Laserspray ionization (LSI) ion mobility spectrometry (IMS) mass spectrometry. *Journal of the American Society for Mass Spectrometry*, 21, 1260-1264.
- ¹²² Trimpin, S.; Wang, B.; Inutan, E.D.; Li, J.; Lietz, C.B.; Harron, A.; Pagnotti, V.S.; Sardelis, D.; McEwen, C.N. (2013). A Mechanism for Ionization of Nonvolatile Compounds in Mass Spectrometry: Considerations from MALDI and Inlet Ionization. *Journal of the American Society for Mass Spectrometry* 23, 1644-1660.
- ¹²³ Bhattacharyya, I.; Maze, J.T.; Ewing, G.E.; Jarrold, M.F. (2011). Charge Separation from the Bursting of Bubbles on Water. *Journal of Physical Chemistry A* 115, 5723-5728.

- ¹²⁴ Vestal, M.L. (1983). Ionization Techniques for Non-Volatile Molecules. *Mass Spectrometry Reviews* 2, 447-480.
- ¹²⁵ Trimpin, S.; Wang, B. (2015). *Inlet and Vacuum Ionization from Ambient Conditions*, in: *Ambient Ionization Mass Spectrometry*, Royal Society of Chemistry, by Eds. Marek Domin and Robert Cody, 423-444.
- ¹²⁶ Chakrabarty, S.; Pagnotti, V.; Wang, B.; Trimpin, S.; McEwen, C.N. (2014). Ionization from Ice in Mass Spectrometry and a Possible Connection to Thunderstorms, *Analytical Chemistry* 86, 7343-7350.
- ¹²⁷ Trimpin, S.; Lutomski, C. A.; El-Baba, T. J.; Woodall, D. W.; Foley, C. D.; Manly, C. D.; Wang, B.; Liu, C.; Harless, B. M.; Kumar, R.; Imperial, L. F.; Inutan, E. D. (2014). Magic matrices for ionization in mass spectrometry. *International Journal of Mass Spectrometry*, doi: 10.1016/j.ijms.2014.07.033.
- ¹²⁸ Van Berkel, G. J., Pasilis, S. P., & Ovchinnikova, O. (2008). Established and emerging atmospheric pressure surface sampling/ionization techniques for mass spectrometry. *Journal of Mass Spectrometry*, 43, 1161-1180.
- ¹²⁹ Trimpin, S., Herath, T. N., Inutan, E. D., Cernat, S. A., Miller, J. B., Mackie, K., & Walker, J. M. (2009). Field-free transmission geometry atmospheric pressure matrix-assisted laser desorption/ionization for rapid analysis of unadulterated tissue samples. *Rapid Communications in Mass Spectrometry*, 23, 3023-3027.
- ¹³⁰ Zydel, F., Trimpin, S., & McEwen, C. N. (2010). Laserspray ionization using an atmospheric solids analysis probe for sample introduction. *Journal of the American Society for Mass Spectrometry*, 21, 1889-1892.

- ¹³¹ McEwen, C. N., & Trimpin, S. (2011). An alternative ionization paradigm for atmospheric pressure mass spectrometry: flying elephants from Trojan horses. *International Journal of Mass Spectrometry*, *300*, 167-172.
- ¹³² Inutan, E. D., & Trimpin, S. (2010). Laserspray Ionization-Ion Mobility Spectrometry– Mass Spectrometry: Baseline Separation of Isomeric Amyloids without the Use of Solvents Desorbed and Ionized Directly from a Surface. *Journal of proteome research*, *9*, 6077-6081.
- ¹³³ Richards, A. L., Marshall, D. D., Inutan, E. D., McEwen, C. N., & Trimpin, S. (2011). High-throughput analysis of peptides and proteins by laserspray ionization mass spectrometry. *Rapid Communications in Mass Spectrometry*, *25*, 247-250.
- ¹³⁴ Inutan, E. D., Richards, A. L., Wager-Miller, J., Mackie, K., McEwen, C. N., & Trimpin, S. (2011). Laserspray ionization, a new method for protein analysis directly from tissue at atmospheric pressure with ultrahigh mass resolution and electron transfer dissociation. *Molecular & Cellular Proteomics*, *10*, M110-000760.
- ¹³⁵ Richards, A. L., Lietz, C. B., Wager-Miller, J. B., Mackie, K., & Trimpin, S. (2011). Imaging mass spectrometry in transmission geometry. *Rapid Communications in Mass Spectrometry*, *25*, 815-820.
- ¹³⁶ Trimpin, S., Herath, T. N., Inutan, E. D., Wager-Miller, J., Kowalski, P., Claude, E., Walker, J. M., & Mackie, K. (2009). Automated solvent-free matrix deposition for tissue imaging by mass spectrometry. *Analytical Chemistry*, *82*, 359-367.
- ¹³⁷ Schilling, B.; Miller, A; Miller, J. P.; Gaman, E. A.; Ellerby, L. M.; Gibson, B. W.; Hughes, R. E. Proceedings of the 55th ASMS Conference on Mass Spectrometry and Allied Topics, 2007, Indianapolis, IN, ThPZ7.

- ¹³⁸ Hanton, S. D., & Parees, D. M. (2005). Extending the solvent-free MALDI sample preparation method. *Journal of the American Society for Mass Spectrometry*, *16*, 90-93.
- ¹³⁹ Trimpin, S., Wijerathne, K., & McEwen, C. N. (2009). Rapid methods of polymer and polymer additives identification: multi-sample solvent-free MALDI, pyrolysis at atmospheric pressure, and atmospheric solids analysis probe mass spectrometry. *Analytica Chimica Acta*, *654*, 20-25.
- ¹⁴⁰ Trimpin, S., & McEwen, C. N. (2007). Multisample preparation methods for the solvent-free MALDI-MS analysis of synthetic polymers. *Journal of the American Society for Mass Spectrometry*, *18*, 377-381.
- ¹⁴¹ Pomerantz, A.E., Ventura, G.T., McKenna, A.M., Cañas, J.A., Auman, J., Koerner, K., Curry, D., Nelson, R.K., Reddy, C.M., Rodgers, R.P., Marshall, A.G., Peters, K.E., & Mullins, O.C. (2010). The geochemical origin of a viscosity gradient in a petroleum reservoir. *Organic Geochemistry* *41*, 812-821.
- ¹⁴² Pringle, S. D., Giles, K., Wildgoose, J. L., Williams, J. P., Slade, S. E., Thalassinou, K., Bateman, R. H., Bwers, M. T., & Scrivens, J. H. (2007). An investigation of the mobility separation of some peptide and protein ions using a new hybrid quadrupole/travelling wave IMS/oa-ToF instrument. *International Journal of Mass Spectrometry*, *261*, 1-12.
- ¹⁴³ Trimpin, S., Clemmer, D. E., & McEwen, C. N. (2007). Charge-remote fragmentation of lithiated fatty acids on a TOF-TOF instrument using matrix-ionization. *Journal of the American Society for Mass Spectrometry*, *18*, 1967-1972.

- ¹⁴⁴ McLean, J. A., Ruotolo, B. T., Gillig, K. J., & Russell, D. H. (2005). Ion mobility–mass spectrometry: a new paradigm for proteomics. *International Journal of Mass Spectrometry*, *240*, 301-315.
- ¹⁴⁵ Rodgers, R. P., Schaub, T. M., & Marshall, A. G. (2005). Petroleomics: MS Returns to Its Roots. *Analytical Chemistry*, *77*, 20-27A.
- ¹⁴⁶ Fernandez-Lima, F. A., Becker, C., McKenna, A. M., Rodgers, R. P., Marshall, A. G., & Russell, D. H. (2009). Petroleum crude oil characterization by IMS-MS and FTICR MS. *Analytical Chemistry*, *81*, 9941-9947.
- ¹⁴⁷ Ahmed, A., Cho, Y. J., No, M. H., Koh, J., Tomczyk, N., Giles, K., Yoo, J. S., & Kim, S. (2010). Application of the Mason– Schamp equation and ion mobility mass spectrometry to identify structurally related compounds in crude oil. *Analytical Chemistry*, *83*, 77-83.
- ¹⁴⁸ Purcell, J. M., Hendrickson, C. L., Rodgers, R. P., & Marshall, A. G. (2006). Atmospheric pressure photoionization Fourier transform ion cyclotron resonance mass spectrometry for complex mixture analysis. *Analytical Chemistry*, *78*, 5906-5912.
- ¹⁴⁹ Yoshimura, K., Przybilla, L., Ito, S., Brand, J. D., Wehmeir, M., Räder, H. J., & Müllen, K. (2001). Characterization of large synthetic polycyclic aromatic hydrocarbons by MALDI-and LD-TOF mass spectrometry. *Macromolecular Chemistry and Physics*, *202*, 215-222.
- ¹⁵⁰ Przybilla, L., Brand, J. D., Yoshimura, K., Räder, H. J., & Müllen, K. (2000). MALDI-TOF mass spectrometry of insoluble giant polycyclic aromatic hydrocarbons by a new method of sample preparation. *Analytical Chemistry*, *72*, 4591-4597.

- ¹⁵¹ Cristadoro, A., Kulkarni, S. U., Burgess, W. A., Cervo, E. G., Räder, H. J., Müllen, K., Bruce, D. A., & Thies, M. C. (2009). Structural characterization of the oligomeric constituents of petroleum pitches. *Carbon*, *47*, 2358-2370.
- ¹⁵² Cristadoro, A., Räder, H. J., & Müllen, K. (2008). Quantitative analyses of fullerene and polycyclic aromatic hydrocarbon mixtures via solvent-free matrix-assisted laser desorption/ionization mass spectrometry. *Rapid Communications in Mass Spectrometry*, *22*, 2463-2470.
- ¹⁵³ Pinkston, D. S., Duan, P., Gallardo, V. A., Habicht, S. C., Tan, X., Qian, K., Gray, M., & Kenttamaa, H. I. (2009). Analysis of asphaltenes and asphaltene model compounds by laser-induced acoustic desorption/Fourier transform ion cyclotron resonance mass spectrometry. *Energy & Fuels*, *23*, 5564-5570.
- ¹⁵⁴ Trimpin, S., Keune, S., Räder, H. J., & Müllen, K. (2006). Solvent-free MALDI-MS: developmental improvements in the reliability and the potential of MALDI in the analysis of synthetic polymers and giant organic molecules. *Journal of the American Society for Mass Spectrometry*, *17*, 661-671.
- ¹⁵⁵ Trimpin, S., & Clemmer, D. E. (2008). Ion mobility spectrometry/mass spectrometry snapshots for assessing the molecular compositions of complex polymeric systems. *Analytical Chemistry*, *80*, 9073-9083.
- ¹⁵⁶ Yamashita, M., & Fenn, J. B. (1984). Negative ion production with the electrospray ion source. *The Journal of Physical Chemistry*, *88*, 4671-4675.
- ¹⁵⁷ Zhigilei, L. V., & Garrison, B. J. (2000). Microscopic mechanisms of laser ablation of organic solids in the thermal and stress confinement irradiation regimes. *Journal of Applied Physics*, *88*, 1281-1298.

- ¹⁵⁸ Zhigilei, L. V., Kodali, P., & Garrison, B. J. (1997). On the threshold behavior in laser ablation of organic solids. *Chemical Physics Letters*, *276*, 269-273.
- ¹⁵⁹ Trimpin, S., Räder, H. J., & Müllen, K. (2006). Investigations of theoretical principles for MALDI-MS derived from solvent-free sample preparation: Part I. Preorganization. *International Journal of Mass Spectrometry*, *253*, 13-21.
- ¹⁶⁰ Hanton, S. D., & Stets, J. R. (2009). Determining the time needed for the vortex method for preparing solvent-free MALDI samples of low molecular mass polymers. *Journal of the American Society for Mass Spectrometry*, *20*, 1115-1118.
- ¹⁶¹ Hanton, S. D., McEvoy, T. M., & Stets, J. R. (2008). Imaging the morphology of solvent-free prepared MALDI samples. *Journal of the American Society for Mass Spectrometry*, *19*, 874-881.
- ¹⁶² Pizzala, H., Barrère, C., Mazarin, M., Ziarelli, F., & Charles, L. (2009). Solid state nuclear magnetic resonance as a tool to explore solvent-free MALDI samples. *Journal of the American Society for Mass Spectrometry*, *20*, 1906-1911.
- ¹⁶³ Sroka-Bartnicka, A., Ciesielski, W., Libiszowski, J., Duda, A., Sochacki, M., & Potrzebowski, M. J. (2009). Complementarity of solvent-free MALDI TOF and solid-state NMR spectroscopy in spectral analysis of polylactides. *Analytical Chemistry*, *82*, 323-328.
- ¹⁶⁴ Kononikhin, A. S., Nikolaev, E. N., Frankevich, V., & Zenobi, R. (2005). Letter: Multiply charged ions in matrix-assisted laser desorption/ionization generated from electrosprayed sample layers. *European Journal of Mass Spectrometry*, *11*, 257-260.
- ¹⁶⁵ Glückmann, M., Pfenninger, A., Krüger, R., Thierolf, M., Karasa, M., Horneffer, V., Hillenkamp, F., & Strupat, K. (2001). Mechanisms in MALDI analysis: surface

- interaction or incorporation of analytes?. *International Journal of Mass Spectrometry*, 210, 121-132.
- ¹⁶⁶ Knochenmuss, R. (2003). A quantitative model of ultraviolet matrix-assisted laser desorption/ionization including analyte ion generation. *Analytical Chemistry*, 75, 2199-2207.
- ¹⁶⁷ Wachs, T., Conboy, J. C., Garcia, F., & Henion, J. D. (1991). Liquid chromatography-mass spectrometry and related techniques via atmospheric pressure ionization. *Journal of Chromatographic Science*, 29, 357-366.
- ¹⁶⁸ Niessen, W. M. A., & Tinke, A. P. (1995). Liquid chromatography-mass spectrometry general principles and instrumentation. *Journal of Chromatography A*, 703, 37-57.
- ¹⁶⁹ Mehlis, B., & Kertscher, U. (1997). Liquid chromatography/mass spectrometry of peptides of biological samples. *Analytica Chimica Acta*, 352, 71-83.
- ¹⁷⁰ Srinivas, P., Krishna, P., Sadanandam, M. (2010). Nano liquid chromatography in pharmaceutical analysis – a review. *International Journal of Pharmaceutical Science*, 2, 728-737.
- ¹⁷¹ Shen, Y., Tolic, N., Masselon, C., Paša-Tolic, L., Camp, D. G., Hixson, K. K., Zhao, R., Anderson, G. A., & Smith, R. D. (2004). Ultrasensitive proteomics using high-efficiency on-line micro-SPE-nanoLC-nanoESI MS and MS/MS. *Analytical chemistry* 76, 144-154.
- ¹⁷² Smith, R. D., Shen, Y., & Tang, K. (2004). Ultrasensitive and quantitative analyses from combined separations-mass spectrometry for the characterization of proteomes. *Accounts of Chemical Research*, 37, 269-278.

- ¹⁷³ Wilm, M., & Mann, M. (1996). Analytical properties of the nanoelectrospray ion source. *Analytical Chemistry*, *68*, 1-8.
- ¹⁷⁴ Tang, K., Page, J. S., Marginean, I., Kelly, R. T., & Smith, R. D. (2011). Improving liquid chromatography-mass spectrometry sensitivity using a subambient pressure ionization with nanoelectrospray (SPIN) interface. *Journal of the American Society for Mass Spectrometry*, *22*, 1318-1325.
- ¹⁷⁵ Page, J. S., Tang, K., Kelly, R. T., & Smith, R. D. (2008). Subambient pressure ionization with nanoelectrospray source and interface for improved sensitivity in mass spectrometry. *Analytical Chemistry*, *80*, 1800-1805.
- ¹⁷⁶ Hirabayashi, A., Sakairi, M., Koizumi, H. (1994) Sonic Spray Ionization method for atmospheric-pressure ionization mass-spectrometry. *Analytical Chemistry* *66*, 4557-4559.
- ¹⁷⁷ Hirabayashi, A., Hirabayashi, Y., Sakairi, M, Koizumi, H. (1996) Multiply-charged ion formation by sonic spray, *Rapid Communications in Mass Spectrometry* *10*, 1703-1705
- ¹⁷⁸ Koehn, F. E., & Carter, G. T. (2005). The evolving role of natural products in drug discovery. *Nature Reviews Drug Discovery*, *4*, 206-220.
- ¹⁷⁹ Leszczyniecka, M., Roberts, T., Dent, P., Grant, S., & Fisher, P. B. (2001). Differentiation therapy of human cancer: basic science and clinical applications. *Pharmacology & Therapeutics*, *90*, 105-156.
- ¹⁸⁰ Brown, D., & Superti-Furga, G. (2003). Rediscovering the sweet spot in drug discovery. *Drug Discovery Today*, *8*, 1067-1077.

- ¹⁸¹ Hertzberg, R. P., & Pope, A. J. (2000). High-throughput screening: new technology for the 21st century. *Current Opinion in Chemical Biology*, *4*, 445-451.
- ¹⁸² Lapos, J. A., Manica, D. P., & Ewing, A. G. (2002). Dual fluorescence and electrochemical detection on an electrophoresis microchip. *Analytical Chemistry*, *74*, 3348-3353.
- ¹⁸³ Wang, M., Roman, G. T., Perry, M. L., & Kennedy, R. T. (2009). Microfluidic chip for high efficiency electrophoretic analysis of segmented flow from a microdialysis probe and in vivo chemical monitoring. *Analytical Chemistry*, *81*, 9072-9078.
- ¹⁸⁴ Trim, P. J., Djidja, M. C., Atkinson, S. J., Oakes, K., Cole, L. M., Anderson, D. M., Hart, P. J., Francese, S., & Clench, M. R. (2010). Introduction of a 20 kHz Nd: YVO4 laser into a hybrid quadrupole time-of-flight mass spectrometer for MALDI-MS imaging. *Analytical and Bioanalytical Chemistry*, *397*, 3409-3419.
- ¹⁸⁵ Kim, T., Udseth, H. R., & Smith, R. D. (2000). Improved ion transmission from atmospheric pressure to high vacuum using a multicapillary inlet and electrodynamic ion funnel interface. *Analytical Chemistry*, *72*, 5014-5019.
- ¹⁸⁶ Moini, M., Jiang, L., & Bootwala, S. (2011). High-throughput analysis using gated multi-inlet mass spectrometry. *Rapid Communications in Mass Spectrometry*, *25*, 789-794.
- ¹⁸⁷ Li, J. Y., Chen, Y., Deninno, M. P., O'Connell, T. N., & Hop, C. E. (2005). Identification of a novel glutathione adduct of diclofenac, 4'-hydroxy-2'-glutathion-deschloro-diclofenac, upon incubation with human liver microsomes. *Drug Metabolism and Disposition* *33*, 484-488.

- ¹⁸⁸ Kim, S., Rodgers, R. P., Blakney, G. T., Hendrickson, C. L., & Marshall, A. G. (2009). Automated electrospray ionization FT-ICR mass spectrometry for petroleum analysis. *Journal of the American Society for Mass Spectrometry*, *20*, 263-268.
- ¹⁸⁹ Kertesz, V., & Van Berkel, G. J. (2010). Fully automated liquid extraction-based surface sampling and ionization using a chip-based robotic nanoelectrospray platform. *Journal of Mass Spectrometry*, *45*, 252-260.
- ¹⁹⁰ Edwards, R. L., Creese, A. J., Baumert, M., Griffiths, P., Bunch, J., & Cooper, H. J. (2011). Hemoglobin variant analysis via direct surface sampling of dried blood spots coupled with high-resolution mass spectrometry. *Analytical Chemistry*, *83*, 2265-2270.
- ¹⁹¹ van der Hooft, J. J., Vervoort, J., Bino, R. J., & de Vos, R. C. (2012). Spectral trees as a robust annotation tool in LC-MS based metabolomics. *Metabolomics*, *8*, 691-703.
- ¹⁹² Pei, J., Li, Q., Lee, M. S., Valaskovic, G. A., & Kennedy, R. T. (2009). Analysis of samples stored as individual plugs in a capillary by electrospray ionization mass spectrometry. *Analytical Chemistry*, *81*, 6558-6561.
- ¹⁹³ Sun, S., Slaney, T. R., & Kennedy, R. T. (2012). Label free screening of enzyme inhibitors at femtomole scale using segmented flow electrospray ionization mass spectrometry. *Analytical Chemistry*, *84*, 5794-5800.
- ¹⁹⁴ Sterling, H. J., Cassou, C. A., Susa, A. C., & Williams, E. R. (2012). Electrothermal supercharging of proteins in native electrospray ionization. *Analytical Chemistry*, *84*, 3795-3801.

- ¹⁹⁵ Richards, A. L., Lietz, C. B., Wager-Miller, J., Mackie, K., & Trimpin, S. (2012). Localization and imaging of gangliosides in mouse brain tissue sections by laserspray ionization inlet. *Journal of Lipid Research*, *53*, 1390-1398.
- ¹⁹⁶ Chubatyi, N. D., Pagnotti, V. S., Bentzley, C. M., & McEwen, C. N. (2012). High sensitivity steroid analysis using liquid chromatography/solvent-assisted inlet ionization mass spectrometry. *Rapid Communications in Mass Spectrometry*, *26*, 887-892.
- ¹⁹⁷ Wang, B., Inutan, E. D., & Trimpin, S. (2012). A new approach to high sensitivity liquid chromatography-mass spectrometry of peptides using nanoflow solvent assisted inlet ionization. *Journal of the American Society for Mass Spectrometry*, *23*, 442-445.
- ¹⁹⁸ Pagnotti, V.S., Inutan, E.D., Marshall, D.D., McEwen, C.N., Trimpin, S. (2011). Inlet ionization: a new highly sensitive approach for liquid chromatography/mass spectrometry of small and large molecules. *Analytical Chemistry* *83*, 7591-7594.
- ¹⁹⁹ Rohner, T. C., Staab, D., & Stoeckli, M. (2005). MALDI mass spectrometric imaging of biological tissue sections. *Mechanisms of Ageing and Development*, *126*, 177-185.
- ²⁰⁰ Bushee, J. L., & Argikar, U. A. (2011). An experimental approach to enhance precursor ion fragmentation for metabolite identification studies: application of dual collision cells in an orbital trap. *Rapid Communications in Mass Spectrometry*, *25*, 1356-1362.
- ²⁰¹ Oswald, S., Peters, J., Venner, M., & Siegmund, W. (2011). LC-MS/MS method for the simultaneous determination of clarithromycin, rifampicin and their main

- metabolites in horse plasma, epithelial lining fluid and broncho-alveolar cells. *Journal of Pharmaceutical and Biomedical Analysis*, 55, 194-201.
- ²⁰² Qin, J., & Chait, B. T. (1996). Matrix-assisted laser desorption ion trap mass spectrometry: efficient trapping and ejection of ions. *Analytical Chemistry*, 68, 2102-2107.
- ²⁰³ Ding, L., Sudakov, M., Brancia, F. L., Giles, R., & Kumashiro, S. (2004). A digital ion trap mass spectrometer coupled with atmospheric pressure ion sources. *Journal of Mass Spectrometry*, 39, 471-484.
- ²⁰⁴ Chi, L., Wolff, J. J., Laremore, T. N., Restaino, O. F., Xie, J., Schiraldi, C., Toida, T., Amster, I. J., & Linhardt, R. J. (2008). Structural analysis of bikunin glycosaminoglycan. *Journal of the American Chemical Society*, 130, 2617-2625.
- ²⁰⁵ Laremore, T. N., Leach III, F. E., Solakyildirim, K., Amster, I. J., & Linhardt, R. J. (2010). Chapter Three-Glycosaminoglycan Characterization by Electrospray Ionization Mass Spectrometry Including Fourier Transform Mass Spectrometry. *Methods in Enzymology*, 478, 79-108.
- ²⁰⁶ Valentine, S. J., Plasencia, M. D., Liu, X., Krishnan, M., Naylor, S., Udseth, H. R., Smith, R. D., & Clemmer, D. E. (2006). Toward plasma proteome profiling with ion mobility-mass spectrometry. *Journal of Proteome Research*, 5, 2977-2984.
- ²⁰⁷ Dwivedi, P., & Schultz, A. J. (2010). Metabolic profiling of human blood by high-resolution ion mobility mass spectrometry (IM-MS). *International Journal of Mass Spectrometry*, 298, 78-90.
- ²⁰⁸ Devenport, N. A., Reynolds, J. C., Weston, D. J., Wilson, I. D., & Creaser, C. S. (2012). Direct extraction of urinary analytes from undeveloped reversed-phase thin

- layer chromatography plates using a solvent gradient combined with on-line electrospray ionisation ion mobility-mass spectrometry. *Analyst*, *137*, 3510-3513.
- ²⁰⁹ Wuhrer, M., Stam, J. C., van de Geijn, F. E., Koeleman, C. A., Verrips, C. T., Dolhain, R. J., Hokke, C. H. & Deelder, A. M. (2007). Glycosylation profiling of immunoglobulin G (IgG) subclasses from human serum. *Proteomics*, *7*, 4070-4081.
- ²¹⁰ Swaney, D. L., Wenger, C. D., Thomson, J. A., & Coon, J. J. (2009). Human embryonic stem cell phosphoproteome revealed by electron transfer dissociation tandem mass spectrometry. *Proceedings of the National Academy of Sciences*, *106*, 995-1000.
- ²¹¹ Garcia, B. A., Busby, S. A., Barber, C. M., Shabanowitz, J., Allis, C. D., & Hunt, D. F. (2004). Characterization of phosphorylation sites on histone H1 isoforms by tandem mass spectrometry. *Journal of Proteome Research*, *3*, 1219-1227.
- ²¹² Udeshi, N. D., Compton, P. D., Shabanowitz, J., Hunt, D. F., & Rose, K. L. (2008). Methods for analyzing peptides and proteins on a chromatographic timescale by electron-transfer dissociation mass spectrometry. *Nature Protocols*, *3*, 1709-1717.
- ²¹³ Motoyama, A., & Yates III, J. R. (2008). Multidimensional LC separations in shotgun proteomics. *Analytical Chemistry*, *80*, 7187-7193.
- ²¹⁴ Delahunty, C., & Yates Iii, J. R. (2005). Protein identification using 2d-lc-ms/ms. *Methods*, *35*, 248-255.
- ²¹⁵ Nyadong, L., Inutan, E. D., Wang, X., Hendrickson, C. L., Trimpin, S., & Marshall, A. G. (2013). Laserspray and matrix-assisted ionization inlet coupled to high-field FT-ICR mass spectrometry for peptide and protein analysis. *Journal of the American Society for Mass Spectrometry*, *24*, 320-328.

- ²¹⁶ Marshall, A. G., Hendrickson, C. L., & Jackson, G. S. (1998). Fourier transform ion cyclotron resonance mass spectrometry: a primer. *Mass Spectrometry Reviews*, *17*, 1-35.
- ²¹⁷ Zenobi, R., & Knochenmuss, R. (1998). Ion formation in MALDI mass spectrometry. *Mass Spectrometry Reviews*, *17*, 337-366.
- ²¹⁸ Kinsel, G. R., Gimon-Kinsel, M. E., Gillig, K. J., & Russell, D. H. (1999). Investigation of the dynamics of matrix-assisted laser desorption/ionization ion formation using an electrostatic analyzer/time-of-flight mass spectrometer. *Journal of Mass Spectrometry*, *34*, 684-690.
- ²¹⁹ Fournier, I., Brunot, A., Tabet, J. C., & Bolbach, G. (2002). Delayed extraction experiments using a repulsive potential before ion extraction: evidence of clusters as ion precursors in UV-MALDI. Part I: dynamical effects with the matrix 2, 5-dihydroxybenzoic acid. *International Journal of Mass Spectrometry*, *213*, 203-215.
- ²²⁰ Vestal, M. L. (2009). Modern MALDI time-of-flight mass spectrometry. *Journal of Mass Spectrometry*, *44*, 303-317.
- ²²¹ Stavenhagen, K., Hinneburg, H., Thaysen-Andersen, M., Hartmann, L., Silva, D. V., Fuchser, J., Kaspar, S., Rapp, E., Seeberger, P. H., & Kolarich, D. (2013). Quantitative mapping of glycoprotein micro-heterogeneity and macro-heterogeneity: an evaluation of mass spectrometry signal strengths using synthetic peptides and glycopeptides. *Journal of Mass Spectrometry*, *48*, 627-639.
- ²²² Chakrabarty, S., Pagnotti, V. S., Inutan, E. D., Trimpin, S., & McEwen, C. N. (2013). A new matrix assisted ionization method for the analysis of volatile and nonvolatile

- compounds by atmospheric probe mass spectrometry. *Journal of The American Society for Mass Spectrometry*, 24, 1102-1107.
- ²²³ Mitchell, J. Jr., Deveraux, H. D. (1978) Determination of traces of organic-compounds in atmosphere – role of detectors in gas-chromatography. *Analytica Chimica Acta* 100, 45-52.
- ²²⁴ Sweeting, L. M., Cashel, M. L., & Rosenblatt, M. M. (1992). Triboluminescence spectra of organic crystals are sensitive to conditions of acquisition. *Journal of Luminescence*, 52, 281-291.
- ²²⁵ Sweeting, L. M. (2001). Triboluminescence with and without air. *Chemistry of Materials*, 13, 854-870.
- ²²⁶ Batoy, S. M. A., Borgmann, S., Flick, K., Griffith, J., Jones, J. J., Saraswathi, V., Hasty, A. H., Kaiser, P., & Wilkins, C. L. (2009). Lipid and phospholipid profiling of biological samples using MALDI Fourier transform mass spectrometry. *Lipids*, 44, 367-371.
- ²²⁷ Catherman, A. D., Li, M., Tran, J. C., Durbin, K. R., Compton, P. D., Early, B. P., Thomas, P. M., & Kelleher, N. L. (2013). Top down proteomics of human membrane proteins from enriched mitochondrial fractions. *Analytical Chemistry*, 85, 1880-1888.
- ²²⁸ Cooper, H. J., Håkansson, K., & Marshall, A. G. (2005). The role of electron capture dissociation in biomolecular analysis. *Mass Spectrometry Reviews*, 24, 201-222.
- ²²⁹ Zubarev, R. A., Kelleher, N. L., & McLafferty, F. W. (1998). Electron capture dissociation of multiply charged protein cations. A nonergodic process. *Journal of the American Chemical Society*, 120, 3265-3266.

- ²³⁰ Chi, A., Huttenhower, C., Geer, L. Y., Coon, J. J., Syka, J. E., Bai, D. L., ... & Hunt, D. F. (2007). Analysis of phosphorylation sites on proteins from *Saccharomyces cerevisiae* by electron transfer dissociation (ETD) mass spectrometry. *Proceedings of the National Academy of Sciences*, *104*, 2193-2198.
- ²³¹ Lee, M. S., & Kerns, E. H. (1999). LC/MS applications in drug development. *Mass Spectrometry Reviews*, *18*, 187-279.
- ²³² Fenselau, C., & Demirev, P. A. (2001). Characterization of intact microorganisms by MALDI mass spectrometry. *Mass Spectrometry Reviews*, *20*, 157-171.
- ²³³ Vismeh, R., Waldon, D. J., Teffera, Y., & Zhao, Z. (2012). Localization and quantification of drugs in animal tissues by use of desorption electrospray ionization mass spectrometry imaging. *Analytical Chemistry*, *84*, 5439-5445.
- ²³⁴ Gygi, S. P., Rist, B., Gerber, S. A., Turecek, F., Gelb, M. H., & Aebersold, R. (1999). Quantitative analysis of complex protein mixtures using isotope-coded affinity tags. *Nature Biotechnology*, *17*, 994-999.
- ²³⁵ Li, X., Fang, X., Yu, Z., Sheng, G., Wu, M., Fu, J., & Chen, H. (2012). Direct quantification of creatinine in human urine by using isotope dilution extractive electrospray ionization tandem mass spectrometry. *Analytica Chimica Acta*, *748*, 53-57.
- ²³⁶ Vanderford, B. J., & Snyder, S. A. (2006). Analysis of pharmaceuticals in water by isotope dilution liquid chromatography/tandem mass spectrometry. *Environmental Science & Technology*, *40*, 7312-7320.
- ²³⁷ Keshishian, H., Addona, T., Burgess, M., Kuhn, E., & Carr, S. A. (2007). Quantitative, multiplexed assays for low abundance proteins in plasma by targeted

- mass spectrometry and stable isotope dilution. *Molecular & Cellular Proteomics*, 6, 2212-2229.
- ²³⁸ Dams, R., Huestis, M. A., Lambert, W. E., & Murphy, C. M. (2003). Matrix effect in bio-analysis of illicit drugs with LC-MS/MS: influence of ionization type, sample preparation, and biofluid. *Journal of the American Society for Mass Spectrometry*, 14, 1290-1294.
- ²³⁹ Benijts, T., Dams, R., Lambert, W., & De Leenheer, A. (2004). Countering matrix effects in environmental liquid chromatography–electrospray ionization tandem mass spectrometry water analysis for endocrine disrupting chemicals. *Journal of Chromatography A*, 1029, 153-159.
- ²⁴⁰ Jackson, S. N., Wang, H. Y. J., & Woods, A. S. (2005). Direct profiling of lipid distribution in brain tissue using MALDI-TOFMS. *Analytical Chemistry*, 77, 4523-4527.
- ²⁴¹ Stoeckli, M., Staab, D., & Schweitzer, A. (2007). Compound and metabolite distribution measured by MALDI mass spectrometric imaging in whole-body tissue sections. *International Journal of Mass Spectrometry*, 260, 195-202.
- ²⁴² Cornett, D. S., Reyzer, M. L., Chaurand, P., & Caprioli, R. M. (2007). MALDI imaging mass spectrometry: molecular snapshots of biochemical systems. *Nature methods*, 4, 828-833.
- ²⁴³ Stoeckli, M., Chaurand, P., Hallahan, D. E., & Caprioli, R. M. (2001). Imaging mass spectrometry: a new technology for the analysis of protein expression in mammalian tissues. *Nature medicine*, 7, 493-496.

- ²⁴⁴ Krutchinsky, A. N., & Chait, B. T. (2002). On the nature of the chemical noise in MALDI mass spectra. *Journal of the American Society for Mass Spectrometry*, *13*, 129-134.
- ²⁴⁵ Puolitaival, S. M., Burnum, K. E., Cornett, D. S., & Caprioli, R. M. (2008). Solvent-free matrix dry-coating for MALDI imaging of phospholipids. *Journal of the American Society for Mass Spectrometry*, *19*, 882-886.
- ²⁴⁶ Wiseman, J. M., Evans, C. A., Bowen, C. L., & Kennedy, J. H. (2010). Direct analysis of dried blood spots utilizing desorption electrospray ionization (DESI) mass spectrometry. *Analyst*, *135*, 720-725.
- ²⁴⁷ Eberlin, L. S., Ferreira, C. R., Dill, A. L., Ifa, D. R., & Cooks, R. G. (2011). Desorption electrospray ionization mass spectrometry for lipid characterization and biological tissue imaging. *Biochimica et Biophysica Acta (BBA)-Molecular and Cell Biology of Lipids*, *1811*, 946-960.
- ²⁴⁸ Cooks, R. G., Manicke, N. E., Dill, A. L., Ifa, D. R., Eberlin, L. S., Costa, A. B., ... & Ouyang, Z. (2011). New ionization methods and miniature mass spectrometers for biomedicine: DESI imaging for cancer diagnostics and paper spray ionization for therapeutic drug monitoring. *Faraday Discussions*, *149*, 247-267.
- ²⁴⁹ Ifa, D. R., Wu, C., Ouyang, Z., & Cooks, R. G. (2010). Desorption electrospray ionization and other ambient ionization methods: current progress and preview. *Analyst*, *135*, 669-681.
- ²⁵⁰ Norris, J. L., & Caprioli, R. M. (2013). Analysis of tissue specimens by matrix-assisted laser desorption/ionization imaging mass spectrometry in biological and clinical research. *Chemical Reviews*, *113*, 2309-2342.

- ²⁵¹ Chaurand, P., Schriver, K. E., & Caprioli, R. M. (2007). Instrument design and characterization for high resolution MALDI-MS imaging of tissue sections. *Journal of Mass Spectrometry*, *42*, 476-489.
- ²⁵² Schäfer, K. C., Dénes, J., Albrecht, K., Szaniszló, T., Balog, J., Skoumal, R., ... & Takáts, Z. (2009). In vivo, in situ tissue analysis using rapid evaporative ionization mass spectrometry. *Angewandte Chemie International Edition*, *48*, 8240-8242.
- ²⁵³ Wang, B., & Trimpin, S. (2013). High-throughput solvent assisted ionization inlet for use in mass spectrometry. *Analytical chemistry*, *86*, 1000-1006.
- ²⁵⁴ Webb, K. J., Xu, T., Park, S. K., & Yates III, J. R. (2013). Modified MuDPIT separation identified 4488 proteins in a system-wide analysis of quiescence in yeast. *Journal of Proteome Research*, *12*, 2177-2184.
- ²⁵⁵ Lutomski, C. A., El-Baba, T. J., Inutan, E. D. V., Manly, C. D., Wager-Miller, J., Mackie, K., & Trimpin, S. (2014). Transmission Geometry Laserspray Ionization Vacuum Using an Atmospheric Pressure Inlet. *Analytical Chemistry*.
- ²⁵⁶ Laskin, J., Heath, B. S., Roach, P. J., Cazares, L., & Semmes, O. J. (2011). Tissue imaging using nanospray desorption electrospray ionization mass spectrometry. *Analytical chemistry*, *84*, 141-148.
- ²⁵⁷ Harvey, D. J. (1995). Matrix-assisted laser desorption/ionization mass spectrometry of phospholipids. *Journal of Mass Spectrometry*, *30*, 1333-1346.
- ²⁵⁸ Jackson, S. N., Wang, H. Y. J., & Woods, A. S. (2005). In situ structural characterization of phosphatidylcholines in brain tissue using MALDI-MS/MS. *Journal of the American Society for Mass Spectrometry*, *16*, 2052-2056.

- ²⁵⁹ Baldessarini, R. J., Centorrino, F., Flood, J. G., Volpicelli, S. A., Huston-Lyons, D., & Cohen, B. M. (1993). Tissue concentrations of clozapine and its metabolites in the rat. *Neuropsychopharmacology*, *9*, 117-124.
- ²⁶⁰ Shrestha, B., Nemes, P., Nazarian, J., Hathout, Y., Hoffman, E. P., & Vertes, A. (2010). Direct analysis of lipids and small metabolites in mouse brain tissue by AP IR-MALDI and reactive LAESI mass spectrometry. *Analyst*, *135*, 751-758.

ABSTRACT

DEVELOPMENT OF *INLET* AND *VACUUM* IONIZATION METHODS FOR CHARACTERIZATION OF BIOLOGICAL MATERIALS BY MASS SPECTROMETRY

by

BEIXI WANG

May 2015

Advisor: Dr. Sarah Trimpin

Major: Chemistry (Analytical)

Degree: Doctor of Philosophy

Inlet ionization and *vacuum* ionization are novel ionization methods to produce electrospray ionization (ESI)-like ions from the solid or liquid states, operating from atmospheric pressure (AP) or vacuum, without the use of voltage or the necessity of high energy input such as a laser or particle beam. The fundamental aspects were probed for better understanding of the novel ionization processes. Initial applications were attempted to utilize the novel ionization methods for fast, robust, and quantitative analyses.

For *inlet* ionizations (laserspray ionization *inlet*, **LSII**; matrix assisted ionization *inlet*, **MAII**; and solvent assisted ionization *inlet*, **SAII**), small (e.g. drugs) to large (e.g. proteins) non-volatile molecules are ionized with the assistance of heat and pressure drop, and are operated from AP. The ease of operation, rapidness of data acquisition, and simplicity of coupling with other techniques achieved by SAI, have enabled the *inlet* ionization for high throughput multiplexing analyses, hyphenation with liquid chromatography (especially at low flow rates), and fast surface assessment and drug

quantifications. LSII has been utilized together with solvent-free sample preparation and solvent-free gas-phase separation for total solvent-free analysis.

The production of multiply charged ions from solid states by *vacuum* ionization was utilized to encompass the advantages from ESI and matrix-assisted laser desorption/ionization (**MALDI**), for better characterization from surfaces and extending the mass range of high performance mass spectrometers. Operating from AP provides the potential for *vacuum* ionization to be applied in high throughput analysis. The continuous ion formation also benefits matrix assisted ionization *vacuum* (**MAIV**) for drug quantification with better reproducibility.

AUTOBIOGRAPHICAL STATEMENT

Beixi Wang

Education

Wayne State University, Detroit, MI

August 2009 – 2014

Major: Analytical Chemistry

Fuzhou University, Fujian, China

September 2005 – July 2009

Major: Chemistry

Degree: B.S.

Honors and Awards

David F. Boltz Award Analytical Chemistry, April 2014

A. Paul and Carol C. Schaap Endowed Distinguished Graduate Student Fellowships, 2013-2014

Graduate School Citation for Excellence in Teaching Service, 2013

Thomas C. Rumble University Graduate Fellowships, 2012-2013

Department Citation for Excellence in Teaching Service, 2012

Graduate Travel Award from Wayne State University, May 2012

Travel Award from Thermo Fisher Scientific Inc., April 2012

Selected Publications

A. Journal Publications

- 1) **Wang, B.**; Dearing, C.L.; Wager-Miller, J.; Mackie, K.; Trimpin, S. *Anal. Chem.*, submitted.
- 2) **Wang, B.**; Tisdale, E., Trimpin, S., Wilkins, C.L. *Anal. Chem.* **2014**, *86*, 6792-6796.
- 3) **Wang, B.**; Trimpin, S. *Anal. Chem.*, **2014**, *86*, 1000-1006.
- 4) **Wang, B.**; Inutan, E.D.; Trimpin, S. *J. Am. Soc. Mass Spectrom.* **2012**, *23*, 442-445.
- 5) **Wang, B.**; Lietz, C.B.; Inutan, E.D.; Leach, S.M.; Trimpin, S. *Anal. Chem.* **2011**, *83*, 4076-4084.

B. Book Chapter

- 1) Trimpin, S.; **Wang, B.** Inlet and Vacuum Ionization from Ambient Conditions, in: *Ambient Ionization Mass Spectrometry*, Royal Society of Chemistry, by Eds. Marek Domin and Robert Cody, **2015**, 423-444.